THE CHARACTERISATION OF A GM-CSF AND IL-2 INHIBITORY PROTEIN ENCODED BY ORF VIRUS

DAVID LESLIE DEANE

A THESIS SUBMITTED FOR THE DEGREE OF

DOCTOR OF PHILOSOPHY

IN THE

FACULTY OF MEDICINE,

UNIVERSITY OF EDINBURGH

VIROLOGY DIVISION

MOREDUN RESEARCH INSTITUTE,

PENICUIK

JANUARY 2001

DECLARATION

I hereby declare that:

(i) This thesis has been composed by myself

(ii) It has not been accepted in any previous application

(iii) The work described has been carried out by myself or, where jointly, this fact has been acknowledged.

David Leslie Deane

Moredun Research Institute

January 2001

ACKNOWLEDGEMENTS

I would like to thank the following for their invaluable assistance during the preparation of this thesis:

My supervisor at the Moredun Research Institute, Dr. David Haig for all his unstinting advice and encouragement.

Professor Mary Norval for acting as my University supervisor, providing advice and encouragement, liasing with the Medical Faculty Office and proof reading manuscripts.

Dr. Colin McInnes and Miss Ann Wood for their contribution to the isolation and characterisation of the GIF gene described in chapter 3 and for advice and helpful discussion throughout this study.

Dr. Gary Entrican, Dr. Heng-Fong Seow, Dr. Paul Wood and Dr.Sarah Duggan for supplying recombinant ovine and bovine cytokine reagents.

Dr. Tony Hunter for advice on statistical analysis of data.

Dr. Andy Mercer for supplying the vaccinia virus-orf virus recombinant library required for the identification of the GIF gene.

Dr. Peter Nettleton and Mrs. Janice Gilray for advice and assistance with virus work.

Dr. Alex Schock and Mr. Ian Anderson for advice on immunohistochemical techniques described in chapter 7.

Mrs Ann Percival, Miss Jackie Thomson, Mrs Ann Gardiner, Mrs Mary MacLean and Mr. Jim Redmond for their expert technical assistance.

Mary, Maggie and Jenny for their support and patience.

ABSTRACT

Orf virus is a 139 kb double-stranded DNA parapoxvirus that has a world wide distribution and infects sheep, goats and man. The virus infects broken or scarified skin and replicates in regenerating epidermal keratinocytes. Infections are acute, contained locally and give rise to pustular lesions that turn to scabs. Virus is shed with the scab. The immune response to orf virus is characterised by a local accumulation of $CD4^+$ and $CD8^+$ T cells, B cells, neutrophils and a dense network of dermal dendritic cells. Evasion of the host immune system by orf virus is implicated since the virus can repeatedly infect previously exposed sheep in spite of an apparently normal host antiviral immune and inflammatory response.

The orf virus genome has been sequenced but only 31 gene sequences have been recorded in the public databases. Several putative immunomodulatory genes have been discovered: a viral homologue of mammalian vascular endothelial growth factor, a viral homologue of IL-10 and a homologue of the vaccinia virus E3L gene which encodes for an interferon resistance protein.

A granulocyte-macrophage colony stimulating factor (GM-CSF) inhibitory activity associated with virus-infected cells was first detected in a previous study of cytokine production by sheep keratinocytes infected with orf virus. Although IL-8, TNF-α and GM-CSF mRNAs and IL-8 and TNF-α protein were detected in infected keratinocyte cultures, GM-CSF protein was not. In this study, the gene encoding the GM-CSF- inhibitory factor (GIF) was isolated and mapped to the right terminal quarter of the orf virus genome. The orf virus GIF cDNA was expressed as a secreted protein in Chinese hamster ovarian cells as detected by GM-CSF inhibition ELISA. Recombinant GIF was purified by ovine GM-CSF affinity chromatography and gel filtration. Sequence analysis of the 20 N-terminal amino acids was performed on the purified GIF. The GIF gene encodes a 28 kD protein that exhibits 32% amino acid sequence similarity to the predicted sequence of the A41L gene product encoded by vaccinia virus. Although the vaccinia virus A41L protein has sequence similarity to the T1 secreted chemokine-binding proteins of leporipoxviruses, its function is not known. GIF did not share any homology with any cytokine receptor molecule identified to date. In contrast to other parapovxirus immunomodulatory proteins that are products of early viral genes, GIF was found to be the product of an intermediate /late viral gene in orf virus-infected cells. GIF formed homodimers and homotetramers in solution and bound ovine GM-CSF with a Kd of 369 pM. In addition GIF bound ovine IL-2 with a Kd of 1.04 nM. Although orf virus infects humans, GIF did not bind human GM-CSF or IL-2.

GIF was shown to inhibit the binding of ovine ^{125}I-GM-CSF to its receptor on isolated sheep neutrophils and to inhibit the haematopoietic activity of ovine GM-CSF in a soft agar bone marrow colony assay. GIF also inhibited the binding of ovine ^{125}I-IL-2 to $CD4^+$ T cells and inhibited the stimulatory activity of ovine IL-2 in a T cell proliferation assay. This inhibitory activity was neutralised by a rabbit antiserum raised against purified GIF.

GIF was produced *in vivo* during orf virus reinfection. GIF was detected in skin, localised to the area of orf virus infected cells and in afferent lymph draining the skin site of infection. The presence of GIF, 3-7 days after virus infection was associated with reduced levels of GM-CSF in the lymph plasma and the period of maximum viral replication in the skin.

Thus the GM-CSF and IL-2 inhibitory factor represents a growing number of immunomodulatory proteins encoded by poxviruses and other large DNA viruses that inhibit or mimic key effector molecules of the host immune system.

TABLE OF CONTENTS

LIST OF ABBREVIATIONS

APC	antigen presenting cell
BCA	bichinoic acid
BLAST	basic local alignment search tool
bo	bovine
bp	base pair
BPSV	bovine papular stomatitis virus
BSA	bovine serum albumin
CA	cytosine arabinoside
CD	cluster determinant
cDNA	complementary DNA
DNA	deoxyribonucleic acid
CHAPS	3-[(3-cholamidopropyl)-dimethylammonio]-1-propanesulfonate
CHO	Chinese hamster ovarian
ConA	concanavalin A
CPE	cytopathic effect
CPV	cowpoxvirus
cpm	counts per minute
DC	dendritic cell
DMEM	Dulbecco's modified eagle medium
DMSO	dimethylsulphoxide
DTT	dithiothreitol
ECL	enhanced chemiluminescence
EDC	1-ethyl-3-(3-dimethylaminopropyl)carbodiimide
ELISA	enzyme-linked immunosorbent assay
EV	ectromelia virus
FCS	foetal calf serum
FITC	fluoroscein isothiocyanate
FLM	foetal lamb muscle
FPLC	fast protein liquid chromatography
g	gram (or gravity for centrifugation)
G-CSF	granulocyte-colony stimulating factor
GIF	GM-CSF inhibitory factor
GM-CSF	granulocyte macrophage-colony stimulating factor
GMEM	Glasgow modified Eagle medium
h	hours
HBSS	Hanks' balanced salt solution
HRP	horse radish peroxidase
hu	human
IFN-γ (α,β)	interferons γ (α,β)
Ig	immunoglobulin
IL-1 (2,3,4,5,6,8,10,12,15,18)	interleukin-1 (2,3,4,5,6,8,10,12,15,18)
IMDM	Iscove's modification of Dulbecco's medium
ITR	Inverted terminal repeat
kD	kilodaltons
l	litre
LC	Langerhan's cell

M	molar solution
Mab	monoclonal antibody
MACS	magnetic cell sorting
MCP-1	monocyte chemotactic protein-1
MCV	molluscum contagiosum virus
MHC class I or II	major histocompatibility complex class i or ii
Min	minutes
MIP-1α	macrophage inflammatory protein-1α
MNV	milkers' module virus/pseudocowpox virus
MOI	multiplicity of infection
mol.wt.	molecular weight
MRI	Moredun Research Institute
mRNA	messenger RNA
MSX	methionine sulphoxamine
mu	murine
MV	myxoma virus
NMS	normal mouse serum
NRS	normal rabbit serum
O.D.	optical density
OPD	O-phenylene diamine
OV	orf virus
ov	ovine
PBS	phosphate buffered saline
PEG	polyethylene glycol
r	recombinant
RANTES	regulated upon activation, normal t-cell expressed, and presumably secreted
RNA	ribonucleic acid
rpm	revolutions per minute
RT	room temperature
SCF	stem cell factor
SDS-PAGE	sodium dodecyl sulphate polyacrylamide gel electrophoresis
SEM	standard error of the mean
ShFV	Shope fibroma virus
SFV	Semliki forest virus
SPV	Swinepox virus
TCR	T cell receptor
TNF	tumour necrosis factor
TPV	tanapox virus
UV	ultra violet
v/v	volume in volume
VaV	variola virus
VEGF	vascular endothelial growth factor
VV	vaccinia virus
w/v	weight in volume

CHAPTER 1

GENERAL INTRODUCTION

1.1. Orf

1.1.1. Definition

Orf is an acute and highly contagious skin condition in sheep and goats (Glover, 1928; Abdulassam and Cosslet, 1957; Moore *et al*, 1983; Haig and Mercer 1998). Also known as contagious pustular dermatitis, contagious ecthyma and scabbymouth, orf constitutes a serious welfare problem in sheep and goats world-wide. In the United Kingdom the number of cases of orf has not been documented but annual sales of anti-orf vaccine were estimated in 1996 at 2.5 million doses.

The disease has no systemic phase and is characterised by pustular lesions from which scabs develop. Normally lesions are resolved within six to eight weeks without scarring. Outbreaks of the disease arise all year round but are most common in the spring and summer (Aynaud, 1923; Schmidt and Hardy, 1932). Orf outbreaks typically occur in the more vulnerable young and elderly animals and spread of the disease is often rapid, particularly in animals that have been previously unaffected. Transmission of the disease from the udders of nursing ewes to susceptible lambs can result in severe pustular lesions around the mouth and nares (Fig. 1.1) that may interfere with feeding and an inability to suckle.

Whilst mortality is rare, orf can be fatal in stressed or immunosuppressed animals. Fatalities from orf amongst animals in over-crowded conditions or animals being transported over long distances have been reported (Gumbrell and McGregor, 1997). Orf occurs wherever sheep and goats are raised and can be transmitted to other susceptible animals either in the wild, in captivity or as farmed domesticated species

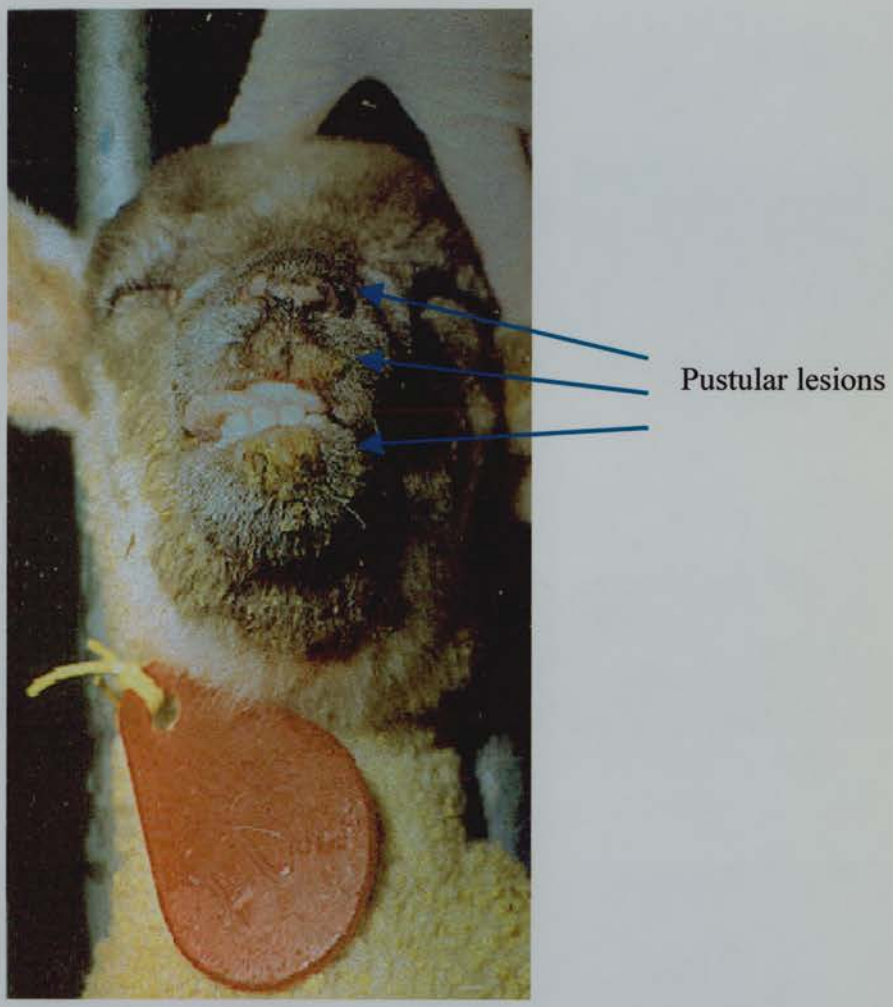

Fig. 1.1 Orf in a young lamb. Lesions around the mouth and nares are indicated.

(Robinson, 1983; Robinson and Balassu, 1981). Other animal species that can contract orf include bighorn sheep, chamois, thar ibex, camels and alpaca (Azwai *et al*, 1995; Dashtseren *et al*, 1984; Hedger *et al*, 1980; Mercer *et al*, 1997a).

Kummeneje and Krogrsrud (1979) have reported outbreaks of orf in herds of musk ox and more recently, Palatsi *et al* (1993) have reported an orf epidemic that affected reindeer in Norway. In reindeer the disease is generally mild. However in musk ox a high mortality rate has been recorded particularly in calves and adult males, with females apparently being more resistant (Mathiesen *et al.* 1985, Moens *et al.* 1990). There is no clear evidence that cattle can contract orf although the condition bovine papular stomatitis is clinically similar (Nagington *et al*, 1967; Czerny *et al.* 1994; Mercer *et al.* 1997a). When kept together with infected sheep, cattle do not become affected (Aynaud, 1923; Darbyshire and Huck, 1966). Horses, pigs, dogs and those laboratory animals in common use (e.g. rabbits, rats, mice) appear to be resistant to the disease (Abdulassam, 1957; Darbyshire, 1961; Buttner *et al*, 1990).

As a zoonotic disease, orf is recognised as an occupational hazard amongst those whose livelihood is associated with sheep and goats, such as veterinary surgeons, farm workers, slaughtermen, butchers and meat process workers (Purdy, 1955; Moore, 1973; Arnaud *et al*, 1986; Groves *et al,* 1991; Yirrell and Vestey, 1994; Buchan, 1996; Mourtada *et al,* 2000).

1.1.2. Epidemiology

Orf virus enters its animal host via broken, or scarified skin, probably caused by grazing in rough pastures or by abrasions from fencing material contaminated with

virus. Thus natural infections are normally localised around the mouth and nares or around the lower limbs. Orf virus-infected animals are also susceptible to secondary infections with bacteria, fungi or blow- fly larvae (Reid, 1991). Complications such as mastitis and 'strawberry footrot' can arise as a result of opportunistic *Staphylococcus aureus* and *Dermatophilus congolensis* infections respectively. In addition, the development of venereal disease with subsequent disruption of breeding and prolonged lambing has also been reported as a consequence of orf virus infection (Reid, 1991; Reid, 1999).

Orf virus is shed (with scabs) into the environment as infectious scab material. It is hardy and will persist in dust and wool that can act as the source of new infections (Glover, 1928; Boughton and Hardy, 1935). Once pasture becomes contaminated, it is difficult to eradicate since the shed scabs from infected animals contribute to the environmental reservoir of infection. However, it is unlikely that the outbreaks observed in the spring in the U.K. are due to over-wintered virus since wet weather conditions found in Northern Europe are not favourable for virus survival and infectivity (McKeever and Reid, 1986a). Orf virus infectivity is also reduced by exposure to ultraviolet radiation (Sawhney and Toschkov, 1972).

Orf virus has been found to persist in previously clean animal accommodation and to survive between outbreaks. It is suggested that this persistence in infected premises is due to the long-term survival of the virus particularly in dry scab form (Glover, 1928; Livingston and Hardy, 1960; Leavell *et al*, 1968). The route by which orf virus is introduced into clean premises is not clear although Gumbrell and McGregor (1997), Greig *et al* (1984) and McKeever (1986) suggest that animals suffering from sub-clinical orf virus infections may act as carriers. This mechanism

of orf virus spread was further established at the Moredun Research Institute when a group of ewes with no clinical orf lesions were housed with lambs that had been kept in isolation. The lambs experienced a severe outbreak of orf resulting from exposure to the ewes (Nettleton *et al*, 1996a).

1.1.3. Clinical course and pathology

The clinical manifestations of orf are variable; in many cases the infection is probably subclinical and goes undetected and at the other end of the spectrum, it may be severe with mortality approaching 80% (Darbyshire, 1961). In natural orf virus infections, the orf lesions produced are restricted to epithelium and oral mucosa, although some cases have been reported of orf virus affecting other tissues of the body e.g. the ocular conjunctiva (Freeman *et al,* 1984). Fever is not normally associated with orf virus infection (McKeever and Reid, 1986b; McKeever *et al,* 1988).

In spite of a vigorous cutaneous immune and inflammatory response, characteristic of an anti-viral response (Haig *et al,* 1997), the virus can repeatedly re-infect sheep. The protection against re-infections is incomplete and of short duration, and vaccination with live attenuated virus is of limited use (Chand *et al,* 1994; Mercer *et al*, 1997b). The route of orf virus infection is via damaged or abraded skin where the virus replicates in the regenerating epidermal layer underlying the damaged epidermis. This freshly regenerated epidermis derives from the basal epidermal cells of the wool follicles (McKeever *et al*, 1988).

In lambs experimentally infected with virus, orf is normally induced by application of virus to scarified skin (Wheeler and Cawley, 1956; Kluge *et al,* 1972).

Generally, in both primary infections and reinfections, the disease progresses from erythema around the sites of scarification, to lesions that develop in four stages from papule, vesicle, pustule and finally to scab. The area of lesion can often encompass 2-4 cm^2 of skin that surrounds the initial site of infection due to the development of secondary papules, vesicles and pustules.

The duration of orf virus infection appears to be self-limiting. In a primary infection of experimental animals, the progression to scab formation occurs within 7-10 days with resolution within 4-6 weeks. Secondary infections are normally less severe and of shorter duration. Scabs are formed within 3-4 days and shed by 14 days (Robinson, 1983; McKeever *et al,* 1988).

Cutaneous lesions of naturally-occurring orf in 7-10 day old lambs were observed to develop through four clinically progressive stages (McKeever *et al,* 1988; Bassioukas *et al,* 1993; Lober *et al,* 1983; McElroy, 1997). The initial papular stage (Stage 1, duration 5-7 days,) gave rise to a stage where the papule became covered with a thin newly-formed scab (Stage 2, duration 4-5 days). The papules subsequently developed a thick scab that was firmly attached and interdigitated with the proliferating epidermis (Stage3, duration 5-7 days). Finally the regressing lesions were covered with a desquamating scab (Stage 4, duration 5-13 days) and healing was completed by the formation of a third epidermis derived from the deeper portion of the wool follicles. Scabs were shed without scarring. Reinfections with orf virus exhibited accelerated healing times (Stage 1 duration: 1-2 days; Stage 2 duration 2-3 days; Stage 3 duration: 2-4 days; Stage 4 duration 3-8 days.) (Jenkinson *et al*, 1990b; Haig *et al*, 1997; Haig and Mercer, 1998; McElroy, 1997).

1.1.4. Persistent orf

Persistent orf is a condition affecting individual sheep in a flock that often results in death of the animal. Affected sheep have extensive and proliferative orf lesions that are often located around the genitalia and ears, and show no evidence of regression at least two months after orf lesions in their companions in the same flock have resolved (Darbyshire, 1961: McKeever, 1984). Persistent orf lesions exhibit the histopathological characteristics of Stage 2 lesions (papules with a thin scab) in normally responding animals with orf but there is a dramatic increase in the degree of epidermal proliferation and an extensive congestion and neo-vascularisation of the superficial dermis.

Highly proliferative lesions have only been observed in natural infections. These lesions form dense papillomatous outgrowths that, together with secondary complications, become ulcerative and necrotic without scab formation (Glover, 1928; Selbie, 1944; Darbyshire 1961).

1.1.5. Vaccination

Vaccines for orf virus are available that consist of live unattenuated virus passaged in sheep or in tissue culture (Pye, 1990; Nettleton *et al*, 1996b). Currently two vaccines are licensed for use in the United Kingdom. These are Scabivax produced by Schering-Plough Animal Health (Uxbridge, U.K.) and Vaxall Orf produced by Ford Dodge Animal Health (Kansas City, USA). Since even natural infection does not induce lasting protection against reinfection, these vaccines are of limited use. After vaccination, a typical orf lesion develops at the site of inoculation but subsequent reinfections that occur tend to be milder with faster resolution times.

Vaccines can therefore be useful (in the face of an outbreak) as a means of artificially infecting all animals and ensuring that they experience only mild disease. Vaccination also reduces the severity of the disease at the crucial early stage of lamb development and helps prevent infection of the udder of the nursing ewe, thus reducing production losses that are associated with natural orf virus infections around the mouth of suckling lambs.

However, the virus in scab material that is produced by vaccination can contaminate the environment in the same way as a natural infection and can contribute to the perpetuation of the disease. A mutant strain of orf virus, D1701, has been identified that has undergone gene loss and translocation particularly at the left hand terminus of the genome (Cottone *et al,* 1998). Experimental infection with D1701 virus results in very mild lesions with little or no scab formation (Buttner *et al*,1995). In Germany, D1701 has been approved and licensed for use as a live vaccine. D1701, as with other tissue culture adapted strains of orf virus such as orf11 does not offer the same level of protection against re-infection that is produced by vaccination with more virulent strains (McInnes *et al*, in press).

1.1.6. Human orf

Around 50 cases of human orf a year were reported in the United Kingdom during the period 1991 to 1993 (Health and Safety Executive, 1993). These are likely to be the most serious cases and under-reporting is probable. Paiba *et al* (1999) estimated, from a random serological survey of farmworkers in three areas of England, that the incidence of orf virus infection for the year 1991/92 was 2.8 per cent. Human infection rates have also been estimated at up to 34% in at-risk farming communities

in Wales (Buchan, 1996).

Orf virus is transmitted to man from infected animals, animal products or fomites. Transmission of orf virus from person to person has also been reported (Lang 1962). The risk of orf virus infection is increased if wounds or abrasions are present on the hands and arms (Pask *et al*,1951). Most commonly, orf affects the skin of the fingers and thumbs and sometimes the arms and face. The lesion(s) produced are clinically similar to those resulting from exposure to milker's nodule virus (pseudocowpox virus), the parapoxvirus of cattle (Nagington *et al*, 1965; Bowman *et al*, 1981) and a distinction is usually made on the grounds of the likely animal source.

Although several lesions may be present, single lesions are more common (Fig. 1.2). These are raised, circular or oval and 0.5-1.5 cm in diameter with a depressed yellow centre, a raised white edge and a surrounding red inflammed zone. Often this is accompanied by swelling of the regional lymph nodes and pyrexia due usually to secondary bacterial infection. In general lesions resolve within 4-8 weeks (Nagington *et al*, 1965; Leavell *et al,* 1968; Arnaud *et al*,1986; Johannessen *et al,* 1975; Gill *et al,* 1990).

Orf virus infection of man produces lesions that are not as well characterised as those observed in sheep but some clinical and histological differences have been suggested (Yirrell and Vestey, 1994). The central umbilication and vascular proliferation characteristic of the human lesion is less obvious in the ovine lesion whilst in sheep the most significant feature is a massive accumulation of MHC class II-positive dendritic cells (see Section 1.3.3.). However this accumulation of dendritic cells has not been assayed for in man. In addition, in sheep the incubation period is considerably shorter (2-4 days) than that for man (3-14 days). Yirrell *et al*

Fig 1.2 Human orf.
Raised pustular lesion on a hand.

(1994a) suggest that this difference in incubation times may significantly affect the nature of the host immune response.

Although orf virus infection of sheep fails to provide lasting protection, in humans the situation is less clear. Immunity to orf virus has been reported to be lifelong (Buchan, 1996; Chahidi *et al,* 1993; Hall,1976; Lo and Mathisen, 1996; Pask *et al,* 1951). Nevertheless there is some evidence from surveys of farmers and farmworkers in England that re-infections and subsequent lesion development do re-occur (Tan *et al*, 1991; Gourreau *et al,* 1986; Paiba *et al*, 1999)

1.2. Orf virus

1.2.1. Classification

The causative agent of orf is orf virus, the prototypical member of the parapoxviruses that belong to the Poxvirus family (Table 1.1). Other members of the genus Parapoxvirus include the closely related bovine papular stomatitis virus, pseudocowpox virus and a parapoxvirus that infects deer (Lance *et al,* 1983; Robinson and Mercer, 1995). Candidate members of the genus include poxviruses that infect camels (Dashtseren *et al*, 1984), seals (Munro *et al*, 1988) and red squirrels (Sainsbury and Ward, 1996).

One feature of the parapoxviruses is that whereas as individuals they exhibit a narrow host range, generally one or two related species, they all appear to be capable of infecting man. There is one possible exception, the deer parapoxvirus, where transmission to man has not been recorded (Mercer *et al*, 1997a).

Subfamily	Genus	Representative Member(s)
Chordopoxvirinae	Avipoxvirus	fowlpox virus
	Capripoxvirus	sheepox virus
	Leporipoxvirus	myxoma virus
	Molluscipoxvirus	molluscum contagiosum
	Orthopoxvirus	vaccinia virus, cowpox virus
	Parapoxvirus	orf virus
		bovine papular stomatitis virus
		pseudocowpox virus
		deer parapox virus
	Suipoxvirus	swinepox virus
	Yatapoxvirus	Yaba monkey tumour virus
Entomopoxvirinae	Entomopoxvirus A	Melolontha melolontha entomopoxvirus
	Entomopoxvirus B	Amsacta moorei entomopoxvirus
	Entomopoxvirus C	Chironomus luridus entomopoxvirus

Table 1.1 Taxonomy of the Poxvirus Family.

1.2.2. Structure

Orf virus exhibits morphological similarities with other poxviruses such as vaccinia virus (Nagington and Horne, 1962; Hiramatsu *et al*, 1999). Parapoxviruses may be distinguished from other poxvirus genera by two major features: firstly, the virus particles are more cylindrical and consequently have a higher axial ratio (length:width) and secondly the outer tubular coat of the viral particles is arranged in a regular basket-weave pattern that resembles a 'ball of yarn' and which is unlike the random arrangement exhibited by the orthopoxviruses (Fig. 1.3) (Nagington and Horne, 1962; Kluge *et al,* 1972; Okada *et al,* 1984; Hiramatsu *et al,* 1999). The enveloped virions of orf virus that are released from infected cells or in scabs are ovoid in shape and on average 260 nm long by 160 nm wide (Abdulassam and Cosslet, 1957; Nagington and Horne, 1962; Romero-Mercado *et al*, 1973). The virus coat consists of an inner and outer envelope. An additional membrane is observed in tissue culture isolates of orf virus that appears similar to the outer membrane of vaccinia virus and is thought to be derived from the host cell Golgi apparatus. (Dubochet *et al,* 1994; McElroy, 1997; Moore *et al*, 1977). Analysis of negatively stained orf virus particles by electron microscopy reveals two forms; the mulberry (M) form, in which the outer tubular filaments are highlighted or the clear (C) form, where the capsule of the virus is stained (Balassu and Robinson, 1987; Nagington *et al*, 1964; Rosliakov, 1972; Seifert and Saito, 1977).

Orf virus exhibits a similar internal structure to other poxviruses with a tubular S-shaped construction of nucleoprotein surrounded by a lipoprotein envelope (Nagington *et al,* 1964; Nagington and Horne, 1962; Harkness *et al*, 1977; Loubet.

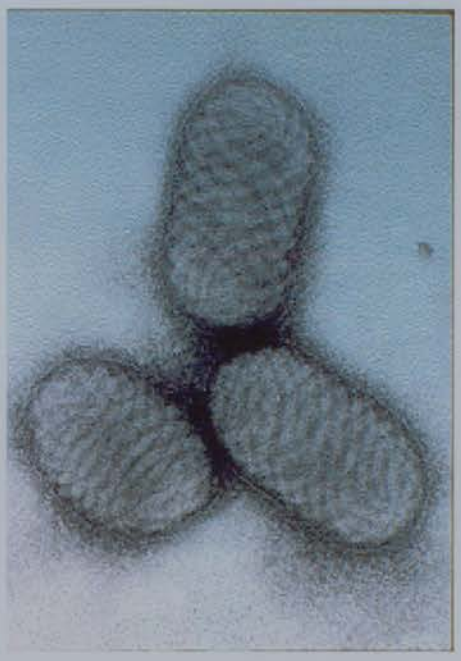

Fig. 1.3 Electronmicrograph of orf virus particles.
The 'ball of yarn' morphology of the virus coat with its outer tubular filaments is characteristic of the 'M' form.
x 80,000.

et al, 1980; Mitchner, 1969; Seifert and Saito, 1977). The viral core is biconcave with two lateral bodies (that are lens-shaped) and contains a folded nucleoprotein thread of linear double-stranded DNA of 140 kb in size (see infectious intracellular virion in Fig. 1.5) (Onwuka *et al,* 1995)

1.2.3. Replication

Orf virus, like other poxviruses, undergoes the process of viral replication and virion assembly exclusively in the cytoplasm of the host cell (Moss, 1996; Onwuka *et al*, 1995; Moyer and Graves, 1981). The genome of these large DNA viruses contains many genes essential for the intracellular phase of their life cycle and which are expressed in a well ordered sequence. Early genes encode factors that regulate the transcription of intermediate genes that in turn regulate the expression of late viral genes (Moss 1996).

Unlike the orthopoxviruses which have been extensively studied, knowledge of the replication cycle of the parapoxviruses is not so comprehensive. Study of the viral replication cycle in *in vivo* infections is restricted by the difficulty of ensuring synchronous infection of target cells. *In vitro* cell infection and virus ultrastructural studies have been developed to overcome this difficulty of non-synchronous infection on the growth cycle of orf virus (Balassu and Robinson, 1987; Hessami *et al*, 1979; Onwuka *et al,* 1995; Pospischil and Bachmann, 1980). The cycle of replication of orf virus in cultured cells can be divided into three phases, an entry phase, an eclipse phase and a stage of morphogenesis and virus release (Fig. 1.4) (Onwuka *et al*, 1995).

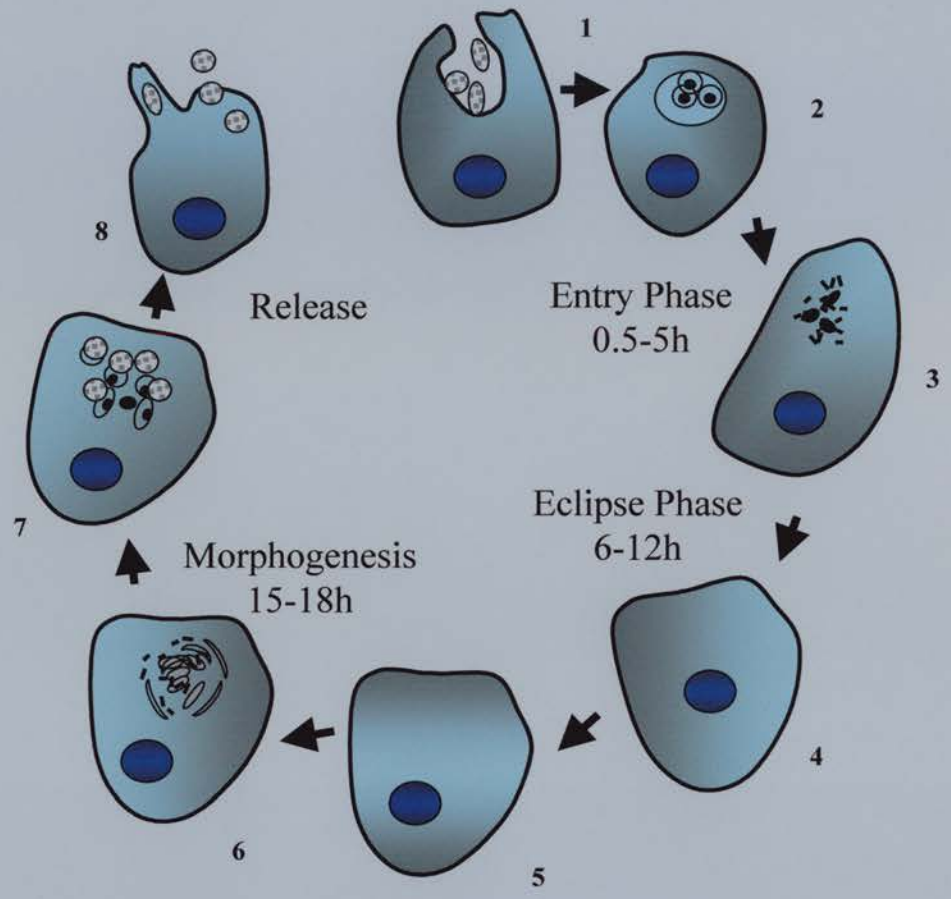

Fig 1.4 Diagramatic representation of the orf virus replication cycle *in vitro* (adapted from Onwuka et al,1995).
1.) Entry of virion(s) possibly by phagocytosis/pinocytosis. 2.) Virus particles retained within vesicles. 3.) Vesicle membranes are lost and the virus particles uncoat. 4.) The eclipse phase when no virus is detected. 5.) The formation of electron dense zones or viroplasm where the maturation of progeny virions takes place 6.) and 7.) Mature virions migrate to the periphery of the viroplasm prior to release. 8.) Release of mature virions either by budding, exocytosis or cell disruption.

i). Entry of the virus

Orf virus infection of an *in vitro* cell population (e.g. fetal lamb skin fibroblasts or fetal lamb kidney cells) originates with the entry of the virus into cells within 5 hours after addition to cultures (Onwuka *et al*, 1995). Internalisation of the virus occurs probably by phagocytosis/pinocytosis whereby the cell extends pseudopodia that surround the virus particles and produce, within the cytoplasm, membrane-bound vesicles enclosing the virions. There is no evidence that, in the entry of orf virus, the viral membrane fuses with that of the cell via some as yet unidentified cell surface receptor as reported for other poxviruses (Armstrong *et al*, 1973; Hsiao *et al*, 1999; Janeczko *et al,* 1987; Payne and Norrby, 1978; Smith and Vanderplasschen, 1998). As the cell vesicles move deeper into the cytoplasm, the vesicle membrane is lost and the virions are released into the cytoplasm where they uncoat. Naked (uncoated) virions have not been observed and the factors that control the uncoating process have yet to be determined. It is suggested that the disintegration of the outer envelope is followed by release of the viral core which subsequently disaggregates to free the viral DNA (Onwuka *et al* 1995).

Evidence from vaccinia virus studies suggest that prior to the second uncoating step, the early transcription system packaged within the virus core initiates the synthesis of mRNA (Kates and McAuslan, 1967). RNA/DNA hybridisation studies have shown that approximately half of the vaccinia virus genome has been transcribed prior to DNA replication (Beaud, 1995; Golini and Kates, 1984; Golini and Kates, 1985). The early genes encode proteins involved in viral DNA replication, intermediate gene expression and virus–host interactions (Moss 1996).

ii). The eclipse phase

The eclipse phase is characterised by the total absence of visible virus within the infected cells and lasts for 8-10 hours after completion of the entry phase. It is suggested that the virus exists as strands of DNA that may well be undergoing replication during this phase (Onwuka *et al* 1995).

iii). Viral morphogenesis and release

The third phase of the orf virus cycle begins between 10 h and 12 h after infection with the appearance of viroplasm. This constitutes the site of new virus assembly and corresponds to the B-type inclusion bodies that are observed in cells infected with poxviruses (Hollos and Lovas, 1968; Kluge *et al,* 1972; Okada and Fujimoto, 1975; Sawhney and Toschkov, 1972; Yeh and Soltani, 1974). Viroplasm occurs free in the cytoplasm without an encircling membrane. Several foci of viroplasm have been detected in infected cells and may reflect a multiple infection with orf virus as seen in infected sheep epidermal cells (Kluge *et al*, 1972; Onwuka *et al* 1995).

In the developing stages of orf virus morphogenesis, the virus particles move from the centre of the viroplasm to the periphery. The absence of rough endoplasmic reticulum and polysomes within the viroplasm suggest that, as for vaccinia virus (Morgan 1976), the late proteins are synthesised elsewhere in the cell and transported to the viral assembly site. In later stages of virus infection, viral DNA and the RNA complex responsible for the transcription of early genes, are packaged into viral particles. The virus is then packaged in a double membrane and will be retained within the cytoplasm until cytolysis is induced. This is the intracellular mature virion (IMV). An alternative form of infectious virus, the extracellular enveloped virion (EEV), has also been reported. EEVs are virus particles that have acquired two

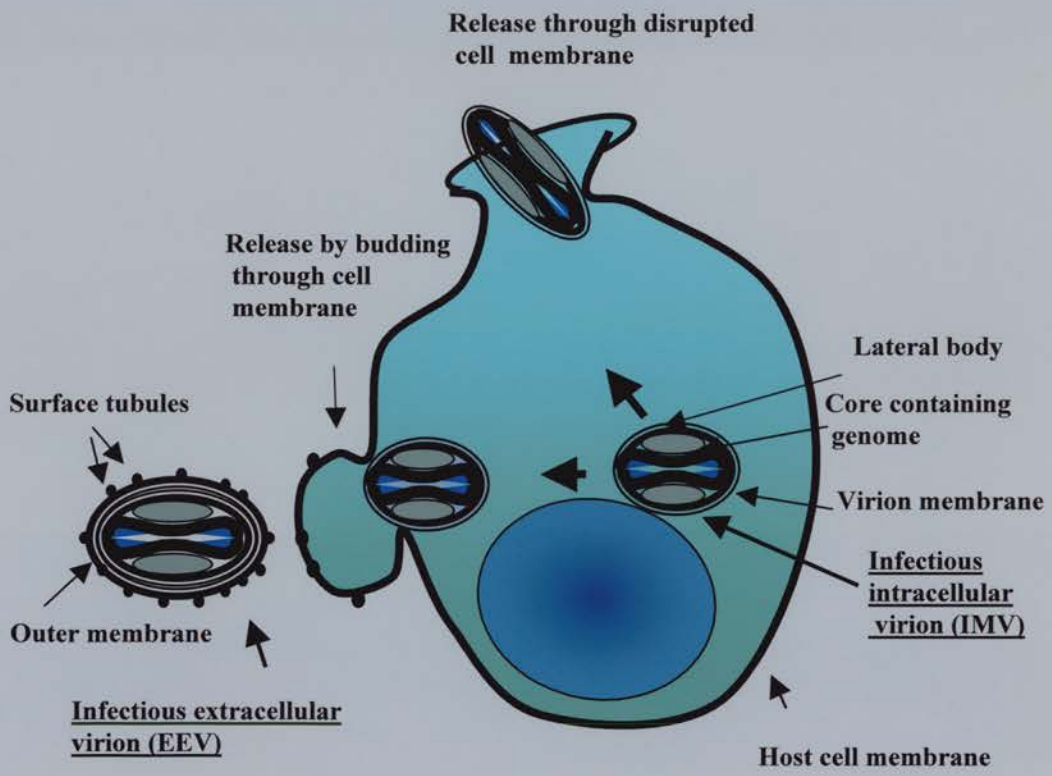

Fig. 1.5 Release of infectious orf virus particles.

A diagrammatic representation of the structure of both EEV and IMV forms of infectious orf virus particles and their release as suggested by Onwuka et al (1995). The release of virions can occur by exocytosis through the cell membrane or as a result of cell disruption.

additional membranes and can fuse with the plasma membrane. Following the loss of the outermost membrane, EEVs can be released from the cell (Fig 1.5) (Kluge *et al,* 1972; Rosenbusch and Reed, 1982; Onwuka *et al*, 1995). Mature virions appear at the cell membrane either freely or contained within vesicles with a bilaminar membrane. Microfibrils of the cytoskeleton, the Golgi apparatus and rough endoplasmic reticulum are thought to be involved in transport of the virions within the infected cell (Florkiewicz *et al,* 1983; Morgan, 1976; Ward and Moss, 2000; Onwuka *et al,* 1995). Release of the virions appears to occur by three mechanisms. Firstly by the ultimate disruption of the infected cell, secondly by the release of the vesicles through exocytosis or finally, by the enclosure of individual virions within microvilli which are pinched off from the cell. Although this latter process whereby the virions bud from the infected cell is common to vaccinia virus release, it has not been observed during the release of orf virus virions, which instead appear to undergo virus-induced exocytosis (Hiramatsu *et al,* 1999).

The duration of the orf virus cycle is considered to be 15-16 hours *in vivo* (Balassu and Robinson, 1987; Hessami *et al,* 1979; Martinez-Pomares *et al*, 1995).

1.2.4. The genome

Orf virions contain one molecule of linear double stranded DNA with a total genome length of approximately140 kb. In common with the DNA of the orthopoxviruses, orf virus DNA is cross-linked at each terminus by 'hair-pin' loops to form a covalently continuous polynucleotide chain (Baroudy *et al*, 1982a and b) The termini consist of inverted terminal sequences which are tandemly repeated, internally reiterated and repeated at the two ends of the genome (Fraser *et al,* 1990).

The lengths of these inverted, terminal-repeat sequences (ITR) can vary within a genus.

The genomes of the different poxviruses are organised in a similar fashion with terminal regions of variable DNA sequence flanked by a conserved central region (Fig. 1.6) (Archard, 1983; Mackett and Archard, 1979; Esposito and Knight, 1985; Pickup *et al,* 1982). The genes contained in the central region are for the most part essential for viral replication and the assembly of new viral particles while 'non-essential' genes in this respect are concentrated in the terminal regions. Some of these genes appear to encode proteins associated with virulence and pathogenesis (Moss, 1996; Alcami and Koszinowski, 2000; Smith, 1999; McFadden *et al*, 1998). Parapoxviruses differ from other poxviruses in possessing DNA with a high G+C content (Wittek *et al,* 1979). In comparing orf virus with vaccinia virus, Mercer *et al* (1997a) reported guanine and cytosine (G+C) values of 65% and 35% respectively. Accordingly the orf virus genome does not cross-hybridise with those of the orthopoxviruses. However a number of genes mapped to the orf virus genome have homologues in vaccinia virus (Fig. 1.6). Genomic alignment of both orf virus and vaccinia virus reveals a conserved core of approximately 88 kb from 15 kb to 103 kb in the orf virus genome. This region encodes homologues of vaccinia virus genes and proteins as identified from DNA and predicted amino acid sequences and that map to the same relative positions as their vaccinia virus counterparts. Some of these orf virus DNA homologues of vaccinia virus DNA have been studied in some depth and include;

1.) A 3.3 kb fragment mapped to the centre of the orf virus genome that contains 3 open reading frames (F2L, F3R and F4R) (Fig. 1.6) (Fleming *et al,* 1993) that are

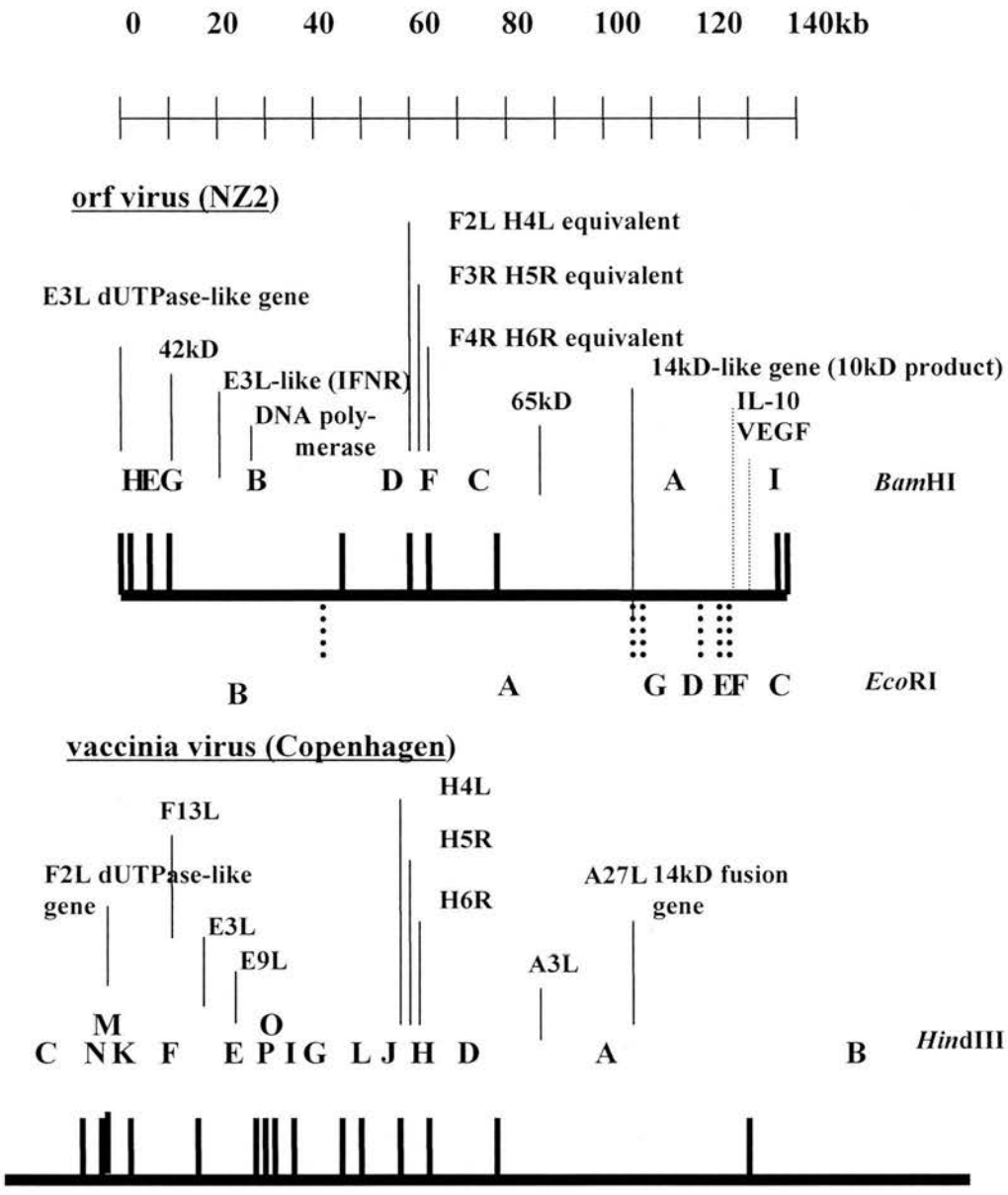

Fig. 1.6 Alignment of the orf virus and vaccinia virus genomes (Fleming *et al*,1993).
The two horizontal heavy lines represent the genomes of the NZ2 strain of orf virus (upper) and the Copenhagen strain of vaccinia virus (lower). Marked on each genome are the locations of restriction enzyme cleavage sites *Bam*HI (solid vertical lines) and *Eco*RI (dotted vertical lines) for orf virus and *Hin*dIII (solid vertical lines) for vaccinia virus and the location of homologous genes as outlined in the text. The position of the genes encoding the orf virus homologues of mammalian IL-10 and vascular endothelial growth factor (VEGF) are also marked on the orf virus genome (dashed lines).

homologous to the vaccinia virus genes H4L (RNA polymerase-associated protein RAP 94), H5R (35 kD virion envelope antigen) and H6R (topoisomerase) respectively (Rosel and Moss, 1985; Goebel *et al,* 1990). The DNA topoisomerase encoded for by H6R appears to be highly conserved among the genera of the vertebrate poxviruses (Moss, 1996).

2.) Orf virus genes that encode structural proteins of 42 kD (Fleming *et al*, 1993, Sullivan *et al,* 1994), 65 kD (Fig.1.6) (Sullivan *et al,* 1995) and 10 kD (Fig.1.6) (Housawi *et al*, 1998) that are homologous to the vaccinia virus proteins encoded by the genes F13L (Blasco and Moss, 1991), A3L (Rosel and Moss, 1985) and A27L (Rodriguez and Esteban, 1987, Gong *et al,* 1990) respectively. The10 kD peptide has been shown to share a 31% amino acid identity with a 14 kD protein, encoded by the A27L gene of vaccinia virus (Fleming *et al,* 1993; Mercer *et al*, 1997a). Whilst the 14 kD protein is associated with the fusion of the vaccinia virus particle to its target cell (Gong *et al*, 1990: Vasquez and Esteban, 1999), there is no evidence that the orf virus 10 kD protein has similar function.

3.) A homologue of the vaccinia virus interferon-resistance gene E3L, called interferon resistance gene (IFNR) (Fig. 1.6) (McInnes *et al,* 1998).

4.) A dUTPase like gene, homologous to the F2L gene of vaccinia virus, 5 kb from the left end of the genome (Fig. 1.6) (Fraser *et al,* 1990)

5.) A DNA polymerase-like gene at position 26.4 kb from the left hand end (Fig. 1.6) homologous to the E9L gene of vaccinia virus (Mercer *et al,* 1997a).

In contrast, the major genetic differences between vaccinia virus and orf virus lie in the terminal regions of their genomes and are thought to contribute to the differences seen in their respective pathologies. In particular, a 20 kb region of DNA

at the right hand end of the orf virus genome has no counterpart in the genome of vaccinia virus (Mercer *et al,* 1997a). Two genes have been identified from this region to date (2000). One gene encodes a polypeptide with homology to mammalian vascular endothelial growth factor (VEGF) (Lyttle *et al,* 1994). The other, neighbouring gene encodes a homologue of mammalian IL-10 (Fleming *et al,* 1997). It is suggested that these genes may have been acquired from a mammalian host during the co-evolution of host and virus.

In tissue culture, orf virus (NZ2) has been reported to undergo genetic changes that involve the duplication and translocation of approximately 19.3 kb of DNA at the right-hand terminus to the left terminus (Fleming *et al*, 1995). This translocation results in the deletion of three orf virus genes from the left-hand terminus. The genes lost are; a homologue of the vaccinia virus F2L (a dUTPase) gene, a homologue of the vaccinia virus 5K gene and a gene encoding an ankyrin repeat protein (Fig. 1.7) (Sullivan *et al*, 1994). The tissue culture adapted isolates D1701 and orf 11 are also representative of orf virus variants with similar translocations and deletions, and like the NZ2 variant are reported to induce smaller lesions when compared with wild-type orf virus (Mcinnes *et al*, in press). Thus the deleted genes are considered to be non-essential to viral replication but may be associated with virulence *in vivo*.

1.3. The immune response to orf virus infection

1.3.1. The ovine immune system

The structure and function of the mammalian immune system is generally conserved in the sheep and other ruminants. There is apparent conservation of leukocyte surface molecules, the structure and function of cytokines, MHC

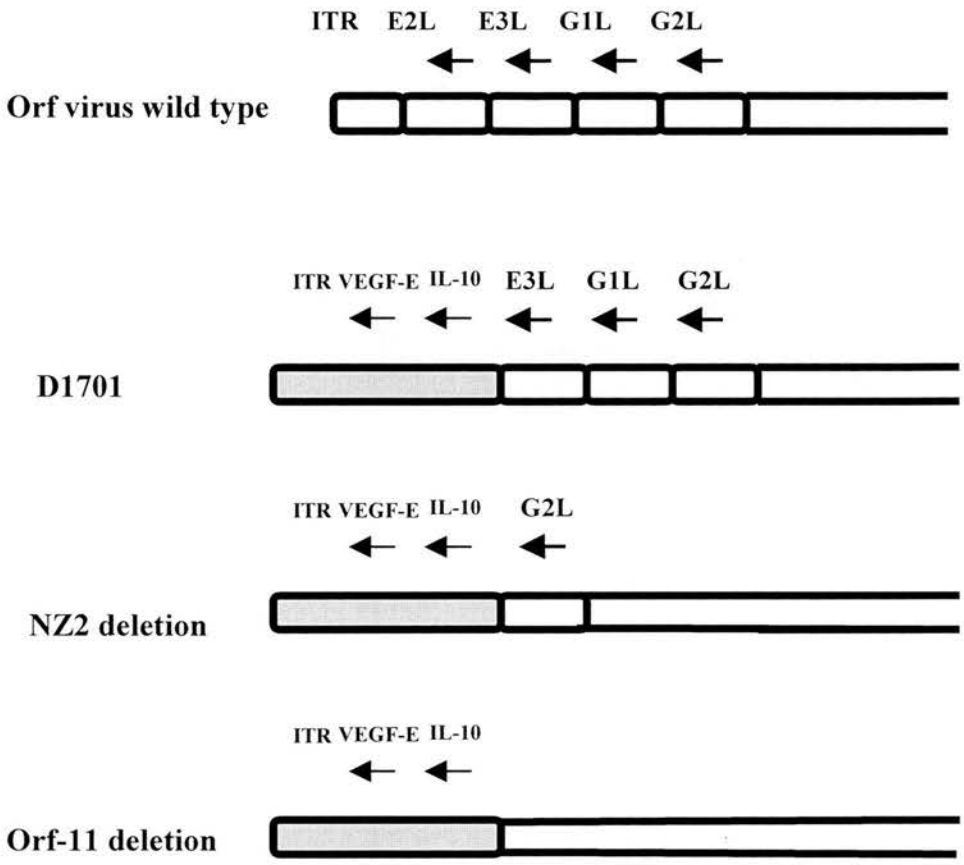

Fig 1.7 Non-essential gene loss and translocation at the left hand termini of attenuated strains of orf virus.
Each segmented strand shown above represents the left hand terminus of the genome for a different orf virus strain.
A 16.5 kb DNA fragment at the right hand terminus of the orf virus genome is duplicated and translocated to the the left hand end with the loss of one or more genes. This fragment (shaded) contains, among others, the genes that encode the homologues of VEGF and IL-10.
The deleted sequences encode the early transcribed genes, E2L, E3L, G1L and G2L. E2L encodes a peptide homologous to the 5 kD peptide of unknown origin in vaccinia virus. E3L is homologous to dUTPase encoded by the herpes viruses. G1L encodes a protein that contains 8 ankyrin-like repeat sequences and is of unknown function. G2L is homologous to the F11L gene of vaccinia virus which is also of unknown function (Fraser et al, 1990; Fleming et al, 1995).

organisation (except for sheep lacking primate MHC class II DQ2 genes whilst possessing MHC class II DY genes not found in rodents or man; Ballingal *et al*, 1992; Hopkins *et al*, 1986) and the complement cascade (Oswald *et al*, 1990). However, there are differences in γδ T cell population dynamics and B lymphogenesis between ruminants and rodents or man (Mackay *et al*, 1988; Griebel and Hein, 1996).

i). T cells

As in other species, sheep γδ T cells differ from αβ ($CD4^+$ and $CD8^+$) T cells by the expression and utilisation of a different set of T cell antigen receptor genes (γ and δ) and surface receptor molecules. Young ruminants differ from other mammals in having an unusually large number of γδ T cells, particularly in blood. In young sheep the γδ T cell population may account for up to 60% of peripheral blood mononuclear cells and is thought to provide early cover of non-MHC-restricted cellular immunity until a more mature αβ T- cell system becomes established (Hein and Mackay, 1991). As proposed in other species, a major function of γδ T cells in sheep is the immune surveillance of epithelial surfaces that include the intestinal epithelium and lamina propria (Mackay *et al*, 1989; Janeway *et al,* 1988). In sheep, γδ T cells are the predominant lymphoid population in skin surfaces that are not covered by wool (Mackay and Hein, 1989; Haig *et al*, 1999).

ii) Immunoglobulin repertoire

Sheep express IgM, IgG1, IgG2, IgA and IgE either as membrane-anchored B cell antigen receptors or as secreted antibodies (Beh *et al,* 1986). There is no evidence that sheep express IgD. The generation of the sheep Ig repertoire is unusual, in so far

as it occurs by a hypermutation process that appears to operate autonomously during B cell development in the follicles of the ileal Peyer's patch (Reynaud *et al,* 1995).

The sheep has proved extremely useful in the investigation into the physiology of the immune system (Hein, 1995). Lymphatic duct cannulation has provided direct access to a number of lymphoid micro-environments and can be used to investigate the interaction between viruses and the local host immune system *in vivo* (Yirrell *et al,* 1991; Haig *et al*, 1999).

1.3.2. The skin response to orf virus infection

In ovine skin, the host response to experimental infection (described in Section 2.6.) has been characterised histologically. Within the first 48h after a primary orf virus infection, an early influx of neutrophils into the region surrounding orf virus-infected epidermal cells was followed by an accumulation of MHC class II^+ dendritic cells, $\gamma\delta$ TCR^+ T cells, $CD4^+$ T cells, $CD8^+$ T cells and B cells. This cell influx was observed to peak between 9-15 days post infection and had returned to preinfection levels by day 30 (Jenkinson *et al,* 1990a; Jenkinson *et al,* 1992; Lear *et al*, 1996; Haig and Mercer, 1998). Throughout all four clinical stages of virus infection, the majority of infiltrating lymphocytes were T cells (Haig *et al* 1996a, McElroy 1997).

In Stage 1 lesions (the initial papular stage), $CD4^+$ T cells predominated but as the lesions aged and regressed (Stage 4), the number of $CD8^+$ T cells recruited to the lesion site during viral replication and in the afferent lymph draining the site of infection increased. The proportion of activated $CD8^+$ T cells in lymph and skin was determined by the expression of the tryptase serine protease, BLT esterase, that is associated with cytotoxicity (Haig *et al,* 1996b; McElroy, 1997). The number of $\gamma\delta$

TCR^+ T cells did not change significantly as the lesions aged.

In reinfections with orf virus, there was a parallel increase and decrease in the accumulation of T cells, B cells and dendritic cells with the time course of viral replication (Jenkinson *et al*, 1990c; Jenkinson *et al*, 1990a; Jenkinson *et al*, 1991; Jenkinson *et al,* 1992; McKeever *et al,* 1988; Lear, 1995; Lear *et al,* 1996). Experimentally-induced lesions were also smaller than those associated with the naturally-occurring disease. Virus antigen was not detectable 11 days post-challenge. The predominant lymphocyte subset obseved in the resolving phase of reinfection lesions was the $CD4^+$ T cell; these resolving lesions also contained significantly greater numbers of $\gamma\delta$ TCR^+ T cells than lesions in primary infections (McElroy, 1997; Haig *et al*, 1996d; Haig *et al*, 1997). The systemic depletion of different T cell subsets prior to infection using mouse monoclonal antibodies directed against specific cell subsets revealed that in animals depleted of $CD8^+$ T cells or $\gamma\delta$ TCR^+ T cells, lesion size and resolution times did not differ from those in the untreated infected control group, although there was some evidence that $CD8^+$ T cells may be involved in an early immune response to orf virus reinfection (Lloyd *et al,* 2000). However, those sheep, depleted of $CD4^+$ T cells, developed larger lesions that took longer to resolve. Accelerated healing times in reinfections indicates the development of a degree of immunity to orf virus. The greater numbers of $CD4^+$ and $\gamma\delta$ TCR^+ T lymphocytes in the rechallenge lesions compared to the primary lesions suggests that these cells may have a role in this resistance.

1.3.3. The dendritic cell response

MHC class II^+ dendritic cells are widely distributed throughout normal skin in

two locations, namely in the epidermis and in the dermis in the vicinity of the dermal structures e.g hair follicles, sweat glands and blood vessels (Jenkinson *et al*,1991; Lear, 1995; Lear *et al,* 1996). They are considered to constitute a population of specialised antigen processing and presenting cells responsible for the induction and maintenance of the immune response and may be involved in epidermal repair processes (Jenkinson *et al,* 1991). After orf virus infection a dense mass of closely associated MHC class II^+ dendritic cells develop in the dermis adjacent to the infected hair follicles and under and adjacent to infected degenerating epidermis (Fig. 1.8). These cells interconnect and appear to form a barrier around the site of infection with a network of processes interdigitating with the overlying epidermis (Jenkinson *et al,* 1990a; Jenkinson *et al*, 1991; Lear, 1995; Lear *et al*, 1996).

This dense accumulation of MHC class II^+ dendritic cells, a majority (>90%) of which are $CD1^-$, $CD11b^-$, $CD11c^-$ is representative of a minor dendritic cell population that is found in uninfected sheep skin (Lear, 1995; Lear *et al;* 1996). (The majority in normal skin are $CD1^+$). The origin and function of these cells which lack both the CD1 antigen of the antigen–capturing Langerhans cells of the epidermis or the CD11b/CD11c antigens of tissue macrophages, is not yet known. Although possible roles in skin repair, antigen processing and presentation and/or in containing the spread of the virus directly, have been put forward (Jenkinson *et al,* 1991; Haig *et al*, 1995; Haig *et al,* 1999; Haig and Mercer, 1998).

The control of different dendritic cell subsets and their function in host immunity appears to be regulated by different cytokines and cytokine combinations. Haig *et al* (1995) have shown that the intradermal injection of Tumour Necrosis Factor-alpha (TNF-α) and Granulocyte-Macrophage Colony Stimulating Factor (GM-CSF) in

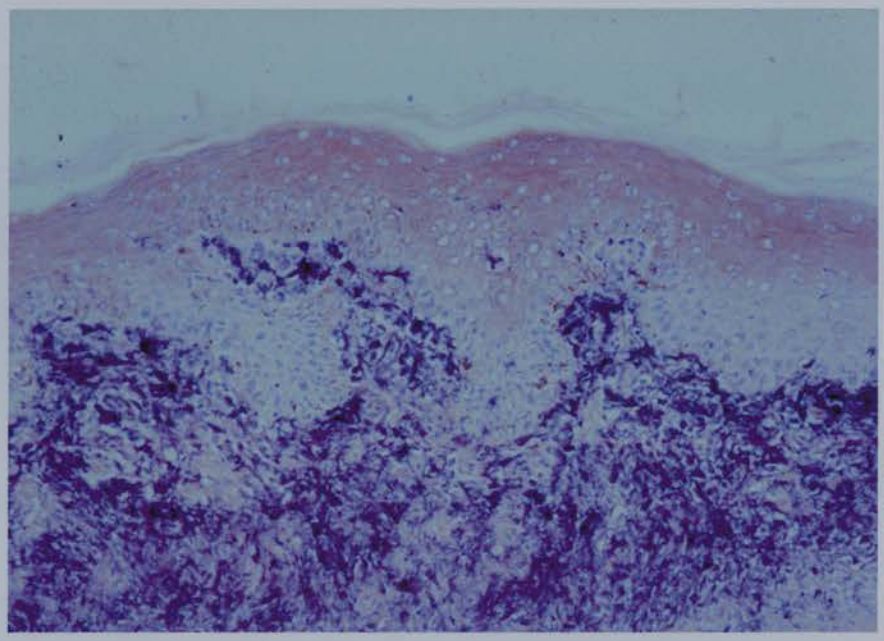

Fig 1.8 Immunohistolological analysis of an ovine orf lesion (Haig et al, 1997).
A paraffin-wax -embedded section (x 350) from a skin biopsy sample taken on day 5 following orf virus reinfection. Orf virus antigen (brown immunoperoxidase staining) is located by specific monoclonal antibody in the epidermal cells showing evidence of vacuolation.
Approximately 50% of MHC class II^+ cells (deep purple immunoperoxidase staining) accumulating under and adjacent to the virus-infected cells, were of dendritic morphology (Lear et al, 1996).

unchallenged sheep promoted the accumulation of MHC class II^+ $CD1^+$ and $CD1^-$ dendritic cells at the site of injection, whereas the injection of GM-CSF alone promoted the infiltration of MHC class II^+ $CD1^-$ dendritic cells. Both GM-CSF and TNF-α in concert are known to support the survival and proliferation of murine dendritic or Langerhans cells in culture and their development into potent T cell stimulators (Heufler *et al,* 1988a and b). Furthermore antigen-presenting sheep veiled dendritic cells found in afferent lymph survive *in vitro* provided TNF-α is present and will increase in number if GM-CSF and TNF-α are added together in cultures (Haig *et al*, 1995).

1.3.4. Lymph components of the immune response

It is possible to study the *in vivo* dynamics of the cellular immune response in terms of the production of antibodies and cytokines in afferent lymph draining the site of experimental orf virus reinfection (the prefemoral or popliteal lymph node drainage area) and efferent lymph exiting the draining node (reviewed by Haig *et al*, 1999). The measurements obtained can be compared with those from lymph cannulated from unchallenged sheep (Fig. 1.9) (McKeever and Reid, 1987; Yirrell *et al,* 1991; Bujdoso *et al,* 1989; Haig *et al,* 1999). Afferent lymph in unchallenged sheep contains $CD4^+$ T cells, $CD8^+$ T cells, γδ TCR^+ T cells, B cells and 5-15% of potent antigen-presenting veiled dendritic cells (Bujdoso *et al,* 1989; Mackay *et al*, 1989; Haig *et al,* 1999). Efferent lymph contains > 98% lymphocytes, the majority of which are $CD4^+$ T cells and B cells with fewer $CD8^+$ T cells and γδ TCR^+ T cells. Over 90% of these are derived from the blood filtering into the lymph node via high endothelial venules and exiting by the efferent ducts (Mackay *et al*, 1989; Bujdoso

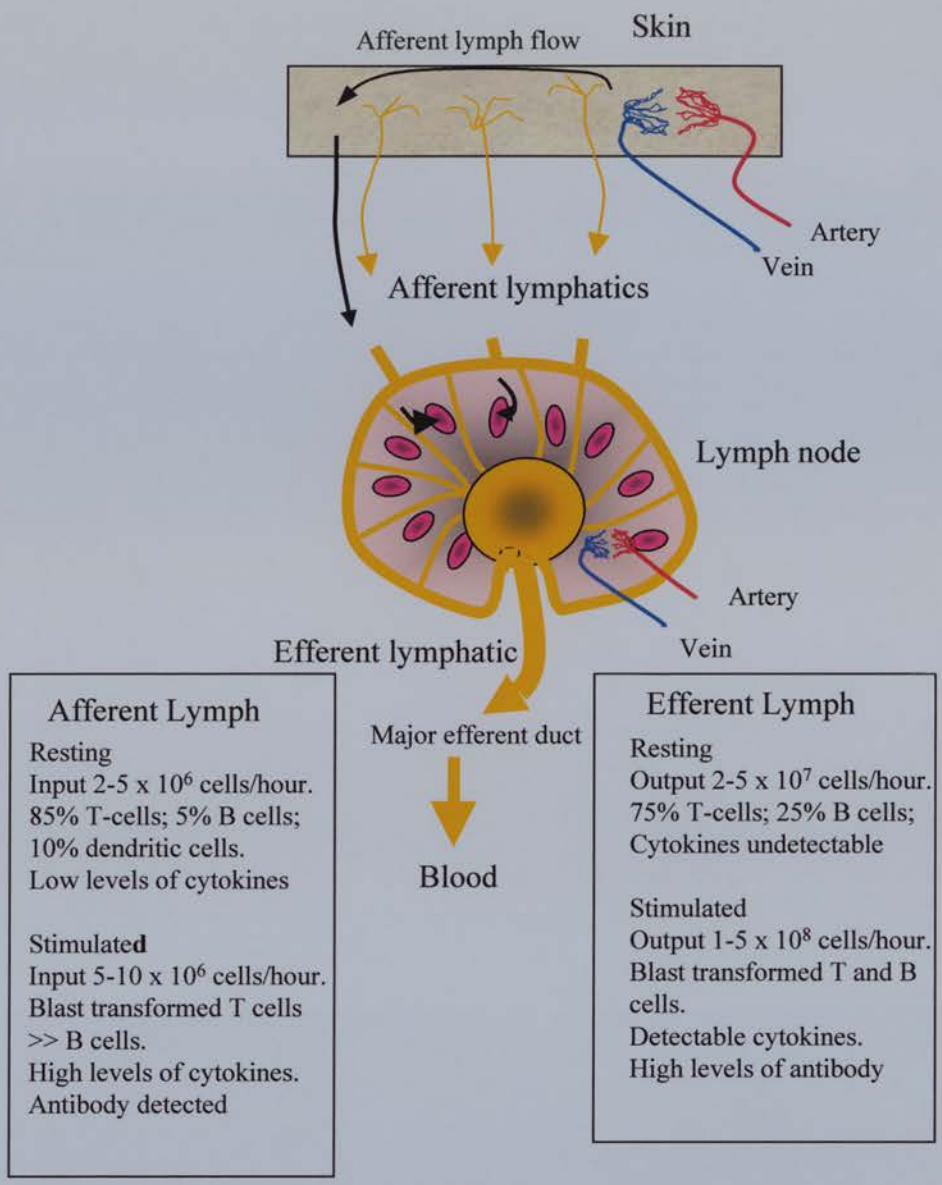

Fig. 1.9 Cellular composition and flow rates of afferent and efferent lymph circulating around a single skin-draining lymph node (Haig et al, 1999). Afferent lymph contains antigen presenting cells, T cells and a small proportion of B cells. Following orf virus challenge there is an increase in the frequency of lymphoblasts, particularly $CD4^+$ T cell blasts, antibodies can be detected and there is an increase in cytokine levels, particularly IL-2, IFNγ and GM-CSF. Furthermore afferent lymph cell input can triple. Efferent lymph contains >98% lymphocytes with a higher proportion of B cells and much higher flow and cell output rates than the input rates of afferent lymph.

Following infection, in efferent lymph there is often an initial shutdown of lymphocyte output, followed by a recruitment phase whereby lymphocyte output increases along with increased blood flow to the node. Efferent T and B lymphoblasts appear after this phase with B cell blasts and antibody produced within the lymph node. Finally with resolution, lymph flow rate and cellular composition return to pre-stimulation levels.

et al, 1989; Harp *et al*, 1988). The remaining 10% of efferent lymph lymphocytes are derived from within the lymph node or from afferent lymph (Hall and Morris, 1962).

Following control scarification of the skin there are no significant or only small changes in total cell output, lymphoblast transformation or the proportions of different cell types in afferent or efferent lymph (Haig *et al,* 1996a; Haig *et al,* 1999).

Following orf virus challenge, total cellular and lymphoblast output is biphasic in afferent and efferent lymph. The first peak response in both compartments was thought to reflect an immediate antigen specific immune memory reaction to orf virus antigen and the second to viral replication in the skin which occurs between 3 and 9 days post reinfection (Haig *et al,* 1996a and b). However, Haig *et al*, (1999) more recently have suggested that the delay between the observed lymphoblast responses to orf virus reinfection may be due to the effect of viral immunomodulators (see Section 1.4.). In contrast, challenge with UV-inactivated orf virus stimulates a delayed type hypersensitivity reaction in the skin and a single peak response in both lymph compartments (Haig *et al,* 1999)

In the infected animal, total and blast-transformed $CD4^+$ Tcell output precedes and exceeds that of $CD8^+$ T and B cells in both afferent and efferent lymph as was observed in the skin. $\gamma\delta$ TCR^+ T cells show only a slight increase early in the infection, between days 1-4. Antibody titres to orf virus antigens increase in both lymph compartments following challenge (Yirrell *et al,* 1989; Yirrell *et al*, 1991). Afferent lymph contains antigen-specific memory T cells that are able to respond rapidly to reinfection by blast transformation and cytokine production whilst efferent lymph cell output is delayed slightly by comparison. Effector cells in efferent lymph are recruited from the blood prior to activation within the node thus amplifying the

number of antigen specific T and B cells able to react with orf virus antigens in the skin (Haig *et al,* 1996a and b).

1.3.5. Cytokine production

The activation status of the skin and lymph following orf virus reinfection can be determined by analysis of skin and lymph samples for the presence of those cytokines that are involved in anti-viral immune responses.

Messenger RNA transcripts for the cytokines, IL-1β, IL-2, IL-3, TNF-α, GM-CSF and IFN-γ are detected in lesion biopsies taken from the skin of orf virus re-infected sheep. These transcripts are not detected in control sheep that undergo a mock scarification (Haig *et al,* 1996c). This spectrum of cytokines produced following orf virus challenge is indicative of a typical anti-viral immune and inflammatory response. (Haig *et al,* 1997; Seow *et al,* 1994).

Similarly, cytokine mRNA and/or cytokine expression can be analysed in both afferent and efferent lymph. Lymph plasma contains cytokine activity generated in the skin as well as from the cells contained in the lymph. Cytokines, namely IL-1β, IL-2, IL-8, TNF-α, GM-CSF, IFN-α and IFN-γ, are detected in afferent lymph during the course of orf virus infection (Haig *et al,* 1996c; Haig and Fleming, 1999; Haig and Mercer, 1998). IL-1β and IL-8 appear rapidly in both afferent and efferent lymph and in cell-free supernatants from cultures of afferent and efferent lymph cells within the first 24h following orf virus reinfection. This is consistent with the involvement of these cytokines in the early stages of both innate and specific immune responses (Haig *et al,* 1997; Seow *et al*, 1994). GM-CSF appears in afferent lymph also in the early stages of infection but after IL-1β and IL-8. GM-CSF and

IFN-γ peak in parallel with the lymphoblast output that peaks on days 4-6 and 8-12 in afferent lymph and days 5-8 and 10-14 in efferent lymph (Haig *et al,* 1997). In efferent lymph, Haig *et al* (1996a) suggest that those T cells subsets activated as a result of orf virus reinfection and expressing the $CD45RA^-$ phenotype of memory T cells, are the principal cellular sources of IL-2, IFN-γ and GM-CSF.

The importance of T cell and cytokine function in immunity to orf virus infection was highlighted in an experiment where 6 month old lambs were given a course of the immuno-suppressive drug cyclosporin-A (CSA) for a period of 9 days prior to and during re-infection. These animals developed severe lesions that were typical of a primary infection (Haig *et al,* 1996d). CSA is reported to inhibit the transcription of the genes for IL-2 and IFN-γ via a calcineurin-dependent mechanism (Schreiber and Crabtree, 1992). At the site of infection in the treated group, there was a marked reduction in the recruitment of $CD4^+$ T cells, $CD8^+$ T cells, B cells and dendritic cells. Futhermore the expression of IL-2 and IFN-γ witnessed on days 3 and 9 post challenge in the untreated group was not present in CSA-treated animals. However on cessation of treatment, there was a rapid influx of immune cells ($CD4^+$ T cells followed by dendritic cells, then B cells, then finally $CD8^+$ T cells) to the site of infection (Haig *et al,* 1996d).

1.3.6. Humoral response

Sheep infected with orf virus produce detectable antibodies specific for a small number (4 or 5) of immuno-dominant viral antigens (McKeever *et al,* 1987; Yirrell *et al,* 1989; Housawi *et al,* 1998). However none of these antibodies appears to neutralise virus or provide protection to virus challenge through passive transfer

(Yirrell *et al,* 1989; Mercer *et al*, 1997b). In spite of high antibody titres in the sera of infected sheep, the humoral response to orf virus infection is short lived (up to a few months post infection) (McKeever *et al,* 1987; Mercer *et al,* 1994). Passive antibody transfer studies imply a minor role if any for antibody in orf immunity (Buddle and Pulford, 1984; Mercer *et al,* 1997b). In contrast, Lloyd *et al* (2000) observed that in sheep with high orf virus–specific antibody titres at the time of infection, orf lesions healed faster than in sheep with low antibody levels. In persistent orf virus infections, McElroy (1997) suggests that in spite of a considerable antibody response characterised by high antibody titres against orf virus antigen, it is a defective T cell response marked by a local absence of T cells, particularly $CD4^+$ and $\gamma\delta TCR^+$ T cells, that prevents resolution of the infection.

Whilst it is still unclear whether antibodies play a minor role, $CD4^+$ T cells, $CD8^+$ T cells, and IFN-γ fulfil major roles in the protective immune response to orf virus infection (Haig and Mercer 1998). In spite of this, orf virus along with other parapoxviruses can repeatedly infect their hosts; a phenomenon that suggested a role for orf virus-encoded immuno-modulatory proteins.

1.4. Interference with host immunity

1.4.1. Poxvirus immuno-modulatory genes

Poxviruses, like other large DNA viruses, have evolved a number of mechanisms by which they are able to survive and replicate in a wide range of species in spite of an active host immune response. Orthopoxviruses, as represented by vaccinia virus and cowpox virus and the leporipoxviruses, as represented by myxoma virus, have been extensively investigated as models of poxvirus infections and of immune

evasion of the host response. (Reviewed by: Palumbo *et al,* 1994; Smith, 1993; Smith, 1999; Haig, 1998; McFadden *et al,* 1995; Alcami and Koszinowski, 2000). Through the co-evolution of poxvirus and host, host immuno-modulatory genes have been acquired and modified by the poxviruses in order to counteract many of the key components of the host immune response (Table 1.2).

1.4.2. Orf virus interaction with host immune responses

Unlike either the orthopoxviruses or leporipoxviruses, the parapoxviruses fail to develop a systemic infection and seldom give rise to fatal infections. However, an intriguing characteristic of parapoxviruses is the ability to reinfect their host despite an apparently typical anti-viral host immune response (Haig and Mercer, 1998). The orthopoxviruses (represented by vaccinia virus) have evolved multiple mechanisms that interfere with host anti-viral defences and although the parapoxviruses have not been analysed to the same degree, there are several possible reasons why orf virus may be able to survive host anti-viral mechanisms, particularly on reinfection.

Haig and Mercer (1998) suggest that since orf virus infects epidermal cells, the period before anti-viral cellular and molecular components reach the infected site may be sufficient time for limited viral replication. Furthermore, by infecting regenerating epidermal cells, the virus may not stimulate apoptosis to the same degree as in those cells not committed to proliferation. Lastly, the dense network of accumulating MHC class II^+ dendritic cells underlying the site of infection may act as a barrier to further spread of orf virus infection.

Finally, several immuno-modulatory genes have recently been identified in the terminal regions of the orf virus genome. The genes encode a viral vascular

Table 1.2 Poxvirus products that counteract host defences

Host response	Virus	Virus gene/product	Function/mechanism	Reference
Apoptosis	CPV, VV, MV	CrmA, SPI-2, Serp2	Secreted, show homology to serpins and inhibit the caspase cascade of serine proteases that induce apoptosis.	Zhou *et al*, 1997 (CrmA) Dobbelstein and Shenk 1996 (SPI-2)
	MCV	159L, 160L	Secreted, viral fas-ligand inhibitory proteins that block apoptosis induced by cascade triggered by fas-fas-ligand binding..	Senkevich *et al*, 1997 (159L, 160L)
	MV	M-T2 , M-T4 , MT5	Secreted, inhibits T cell-induced apoptosis	Alcami and Koszinowski, 2000 (review) Schreiber *et al*, 1997 (M-T2) Barry *et al*, 1997 (M-T4) Mossman *et al*, 1996 (M-T5)
	CPV	CHOhr		Ink *et al*, 1995 (CHOhr)
	MV	M11L	Inhibits apoptotic response in monocytes and macrophages.	Everett *et al*, 2000 (M11L)
	MCV	MC66	An anti-oxidant selenoprotein that scavenges reactive oxides, blocks H_2O_2 and UV-induced apoptosis.	Bugert *et al*, 1999 (MC66)
Inflammation	CPV, VV, MV	CrmA, B14R, Serp1	Serpins that inhibit proteolytic cleavage and activation of pro-inflammatory cytokine IL-1β.	Ray *et al*, 1992 (CrmA)
		B15R	Secreted, binds IL1-β and inhibits the induction of fever in response to viral infection.	Alcami and Smith, 1992 (B14R) Alcami and Smith, 1996 (B15R)
				Nash *et al*, 1997 (Serp1)
	ShFV, MV	T2, M-T2	Secreted TNF receptor homologues that block the pro-inflammatory cytokines TNF-α and TNF-β	Smith *et al*, 1991(T2) Sedger and McFadden, 1996 (M-T2)
	VV, VaV	A53R, G2R/G4R	Secreted, binds TNF-α with high affinity, also inhibits CTL-induced apoptosis.	Alcami *et al*, 1999 (A53R etc.)
	CPV	CrmB, CrmC , CrmD, CrmE	Secreted TNF-binding proteins.	Smith *et al*, 1996 (CrmB/C)) Loparev *et al*, 1998 (CrmD) Alcami and Koszinowski, 2000 (CrmE)
	VV, SPV	B28R, K2R	Membrane bound IL-8 receptor, inhibits IL-8 activity.	Alcami *et al*, 1999 (B28R)
	VV	3β-HSD	Promotes the production of steroids with immunosuppressive properties.	Cao *et al*, 1995 (K2R) Smith *et al*, 1997 (3β-HSD)
Interferon	MV, ShFV	M-T7 , T-7	Secreted, acts as IFN-γ receptor, neutralises the antiviral activity of IFN-γ.	Goodbourn *et al*, 2000 (review)
	VV, TPV	B8R , C8L		Upton *et al*, 1992 (M-T7)
	VV, OV	E3L, 20.0L	Binds dsRNA, inhibits PKR kinase-activated host cell apoptosis and prevents activation of RNase L system that degrades RNA.	Mossman *et al*, 1995 (T-7) Alcami and Smith 1995 (B8R)
	VV	K3L	Inhibits the activation of eIF2α and blocks PKR activated apoptosis	Kawagishi-Kobayashi *et al*, 2000 (C8L)
	VV	B18R	IFN-α/β receptor present on cell surface and extra-cellular medium that inhibits the effects of type-1 IFNs.	Ho and Shuman, 1996 (E3L) Haig *et al*, 1998 (20.0L)
	MCV	MC53, MC54	Secreted, binds IL-18 and inhibits IL-18-induced IFN-γ production.	Carroll *et al*, 1993 (K3L)
	EV, VV, CPV	D7L		Alcami *et al*, 2000 (B18R) Smith *et al*, 2000 (IL-18BPs)

Table 1.2 continued. Poxvirus products that counteract host defences

Host response	Virus	Virus gene/product	Function/mechanism	Reference
Chemokines	MV, VV	M-T7, vCKBPI	Secreted, promiscously binds CXC, CC and C chemokines through heparin binding domains. Thought to block interaction of chemokines with proteoglycans *in vivo*.	Lalani *et al*, 1997 (M-T7) Alcami *et al*, 1998 (review)
	VV, EV, VaV CPV, MV, ShFV	vCKBPII, B29R, vCC1, M-T1, S-T1	Secreted, binds CC-(e.g. RANTES) but not CXC- or C chemokines.	Graham *et al*, 1997 (M-T1) Carfi *et al*, 1999 (vCC1)
	MCV	MC148/MCC-1	Chemokine analogues, specific CCR8 antagonists, that may interfere with monocyte and dendritic cell function.	Luttichau *et al*, 2000 (MC148) Lalani *et al*, 1999b (review)
Complement	CPV, VV	C21L, vCP	Secreted viral proteins that bind C3b and C4b thus inhibiting activation of classic and alternative pathways.	Rosengard *et al*, 1999 (VCP) Isaacs *et al*, 1992 (C21L)
	CPV	IMP	Blocks immunopathological tissue damage at the site of infection by inhibiting production of macrophage chemoattractant factors C3a and C5a.	Kotwal, 2000 (review, IMP) Vanderplasschen *et al*, 1998 (CD46, CD55, CD59)
	VV	CD46, CD55, CD59	Host complement control proteins incorporated into virion envelope or infected cell membrane that block formation of the membrane-attack complex and confer protection against lysis.	
MHC	VV, MV	Late viral proteins	MHC class I antigen expression reduced. Late viral proteins involved in regulating MHC turnover and expression.	Boshkov *et al*, 1992 (LVPs)
	EV	viral serpins	Inhibit processing of viral antigens through serpin inactivation of proteolysis.	Mullbacher *et al*, 1999 (serpins) Smith *et al*, 1997 (review)
Cytokines	TPV	35kD	Secreted, binds IL-2 , IL-5 and IFN-γ, thus disarming Th1 (IL-2 and IFN-γ) and Th2 (IL-5) effector mechanisms.	Alcami *et al*, 1998 (review) Essani *et al*, 1994 (B8R)
	OV	vIL-10	Secreted, with inhibitory effects on non-specific immunity and Th1 effector functions.	Fleming *et al*, 1997 (vIL-10)

Abbreviations in table.

3β-HSD, 3β-hydroxysteroid dehydrogenase; BP, binding protein; CKBP, chemokine binding protein; CP, complement control protein; CPV, cowpox virus; Crm, cytokine response modifier; eIF-2α, eukaryotic translation initiation factor 2α; EV, ectromelia virus; IMP, inflammation modulatory protein; LVP, late viral protein; MCV molluscum contagiosum virus; MV, myxoma virus; OV, orf virus; PKR, dsRNA-dependent protein kinase; RANTES, regulated upon activation normal T cell expressed and secreted; Serpin, serine protease inhibitor; ShFV, Shope fibroma virus; SPV, swinepox virus; TPV, Tanapox virus; v, viral; VaV, variola virus; VV, vaccinia virus.

endothelial growth factor (VEGF), a viral IL-10, and a viral interferon-resistance factor (IFNR) (Haig and Mercer, 1998).

i). Orf virus vascular endothelial growth factor (VEGF)

The first orf virus virulence gene to be identified was a homologue of the mammalian VEGF gene (Lyttle *et al,* 1994). VEGF is a secreted homodimeric glycoprotein that stimulates the proliferation of vascular and lymphatic endothelial cells and has a key role in normal and abnormal angiogenesis (Fava *et al,* 1994). A feature of orf virus infection, in sheep and man, is the extensive capillary proliferation and dilation found in the area of the lesion and it seems likely that orf virus VEGF, an early expressed gene, is involved in the promotion of this condition (Meyer *et al,* 1999). VEGF also promotes the expression of the integrins, VCAM-1 and ICAM-1 in endothelial cells (Melder *et al,* 1996) and may interfere with the maturation of dendritic cells (Gabrilovich *et al,* 1998). Futhermore Haig and Mercer (1998) suggest that the accumulation of MHC class II^+ dendritic cells adjacent to the site of infection and characteristic of orf may be a result of viral VEGF released by infected cells. Meyer *et al,* (1999) report that in contrast to mammalian VEGF, orf virus VEGF binds to only one of 2 VEGF receptors, namely VEGF receptor-2 (VEGFR-2). VEGFR-2 is thought to dominate the angiogenic response (Waltenberger *et al,* 1996).

Interestingly, there are 2 major forms of the orf virus VEGF gene as expressed by the different orf virus strains NZ2 and NZ7 and which differ from one another in DNA sequence to a degree whereby they share a predicted amino acid identity of only 41%. However orf virus isolates appear to contain only a single gene copy encoding one of the VEGF isoforms, but not both (Lyttle *et al,* 1994). As to why

different orf viruses should acquire one or other of 2 different VEGF genes is not known. Haig and Mercer (1998) suggest that since multiple VEGF forms exist in mammals (potentially 4-6 in man and sheep), it is possible that whilst different strains of orf virus can acquire a single copy of several VEGF genes available in infected tissue, they have not the capability of capturing another. The acquisition, by individual orf viruses, of different VEGF genes with possible subtle differences in biological activity may confer a specific advantage to that particular virus (Ferrara and Davis-Smyth, 1997).

A recombinant orf virus in which the orf virus VEGF gene has been removed has been tested for virulence and although no significant difference in virus growth in tissue culture was observed, in sheep, lesion development was significantly reduced in the 'knocked out' virus (Wise *et al,* 1999).

From the evidence accumulated so far, Haig and Mercer (1998) propose that orf virus VEGF, either directly or indirectly, provides proliferating epithelial cells as targets for virus replication and may prevent viral induced cell apoptosis in a similar way to vaccinia virus epidermal growth factor (Reisner, 1985).

ii). Orf virus IL-10

An orf virus homologue of the ovine IL-10 gene has been identified (Fleming *et al,* 1997). IL-10 is a pleiotropic cytokine that is involved in the general down-regulation of the Th1 cell mediated immune response in favour of the promotion of Th2 and B cell responses (Fig. 1.10) (Itoh *et al,* 1994; Perrin *et al,* 1999).

Th1 and Th2 responses represent two different types of immunity mediated by two distinct types of helper T cells (Th) (reviewed by Mosmann and Moore, 1991; Romagnani, 1992, 1997). Th1 cells produce those cytokines that stimulate strong

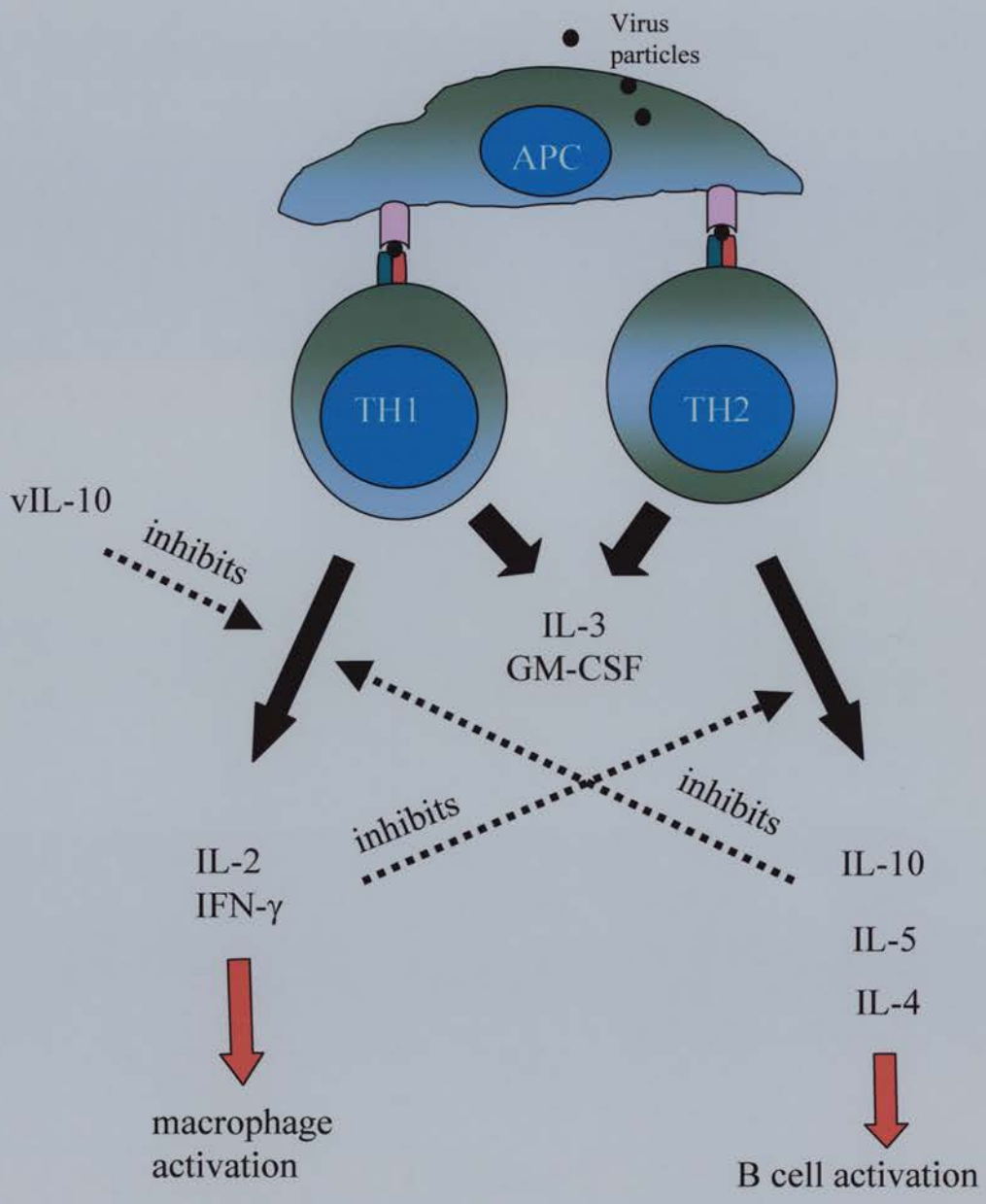

Fig. 1.10 Mediation of effector mechanisms by Th1 and Th2 cells.
Activation of either Th subset by antigen presenting cells (APC) leads to the output of cytokines which drive different effector pathways. However the activation of Th1 cells will tend to switch off the activation of Th2 cells and vice versa. Th2 cells release IL-10 which inhibits the Th1-driven response. Viral IL-10 (vIL-10) is considered to act in a similar fashion.

cellular immunity but only weak and transient antibody responses. In contrast, Th2 cells produce an array of cytokines that evoke strong antibody responses but weak cellular immunity. In general, the immune response to most individual pathogens involves both, with one or other predominating to most effectively combat the invasion. By occurring together, Th1 and Th2 responses, through the cytokines produced, can suppress or moderate the activity of the other. However the action of certain cytokines can sometimes alter the balance of the Th1/Th2 immune response and bring about inappropriate reactions.

The inhibitory effects of IL-10 on Th1 responses were found to be indirect and due to the inhibition of accessory function and antigen presenting capacity of monocytes and macrophages (Fiorentino *et al,* 1991). IL-10 blocks the production of the Th1 cytokines, IL-2 and IFN-γ (Moore *et al*, 1993) and also the production of pro-inflammatory cytokines that include TNF-α, IL-1β, IL-6 and IL-8 (de Waal *et al,* 1991; Wang *et al*, 1994; Mosmann, 1994). Finally, IL-10 has been reported to suppress nitric oxide synthesis in both activated macrophages and keratinocytes in culture (Corradi *et al,* 1993; Becherel *et al,* 1995).

Viral homologues of IL-10 have also been identified in Epstein Barr virus (EBV) (Hsu *et al,* 1990; Moore *et al,* 1990) and equine herpes virus-2 (Telford *et al,* 1995) but not in poxviruses other than orf virus so far.

Orf virus IL-10 is an early gene and the predicted protein sequence has 80% amino acid identity with ovine IL-10, with major differences occurring at the N-terminus. Orf virus IL-10 and ovine IL-10 have been shown to have similar activities in a thymocyte proliferation assay (Fleming *et al,* 1997) but whether or not orf virus IL-10 has both the inhibitory and stimulatory activities of host IL-10 is as yet

unclear.

It is thought that orf virus IL-10 acts in the vicinity of virus infection to suppress the inflammatory response via down-regulation of pro-inflammatory cytokines and the cell mediated response via inhibition of Th1 cytokines (Haig and Mercer 1998).

iii) Orf virus interferon-resistance factor

Tissue culture-adapted strains of orf virus have been shown to be resistant to the antiviral effects of IFN α,β and γ (Haig *et al,* 1998). A homologue of the vaccinia virus E3L interferon-resistance (IFNR) gene has been found in the left hand terminal region of the genome of orf virus strain NZ2 (Mercer *et al,* 1997a). The orf virus INFR gene is transcribed early and has a predicted 30% amino acid sequence homology to vaccinia virus E3L gene product (McInnes *et al,* 1998). Vaccinia virus E3L product binds double stranded (ds) RNA and inhibits the ds RNA-dependent activation of both an IFN-inducible protein kinase (PKR) and the IFN-inducible 2-5 polyadenosine synthetase (Chang *et al*, 1992). Activation of PKR kinase would normally result in the phosphorylation of the translation initiation factor eIF2 and inhibition of the initiation of protein translation. On the other hand, activation of the 2-5 polyadenosine synthetase inhibits protein synthesis by activating RNAse L which cleaves both mRNA and ribosomal RNA (Chang *et al,* 1992; Beattie *et al,* 1995). Similarly, the orf virus INFR protein has been shown to bind dsRNA and inhibit ovine PKR phosphorylation thus effectively suppressing the anti-viral state induced by both type 1 and type 2 IFN (McInnes *et al,* 1998; Haig *et al*, 1998). The transient expression of orf virus IFNR in ovine fibroblasts infected with the unrelated Semliki forest virus suppressed the anti-viral effects of type 1 and 2 IFN that would normally restrict the growth of the virus (Haig *et al,* 1998).

Thus orf virus is one of several poxviruses that contain a gene or genes, the products of which interact with one or more of the host components involved in the IFN-induced and dsRNA-dependent shutdown of viral and host protein synthesis. By targeting IFN, those viruses indicate the importance of the interferons in host anti-viral defence.

1.4.3. A GM-CSF-inhibitory factor (GIF) associated with orf virus infection

As a result of a previous study (Lear, 1995), a factor was discovered which was expressed by orf virus-infected ovine keratinocytes in culture that cleared both constitutively produced GM-CSF and exogenous recombinant ovine GM-CSF as measured by a GM-CSF ELISA (described by Entrican *et al,* 1996). This activity was a consequence of orf virus infection and was not due to proteolysis of the GM-CSF, since addition of protease inhibitors failed to prevent GM-CSF clearance (Lear, 1995).

In the skin, GM-CSF is up-regulated in a number of skin inflammatory diseases. Introduction of GM-CSF intradermally either as soluble protein (Haig *et al*, 1994) or by the expression of transgene protein (Xing *et al,* 1997) promotes the influx and accumulation in the dermis of neutrophils, eosinophils, macrophages, MHC class II^+ $CD1^-$ dendritic cells and lymphocytes, particularly T cells. An increase in the number of epidermal Langerhans cells, endothelial cells and keratinocytes was also observed (Ruef and Coleman, 1990; Xing *et al*, 1997). From studies with transgenic mice, Sato *et al,* (1999) suggest that GM-CSF is involved in the maturation of a specific sub-population of natural killer cells.

Whilst GM-CSF in the context of local immune responses stimulates

macrophages and granulocytes, and enhances healing and repair by its action on fibroblasts and epidermal cells, a more pivotal role may be as a mediator of the maturation and function of dendritic cells and their induction of the primary T cell immune response (Baldwin, 1992; Tarr, 1996; Wada *et al,* 1997). An orf virus-induced protein that binds GM-CSF and so inhibits normal GM-CSF function may contribute significantly to the suppression of anti-viral defences to the advantage of orf virus.

1.5. Objectives of this study

GM-CSF inhibitory activity (GIF) has not been associated with other viruses or pathogens and so the GIF activity found in orf virus infection represented an important focus of study. This thesis was designed to further our understanding of the mechanisms by which viruses block host anti-viral immune responses by characterising in detail this novel immuno-modulatory protein.

The initial aim of the project was to determine whether the GIF protein was the product of an orf virus gene or a host cell gene under virus control (see Chapter 3). A vaccinia virus-orf virus library comprising restriction fragments of orf virus DNA inserted into a vaccinia virus vector was used to screen cells infected with the vaccinia-virus-orf virus recombinants for the expression of GIF by ELISA. In this way the orf virus gene associated with GIF activity was isolated. This gene was then expressed in a suitable expression vector and the protein isolated. N-terminal amino acid sequence analysis was carried out on the GIF protein to determine whether or not it was the product of the isolated orf virus gene. Protein sequences recorded in protein databases were examined for any similarity with the sequence of the GIF

protein. In addition, ovine fibroblast cultures were infected with orf virus *in vitro* to determine the kinetics of GIF gene expression. Antibodies to the isolated GIF protein were raised for this and other purposes.

The interaction of the GIF protein with GM-CSF was examined by ELISA and Western blotting to determine the physio-chemical properties of the GIF (Chapter 4).

Since a number of poxvirus immuno-modulatory proteins have been reported as possessing multiple reactivities with host cytokines, the specificity of GIF for cytokines other than ovine GM-CSF was tested by ELISA and ligand blotting (Chapter 5).

A soft agar clonogenic assay that measured GM-CSF–driven proliferation of bone marrow myeloid progenitor cells was used to determine the effect of GIF on GM-CSF function (Chapter 6).

Finally skin biopsy tissue and samples of afferent and efferent lymph taken from sheep experimentally infected with orf virus were examined for the presence of GIF to determine whether GIF has an important role *in vivo* (Chapter 7).

CHAPTER 2

MATERIALS AND METHODS

2.1. General Materials and Methods

2.1.1. Reagents

Unless stated otherwise, the chemicals used in this study were obtained from Sigma Chemicals (Poole, U.K).

2.1.2. Animals

Female Suffolk-cross sheep were used in experiments involving sheep. Antiserum was raised against GIF in female New Zealand strain rabbits and female BALB/c strain mice.

2.1.3. Viruses

The orf virus strains used in this study were orf11 (generated at the Moredun Research Institute, McInnes *et al*, in press), scabbymouth (Pye, 1990), D1701 (Czerny *et al*, 1997), NZ2 (Mercer *et al*, 1987; Lyttle *et al*, 1994) and the field isolate MRI Scab (McKeever and Reid 1987).

The orf11, scabbymouth, D1701 and NZ2 orf virus strains were originally isolated from sheep scab material and subsequently propagated in primary bovine testes cells or primary fetal lamb muscle or kidney cells. The field isolate, MRI Scab virus, is propagated in sheep and has not been adapted to grow in cell culture.

German isolates of bovine papular stomatitis virus (V660) and pseudocowpox virus (B074) were kindly provided by Dr. M. Buttner, Federal Virus Laboratory, Tubingen. Both isolates had been adapted to cell culture by passage in bovine lung epithelial cells followed by passage in fetal lamb muscle cells (Mayr *et al*, 1974).

The vaccinia virus strain Lister was used in this study (Robinson and Mercer,

1988). This strain was originally isolated in the Lister Institute of Preventive Medicine, U.K. for use as a smallpox vaccine.

Semliki Forest virus (SFV) was used in this study as an unrelated virus control. SFV is a positive stranded RNA virus of the genus, Alphavirus, that is transmitted by mosquitoes and has been isolated in central, eastern and southern Africa. Infection of sheep fibroblast cell cultures with SFV resulted in a cytopathic effect similar to that observed after infection with orf virus. It was propagated by passage in ST-6 ovine fibroblasts (Entrican *et al*, 1989).

2.1.4. Cells

i). Cell maintenance

Orf virus, bovine papular stomatitis virus and pseudocowpox virus were grown in fetal lamb muscle (FLM) fibroblast cells maintained at Moredun Research Institute as a primary cell line in Medium 199. Vaccinia virus was grown in CV-1 cells, a monkey kidney fibroblast cell line (European Collection of Cell Cultures [ECACC], CAMR, Salisbury U.K.), maintained in Eagles minimal essential medium (MEM).

The mouse hybridoma lines 3C2 and 8D8 that secrete monoclonal antibodies to ovine GM-CSF (Entrican *et al*, 1996), were maintained in RPMI-1640 medium.

Chinese hamster ovarian epithelial (CHO) cells (ECACC) were maintained in Glasgow's modified Eagle medium (GMEM) supplemented with 7.5% heat - inactivated dialysed fetal bovine serum (PAA Laboratories, Kingston upon Thames, U.K). CHO cells transfected with orf virus DNA or ovine DNA were maintained in glutamine-free GMEM supplemented with 7.5% heat -inactivated dialysed fetal bovine serum and methionine sulphoxamine (see Section 2.2.3.ii).

Media were obtained from Life Technologies Ltd (Paisley, U.K.) and with the exception of GMEM, supplemented with 10% fetal bovine serum, 1mM glutamine and 100 units/ml penicillin and streptomycin. Cell cultures were propagated in plastic tissue culture plates and flasks supplied by Corning Costar Ltd (High Wycombe, U.K.).

ii). Cryopreservation

Cells (2-5 x 10^6) were harvested (see Section 2.2.3.i) and washed once in medium containing serum before gentle resuspension in 1 ml of fetal calf serum containing 10% dimethyl sulfoxide (DMSO) and transferred into a cryotube (Nunc Inc., Naperville, Illinois) The tubes were placed in a Cryo freezing container (Nalge Nunc International, Hereford, U.K.) and stored at –75°C for 24 hours. The tubes were then transferred to a liquid nitrogen tank for storage until required.

Cells removed from frozen storage were thawed rapidly in a 37°C waterbath and the suspension diluted in 5 ml of warm culture medium. The cells were then washed and inoculated into 25 cm^2 and 75 cm^2 flasks at 5 x 10^5 cells/ml.

2.1.5. Chromatography

i). Equipment

All chromatography described in this study was carried out using the Fast Protein Liquid Chromatography (FPLC) system (Amersham Pharmacia Biotech Ltd (APB), Little Chalfont, U.K.). Column buffer flow rates were controlled by an integrated Liquid Chromatography Controller LCC-550 and the protein concentrations in column effluents were measured by a UV-M absorbance detector with 280 nm wavelength filter.

ii). Affinity Chromatography

Proteins were separated by adsorption to specific ligands immobilised on Sepharose 4B (APB) as outlined in Section 2.1.7.

iii). Gel Filtration Chromatography

Recombinant proteins were separated on the basis of size by gel filtration chromatography on Sephacryl S200HR (APB). Prior to separation protein mixtures were concentrated at least 10-fold by ultrafiltration in a Centricon YM-10 (molecular weight cut-off 10,000) microconcentrator cell (Amicon, Stonehouse, UK) at 6000 x g for 3 hours.

Volumes of 0.2-0.5 ml were generally loaded onto a 16 x 600 mm Sephacryl S200HR column equilibrated with PBS containing 0.02% sodium azide or PBS containing 0.5 M NaCl and 0.1 % CHAPS (3-[(3-cholamidopropyl)-dimethylammonio]-1-propanesulfonate) if protein concentrations were < 100μg/ml and adsorption of protein to the gel matrix was suspected. Column flow rate was 0.5 ml/min and 1ml fractions were collected. Fractions were analysed by ELISA (Section 2.1.7.) and/or sodium dodecyl sulphate-polyacrylamide gel electrophoresis (SDS-PAGE) run under reducing conditions (Section 2.1.6.).

The apparent molecular weights of separated proteins were estimated by comparison with the retention times for a range of gel filtration protein standards (Roche Diagnostics Ltd, Lewes, U.K.) run under identical conditions on the same column.

2.1.6. Gel electrophoresis

i). Separation of proteins

Proteins were separated by gel electrophoresis as outlined by Laemmli (1970), using the Mini-Protean gel system (Bio-Rad, Hemel Hempstead, U.K.). Samples (10-15 µl) were reduced in an equal volume of SDS-PAGE sample buffer (0.0625 M Tris-HCL [pH 6.8], 2% SDS, 5% 2-mercaptoethanol, 10% glycerol, 0.002% bromophenol blue) and immersed in boiling water for 2 min. Samples, run under non-reducing conditions, were mixed with sample buffer without 2-mercaptoethanol and were not heated. Electrophoresis buffer consisted of 25mM Tris, 0.19M glycine, 0.1% SDS (pH 8.3). Samples were loaded into the wells of discontinuous SDS-PAGE minigels comprising a 4% stacking gel and a separating gel of either 7.5%, 12% or 15% and electrophoresed at 200 V until the dye had reached the bottom of the gel. Generally, gels were produced from a 30% stock acrylamide solution containing 0.8% bis acrylamide (Severn Biotech Ltd. Kidderminster, U.K). However the use of ProSieve 50 acrylamide gel solution (FMC, Rockland, USA.) to generate the 12 % separating gel was found to improve the separation of reduced proteins (with molecular masses in the range 25-60 kD) when compared with conventional acrylamide solutions.

ii). Silver staining of separated proteins

In general, separated proteins were visualised by silver staining. Gels were fixed in 50% methanol, 10% acetic acid in distilled water for 15 min, rehydrated twice in 5% methanol, 7% acetic acid in distilled water for 10 min then washed twice in distilled water. Proteins were reduced in 5 µg/ml dithiothreitol in distilled water for 15 min, washed again, immersed in 0.1% silver nitrate in distilled water for 20 min,

washed briefly and finally developed for stained protein by immersion in 3% sodium carbonate containing 0.05% formaldehyde. Development was terminated by the addition of citric acid to 1% w/v.

Molecular weight markers (SDS-PAGE standards, Bio-Rad.) that consisted of phosphorylase b (97,400 Daltons), bovine serum albumin, (66,200), ovalbumin, (45,000), carbonic anhydrase (31,000), trypsin inhibitor (21,500) and lysozyme (14,400) were included in all gels.

iii). Estimation of molecular mass of separated proteins

All molecular mass estimations were carried out using the standard curve generating tool provided with Microcal Origin Data Analysis software version 4.0/5.0 (Plikaytis *et al*, 1986). Standard curves were generated from either retention times (gel filtration) or mobilities (SDS-PAGE) of protein standards run either in parallel or under identical conditions.

2.1.7. Detection of GIF by ELISA

i). Introduction

The binding of recombinant GIF to recombinant ovine GM-CSF (rovGM-CSF) was measured by the decrease in unbound rovGM-CSF as detected by GM-CSF sandwich ELISA (Entrican *et al*, 1996). This exploits the fact that GM-CSF bound to GIF is no longer detected in the GM-CSF ELISA. The ELISA uses two affinity-purified monoclonal antibodies 8D8 and 3C2 that recognise mutually exclusive epitopes of GM-CSF (Entrican *et al*, 1996).

ii). Antibodies and rovGM-CSF

The generation of rovGM-CSF and the anti-GM-CSF Mabs 3C2 and 8D8 has

been described (Entrican *et al*, 1996). An IgG fraction of 3C2 was prepared from three 300-400 ml volumes of 3C2 hybridoma conditioned medium by separation over 2.5 mls of Protein A-Sepharose 4 fast flow (APB) equilibrated with PBS containing 0.02% sodium azide.

Bound material was eluted by the addition of 0.5 M NaCl in 0.1 M glycine pH 2.9. The collected fractions (1ml) were immediately neutralised by the addition of (38µl) 1M Tris-HCl pH 11, then concentrated at least 10-fold by ultrafiltration. The pooled IgG fractions (10 mg) were dialysed against 0.1 M $NaHCO_3$ buffer, pH 8.2, overnight then coupled to 1 g (dry weight) of CNBr-Sepharose (APB) to prepare an affinity column according to the manufacturer's instructions.

Cell free supernatants (supernatant, 50 to100 ml; containing a total of 0.5-3 mg rovGM-CSF) from the stable rovGM-CSF transfectant CHO cell line 1G10 , maintained in serumless- GMEM (Gibco BRL, Paisley, UK) for 4 days, were applied to the 3C2-affinity column equilibrated with PBS and the eluants monitored for protein content at OD 280nm. Bound material was treated as described above and aliquots taken for analysis by SDS-PAGE.

In a similar manner, purified rovGM-CSF (5-10 mg) was bound to CNBr-Sepharose. The rovGM-CSF-Sepharose affinity column was then used to purify the anti-GM-CSF Mab 8D8 from hybridoma conditioned medium as described for the Mab 3C2.

The Mab 8D8 was used to coat the ELISA plate and so capture any GM-CSF present in the samples and the second Mab 3C2 conjugated to horse radish peroxidase (HRP) then bound to the second epitope on the captured GM-CSF. The captured GM-CSF was quantified by comparison with a standard curve using

rovGM-CSF (McInnes and Haig, 1991; McInnes *et al*, 1993).

iii). Conjugation of Horse Radish Peroxidase (HRP) to 3C2 antibody

A HRP-aldehyde was formed by the addition of 50 µl $NaIO_4$ (38.5 mg/ml) to 4 mg HRP (Boehringer Mannheim, Lewes, UK) in 1 ml of distilled water for 20 min with stirring at room temperature (RT). The HRP-aldehyde solution was dialysed against 1mM acetate buffer pH 4.5 overnight before the pH was raised by the addition of 20 µl of 0.2 M sodium carbonate pH 9.5 to >9.0 and 5-8 mg of purified 3C2 in 1 ml of 0.01M sodium carbonate pH 9.5 added immediately. The reaction mixture was stirred for 2 h at RT. The reaction was terminated by the addition of 100 µl of freshly prepared sodium borohydride solution (4 mg/ml in water) at 4°C for 2 hours. The conjugate mixture was then fractionated by gel filtration on Sephacryl S-200HR (APB) equilibrated with PBS. From the measured absorbances at 280 nm, the first peak fractions were pooled and tested for function in the GM-CSF clearance ELISA.

iv). The modified GM-CSF ELISA for the detection of GIF

M129B 96 well ELISA plates (Greiner Laborotechnik, Dursley, UK) were coated with 50 µl per well purified anti-GM-CSF Mab 8D8 at a concentration of 2 µg/ml in 0.1 M carbonate buffer pH 9.6, at 4°C overnight. Plates were washed twice with PBS containing 0.05% Tween 20 (PBST), then blocked for 30 min at RT with 100 µl per well PBST containing 4% BSA. At this stage 20 µl of affinity purified recombinant ovine GM-CSF at 40 ng/ml or 80 ng/ml in wash buffer was added to 180 µl of sample to be tested for the presence of GIF and the mixture incubated for 1hour at 37°C.

A range of GM-CSF standards were prepared from a stock of rovGM-CSF at a concentration of 20 μg/ml which was diluted to 8000, 4000, 2000, 1000, 500, 400, 200 and 100 pg/ml in wash buffer. After blocking with 100 μl of 4% BSA in PBS, the plates were washed twice with wash buffer and 50 μl/well of standards, samples, controls or buffer alone were added to the plate in duplicate. The plate was left at RT for 1h, washed 3 times in wash buffer, then 50 μl of affinity-purified anti-GM-CSF Mab 3C2 (1 μg/ml) conjugated to HRP were added to each well. The plate was incubated for a further 1 hour, washed as before, then 50 μl of substrate solution produced from orthophenylene diamine tablet sets (OPD) following the manufacturer's recommendations, were added to each well. Colour was allowed to develop for approximately 15 min. The reaction was terminated by the addition of 25 μl per well 2.5 M H_2SO_4.

The optical density (OD) of the reaction mixture was measured using a MRX Microplate reader (Dynex Tecnologies Ltd. Billingshurst, U.K.) equipped with a 492 nm filter. The level of GM-CSF bound to GIF was estimated by comparison of measured unbound cytokine with a standard curve generated from the range of GM-CSF concentrations using dedicated EndPoint software (Dynex).

2.1.8. Western blot analysis

Ligand or immuno-blot analysis was performed on proteins separated by SDS-PAGE under reducing and non-reducing conditions and electrotransferred to BA 83 nitrocellulose membranes (Schleicher and Schull, Anderman, Kingston upon Thames, U.K.) for 3 hours at 70mA/gel (2 mA/cm^2 of gel). The membranes were then blocked in PBS containing 4 % non-fat milk powder (Marvel; Chivers, Dublin,

then blocked in PBS containing 4 % non-fat milk powder (Marvel; Chivers, Dublin, Ireland) for 1 h at RT before probing with antibody or radioiodinated ligand diluted in blot wash buffer; PBS containing 0.35M NaCl and 0.5% (v/v) Tween 80 (Sigma) for 1h at RT. After extensive washing of the blot, bound ^{125}I-ligand was visualised by autoradiography whereby the dried blot was exposed to Hyperfilm MP x-ray film (APB) overnight.

Bound antibody was visualised by a further 1 hour incubation with a 1:1000 dilution of goat anti-rabbit IgG conjugated to horse-radish peroxidase (HRP) (DAKO, Ely, UK) in wash buffer, followed by treatment with the enhanced chemiluminescence (ECL) reagent (APB), according to the manufacturer's instructions, and exposure to Hyperfilm ECL (APB) for 30 secs to 5 min before development.

2.1.9. Radioiodination of proteins

Purified proteins were radioiodinated by the chloramine-T method as described by McConahey and Dixon (1980). Protein (20-30 μg) in 20-50 μl of PBS was added to 20 μl of 0.5 M sodium phosphate buffer pH 7.5 and 0.5 mCi (18.7 MBq) of Na^{125}I (free of carrier, 3.7 GBq/ml, APB) in a 1.8 ml microfuge tube. The reaction was initiated with the addition of 60μl of chloramine T (1 mg/ml) in distilled water to the mixture which was vigorously shaken and left for 2 min at RT. The reaction was terminated by addition of 60 μl of stop buffer containing 1 mg/ml L-tyrosine (Sigma), 1 mg/ml potassium iodide in water and the volume made up to 1 ml with PBS. ^{125}I-labelled protein was separated from free Na^{125}I by gel filtration on a 10 ml column of Sephadex G-25 (APB) equilibrated with PBS. Aliquots (10 μl) were taken

counter, Packard, Pangbourne, U.K.) to identify radiolabelled protein fractions and to determine the efficiency of labelling and the specific activity of the recovered protein.

2.1.10. Statistical analysis of data

Throughout this project statistical tests were applied to data obtained where appropriate. Tests were based on within-sample variation and were performed using a standard error of differences established from an analysis of variance (ANOVA) applied to data normalised by $\log_{10}(x + 1)$ transformation. In this study, the values given in tables and figures are the mean of 3 or 4 samples +/- standard error of the mean unless stated otherwise.

2.2. Isolation and characterisation of the orf virus gene encoding the GM-CSF inhibitory factor

2.2.1. Expression of the VVOV recombinant library

CV-1 and FLM cells were grown to confluence in 25 cm^2 flasks. After washing with 5 ml of PBS, the cells were inoculated with one of 16 VVOV recombinants in 2ml of DMEM and at a multiplicity of infection (MOI) of 0.1. [The multiplicity of infection is the average number of infectious virus particles per host cell. Virus titre was calculated by the Spearman-Kärber formula for the determination of 50% endpoints as outlined by Klement and Nicolson (1977)]. Other cells were inoculated with vaccinia virus (strain Lister) or orf virus (strain NZ2) at a MOI of 0.1. After 2 hours the inoculum was removed, the cells washed and 5 ml of DMEM supplemented with 10% FCS added. Uninfected cell cultures were used as a control.

After 18-20 hours cell free supernatants were collected from each culture and tested for GIF activity.

2.2.2. Expression of subclones of VVOV85

Eight overlapping orf virus DNA fragments that together corresponded to the orf virus insert of VVOV85 plus 1 kb of DNA on either side were cloned into the pUC8 expression vector by A. Mercer (Mercer *et al*, 1987). (This vector requires the presence of the transcriptional machinery of vaccinia virus for expression). Recombinant plasmids were designated pVU followed by the clone number. Plasmid DNAs were transfected with the cationic lipid carrier, lipofectin (GIBCO BRL), into FLM cells infected with vaccinia virus (Mercer *et al*, 1997b). After 20 hours cell-free supernatant from each culture were collected for GIF analysis.

2.2.3. Expression of recombinant GIF

i). Transfection of the GIF cDNA into Chinese hamster ovary cells

Stable expression of recombinant GIF was achieved in CHO cells using the Celltech pEE14 vector (Fig. 2.1) and recommended procedures (Cockett *et al*, 1990). The plasmid pEE14 allows the expression of DNA under the control of human cytomegalovirus major immediate early promoter. The cloning of orf viral GIF DNA followed methods described previously (McInnes *et al*, 1993). The pEE14 vector contains a glutamine synthetase (GS) gene as an amplifiable marker in CHO cells. Transfectants expressing GS were selected by cloning the transfected cells, by limiting dilution, in glutamine deficient medium containing dialysed fetal calf serum and 25 μM methionine sulphoxamine (MSX; an inhibitor of glutamine synthetase).

The lipid-mediated transfection of plasmid DNA into CHO cells was optimised

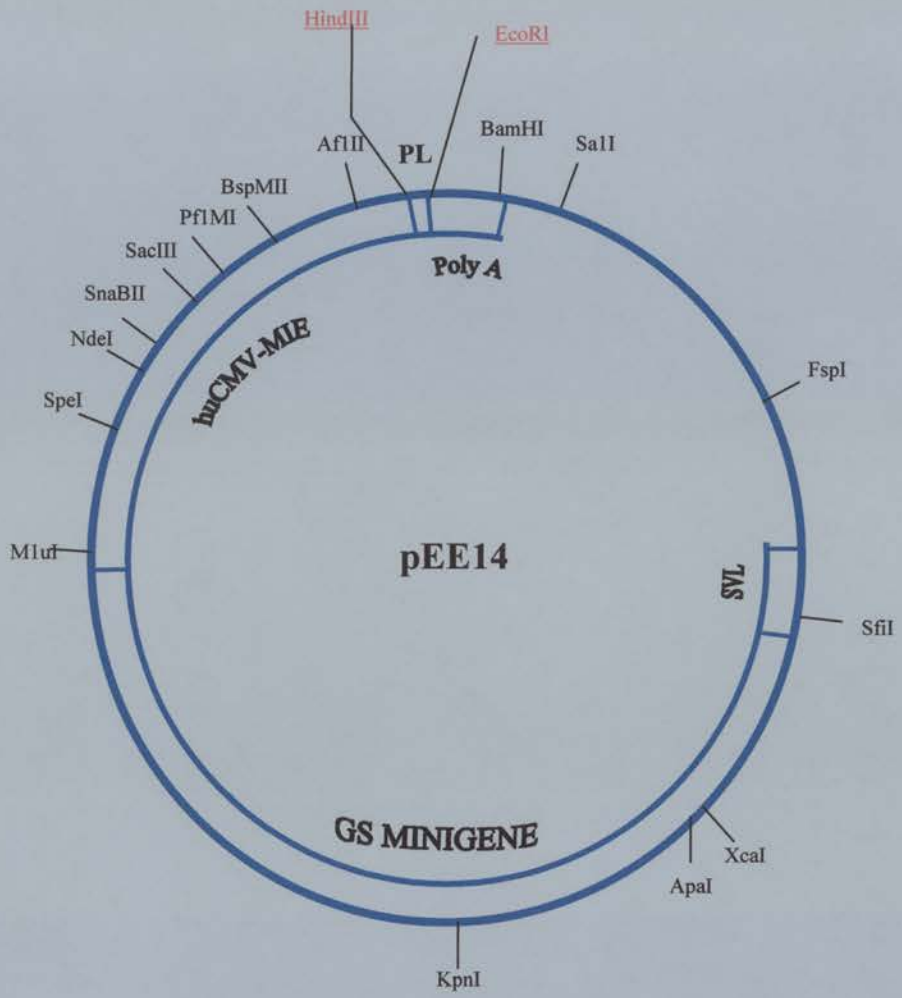

Fig. 2.1 Restriction map of the pEE14 mammalian expression vector. The plasmid pEE14 allows the expression of cDNA under the control of human cytomegalovirus major immediate early promoter (huCMV-MIE). It contains the glutamine synthetase selectable marker gene (GS MINIGENE) that is transcribed from the SV40 late promoter (SVL). Restriction endonucleases which cut once in the plasmid are shown. PL = polylinker. Poly A = SV40 early polyadenylation signal. The rest of the vector sequences in pEE14 are from plasmid pEE6hCMV and contain an ampicillin-resistance gene and an origin of replication for propagation in E. coli (Stephens and Cocket, 1989).
The cDNA incorporating the gene(s) of interest are ligated into the polylinker region between the HindIII and EcoRI cleavage sites (underlined).

using the Superfect® DNA-transfection kit (Quiagen, Crawley, UK). In addition to a range of different lipid transfection reagents (Pfx1-8) this kit contained a control plasmid pcDNA3.1/His/lacZ that encoded the gene for β-galactosidase. The efficiency of different lipid reagents and optimum exposure times were then determined by staining those cells transfected with the control plasmid for β-galactosidase activity.

CHO cells were grown at 37°C in a humid 5% CO_2 in air atmosphere to log phase (50-60% confluent, 1-2.5 X 10^6 cells/flask) in 25 cm^2 flasks in GMEM buffered with (7.5%) sodium bicarbonate and containing 7.5 % heat-inactivated, dialysed fetal bovine serum (FBS), 1% non-essential amino acids, 0.6% glutamate and 0.6% aparagine, 1mM sodium pyruvate and nucleosides (0.7% each of adenosine, guanosine, cytidine, and uridine; 0.24% thymidine), 100U/ml penicillin, 0.01% streptomycin, and 0.03% glutamine.

The medium was removed and cells washed twice with 5 mls of PBS. To duplicate flasks was added 30 µl of a different lipid reagent (Pfx 1-8) and 10 µl of control plasmid pcDNA3.1/His/lacZ at 1 µg/ml in 5 ml of GMEM without serum or glutamine. The flasks were left for 2, 4,6 8 and 20 hours at 37°C then the medium was replaced with 5 mls glutamine-free GMEM containing 7.5 % dialysed FBS and incubated for a further 24 hours. After 24 hours, cells were stained for β-galacosidase activity. Flasks were rinsed twice with 5 ml PBS and cells fixed with 2.5 ml 2 % formaldehyde, 0.2 % glutaraldehyde in PBS, pH 7.3 for 10 min at RT. Flasks were again rinsed twice with PBS before addition of 2.5 ml X-gal reagent (Quiagen) and left at RT overnight. The percentage of cells that were successfully transfected with the plasmid pcDNA3.1/His/lacZ as denoted by blue staining, was determined for

Lipid	Lipid:DNA 6:1			Lipid:DNA 9:1		
	4h	6h	24h	4h	6h	24h
Pfx1	13.5 (-)	10.5 (+/-)	7 (-)	5.5 (-)	10 (+/-)	6 (-)
Pfx2	12.5 (-)	24.5 (+/-)	33 (-)	14 (-)	26.5 (-)	30.5 (+/-)
Pfx3	13.5 (+)	31 (+/-)	32 (+/-)	10.5 (+)	14.5 (+)	27 (+)
Pfx4	16 (-)	19 (-)	7 (-)	8.5 (-)	13.5 (-)	6 (-)
Pfx5	19 (-)	21 (-)	28.5 (-)	18.5 (-)	26 (-)	6 (-)
Pfx6	14 (+)	12.5 (+)	19.5 (-)	5.5 (+)	11.5 (+)	24.5 (+/-)
Pfx7	10.5 (+)	28 (+)	35.5 (+/-)	9 (+)	18 (+/-)	22.5 (+/-)
Pfx8	21.5 (-)	19 (-)	16.5 (+/-)	18.5 (+)	23.5 (-)	20.5 (+)

Table 2.1 Superfect lipid reagents tested for transfection efficiency on CHO cells.
Values given represent the mean of β-galactosidase-positive cells from duplicate flasks of cultures transfected with a control plasmid pcDNA3.1/His/lacZ (containing the β-galactosidase gene) and taken at 26 hours after the addition of each lipid (Pfx1-8) at 2 different lipid:DNA ratios (6:1 and 9:1) and for different incubation times (4h, 6h, and 24h). Cultures were also scored for their condition i.e. (+) good: cells clear and the majority adherent, (+/-) acceptable: <30% cells rounded up and (-) poor: >30% cells rounded up.

each flask (Table 2.1). From this experiment it was deduced that for the transfection of the plasmids pEE14GM1 and pEE14GM2 into CHO cells, a high transfection efficiency could be achieved with the transfection lipid reagent Pfx 7 and an incubation time of 8 hours. This medium was then replaced with 5 ml glutamine-free GMEM containing 7.5% dialysed FBS and the flasks incubated for a further 24 hours. Cells were detached from the flasks by first rinsing with PBS then by incubating with 1 ml/flask of 0.25% trypsin/EDTA at 37°C for 10-15 min. Further unwanted digestion of detached cells was prevented by the addition of 2 ml of culture medium without growth factors. Clumps of detached cells were broken up by pipetting vigorously and the suspension was then centrifuged at 400 x g for 5 min to pellet the cells. The cells were washed twice with PBS and harvested. After counting cells were resuspended in medium containing 25 μM MSX to 100 cells/ml and set up at 1, 2, 5 and 10 cells/well in multiples of 6 wells in 96 well culture plates. Plates were incubated until cell growth was visible and viable cell aggregates could be identified. When viable cells covered approximately 50% of the area of the wells, medium was removed for testing for GIF production in the GM-CSFclearance ELISA. Positive cells were removed by trypsinisation and transferred to 24 well tissue culture plates. GIF production was monitored as cultures were expanded from 24 well plates to 25 cm^2 flasks and cell bank stocks of only the best producing cells were established in liquid nitrogen.

ii). Maintenance of transfected cell cultures

A higher level of recombinant GIF (rGIF) expression was obtained by further cloning of transfectants in increasing concentrations of MSX (Fig. 3.5B). The rGIF CHO cell line, GM1-CHO, used for all experiments was grown in the presence of

0.25mM MSX.

For bulk production of rGIF, the cells were propagated in 175 cm^2 flasks (Life Technologies, Paisley, UK). When the cells became confluent, the culture medium was removed and the mono-layer washed four times in warm phosphate-buffered saline (PBS). The cells were then incubated for 4 days in GMEM without serum or MSX. The serum-free supernate was harvested, clarified by centrifugation at 1000 x g for 20 min at 8°C, aliquoted and stored at –20°C.

2.2.3. Isolation of recombinant GIF

Cell-free supernatant (20-100 ml) from GM1-CHO was applied to the rovGM-CSF-Sepharose affinity column (Section 2.1.7.) and fractions collected throughout the process. After extensive column washing, bound protein was eluted. The collected fractions were tested for the presence of GIF by GM-CSF clearance ELISA. To minimise interference by rovGM-CSF leaking from the column during elution, the column was washed between runs with 2 cycles each of 0.5 M NaCl in 0.1 M $NaHCO_3$, pH 4.5 and 0.5 M NaCl in 0.1M Tris-HCl pH 8.5. The eluted GIF fractions as determined by ELISA (approximately 5-7 ml) were pooled and concentrated in a Centricon YM-10 microconcentrator cell (Amicon) by centrifugation at 6000 x g for 3 hours or until the total volume of the retentate was reduced to 200-400 µl. Aliquots (10 µl) were then analysed by 12 % SDS-PAGE.

2.2.4. The identification of GIF protein

i). N-terminal sequence analysis

Affinity-purified rGIF, separated by SDS-PAGE mini-gel, was transferred by the semi-dry method, as described by Khyse-Anderson (1984) and Matsudaira (1987), to

an inert support material, Immobilon-P (Millipore, Watford, UK). The Immobilon-P was first soaked in methanol then washed in water and finally immersed in 10 mM of 3-[cyclohexylamino]-propane-sulfonic acid (CAPS; Sigma) transfer buffer. Electro-transfer was for 3 h at 70 mA/minigel in a semi-dry blotting apparatus (Sigma).

Transferred protein was stained with 0.02% Coomassie brilliant blue in 50% ethanol for 15 min before rinsing the sheets briefly in 50% ethanol to remove background staining and then allowed to air dry. Stained protein bands were excised and sent for analysis to the Microchemistry Department at the AFRC Institute of Animal Physiology and Genetics Research, Cambridge Research Station, Babraham, Cambridgeshire, UK.

N-terminal protein sequencing of the soluble proteins was performed using liquid phase Edman degradation chemistry (Hunkapillar *et al*, 1983) on a Model 492, Procise Protein Sequencer (PE- Applied Biosystems, Warrington,Cheshire,UK). The purified protein was applied to a polybrene-treated glass fibre filter prior to sequencing. The N-terminal 20 amino acids of each protein were analysed.

ii). Comparative sequence analysis

The amino acid sequence of GIF and the 43 kD protein were compared with sequences recorded in the Swiss-Prot (release 37.0) and TREMBL (release 10.0) databases. The search for a sequence match with the query sequences was carried out using the Basic Local Alignment Search Tool (BLAST) provided by the United States National Center for Biotechnology Information (NCBI). Blast is designed to search all of the available sequence databases using a heuristic algorithm (Altschul *et al*, 1990) which seeks local rather than global alignments and therefore is able to detect relationships among sequences which share only isolated regions of similarity.

Further investigation of protein sequences was carried out using the ExPASy (Expert Protein Analysis System) proteomics server of the Swiss Institute of Bioinformatics (SIB). This server is dedicated to the analysis of protein sequences and structures.

2.2.5. Analysis of GIF expression by virus infected fetal lamb muscle cell cultures

i). Characterisation of rabbit anti-GIF

GIF antiserum was prepared by injecting rabbits intra-muscularly with affinity-purified GIF (10 μg/injection) in 0.5 ml PBS containing 20 μg Quill-A saponin adjuvant (Sperfos Biosector, Kvistgaard, Denmark). Eight days after a third monthly injection, the rabbits were bled from a peripheral ear vein and 5 ml of blood collected. An IgG fraction (400 μg) from 1ml of immune serum (ra101) was isolated on Protein A-Sepharose (APB) as described for the preparation of mAb 3C2. Eluted material was tested for inhibition of GIF clearance of exogenous rovGM-CSF as measured by GM-CSF clearance ELISA. Briefly, 90 μl of GM1-CHO supernatant (rovGM-CSF clearance of approximately 500 ng/ml) was incubated with 90 μl of a range of dilutions of the polyclonal IgG (1:100-1:5000 of a 200 μg/ml protein solution as determined by BCA reagent, Pierce) in PBST for 1 hour at RT before addition of the 20 μl rovGM-CSF 'spike' (100 ng/ml). An IgG fraction from pre-immune rabbit serum was run in parallel as a control.

ii). Virus infection of fetal lamb muscle cell cultures

Fetal lamb muscle (FLM) cells were grown to confluency in 75 cm^2 flasks (Costar) containing 10% FBS in DMEM. The cultures were washed three times with PBS then an inoculum of 2 ml of DMEM containing either NZ2, orf11,

scabbymouth, D1701 strains of orf virus, bovine papular stomatitis virus, pseudocowpox virus or Semliki forest virus at a MOI of 0.1-1 was added for 2 h at 37°C. The inoculum was then removed and replaced with 10 ml of serum-free DMEM. FLM cultures that had not been exposed to virus were taken as uninfected controls. After 24 h, the level of cytopathic effect was noted and cell free supernatants were collected and analysed for GIF activity by GM-CSF clearance ELISA.

A number of FLM cultures were treated before and after orf virus infection with cytosine arabinoside (CA) (40μg/ml) as described by Haig *et al* (1998). At an appropriate dose, CA inhibits viral DNA replication but not the expression of early viral genes (Schreiber and Crabtree, 1992).

Samples of supernatant from cultures were taken prior to and at 1, 2, 4, 6, 8, 10, 12, 18, 20 and 24h intervals after infection. At the same time, cells were harvested by trypsinisation, washed 3 times in PBS then counted. Cell pellets were lysed by resuspension in ice- cold PBS containing 1% NP-40 (Sigma) at 10^7 cells/ml lysis buffer. After 15 min on ice, the lysate was centrifuged at 9200 x g for 10 min and both soluble and insoluble material taken for analysis of GIF activity by GM-CSF clearance ELISA and Western blotting. Insoluble material was assayed as a suspension in ELISA wash buffer (the volume of wash buffer taken was ½ volume of the lysis buffer used).

iii). Western blot analysis of GIF with rabbit anti-GIF

Serumless conditioned media from GM1-CHO, GM2-CHO, untransfected CHO cells and virus-infected and uninfected FLM cell cultures were concentrated ten-fold by ultrafiltration in Centricon YM-10 microconcentrator cells before separation of 10

μl aliquots by 12% SDS-PAGE run under non-reducing conditions and electrotransfer to nitrocellulose as described in Section 2.1.8. After blocking, immobilised proteins were probed with either a 1:500 dilution of the polyclonal IgG fraction or a 1:500 dilution of control IgG (from pre-immune rabbit serum) in blot wash buffer. Bound antibody was visualised by treatment of the blots with HRP-conjugated anti-rabbit IgG followed by ECL reagent as described in Section 2.1.8.

2.3. Analysis of GIF physico-chemical properties

2.3.1. Analysis of affinity-purified GIF activity by gel filtration

To determine whether GIF functions as a monomer, dimer or higher order structure, approximately 500 ml of serum-less GM1-CHO supernatant was partially purified in 60-100 ml volumes over rovGM-CSF-Sepharose. Fractions containing GIF activity as determined by GM-CSF clearance ELISA were pooled and concentrated 50-fold by ultrafiltration at 3000 x g in Centricon YM-10 devices. The concentrated GIF mixture (1.5 ml) was applied to a 16 x 600 mm column of Sephacryl-200HR (APB) equilibrated with PBS containing 0.5 M NaCl, 0.01% CHAPS, 0.02% sodium azide and adjusted to pH 7.2. The mixture was separated over the column at a flow rate of 0.75 ml/min and 1 min fractions collected. The protein content of each fraction was measured by an in-line UV spectrophotometer (APB) at 280 nm. Fractions were tested for GIF activity in the GM-CSF clearance ELISA and analysed by 12% SDS-PAGE. The molecular mass of each protein peak was estimated by comparing the retention times of each peak with a calibration curve generated from the retention times of a mixture of proteins (that ranged from 25 kD-116 kD and were supplied as components of a gel filtration calibration kit (APB).

This standard protein mixture comprised 0.5 mg of each protein and was separated prior to the purification of GIF under identical conditions. Those fractions containing GIF activity were pooled and concentrated to 0.5 ml by ultrafiltration.

The protein content of the GIF isolate (115 kD) was determined by the bichinoic acid (BCA) protein estimation kit (Pierce) using a range of BSA concentrations (50 μg/ml –2 mg/ml) to generate a standard curve as detailed in the manufacturer's instructions. This colourimetric assay was performed in a 96 well ELISA plate (Dynex) and the plate read in a MRX Microplate reader (Dynex). From the BSA standard curve, the concentration of GIF was estimated using dedicated EndPoint software (Dynex).

2.3.2. Dissociation of the GIF complex

In order to test whether the 28 kD GIF bound rovGM-CSF, an aliquot (0.5ml) of the GIF isolate (115 kD) at 20μg/ml was reduced to its 28 kD subunit by boiling in the presence of 1, 2 or 5 mM dithiothreitol. Once the mixture had cooled, aliquots (50 μl) were tested for GM-CSF clearance in the GM-CSF ELISA. The remaining volumes were dialysed overnight against 2000 ml of PBS to remove the dithiothreitol and further aliquots tested for GIF activity by GM-CSF clearance ELISA.

2.3.3. Analysis of ^{125}I-GIF structure and GM-CSF binding activity

i). Radioiodination of GIF

Further investigation into GIF monomer/higher order structural forms was carried out on purified GIF (115 kD) that was radio-iodinated by the chloramine T method as described in Section 2.1.9.

After desalting over a 10 ml Sephadex G-25 gel filtration column equilibrated

with PBS to remove free $Na^{125}I$, a 10 µl sample was taken from 1 ml of radio-labelled protein collected and counted. From this value (2.2×10^6 dpm/min) the specific activity of ^{125}I-GIF was calculated as follows;

^{125}I-GIF count = 220×10^6 dpm/ml

Counting efficiency = 86% (from calibration carried out using the Instrument Performance Assessment feature of the Cobra II Auto-Gamma counter and a ^{125}I source).

Concentration ^{125}I-GIF = 20 µg/ml (assumed 100% recovery of protein from desalting column)

Specific activity (kBq/mg) = [(count dpm/ml/0.86)/6×10^4 dpm/ kBq]/20 µg

= 211 kBq/µg = <u>211 MBq/mg</u>

Molecular mass of isolated GIF = 115 kD

Specific activity (TBq/mM) = (specific activity MBqi/mg x molecular mass mg/mM)

= <u>24.2 TBq/mM</u>

ii). Gel filtration of ^{125}I-GIF

To determine whether the ^{125}I-GIF was affected by the oxidation reaction of the radiolabelling procedure, 0.5 ml of ^{125}I-GIF was analysed by S-200HR gel filtration as described above. Aliquots (10µl) were taken from each fraction for γ-scintillation counting. Fractions from each peak of radioactivity were then sampled (5 µl) and analysed by 12 % SDS-PAGE under reducing conditions. Separated radiolabelled protein was visualised by autoradiography overnight.

iii). ^{125}I-GIF ligand blotting

In order to test whether different ^{125}I-GIF forms separated by S200HR were capable of binding GM-CSF, column fractions were tested in a ligand blot assay.

Affinity purified rovGM-CSF (25 μg) was separated under reducing conditions on a 15% SDS-PAGE gel. All sample wells were loaded with rovGM-CSF save for a single end well retained for molecular mass protein standards. Separated proteins were electrotransferred to nitrocellulose membrane as described previously. After removal of the portion of membrane containing the protein standards for staining [see Section 2.2.4.(i)], the remainder was blocked with 4% powdered milk in PBS. The nitrocellulose membrane was then cut into strips and each strip incubated in a sealed tube containing 60 μl from a pool of 2/3 consecutive column fractions in 1 ml of blot wash buffer. The strips were incubated for 1 hour at RT with continual agitation then washed extensively over a period of 2 hours. The strips were allowed to air dry, realigned on card and autoradiographed overnight.

iv). Gel mobility shift cross-linking assay

The reactive form of GIF was investigated using a chemical cross-linking assay as described by Upton *et al*, (1992). Briefly ^{125}I- GIF (0.6 μg/ml) was incubated with affinity purified rovGM-CSF (5-10 μg/ml protein) for 2 h at RT.

Cell-free supernatant from an IL3-transfectant CHO cell line was concentrated by ultrafiltration in a YM-10 Centricon. An aliquot of IL-3-CHO concentrate that contained 5-10 μg/ml rovIL-3 (as determined by microdensitometry of SDS-PAGE separated IL3-CHO concentrate and a range of concentrations of chymotrypsinogen [2-50 μg/ml] see Section 2.4.3.) was incubated with ^{125}I-GIF in a parallel control experiment.

After incubation, purified ^{125}I-GIF and the ^{125}I-GIF-protein complexes were cross-linked by the addition of 1-ethyl-3-(3-dimethylaminopropyl)carbodiimide (EDC) to a final concentration of 40 mM for 30 min at RT and the reaction was quenched by the

addition of 1/10 volume of 1M Tris pH 7.5. SDS-PAGE sample buffer without mercaptoethanol was added to the mixtures before separation on 5%, 7.5% SDS-PAGE gels. Cross-linked complexes were analysed by autoradiography as described in Section 2.1.8.

2.3.4. Analysis of N-linked carbohydrate associated with the GIF molecule

Aliquots of purified GIF (1-2 μg) or rovGM-CSF (5-10 μg) in 200 μl of 20 mM sodium phosphate buffer pH 7.2 containing 10 mM EDTA, 1% (v/v) 2-mercaptoethanol, 0.1% (w/v) SDS and 1% (v/v) Triton X100 (Sigma) were boiled for 5 min. The mixtures were then allowed to cool before the addition of 1U of endo-glycopeptidase F (PNGase F; Roche) and incubation for 24 hours at 37°C. At the end of this period, a further 1 U of enzyme was added and the incubation repeated. Samples (10 μl) were analysed either by Western blot analysis (GIF) or SDS-PAGE followed by silver staining (rovGM-CSF) for a shift in relative mobilities after separation.

2.3.5. Determination of the isoelectric point of GIF

Purified GIF (2μg) was added to 1 ml aliquots of Q-Sepharose (APB) anion exchange resin (0.1g) that had been equilibrated to different pHs (range pH 5-9.5) by washing 10 times with 10 ml of 0.2M Tris-HCl adjusted to a particular pH. After mixing for 10 min, the gel was allowed to settle and the supernatant assayed for the presence of GIF by GM-CSF clearance ELISA.

2.3.6. Analysis of GIF-rovGM-CSF binding kinetics

i). Reactivity with time

Affinity purified GIF (1 μg/ml) was spiked with increasing amounts of rovGM-CSF (4-50 ng/ml) and incubated for 1 h and 20 h at 37°C. At the end of each incubation time, unbound rovGM-CSF was measured by GM-CSF ELISA.

ii). The effect of temperature

Aliquots of supernatant, from GM1CHO cultures, were spiked with increasing amounts of rovGM-CSF and incubated at different temperatures (4°C- 56°C) for 1 hour. Samples were then immediately assayed for rovGM-CSF.

iii). The effect of high salt concentration

The binding of affinity purified GIF (1 μg/ml) to 8 ng/ml rovGM-CSF in the presence of increasing salt concentration (0.1 M-1 M NaCl) was analysed by GM-CSF clearance ELISA. The effect of high salt concentration on the detection of GM-CSF was evaluated in the absence of GIF.

iv). The effect of extremes of pH

Prior to addition of rovGM-CSF, affinity purified GIF was diluted to 5 μg/ml in either 0.1 M citrate buffer adjusted to pH 3.0 or pH 4.0 or 0.1M carbonate buffer adjusted to pH 10 or pH 11 for 1h at 37°C. After this period, the pH of the solutions were adjusted to pH 7.5 with the addition of either 0.1 M carbonate buffer pH 11 or 0.1M citrate buffer pH 2.5. The GIF was further diluted to 1 μg/ml in wash buffer before analysis by GM-CSF clearance ELISA.

In a similar manner, samples of a mixture of affinity purified GIF (2 μg/ml) and rovGM-CSF (16 ng/ml) were adjusted to either pH 3.0, 4.0, 10, or 11 and after incubation for 1h at 37°C neutralised and analysed. The effect of extremes of pH on

the GM-CSF clearance ELISA was investigated in the absence of GIF.

2.4. Analysis of the binding specificity of GIF

2.4.1. Recombinant cytokines/chemokines

The recombinant ovine cytokines IL-1β, IL-2, IL-3, IL-4, IL-5, GM-CSF, MCP-1, MIP-1α, RANTES, TNF-α and IFN-γ were prepared from serumless supernatant from CHO cells transfected with the respective cytokine or chemokine cDNAs (from Ian Colditz, T. Yoshimura, Heng-Fong Seow, Paul Wood, J-P Scheerlink and Paul Chaplin, CSIRO, Melbourne Australia and Gary Entrican, Moredun Research Institute). The transfected CHO cells were propagated as described in Section 2.2.3.ii.

In order to identify and quantify individual cytokines, supernatant from each transfectant CHO culture was analysed by SDS-PAGE followed by microdensitometry. Supernatant was first concentrated ten-fold by ultrafiltration in a Centricon YM-10 filtration device and the protein content determined by the BCA reagent assay. Aliquots (20 µl) were run on 15% SDS-PAGE and separated proteins visualised by silver staining. Individual gel tracks were analysed by microdensitometry on a GS-670 Imaging Densitometer (BioRad) using the Molecular Analyst Program (BioRad). Recombinant cytokines were identified by comparison with material from untransfected CHO cultures and molecular mass protein standards run simultaneously (Figs. 2.2-2.6 and Table 2.2). The proportion of cytokine present in each supernatant was determined by measuring the area(s) of cytokine peak(s) and those of the other proteins present in the optical density profiles for each sample. Since the protein content of each sample had been determined, an

estimate of the level of expression of each cytokine was obtained (Table 2.2).

Purified human (hu) and murine (mu) GM-CSF and huIL-2 and huIL-4 recombinant cytokines were purchased from R&D Systems (Abington, U.K.). Recombinant ovine IL-8 was a gift from Heng-Fong Seow and Paul Wood, CSIRO, Australia. Recombinant bovine GM-CSF and IL-2 were gifted by Sarah Duggan, BBSRC, Institute of Animal Health, Compton, U.K. The other putative ligands used in this study, heparin and α_2-macroglobulin, were purchased from Sigma.

For soluble ligand binding assays, purified rovGM-CSF was prepared by affinity chromatography as described in Section 2.1.7.ii whilst rovIL-2 was isolated from 1 ml aliquots of a 80 fold concentrate of rovIL-2 cDNA-transfectant CHO supernatant by S200HR gel filtration as described in Section 2.1.5.ii. The concentration of purified rovGM-CSF and rovIL-2 were determined by the BCA reagent assay.

2.4.2. GIF binding assays

GIF reactivity with ligands, other than rovGM-CSF, was tested by a ligand competition assay. A 90 µl aliquot of each recombinant cytokine (100-200 ng/ml), heparin (1-2 µg/ml) or α_2-macroglobulin (1-2 µg/ml) was incubated with 90 µl of GM1-CHO supernatant for 1 h at 37°C before addition of the GM-CSF spike (8 ng/ml) and analysis by GM-CSF clearance ELISA. Ligands were tested in the absence of GIF for any interference with the GM-CSF clearance ELISA.

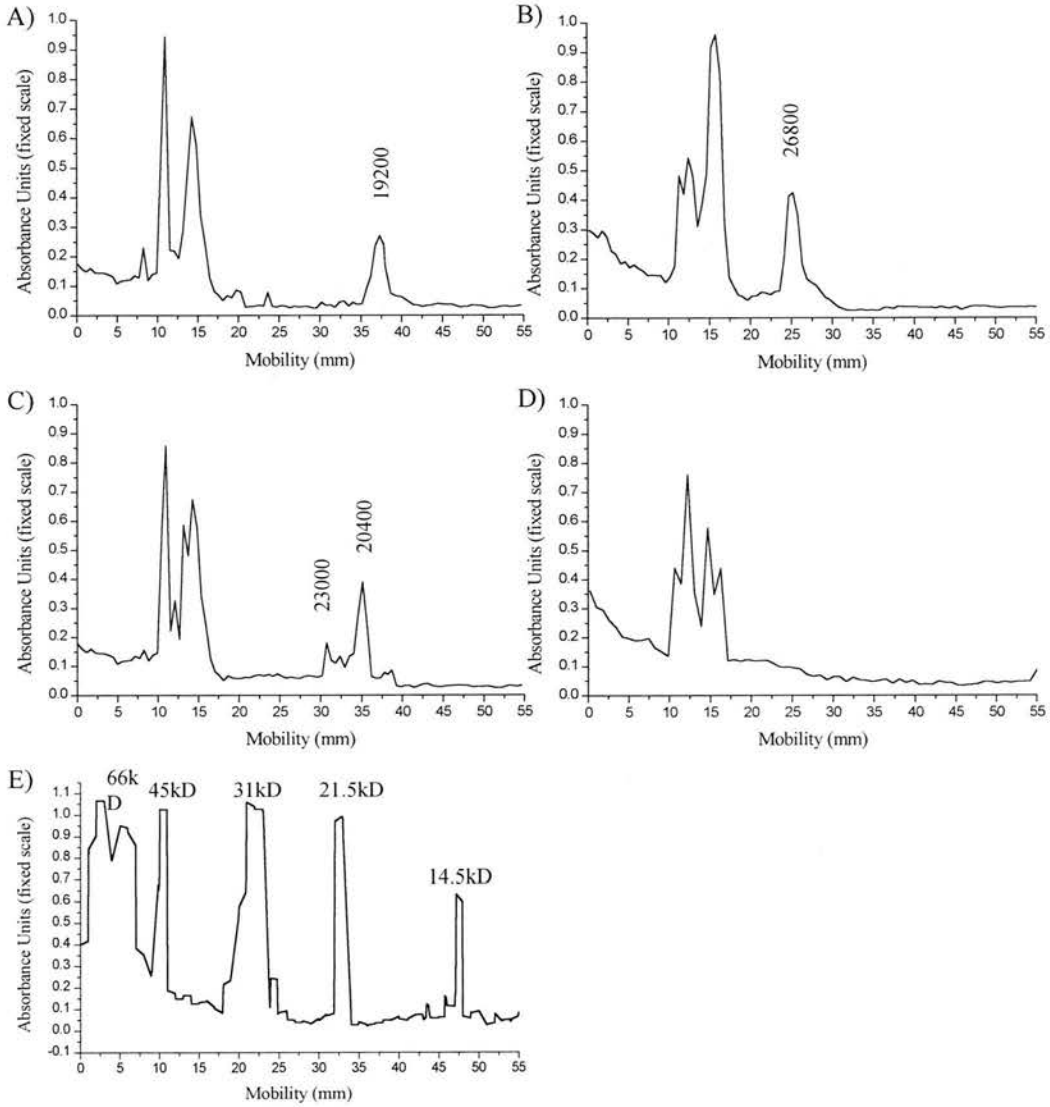

Fig. 2.2 Expression of recombinant ovine cytokines; IL-1β, IL-2 and IL-3. Supernatants from CHO cell cultures transfected with cDNA encoding the ovine cytokines IL-1β (A), IL-2 (B) and IL-3 (C) were separated by 15 % SDS-PAGE under reducing conditions and analysed by microdensitometry. Analysis of individual profiles where protein band optical density (Absorbance, y axis) and protein mobility in the gel (Mobility, x-axis) were measured, allowed both the level of expression and molecular mass of the recombinant protein(s) (given in Table 2.2) to be calculated using the BioRad GS 790 Imaging densitometer and BioRad Molecular Analyst software. Recombinant cytokines were identified by comparison with supernatants taken from untransfected CHO cultures (D) and processed in parallel. The molecular masses (kD) of individual cytokines are given above each peak and were estimated by comparison with a standard curve generated from molecular mass standards run simultaneously (E).

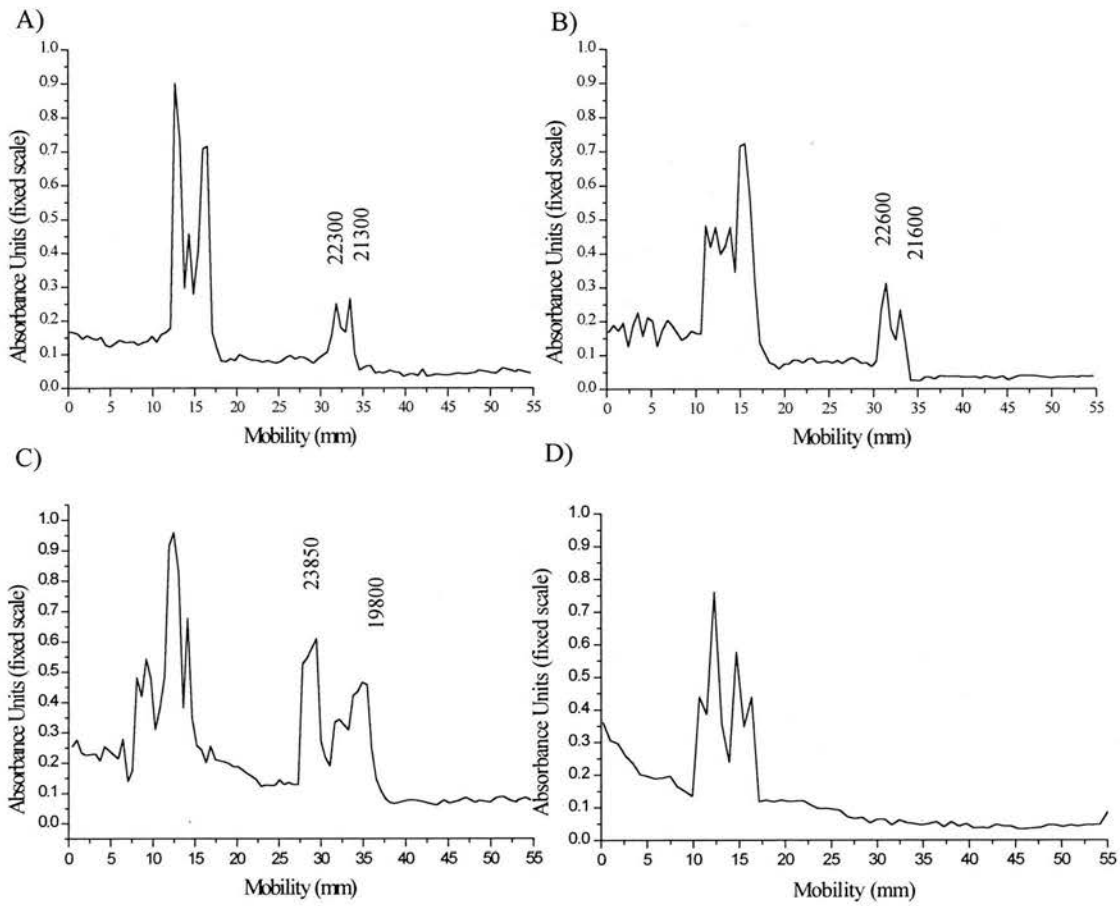

Fig. 2.3 Expression of recombinant ovine cytokines; IL-4, IL-5 and GM-CSF.
Microdensitometry profiles of supernatants from CHO cell cultures transfected with cDNA encoding A) IL-4, B) IL-5 and C) GM-CSF. Supernatant from untransfected CHO cell cultures (D) were included as a control.

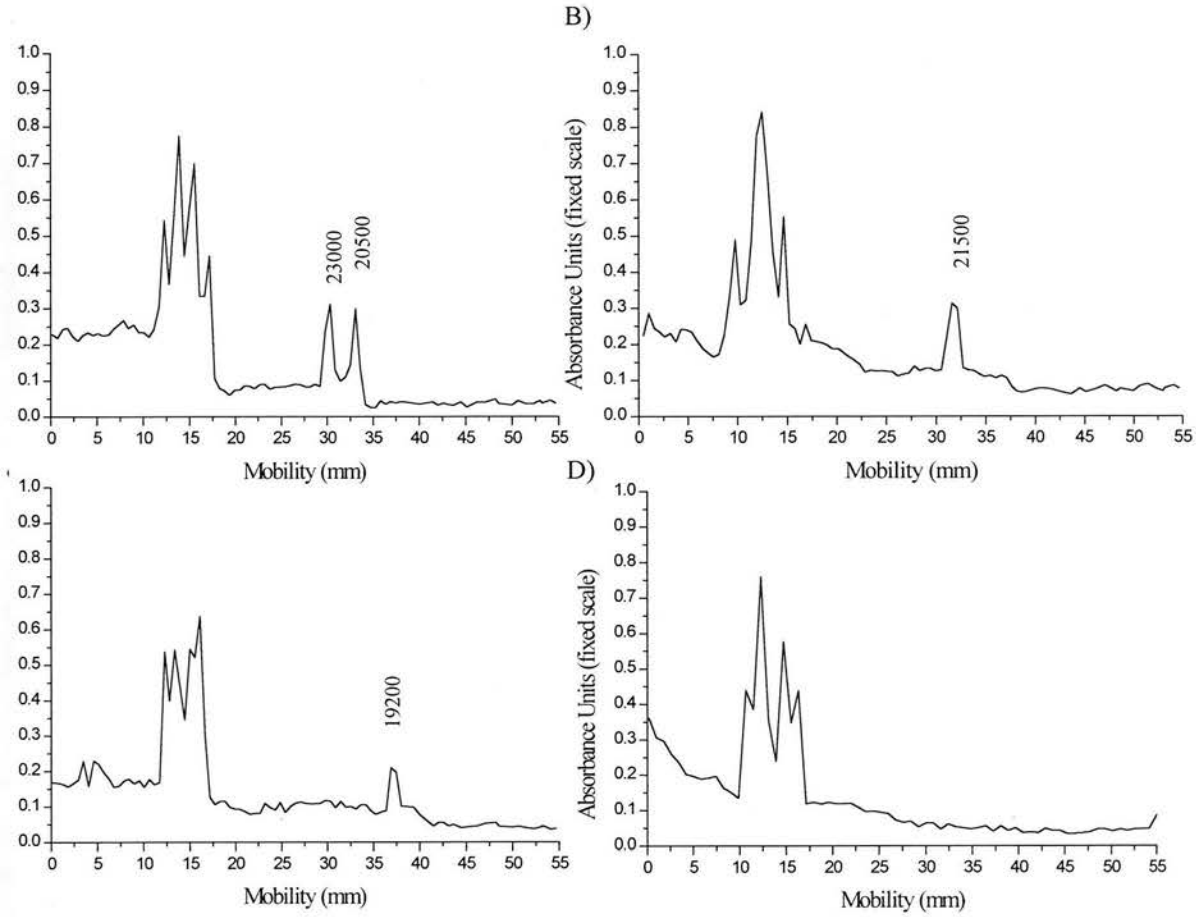

Fig. 2.4 Expression of recombinant ovine cytokines; IFN-γ, SCF and TNF-α.
Microdensitometry profiles of CFS from A) IFN-γ , B) SCF and C) TNF-α -cDNA transfected CHO cell cultures compared with supernatant from untransfected CHO cell cultures (D).

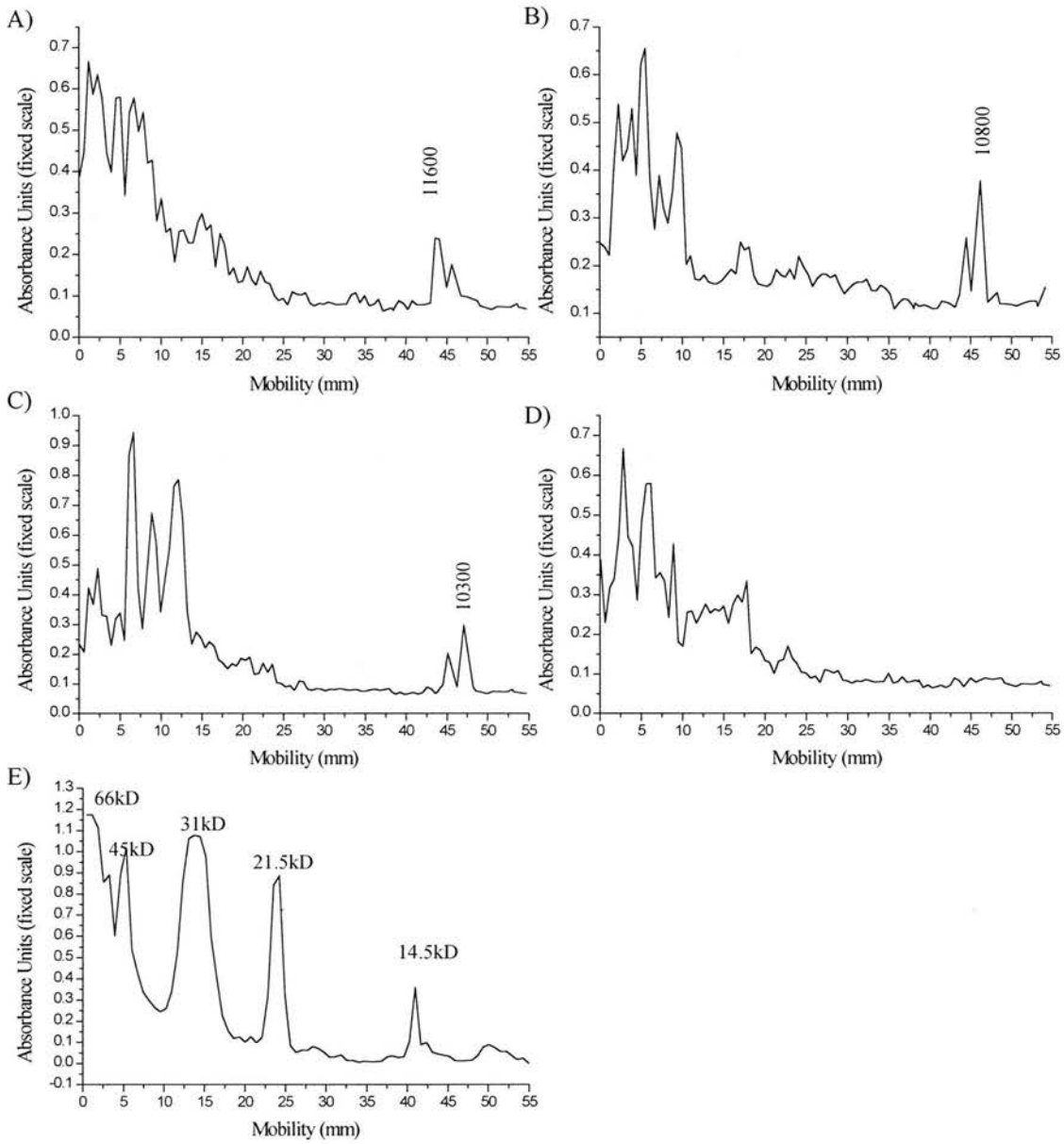

Fig. 2.5 Expression of recombinant ovine chemokines; MCP-1, MIP-1α and RANTES.
Microdensitometry profiles of CFS from A) MCP-1, B) MIP-1α and C) RANTES-cDNA transfected CHO cell cultures compared with CFS from untransfected CHO cell cultures (D).
The molecular masses ascribed to individual chemokine peaks are approximate since the mobilities of the chemokines fall outwith the standard curve generated from the mobilities of the molecular mass standards as shown in (E).

Cytokine	Molecular mass (Observed, kiloDaltons)	Molecular mass (human equivalent, kiloDaltons)	Level of expression (μg/ml)
IL-1β	19.2	17.0-22.0 (Brazel *et al*, 1991)	2.4
IL-2	26.8	15.4 (human, Riske *et al*, 1991); 27.0 (bovine, Arunachalam, 1989)	8.4
IL-3	23.0, 20.4	15.0-17.0 (Zenke *et al*, 1991)	3.6
IL-4	22.3, 21.3	20.0-22.0 (Boulay and Paul, 1992)	2.2
IL-5	22.6, 21.6	45.0 (homodimer, Takatsu *et al*, 1988, Takatsu, 1991)	3.1
GM-CSF	23.8, 19.8	14.0-35.0 (Okamoto *et al*, 1991)	28.5
IFN-γ	23.0, 20.5	20.0, 25.0 (Curling *et al*, 1990)	1.8
SCF	21.5	20.0 (Arakawa *et al*, 1991)	2.4
TNF-α	19.2	51.0 (homotrimer, Eck and Sprang, 1989)	0.9
MCP-1	10.5-13.0#	7.0 (Yoshimura and Leonard, 1992); 30.0 (murine, Liu *et al*, 1996)	1.2
MIP-1α	10.0-12.0#	8.0 (Graham *et al*, 1994)	0.9
RANTES	10.0-12.0#	8.0 (Schall, 1991)	1.4

Table 2.2 Expression of recombinant ovine cytokines
The molecular masses of ovine recombinant cytokines expressed by CHO cells and analysed by SDS-PAGE and microdensitometry under reducing conditions are compared with the molecular masses of cytokines of human origin.
(# = Approximate values since cytokine peaks were outwith the range of molecular mass standards).
The concentration of cytokine (μg/ml) in cell free supernatant collected from confluent CHO transfectant cultures maintained in serum-free medium is also given.

In order to test whether rovIL-2 and rovGM-CSF shared the same (or very close proximity) binding site within the GIF complex, increasing amounts of purified rovIL-2 (10-500 ng/ml) were tested for inhibition of GIF clearance of an 8ng/ml spike of rovGM-CSF in the GM-CSF clearance ELISA.

For GIF-cytokine ligand blots, ^{125}I-GIF was prepared as described in Section 3.3.3.i. Two hundred to 350 ng of each cytokine was separated by 15% SDS-PAGE under reducing and non-reducing conditions and then transferred to nitrocellulose membranes. After blocking and washing, the membranes were incubated with ^{125}I-GIF (100 pM) for 2h at RT. After further washings, cytokine-GIF binding was visualised by autoradiography. In order to demonstrate the specificity of ^{125}I-GIF binding, a 10 nM concentration of unlabelled GIF was used for competitive inhibition of binding of ^{125}I-GIF to the cytokines.

2.4.3. Scatchard Analysis of GIF reactivity

The affinity binding of GIF to ovGM-CSF and ovIL-2 was determined by Scatchard analysis of ^{125}I-cytokine-GIF soluble binding assay as described by Symons *et al* (1990).

RovIL-2 and rovGM-CSF (25 μg) were radio-iodinated by the chloramine T method. The ^{125}I-rovIL-2 fraction was found to contain significant levels of contaminating radio-labelled protein (presumed to be ^{125}I-BSA from trace amounts of FCS in the supernatant from the rovIL-2 CHO transfected cultures) and was further purified by a second S200HR gel filtration stage (Fig. 2.6). Fractions from

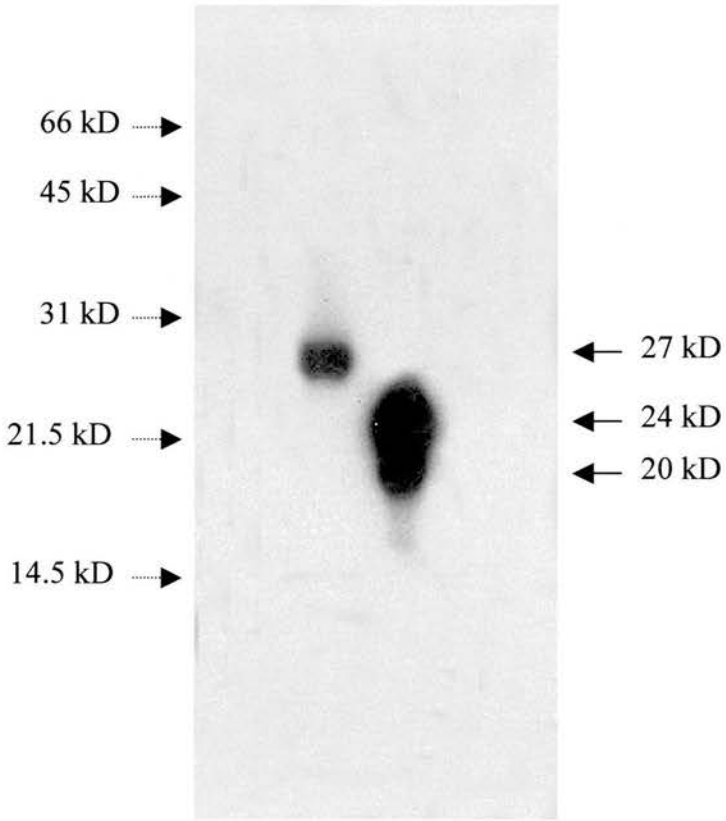

Fig. 2.6 SDS-PAGE analysis of ^{125}I-rovIL-2 and ^{125}I-rovGM-CSF. After radio-iodination and further purification of ^{125}I-rovIL-2 by S200 gel filtration to remove contaminating radio-labelled proteins both ^{125}I-rovIL-2 (27 kD; lane 1) and ^{125}I-rovGM-CSF (20kD and 24 kD; lane 2) were analysed by SDS-PAGE followed by autoradiography. (The 24 kD band of ^{125}I-rovGM-CSF represents a glycosylated form of the 20 kD band). The position of molecular weight markers (14.5 kD-66 kD, dashed arrows) are indicated.

S200HR gel filtration containing ^{125}I-rovIL-2 were pooled and concentrated ten-fold by ultrafiltration in Centricon YM-10 devices. The concentration of each radio-labelled cytokine was estimated by separation of 10 µl aliquots on 12 % SDS-PAGE followed by silver-staining and comparison with a range of concentrations of chymotrypsinogen analysed by micro-densitometry as described previously (Figs. 2.7 and 2.8).

The specific activity of each radio-ligand was calculated as follows;

1.) ^{125}I-GM-CSF count = 384 x 10^6 dpm/ml

Counting efficiency = 86%

Concentration ^{125}I-GM-CSF = 14.2 µg/ml (estimated from microdensitometric analysis)

Specific activity (MBq/mg) = [(count dpm/ml/0.86)/6 x 10^4 dpm/ kBq]/14.2 µg

= 524 kBq/µg = <u>524 MBq/mg</u>

Molecular mass of rovGM-CSF = 20 kD

Specific activity (TBq/mM) = (specific activity MBq/mg x molecular mass mg/mM)

= <u>10.48 TBq/mM</u>

2.) ^{125}I-IL-2 count = 119 x 10^6 dpm/ml

Concentration ^{125}I-IL-2 = 12.5 µg/ml (from microdensitometry)

Specific activity (MBq/mg) = <u>184.5 MBq/mg</u>

Molecular mass of rovIL-2 = 26.8 kD

Specific activity (TBq/mM) = <u>4.94 TBq/mM</u>

A soluble-ligand-binding assay was performed for each cytokine. Briefly, 50 µl volumes of a range of ^{125}I-rovGM-CSF (2-300 pM) and ^{125}I-rovIL-2 (5-1000 pM)

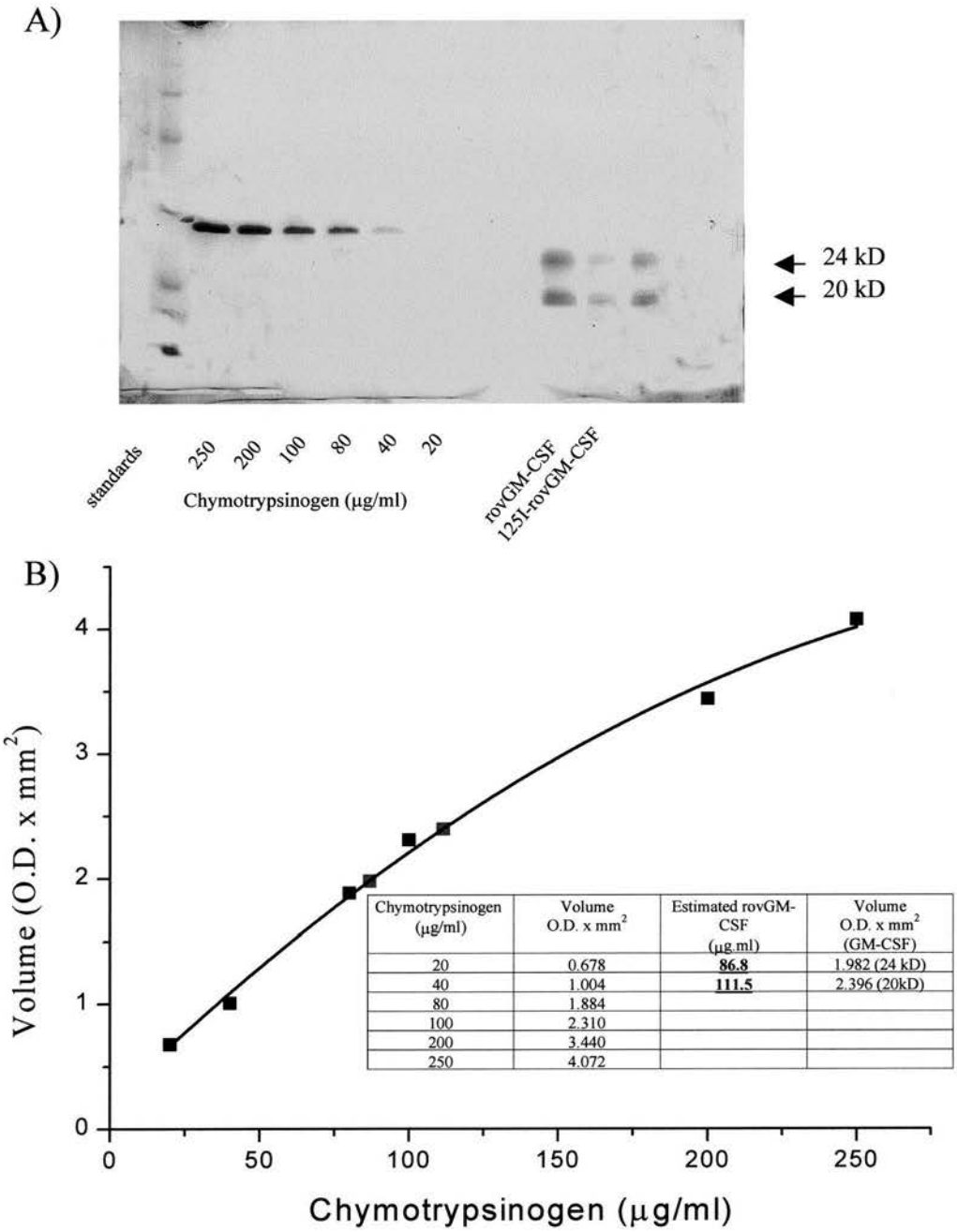

Chymotrypsinogen (µg/ml)	Volume O.D. x mm^2	Estimated rovGM-CSF (µg.ml)	Volume O.D. x mm^2 (GM-CSF)
20	0.678	**86.8**	1.982 (24 kD)
40	1.004	**111.5**	2.396 (20kD)
80	1.884		
100	2.310		
200	3.440		
250	4.072		

Fig. 2.7 Estimation of rovGM-CSF concentration by microdensitometry. A) The optical densities of protein bands separated by 15% SDS-PAGE and silver stained were determined by microdensitometry. The optical densities (1.982 and 2.396 O.D. x mm^2) of both silver stained ^{125}I-rov GM-CSF bands at 20kD and 24 kD were compared with the optical densities of different chymotrypsinogen concentrations (20-250 µg/ml) from which a standard curve (B) was generated. The standard curve (y-axis, O.D. x mm^2 vs x-axis, µg/ml) was generated in the Molecular Analyst Program (BioRad) using a quadratic non-linear fit from which the concentration of ^{125}I-rovGM-CSF was estimated (underlined).

A)

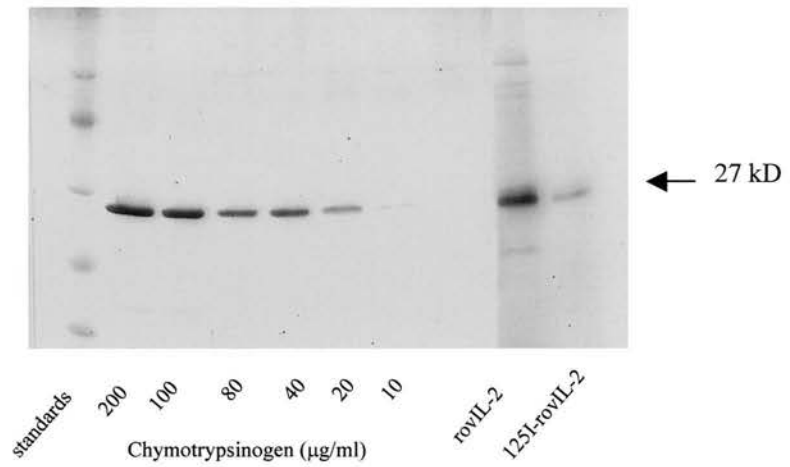

B)

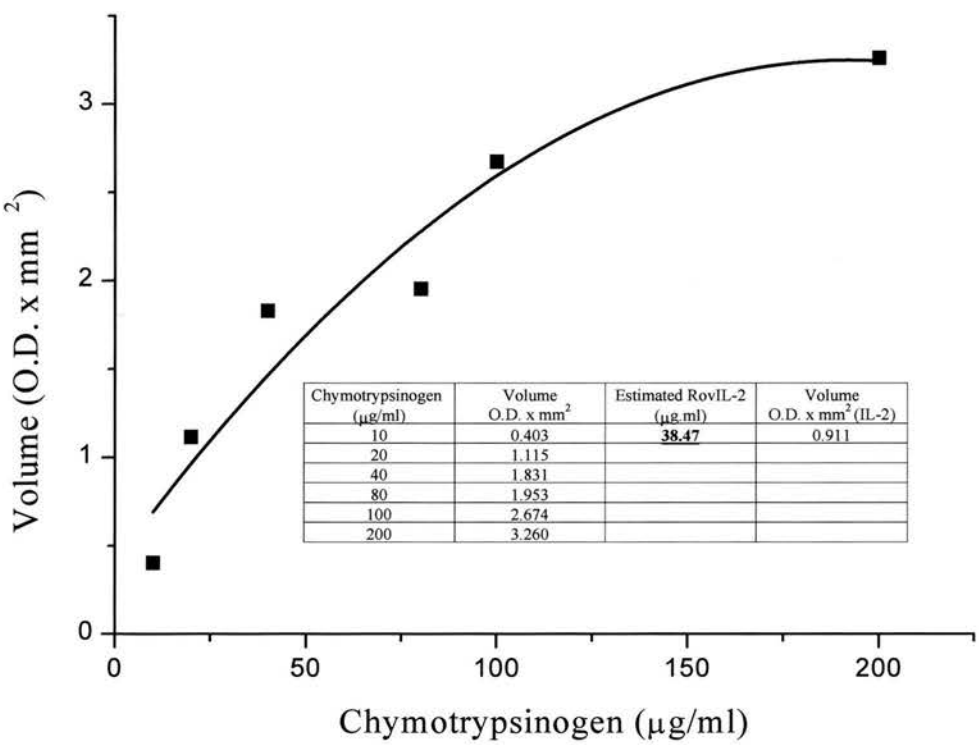

Chymotrypsinogen (μg/ml)	Volume O.D. x mm^2	Estimated RovIL-2 (μg.ml)	Volume O.D. x mm^2 (IL-2)
10	0.403	**38.47**	0.911
20	1.115		
40	1.831		
80	1.953		
100	2.674		
200	3.260		

Fig. 2.8 Estimation of IL-2 concentration by microdensitometry. The optical densities of protein bands separated by 15% SDS-PAGE and silver stained were determined by microdensitometry as described for Fig. 2.8. The optical density (0.911 O.D. x mm^2) of a silver stained ^{125}I-rovIL-2 band at 27 kD was compared with a range of band optical densities of different chymotrypsinogen concentrations (10-200 μg/ml).

were incubated with 100 µl of GIF (100 ng) containing 5% FBS for 2h at RT. Bound proteins were precipitated by the addition of 300 µl of 20 % polyethylene glycol (PEG 6000; Sigma) in PBS and incubation on ice for 30 min. The material precipitated from each sample was collected onto GF/C filter discs (Whatman, Maidstone, U.K.) by filtration under vacuum and after washing with four 10 ml volumes of ice cold PEG 6000 in PBS. Radio-labelled complex was measured by counting the discs in the γ-scintillation counter. The levels of non-specific binding of ^{125}I- cytokines to the filters were obtained in the absence of GIF and the data presented adjusted accordingly. Scatchard analysis as outlined by Segel (1976) was performed on best-fit plots (bound ^{125}I-cytokine [pM, x-axis] versus bound /free [cpm, y-axis]) performed on three separate sets of data for each cytokine using Origin software (Microcal).

2.5. Analysis of GIF inhibition of cytokine binding to cell receptors

GIF was tested for inhibition of ^{125}I-rovGM-CSF binding to GM-CSF receptors on sheep neutrophils and ^{125}I-rovIL-2 binding to IL-2 receptors on sheep CD4$^+$ T cells.

2.5.1. Preparation of ovine neutrophils

In order to measure the binding of GM-CSF to its cellular receptor, neutrophils were isolated from sheep peripheral blood (Nash *et al*, 1997). To minimise contamination of the neutrophil fraction with eosinophils, animals were treated with anti-helminthic for 1-2 weeks prior to blood collection. A 50 ml volume of blood was collected by venipuncture of the jugular vein and immediately mixed with 10 ml of a

solution (ACD) containing 2.2% trisodium citrate, 0.8% citric acid and 2.5% glucose to minimise clotting. Thirty ml volumes of blood were centrifuged at 1500 x g for 30 min without braking and the buffy coat and plasma removed without disturbing the red blood cell (RBC) pellet. The RBC pellet was then resuspended in 15 ml warm (37°C) pyrogen-free water and agitated for 1 min in a 37°C water bath before the addition of 1.5 ml 10x Tyrode's solution consisting of 8% sodium chloride, 0.2% potassium chloride, 0.05% sodium dihydrogen orthophosphate, 1% sodium bicarbonate and 1% glucose. The suspension was then centrifuged at 800 x g for 10 min.

After discarding the supernatant, the cell pellet (between 0.75 - 1.5 $x10^7$ cells total) was resuspended at 2 x 10^6 cells/ml in Hanks' balanced salt solution (HBSS/T, Gibco-BRL) containing 0.1% gelatin and adjusted to pH 7.2 with 1 M Tris-HCl. Approximately 10^5 cells in 200 µl of HBSS were spun down at 6000rpm for 10 min in a Cytospin3 (Shandon) cyto-centrifuge for cytosmears and stained with Leishman's staining solution for a differential count. (Fig. 2.9)

2.5.2. Preparation of ovine $CD4^+$ T cells

Mesenteric lymph nodes were collected post mortem into Hanks' balanced salt solution containing 5 % heat inactivated FBS (Sigma) and 25 µg/ml penicillin and streptomycin (Gibco-BRL) (HBSS). The nodes were then transferred to a 60 mm petri dish, trimmed and finely chopped with a scalpel blade in 5 ml of HBSS. The suspension was transferred to a stomacher bag and processed in a Stomacher 80 (Camlab Ltd. Cambridge, U.K.) for approximately 10 secs. The disrupted tissue was filtered through a double layer of sterile lens tissue that was rinsed with 5 ml of

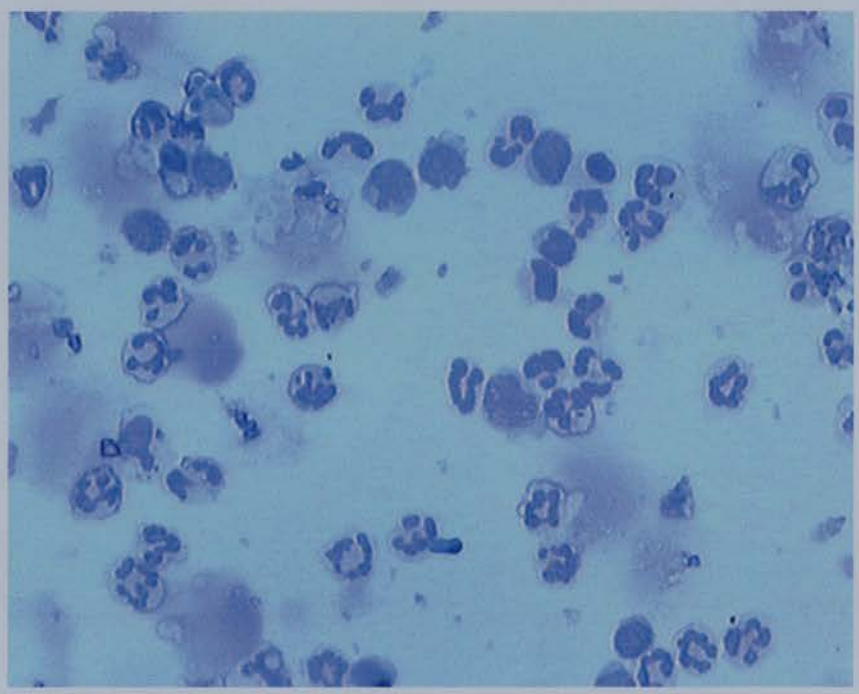

Fig. 2.9 Preparation of neutrophils from ovine peripheral blood. Light micrograph (x 400) of a cytocentrifuged cell suspension, isolated from the cell pellet after hypo-osmotic lysis of red blood cells.
Polymorphonuclear leucocytes (multi-lobed nuclei stained with Leishman's solution) comprise approximately 84% of 500 cells counted in the cytospot

.

HBSS. The filtrate was collected, spun down at 1200 rpm for 5 min and resuspended in 5 ml of HBSS. Lymphocytes were isolated by centrifugation over Lymphoprep (Nycomed, Oslo, Norway) and washed twice in HBSS.

A $CD4^+$ T cell-enriched fraction was prepared from the lymphocyte population by magnetic cell sorting (MACS). $CD8^+$, γδT cells and B cells were labelled with magnetic microbeads coated with specific antibody and then separated using a magnetic separation column placed in a strong magnetic field. The magnetically labeled cells were retained in the column while non-labelled cells (enriched for $CD4^+$ T cells) passed through. Lymphocytes (10^7) were resuspended in 1ml of pre-chilled HBSS containing 5 μg/ml each of an anti-CD8 (7C2; Mackay *et al*, 1986), anti-γδ TCR (86D; Hunig, 1985) and anti-B cell immunoglobulin (VPM8; Hopkins and Dutia, 1990) mAb and incubated for 15 min at 6-12°C (in refrigerator). Cells were washed carefully and resuspended in 80 μl of HBSS/ per 10^7 cells then 20 μl of MACS rat anti-mouse IgG magnetic microbeads (Miltenyi Biotec, Bisley, U.K.) added for a further 15 min at 6-12°C. The magnetically labelled suspension was then loaded onto a MiniMACS (Miltenyi Biotec) separation column (10^7 cells/column) as outlined in the manufacturer's instructions and unlabelled cells collected in the effluent. Aliquots (10^6 cells) were taken from the unlabelled cell fraction to determine the percentage of $CD4^+$ T cells present (Fig 2.10). The cells were resuspended in 100 μl of PBS 2% BSA, 0.02% sodium azide and 1 μg/ml of anti-CD4 mAb (17D; Mackay *et al*, 1986) or 1 μg/ml of an isotype matched negative control mAb VPM21 (specific for border disease viral epitope and obtained from Gary Entrican, Moredun Research Institute) and left for 1hour on ice. The cells were washed twice in 5 ml of PBS/BSA then resuspended in 100 μl of a 1:50 dilution of

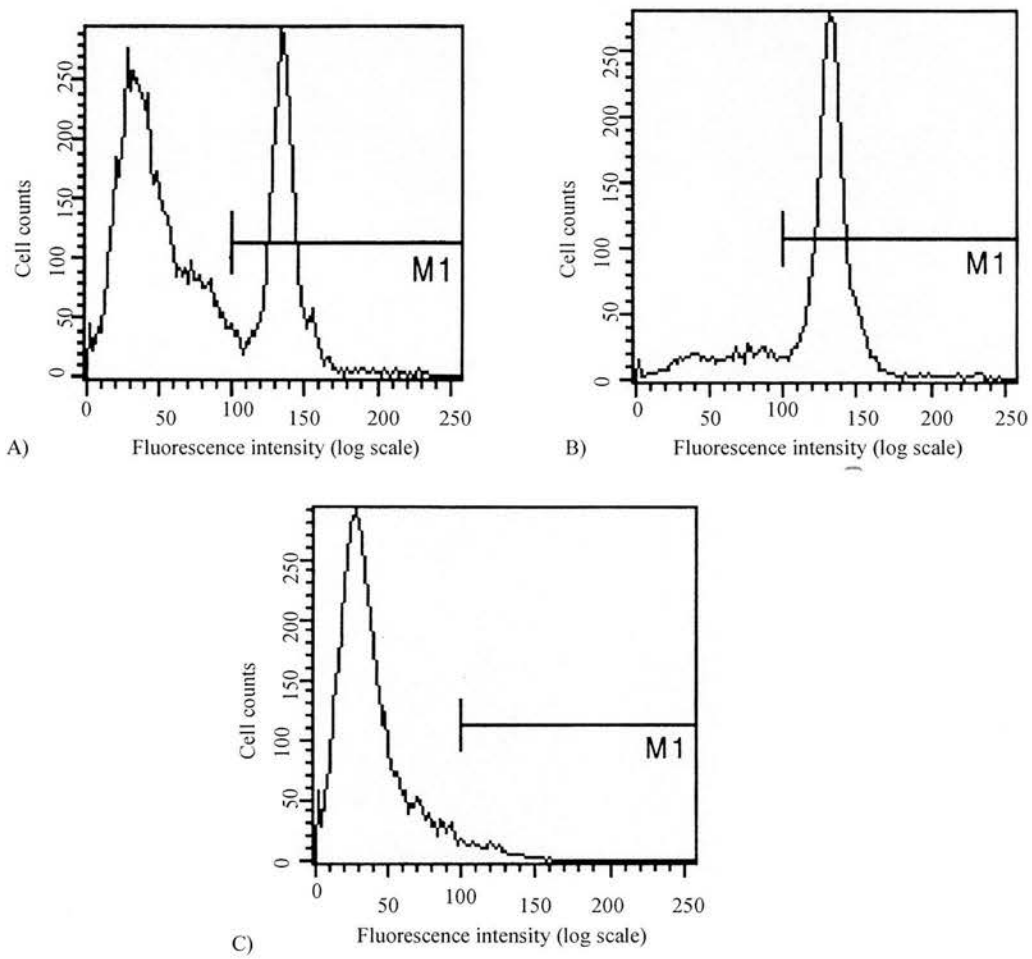

Fig. 2.10 Immunofluorescent analysis of $CD4^+$ T cells.
Lymphocytes from sheep mesenteric lymph node were analysed for $CD4^+$ T cells by flow cytometry using specific mAb 17D before (A) and after (B) depletion of $CD8^+$, $\gamma\delta$ T^+ and B cells. The percentages of $CD4^+$ T cells were as measured by fluorescence intensity within the gate, M1 (determined by comparison with (C) the negative control mAb VPM 21) were A) 32% and B) 89.8%.

fluoroscein (FITC)-conjugated rabbit anti-mouse IgG (Dako, High Wycombe, U.K.) and incubated for 1 hour on ice. After washing, cells were resuspended in 400 μl of PBS before the addition of 100 μl of 4% paraformaldehyde in PBS. The fixed cell suspensions were analysed by flow cytometry on a Facscan (Becton Dickinson, Franklin Lakes, U.S.A.).

2.5.3. Binding assays of ^{125}I-cytokines to cells

The binding of ^{125}I-rovGM-CSF or ^{125}I-rovIL-2 to neutrophil or $CD4^+$ T cell fractions respectively were carried out as suggested by Dr. Antonio Alcami (Department of Pathology, University of Cambridge, U.K.) and based on a method described by Dower *et al*, (1985). Cells were washed twice in binding buffer comprising RPMI 1640 (Gibco-BRL) containing 1% FCS and 20 mM Hepes pH 7.5 then added at 2 x10^6 in 50 μl to 250 μl of binding buffer containing ^{125}I-labelled cytokine (0.1-1nM) for 2h at 4°C. Pretreatment of cytokine with unlabelled cytokine (100nM), GIF (10nM), GIF and anti-GIF (ra101, 2 μg/ml) was carried out at 4°C for 60 min, 60 min and 90 min respectively prior to the addition of the cells.

Cells were isolated from the reaction mix by centrifugation of the cell suspension (300 μl) through 400 μl of a phthalate oil mix comprised of a 1.5 parts of dibutyl phthalate (Sigma) and 1 part of bis(2ethylhexyl)phthalate (Sigma) at 13000 x g for 1 min in 1.5 ml eppendorf tubes. The supernatant was carefully removed and the tip of the tube containing the cell pellet removed with a surgical blade and cell bound radioactivity measured in a γ-counter.

2.5.4. Investigation of GIF inhibition of cytokine stimulatory activity

GIF was tested for inhibition of rovGM-CSF stimulatory activity as measured by a bone marrow soft agar clonogenic assay and rovIL-2 stimulatory activity as measured by $CD4^+$ T cell proliferation assay.

i). Bone marrow soft agar clonogenic assay

GM-CSF stimulation of neutrophil, macrophage, and eosinophil colony development was measured using a soft agar haemopoietic cell clonogenic assay as described by Haig (1997).

Sternal bone marrow cells were obtained from lambs (aged 4 months to 1 year and bred at the Moredun Research Institute) at postmortem. Bone marrow was collected into universals containing 15 ml of HBSS and allowed to settle for 5 min A cell suspension was removed, by syringe from beneath a layer of fat that formed at the top of the universal and filtered through a double layer of sterile lens tissue. Light-density cells (<1.077 g/ml) were prepared from the filtered cell suspension by centrifugation over Lymphoprep (Nycomed). The interphase cells were washed several times in HBSS containing 5% heat-inactivated FBS (Sigma) then resuspended in culture medium, Iscove's modified Dulbecco's modified Eagle's medium (IMDM; Gibco-BRL), at 10^6 cells/ml.

Samples to be tested that included GIF (50 and 520 ng/ml), rovGM-CSF (46, 460 and 4600 pg/ml), rovIL-3 (50 ng/ml) and rabbit anti-GIF (ra101; 2 μg/ml) in a final volume of 200 μl were added to duplicate 35 mm Petri dishes. A 3 % solution of Bacto agar (Difco Laboratories, Detroit, USA) in PBS was prepared by boiling gently, then for each set of 8 dishes, 1 ml of hot agar was transferred to 6.5 ml of IMDM. To this was added 0.5 ml of the cell suspension and the mixture stirred

slowly, avoiding air bubbles. The cells were then dispensed as 0.8 ml aliquots (5 x 10^4 cells/plate) to each dish, ensuring even distribution of the agar and cells.

The medium was allowed to gel for 15 min, then two 35 mm dishes were placed, together with an open 35 mm dish containing distilled and de-ionised water in a 90 mm Petri dish. Lids were then placed on the 90 mm dishes which were incubated for 7-14 days, stacked in a tissue culture incubator at 37°C in a highly humidified atmosphere containing 5% CO2 in air. The analysis of live cell colonies (> 40 cells) and clusters (3-40 cells) were performed on day 7 and again on day 14. The cell count was carried out using an inverted microscope at low power and with the culture dishes placed on a glass plate on which a grid of 2-3 mm^2 squares had been scratched with a diamond pencil.

ii). $CD4^+$ T cell proliferation assay

$CD4^+$ T cells were set up at 2 x 10^6 cells /ml in IMDM containing 10 % FBS, penicillin, streptomycin and 5 μg/ml Con A (Sigma) in 24 well culture plates (Costar) for 3 days at 37°C in the presence of 5 % CO_2 in air. The number of blast cells was determined in Leishman-fixed and stained cytospots of the cell suspension (Haig *et al*, 1996e). The cells were washed and set up in culture in 24 well plates at 5 x 10^5 blasts/ml in IMDM with 10 % FBS and recombinant human IL-2 (Chiron Inc. [formerly Eurocetus], Emeryville, USA) at 20 U/ml for a further 3 days. The cells were washed with IMDM containing 2 % FBS to remove IL-2 and 100 μl of T cell blasts at 5 x 10^5/ml were added to each well of a 96 well plate (Costar). A further 100 μl containing a range of rovIL-2 dilutions (final concentration; 10pg-100ng/ml) in IMDM and either affinity purified GIF (final concentration; 520 ng/ml and 50

ng/ml) or medium were added to quadruplicate wells. After 24 hours, the cultures were pulsed with ^{3}H -thymidine (APB, specific activity 185 GBq/mmol), at 18.5 Mbq/well for a further 24 h before cell harvest onto glass fibre sheets in a Micromate 196 cell harvester (Packard). Incorporated ^{3}H -thymidine in each sample was measured by counting the dried sheets in a Matrix 96 direct beta counter (Packard).

2.6. Detection of GIF and GM-CSF in skin and lymph of sheep infected with orf virus

2.6.1. Immunohistochemistry

Conventionally reared female Suffolk-cross sheep aged between 12 and 14 months were used. All had previous experience of sub-clinical orf virus infection as evidenced by serum ELISA tests for virus-specific antibody (Yirrell *et al*, 1989). The inner thighs were clipped and two days later, scarified (Jenkinson *et al*, 1990a; McKeever *et al*, 1988). Orf virus prepared from scab material and kept as a stock at MRI (McKeever *et al*, 1988) was immediately applied to the scarified skin of half the group of animals and diluent (PBS) to that of the remainder which were housed separately. Skin samples, 6mm in diameter, were taken by biopsy punch from each animal before scarification (day 0) and subsequently across the scar lines at two-three day intervals for up to 21 days.

The skin samples were fixed for 2-3h at 4°C in a cacodylate/formalin solution (4% formaldehyde, 6.8% sucrose in 0.1 M cacodylic acid) and processed to paraffin wax by the St. Marie method (Pearse, 1980). Serial sections, each 10 μm thick, were cut from each block and mounted on Vectabond-coated microscope slides that were air-dried overnight at 38°C and stored at –20°C. Sections were de-waxed in 3 changes of xylene for 5 min each, followed by re-hydration for 20 min in 100%, 95%

and 75% ethanol and finally distilled water. The slides were washed twice in PBS buffer (pH 7.5) containing 0.05% Tween 80 (wash buffer). The sections were dried and the area around the slide isolated by wax pen (PAP pen, Sigma) before 100 µl of blocking solution comprising 25% horse serum in PBS with 0.5 M NaCl (high salt buffer, pH 7.5) was added for 30 min at RT. Slides from every sample were immunostained using a murine mAb for orf virus 39 kD envelope antigen (10E6; Housawi *et al*, 1998), mAb 3C2 and IgG fractions of 1.) rabbit anti-GIF (ra101) and 2.) a rabbit polyclonal antiserum for GIF (ra161) raised against GIF 28 kD–thioredoxin fusion protein expressed in *E. coli* and isolated by electro-elution from a 12% Schagger gel system (Schagger *et al*, 1988) (by Ann Wood and Colin McInnes) and 3.) a mouse polyclonal antiserum for purified GIF (muLT1). Ra161 was raised as described for ra101 (Section 2.2.4.). MuLT1 was raised by injecting Balb/c mice intraperitoneally with firstly, 2-5 µg of purified GIF in 150 µl of a 1:1 mixture of PBS and complete Freunds adjuvant, then at three, 30 day intervals with the same inoculum but in the presence of incomplete Freunds adjuvant. Ten days after the final injection, the mice were exsanguinated. Immunoglobulin-G fractions from pre-immunised mouse serum and pre-immunised rabbit serum were used as controls. Dilutions of primary antibodies at 0.1 –1 µg/ml were made in high salt buffer and incubations were carried out overnight at 4°C in a humidified box. Sections were washed as before and 100 µl of a 1:1000 dilution of biotinylated horse anti-mouse IgG (Vectastain, Vector Laboratories, Peterborough, U.K.) in high salt buffer containing 1% horse serum added to each section for 30 min at RT. After washing endogenous peroxidase activity was blocked by incubating the slides in 1% hydrogen peroxide (30% solution, Sigma) in methanol for 30 min.

The Vectastain ABC reagent was prepared as per the manufacturer's instructions at least 30 min prior to use. After washing 100 µl Vectastain ABC reagent was added to each section for 30 min at RT. After a further washing stage, bound antibody was visualised by addition of DAB substrate solution provided with the Vectastain ABC reagent. After incubation in the dark for 5 min, sections were washed in water Sections were examined after counterstaining in hematoxylin using a Varistain automated staining apparatus (Shandon, Runcorn, U.K.).

2.6.2. Analysis of lymph

The cannulation of lymph node ducts of orf virus-infected and control scarified sheep was carried out in a previous study by Professor High Miller and the techniques used have been described previously (Yirrell *et al*, 1991; Haig *et al*, 1996a and e). Briefly, at least eight weeks before cannulation for afferent lymph, the prefemoral lymph node was removed and the various afferent lymphatics allowed to anastomose (interconnect) with a single efferent duct. This was cannulated to provide pseudo-afferent lymph. Efferent lymph was obtained by cannulating an efferent lymphatic of the prefemoral lymph node as described by Hall and Morris (1962). For the duration of the experiment the animals were kept in metabolic crates. Lymph was collected in plastic bottles that were changed at regular intervals and contained heparin, penicillin and streptomycin.

Animals were rested for 2-4 days following surgery to allow lymph output to settle before scarification of the epidermis and application of live virus or UV-inactivated virus as described above.

For GIF and GM-CSF analysis, lymph samples were centrifuged at 250 x g for 10

min and lymph plasma and cells collected separately. Lymph plasma was re-centrifuged at 1000 x g for 15 min and then passed through a 0.45 μm filter (Millipore, Cramlington, U.K.) to remove any remaining cellular debris before being frozen at –20°C.

To determine whether cells in the lymph were producing cytokine or GIF as a consequence of *in vivo* activation, cells were washed three times in Hanks balanced salt solution containing penicillin/streptomycin and 2% fetal calf serum (FCS) (to remove exogenous cytokines) and then cultured at 2-4 x 10^6 nucleated cells/ml of IMDM + 10% FCS in wells of 24 well tissue culture plates (Costar) or 25 cm^2 tissue culture flasks (Costar) without exogenous stimulation. No GM-CSF was detected in the FCS used in this experiment. Cultures were maintained at 37°C for 24h before supernatant fractions were collected and stored at –20°C prior to analysis by GM-CSF clearance ELISA.

CHAPTER 3

THE ISOLATION AND CHARACTERISATION OF THE ORF VIRUS GENE ENCODING GM-CSF-INHIBITORY FACTOR

3.1. Introduction

The first approach to the identification of the GM-CSF inhibitory/binding activity was to test the hypothesis that an orf virus protein and not a host cell protein is involved in GM-CSF inhibition. The precedence for this was the increasing number of poxvirus and herpesvirus 'immuno-modulatory' proteins described in the literature (reviewed by Davis Poynter *et al*, 1996; Smith, 1996; Alcami and Koszinowski, 2000 and Brander and Walker, 2000). Some of these viral proteins counteract the host immune system by binding to host cytokines and chemokines.

A recombinant vaccinia virus library of recombinant viruses containing between them more than 95% of the orf virus genome (a gift from Dr. Andy Mercer, University of Otago, Dunedin, New Zealand) was employed to identify the putative orf virus gene encoding the GM-CSF-inhibitory factor (GIF). In recent years, vaccinia virus has been used as an expression vector for foreign genes (Moss. 1991; Tartaglia *et al*, 1990). Fleming *et al* (1992) and Sullivan *et al* (1994) have shown that, for a number of orf virus genes, early and late promoter sequences are recognised by the vaccinia virus transcriptional machinery and, as a result, the orf virus genes are transcribed from their own promoters. This has circumvented the need to isolate each orf virus open reading frame (ORF) for fusion to a vaccinia virus promoter. Instead large fragments of orf virus DNA that carry multiple undefined genes can be recombined into vaccinia viruses and the recombinants screened for the expression of orf virus protein. Mercer *et al* (1997b) have constructed in vaccinia virus, an orf virus genomic DNA library consisting of 16 DNA restriction fragments of 10-20 kilobase pairs (kb) that together cover 95% of the orf virus genome in

overlaps. Each recombinant virus from the vaccinia virus-orf virus (VVOV) recombinant library was used to infect foetal lamb muscle cells and CV-1 cells. Supernatants from individual recombinant virus-infected cultures were then tested for GIF activity. GIF activity was assayed by inhibition of ovGM-CSF detection in an ovGM-CSF capture ELISA.

The next stage, if the first was successful, was to identify possible homologues of the GIF gene by comparing the GIF nucleotide and amino acid sequences with those sequences recorded in protein and nucleotide databases. Whilst it was possible that GIF was a homologue of a cellular protein, a number of poxvirus proteins have been identified that bind specific host cytokines and/or chemokines and show homology to host receptors. These include viral receptors for IFN, IL-1β and TNF (Smith and Chan, 1991; Upton *et al*, 1991; Barry and McFadden, 1997; Haig, 1998; McFadden *et al*, 1998).

To determine whether the GIF gene was transcribed early or late in the replication cycle of orf virus, two parallel approaches were adopted, firstly, Northern blot analysis of GIF mRNA isolated from orf virus infected FLM cell cultures treated with cytosine arabinoside (an inhibitor of viral replication) and secondly, Western blot analysis of supernatants from FLM cell cultures sampled at various times and analysed for the presence of GIF by the binding of a rabbit antiserum that was raised against affinity-purified GIF protein.

Finally, the question whether GIF activity was restricted to orf virus infections or whether it is also present in cultures infected with other parapoxviruses such as bovine papular stomatitis and pseudocowpoxvirus was also investigated by GM-CSF clearance ELISA and Western blotting.

In this chapter, all work that involved DNA/RNA manipulations was carried out by Dr. Colin McInnes and Miss Ann Wood (Moredun Research Institute). The results derived from this work are presented in order to give a clear overall picture. The analyses of cultures for GIF activity by ELISA, the expression in CHO cells of orf virus DNA containing the GIF gene and the subsequent isolation and identification of the GIF protein were carried out by the author.

3.2. Results

3.2.1. Mapping of the GIF gene to the OV genome

The VVOV recombinant library (Fig. 3.1) was expressed in CV-1 and FLM cells and supernatants from individual recombinants tested for GIF activity in the GM-CSF clearance ELISA (as outlined in Section 2.2.1.). The only regions of the orf virus genome not included in the library were sections of 1.3kb at each terminus and a 5kb gap between clones VVOV82 and VVOV85. The vaccinia-recombinants containing fragments of orf virus DNA were given the prefix VVOV and a clone number.

The results for the FLM cell cultures are given in Fig. 3.2. GIF activity, as measured by a decrease in O.D. units representing GM-CSF clearance in the GM-CSF ELISA, was detected in supernatant from the cultures infected with the VVOV85 recombinant ($p < 0.001$ when compared with either uninfected cells or cells infected with vaccinia virus, Lister control). GIF was not detected in cells infected with; VVOV330 (which overlaps the 5′ end of VVOV85 by approximately 1.4kb), the remaining members of the VVOV recombinant library or the vaccinia virus control. A similar result (not shown) was achieved with the infection of CV-1 cells.

In order to map the gene encoding GIF activity to a locus within orf virus DNA fragment 85 (rf 85), a number of plasmids that contained overlapping restriction fragments covering the entire rf 85 plus approximately 1kb of flanking DNA on either side were transfected into vaccinia virus-infected FLM cells (Fig. 3.3).

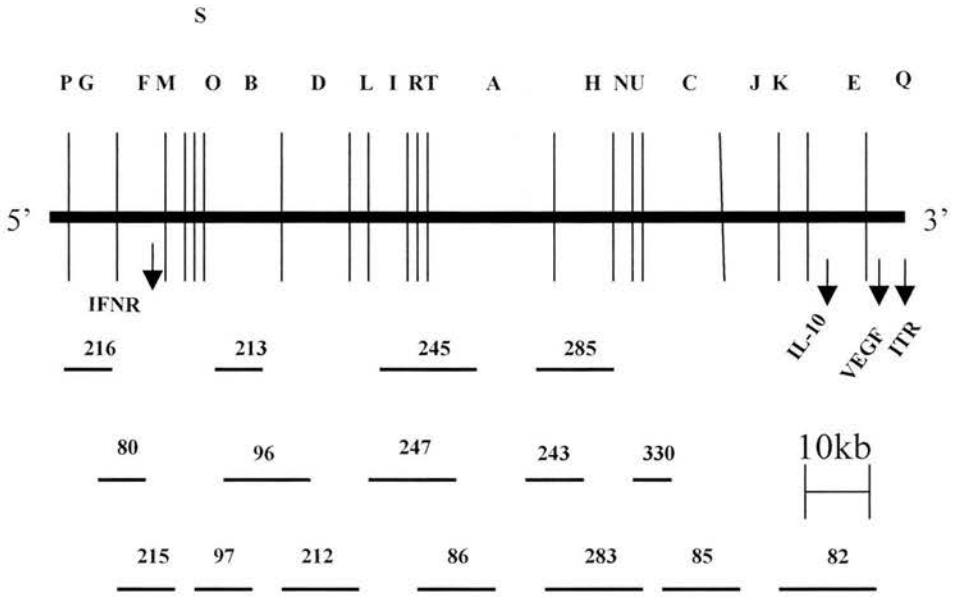

Fig. 3.1 Insertion library of orf virus genomic DNA (restriction fragments) aligned with the *KpnI* map of the orf virus (NZ2) genome (Mercer *et al*, 1997).
To determine whether ovGM-CSF inhibition was produced by a viral gene product, 16 vaccinia virus-orf virus recombinants containing orf virus DNA fragments (numbered, fine lines), the majority of which overlapped one another and together encompassed approximately 95% of the orf virus genome (heavy line), were used to infect FLM cells and the cell free supernatants tested for GIF activity.
The relative positions of the putative virulence genes; interferon resistance gene (IFNR), interleukin-10-like gene (IL-10) and vascular endothelial growth factor (VEGF) are shown marked on the orf virus genome.

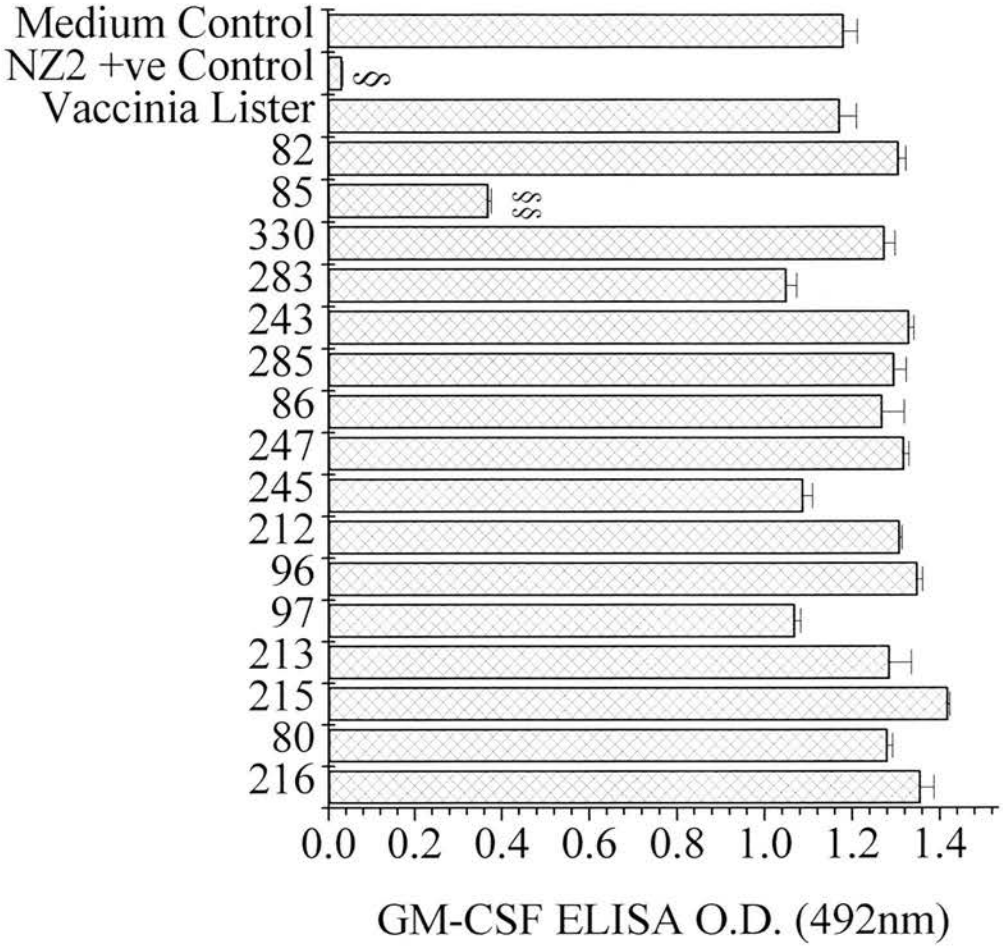

Fig. 3.2 Analysis of vaccinia virus-orf virus recombinants (VVOV, containing orf virus DNA) for expression of GIF activity.
The VVOV clones are numbered on the y axis. Cell-free supernate samples from FLM cell cultures infected with each VVOV recombinant virus were spiked with rovGM-CSF (4 ng/ml) and tested by GM-CSF ELISA for the expression of GIF.
GIF activity was measured as the decrease in O.D. units (x-axis) representing rovGM-CSF clearance in the ELISA. The presence of GIF activity is clearly seen in culture medium taken 24 hours after infection from FLM cells infected with orf virus NZ2 (+ ve control § $p < 0.001$) and VVOV recombinant 85 (§ § $p < 0.001$) when compared with control samples of medium alone. No GIF activity was found in cells infected with vaccinia virus alone. Values given represent the mean of 4 samples and standard error of the mean.

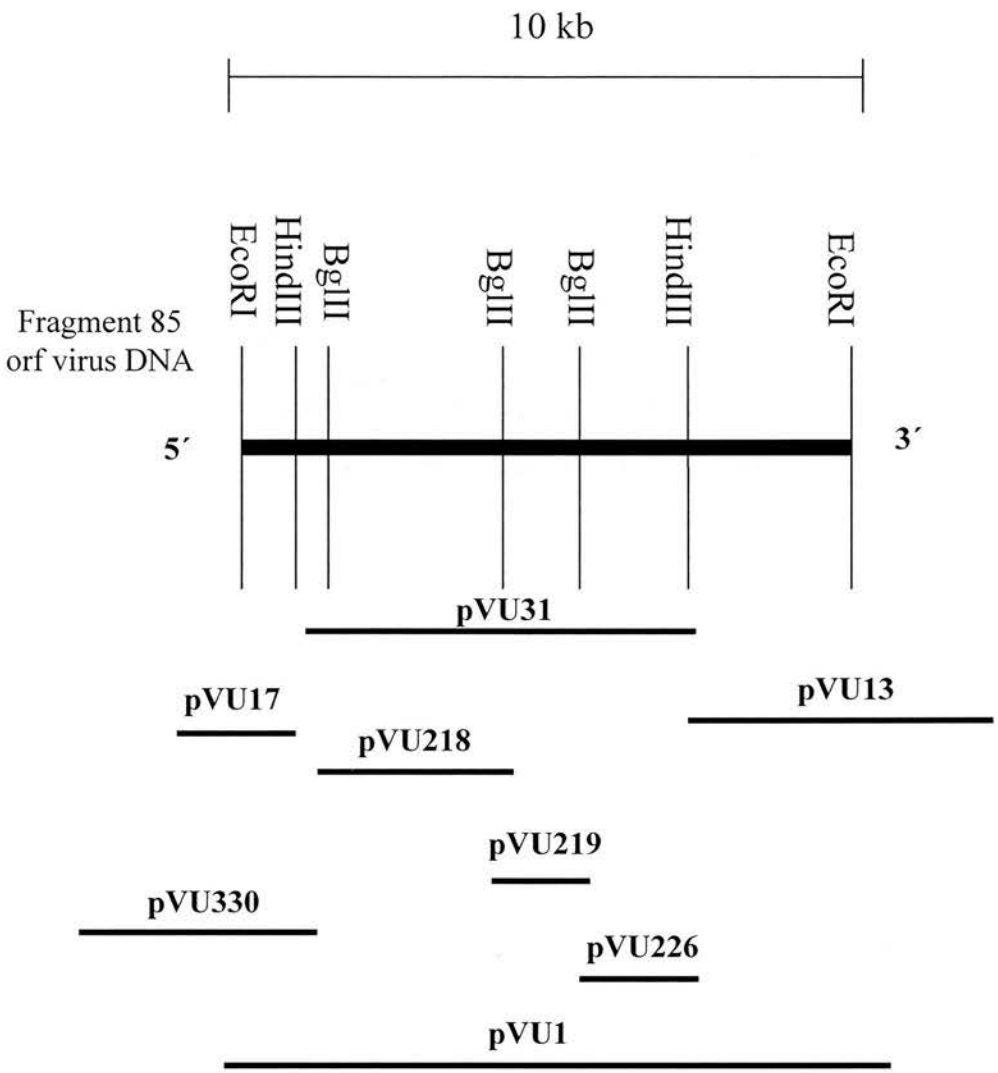

Fig. 3.3 Restriction map of fragment 85 from the genome of orf virus NZ2 and the alignment of subclones from that fragment.
In order to map the gene encoding GIF activity to a locus within restriction fragment 85 a number of overlapping restriction fragments (shown numbered and prefixed pVU) were cloned into the pUC8 expression vector. The resulting plasmids were transfected into FLM cells where orf virus gene expression was initiated and regulated by subsequent infection with vaccinia virus.
Supernatants from infected cell cultures were assayed for GIF activity.

The analysis of cultures of the subclones of rf 85 for GIF activity is given in Fig. 3.4A. GIF activity is clearly seen in cultures transfected with the plasmid pVU1 which contains the entire 10kb of DNA from rf 85 ($p < 0.001$ when compared with a medium control sample or cultures infected with vaccinia virus Lister strain). Of the other clones tested only FLM cells transfected with the plasmid pVU13 were found to express detectable levels of GIF activity ($p < 0.01$ when compared to the control samples). Neither of the clones, pVU31 or pVU226 that overlapped pVU13 at its 5′ end, expressed GIF. A major portion of the orf virus DNA insert of pVU13 covering 2.3 kb at the 3′ end of rf 85 was considered to contain the gene encoding GIF.

In order to determine the direction of transcription of the GIF gene(s) contained in pVU13, the 2.3kb fragment was ligated into the mammalian expression vector pEE14 in both orientations. The plasmids were transfected into CHO cells and the MSX-selected cultures tested for GIF activity (Fig. 3.4B). GIF was expressed by cultures transfected with the orf virus DNA fragment in the 5′-3′ orientation (pEE13.1).

Sequence analysis of clone pVU13 identified 2 potential single ORFs as candidates for the gene encoding the GIF protein. (A third ORF within pVU13 was discounted since its nucleotide sequence matched that of a vaccinia virus gene and was therefore considered unlikely to encode GIF activity).

PEE14 constructs containing both candidate ORFs (designated GM1 and GM2) isolated from DNA prepared from the NZ2 and Moredun Research Institute (prefix MRI) strains of orf virus were transfected into CHO cells. Transfected CHO cell

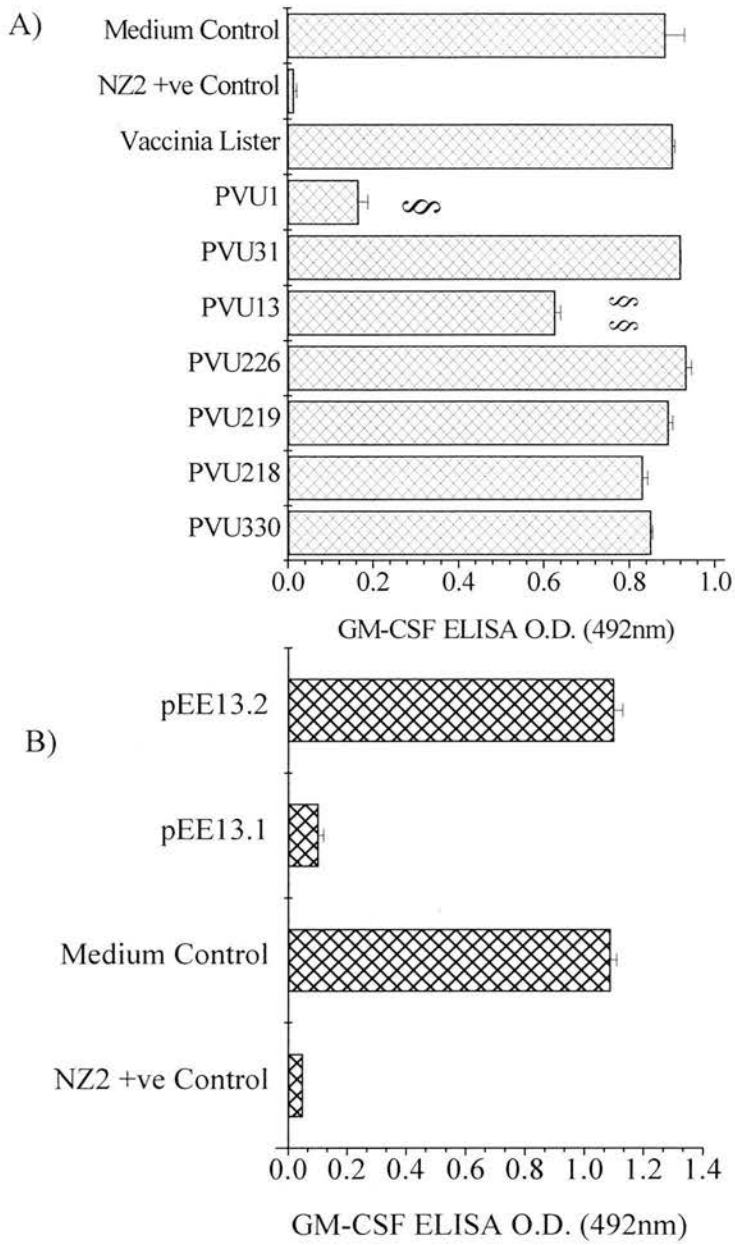

Fig. 3.4 Analysis of orf virus DNA restriction fragment 85 for expression of GIF activity.

A) Samples of supernatants from FLM cells transfected with restriction fragment DNA subclones (pVU series, y-axis) were taken at 20 hours post infection for GIF analysis by the GM-CSF ELISA. GIF activity is clearly seen in cultures transfected with plasmid pVU1 which contains the entire 10kb restriction fragment 85 (§ $p < 0.001$ when compared with medium control). The decrease in O.D. as observed with clone pVU13 indicates that GIF activity is present (§§ $p < 0.01$ versus medium control).

B) Testing for GIF activity in supernatants from CHO cells transfected with plasmid pEE14 that contained the 2.3 kb fragment of orf virus DNA (pVU13) in either orientation (pEE13.1 and pEE13.2). GIF activity was expressed from pEE13.1 but not pEE13.2 CHO transfectants.

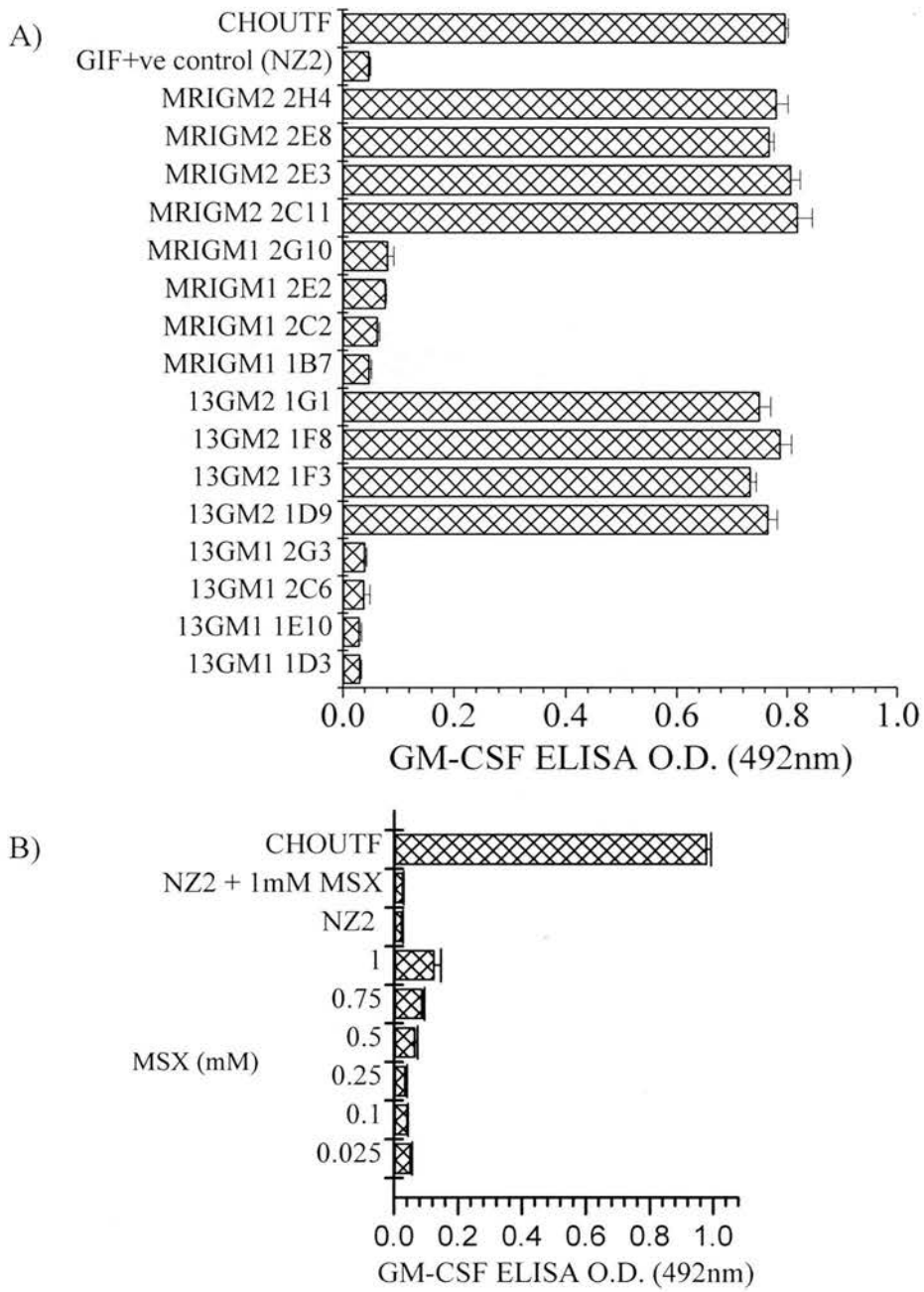

Fig. 3.5 Analysis of GM1 and GM2-transfected CHO cells for GIF expression.

A) The two open reading frames contained within the 2.3 kb restriction fragment of pVU13 and designated GM1 and GM2 were cloned into the mammalian expression vector pEE14 for transfection into CHO cells. Cell free supernatants from individual transfectant cell lines (numbered on the y-axis) were selected by growth in methionine sulphoxamine (MSX, an inhibitor of glutamine synthetase) then tested for GIF activity by GM-CSF ELISA.Plasmids containing DNA from NZ2 (13) and Moredun Research Institute (MRI) orf virus strains were compared for GIF expression.

B) Increasing concentrations of MSX were used to select cultures for high levels of GIF production as measured by low absorbances (x-axis, O.D. 492nm) in the GM-CSF ELISA. Subsequently GM1CHO cells were maintained in medium containing 0.25mM MSX. Samples from supernatants from fetal lamb muscle cells infected with orf virus (NZ2, positive control) with and without 1mM MSX and supernatant from untransfected CHO cells (CHOUTF, negative control) were included as controls.

clones were selected and tested for GIF activity (Fig. 3.5). GIF activity was detected in supernatant from GM1-CHO transfectants containing DNA from both NZ2 and Moredun orf virus strains ($p < 0.001$ when compared with medium control). CHO cells transfected with the GM2 plasmids did not express GIF. The GM1 ORF was mapped to a locus 20.1kb from the right hand terminus of the viral genome.

3.2.2. Isolation and identification of recombinant GIF

Expression of the recombinant GIF protein was carried out using the CHO cell transfectant clone NZ2GM1-1E10 (hereafter referred to as GM1-CHO). Supernatant from GM1-CHO cell cultures maintained at confluency for 4 days in serumless medium was separated over a GM-CSF-Sepharose affinity column (Fig. 3.6). Fractions were collected and analysed for GIF activity. GIF activity was recovered from the elution of bound material from GM-CSF Sepharose. In general, in order minimise the number of column runs and subsequent regeneration cycles, saturating volumes of supernatant (60-80ml) were applied to the column. Consequently significant levels of GIF were detected in the collection of unbound material.

SDS-PAGE analysis of the eluted fraction run under reducing conditions revealed 2 major proteins of 28kD and 43kD (Fig. 3.7).

Sequence analysis of the 20 N-terminal amino acids was carried out on each isolated protein band and is as follows;

28 kD: A Q C? I G E R D F F T A A A Q V V F A R

43 kD: S? Q L P V E A K T G N V Y Q T S N? A V? Y

(The ? after individual amino acid residues denotes some uncertainty with the identification of that residue.)

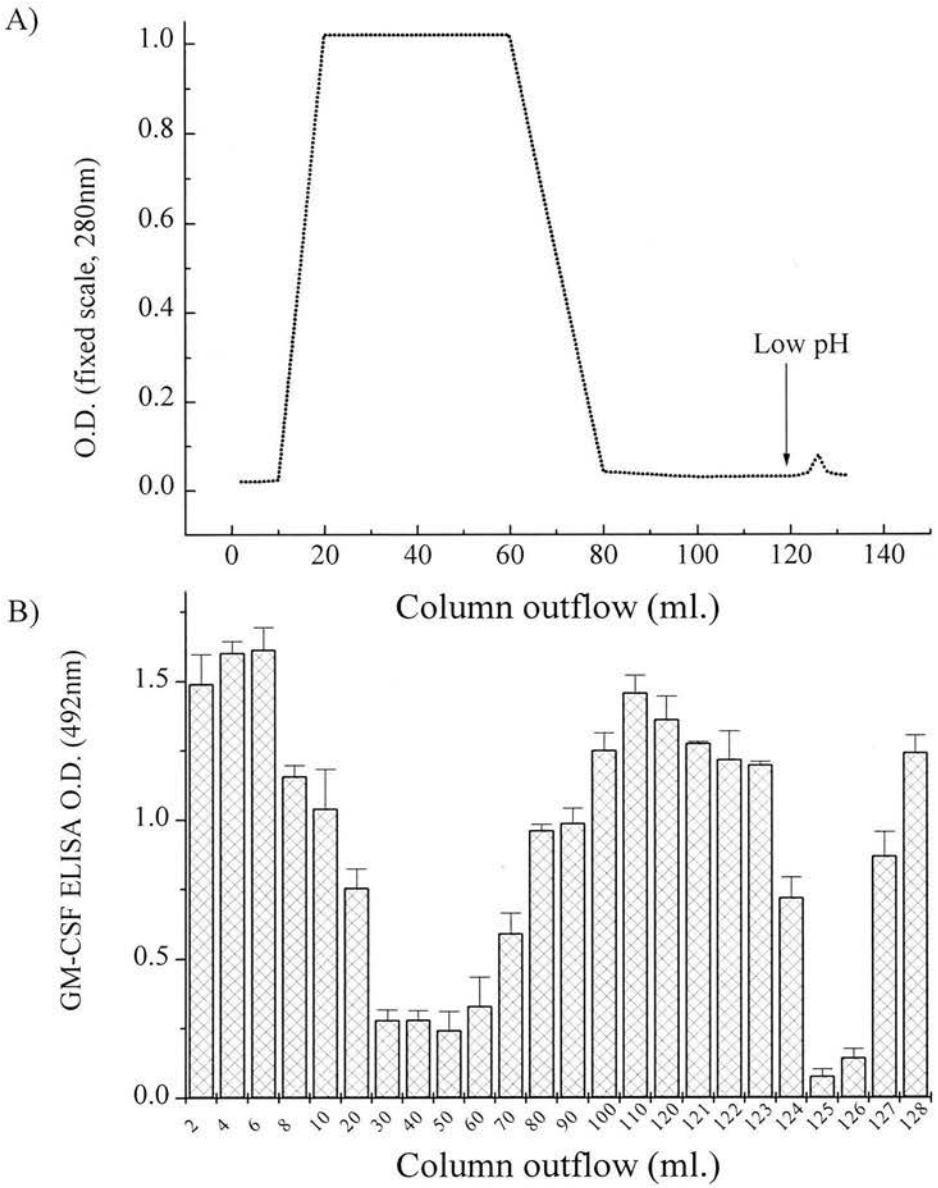

Fig. 3.6 Affinity purification of GIF activity from GM1-CHO transfectant cell cultures.
A) The O.D. (280nm) profile of the column outflow from a GM-CSF -Sepharose affinity column which was loaded with 60 ml of CFS from GM1-CHO cell cultures. After washing (80-120ml column outflow), bound protein was eluted with 0.1M glycine, 0.5M NaCl pH2.8 (Low pH) then neutralised with 1M Tris.
(In order to monitor eluted protein, the sensitivity of the spectrophotometer was set on a higher scale hence the fall-through peak is off-scale).
B) Column outflow fractions were analysed for GIF activity by GM-CSF ELISA. Values given represent the mean of 4 samples and standard error of the mean.

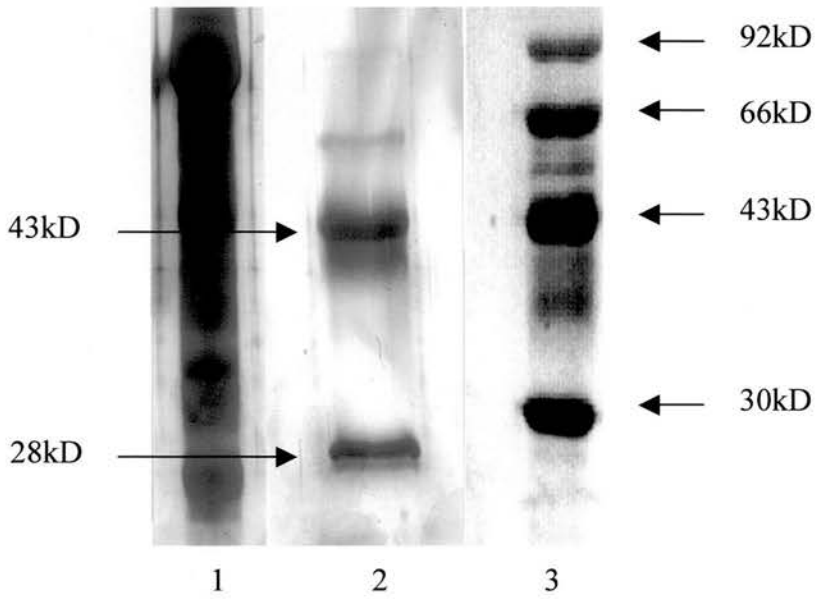

Fig. 3.7 SDS-PAGE analysis of affinity-purified GIF
Aliquots from unbound peak (lane 1) and eluted peak (lane 2) fractions that were collected from the chromatography of GM1-CHO supernatant on the GM-CSF-affinity column, were analysed by 12% SDS-PAGE run under reducing conditions.
Separated proteins were visualised by silver staining. The molecular masses of the major protein bands in the eluted fraction (28kD and 43kD) were calculated from a standard curve of molecular mass vs mobility for a range of molecular mass markers (lane 3) in Microcal Origin 5.0 using a log linear fit .

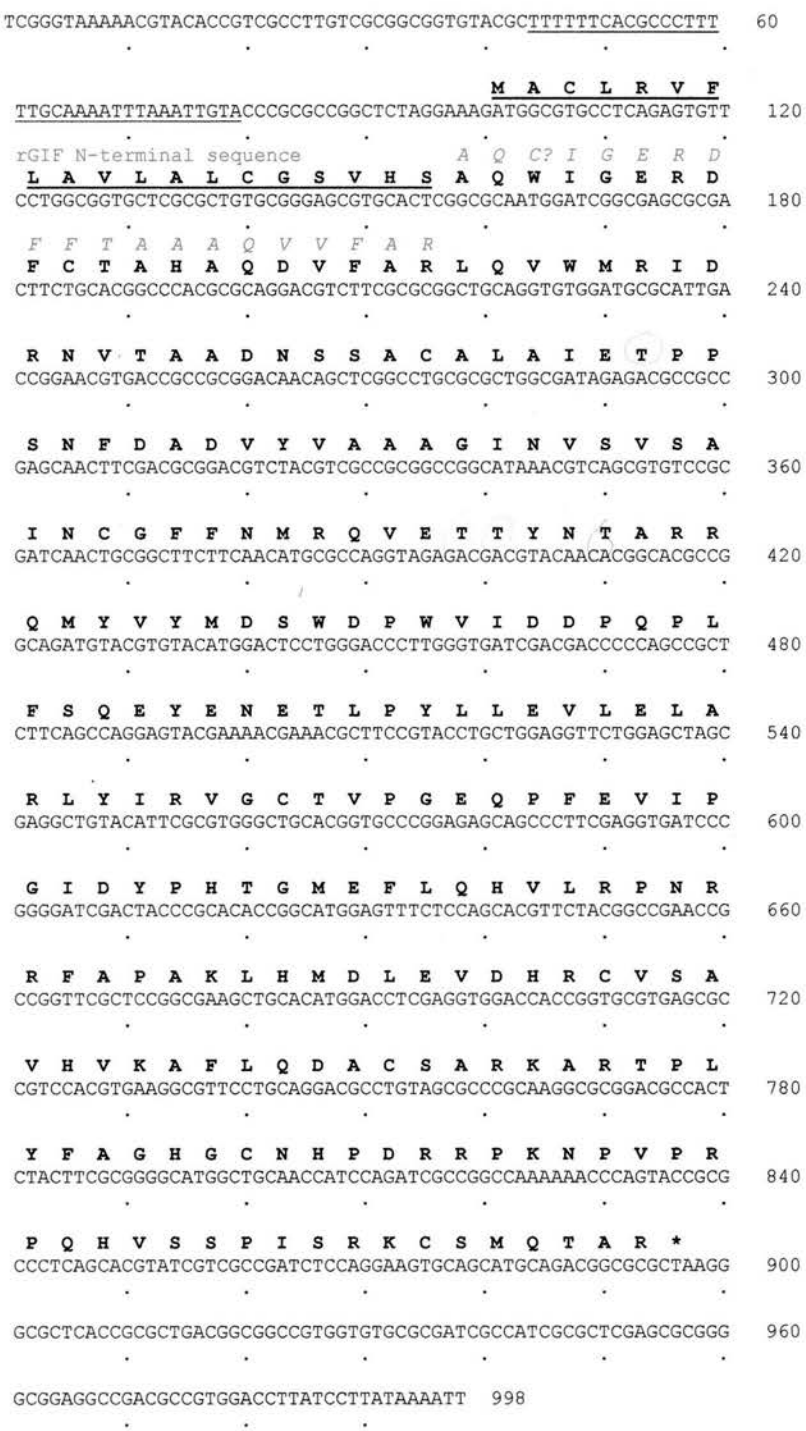

Fig. 3.8 The GIF gene sequence.
Alignment of the nucleotide sequence of open reading frame GM1 (plus 100 bases of flanking sequence 898-998) with the predicted amino acid sequence (bold type) and the sequence of 20 amino acids (italic type) as determined by the N-terminal analysis of the 28kD GIF protein. The first 19 amino acids (underlined) of the predicted a.a. sequence constitute a putative signal peptide.
The region of nucleotide bases containing potential transcription promoter and/or initiator sequences is also underlined
(figure and data courtesy of Colin McInnes).

Comparison of the N-terminal sequence of the 28kD protein with the predicted amino acid sequence computed from the nucleotide sequence of the GM1 ORF, resulted in an almost perfect matched alignment of 20 amino acids (Fig. 3.8, courtesy of Colin McInnes). The recombinant GIF sequence was shown to start at an alanine residue at position 20 of the predicted amino acid sequence and from this alignment a total GIF sequence of 246 amino acids with a putative signal peptide of 19 preceding amino acids was predicted. This polypeptide length corresponds to the observed 28kD molecular mass of the GIF protein. The N-terminal sequence of the 43kD protein did not align with the GIF predicted sequence.

The search for a sequence match for the 246 amino acid GIF sequence and the 20 amino acid sequence of the 43kD protein was carried out using the BLAST. The BLAST failed to return any significant match for the 43kD protein. For the GIF sequence, BLAST returned 4 protein matches with sequences that were similar. These sequences were; 1.) protein A41 precursor of variola virus with 33% identity over a sequence of 88 amino acid residues, 2.) protein A41 precursor of vaccinia virus (Copenhagen and Lister strains) with 32% identity over the same 88 amino acid sequence, 3.) chain 4 of NADH dehydrogenase with 48% identity over 27 residues and 4.) homologue 1 of the cell division protein FTSZ with 26% identity over 118 residues. The position of each protein sequence alignment relative to the GIF sequence is outlined in Fig. 3.9A. The 88 amino acid alignment of GIF with the A41 proteins occurred at the same position of the polypeptide chain in both GIF and A41 (the alignment of GIF and A41 of vaccinia virus is shown in Fig. 3.9B). When the alignments of NADH dehydrogenase and FTSZ with GIF were compared they did not occur at the same position on the respective polypeptide chains.

A)

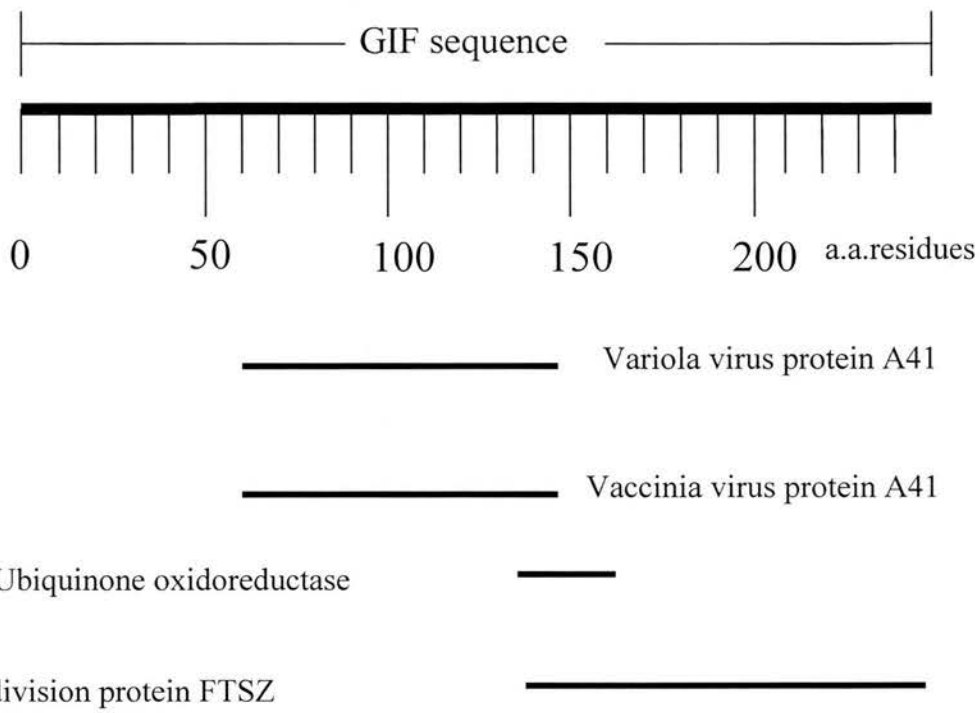

B)

OV GIF

```
57                                                                  116
VAAAGINVSVSAINCGFFNMRQVETTYNTARRQMYVYMDSWDPWVIDDPQPLFSQEYENE
V+  G+N+SV  +NC  F N  V    N  R  +Y    S DPW +    +P+ S  Y++
VSNGGLNISVDLLNC-FLNFHTVGVYTN--RDTVYAKFTSLDPWTM----PINSMTYDD-
64                                                                  116
```

Vaccinia virus A41

```
117                          144
TLPYLLEVLELARLYIRVGCTVPGEQPF
    L+++ E   + I + C V   + F
----LVKLTEECIVDIYLKCEVDKTKDF
117                          140
```

Fig. 3.9 Comparison of GIF amino acid sequence with sequences registered in the Swiss-Prot (37.0) and TREMBL (10.0) databases.
A) A BLAST search identified 4 protein entries that showed amino acid identity with the GIF sequence. The portion of matching polypeptide from each protein (broad lines) is shown aligned with its counterpart GIF sequence contained within the complete GIF sequence of 254 amino acid residues.
B) A more detailed amino acid sequence alignment of the regions of identity of GIF (residues 57-144, underlined) and vaccinia virus (residues 64-140). (Identical amino acids (italics) and conserved substitutions (+)between both sequences are outlined).

3.2.3. Characterisation of a rabbit anti-GIF

In order to facilitate the further characterisation of the GIF, a rabbit anti-GIF reagent was raised against the affinity-isolated GIF protein. The characterisation of the rabbit anti-GIF is outlined in Fig. 3.10. Pre-treatment of GIF with an IgG fraction of anti-GIF was effective in neutralising GIF-GM-CSF binding at dilutions of 1:200 when compared with GIF alone or GIF after treatment with a pre-immune rabbit serum (Fig. 3.10A).

Western blot analysis of supernatant from the GIF-producing GM1-CHO cell line with the anti-GIF revealed reactivity with the 28 kD peptide under reducing conditions (Fig. 3.10B) and both 56 kD and 28 kD peptides under non-reducing conditions (Fig. 3.10C). The anti-GIF also identified a 43 kD peptide expressed by GM1-CHO cells and the two control cell lines GM2-CHO and CHOUTF. Western blot analysis with the pre-immune rabbit serum failed to identify any peptide from the test samples.

3.2.4. Expression of GIF during orf virus infection <u>in vitro</u>

From base sequence analysis (carried out by Colin McInnes), expression of the GIF gene did not appear to be under the control of early transcriptional control sequences that are A+T rich and appear to be conserved in poxviruses (Fleming *et al*, 1991, Prideaux *et al*, 1990). Instead it was thought that the GIF gene start and stop control sequences were more analogous to those of vaccinia virus late genes. In order to determine whether GIF was the product of an early or late orf virus gene, NZ2 virus-infected FLM cell cultures were analysed by ELISA and by Western blotting for the temporal expression of GIF (Table 3.1, Fig. 3.11).

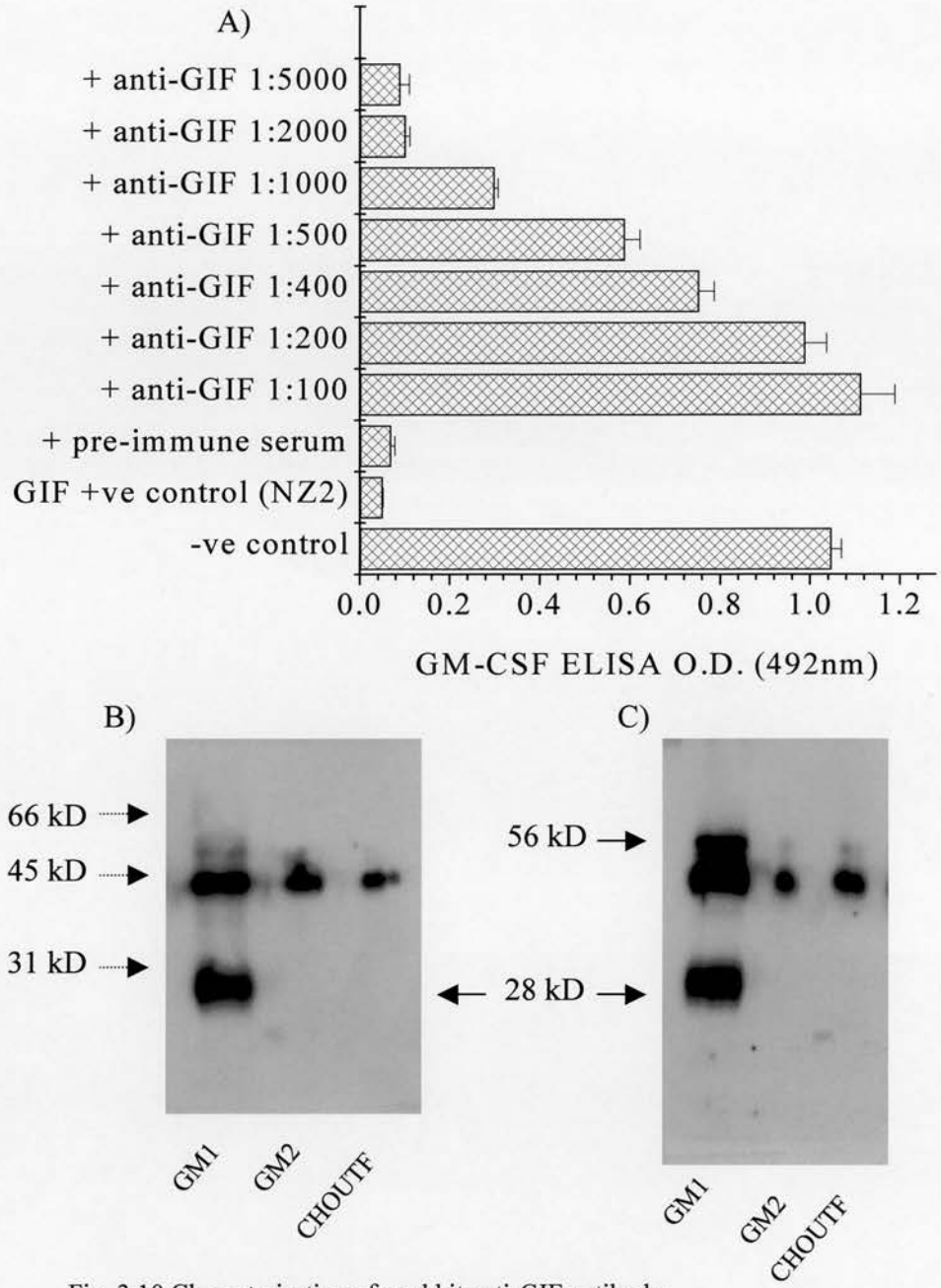

Fig. 3.10 Characterisation of a rabbit anti-GIF antibody.
A range of dilutions of a rabbit antiserum raised against the rovGM-CSF-affinity purified GIF activity were tested for neutralisation of GIF activity in the GM-CSF ELISA (A). Neutralisation by anti-GIF was measured by an increase in O.D. (x-axis, 492nm) as GIF was prevented from clearing rovGM-CSF. Maximum neutralisation of GIF activity was observed at an anti-GIF dilution of 1:200 however significant reactivity of anti-GIF for GIF was detected down to 1:1000 ($p < 0.01$) when compared with GIF activity tested in the presence of pre-immune rabbit serum at 1:500 dilution
The specificity of anti-GIF was tested by Western blot analysis of B) reduced (28kD GIF) and C) non reduced (28 kD and 56 kD GIF) conditioned medium from GM1-CHO cell cultures. Reactivity with the 43 kD protein that co-eluted from the affinity column is also evident in cell-free supernatants from GM2-CHO and untransfected CHO cell cultures (CHOUTF) which were included as controls.

Hours after infection	CFS O.D. (492nm)	Cell lysate O.D. (492nm)	Insoluble Material O.D. (492nm)
0	0.82 +/-0.04	0.74+/-0.05	0.77+/-0.004
1	0.81+/-0.03	0.75+/-0.06	0.85+/-0.01
2	0.80+/-0.05	0.76+/-0.05	0.86+/-0.07
4	0.82+/-0.02	0.76+/-0.03	0.81+/-0.04
6	0.83+/-0.05	0.77+/-0.05	0.84+/-0.02
8	0.78+/-0.03	0.67+/-0.03	0.82+/-0.04
10	0.77+/-0.03	**0.29+/-0.001**	0.79+/-0.05
12	0.63+/-0.02	**0.11+/-0.01**	0.69+/-0.01
18	**0.21+/-0.01**	**0.05+/-0.002**	0.71+/-0.02
20	**0.17+/-0.005**	**0.05+/-0.001**	0.51+/-0.03
24	**0.09+/-001**	**0.18+/-0.002**	0.55+/-0.04

Table 3.1 Expression of GIF during orf virus infection.
Aliquots of cell-free supernatant (CFS), cell lysate and insoluble cellular material (after cell lysis with NP40) from FLM cells infected with orf virus (NZ2) were collected at various times after infection and tested for the presence of GIF by GM-CSF ELISA. GIF activity in both supernatant and cell lysate material was revealed by the lower O.D. (492nm) values which are underlined and with $p < 0.001$ when compared with the value for GM2-CHO GIF negative control (O.D. 0.78 +/- 0.04).
The value for the GM1-CHO GIF positive control for this experiment was 0.048 +/- 0.004. Insoluble material was assayed as a suspension for rovGM-CSF binding activity. No significant GIF activity was detected.
All values represent the mean of 4 samples with +/- standard error of the mean.

Cells were infected at a m.o.i of 0.1 and >75% CPE was observed at 24 hours after infection. Cytoplasmic GIF from cell lysate material was first detected at 10 hours post infection (Table 3.1). Extracellular GIF was first detected 8 hours later. Low levels of GIF were detected in the later stages of infection (after 20 hours), associated with insoluble cellular material.

Western blot analysis of supernatants from NZ2 virus-infected FLM cell cultures, probed by the anti-GIF, identified proteins of 28 kD, 43 kD and 56 kD. (Fig. 3.11A and B). Extracellular GIF was first detected by the anti-GIF 18 hours after virus infection (Fig. 3.11A). Treatment of the cultures with cytosine arabinoside (an inhibitor of viral replication and the expression of late virus genes) was shown to inhibit the production of GIF as detected in the supernatant from untreated cultures (Fig. 3.12B). In addition treatment of infected cultures with cytosine arabinoside prevented the CPE that was observed in its absence.

Western blot analysis of cell lysate material (Fig. 3.11C), taken from cultures at different times after infection, revealed that GIF was present within cells as early as 10 h after infection. Increased levels of GIF were found in lysates taken at 24 h but GIF was not detected in lysates from infected cell cultures taken at 24 h after treatment with cytosine arabinoside. In contrast to supernatants, cell lysate material contained high levels of protein which, under non-reducing conditions, resulted in gel distortion. Western blot analysis of cell lysate material was therefore carried out under reducing conditions and as a consequence the 56 kD protein band observed under non-reducing conditions was not detected in this material.

Northern blot analysis of orf virus infected FLM cells carried out by Colin McInnes (using a DNA probe derived from the sequence within the GIF open

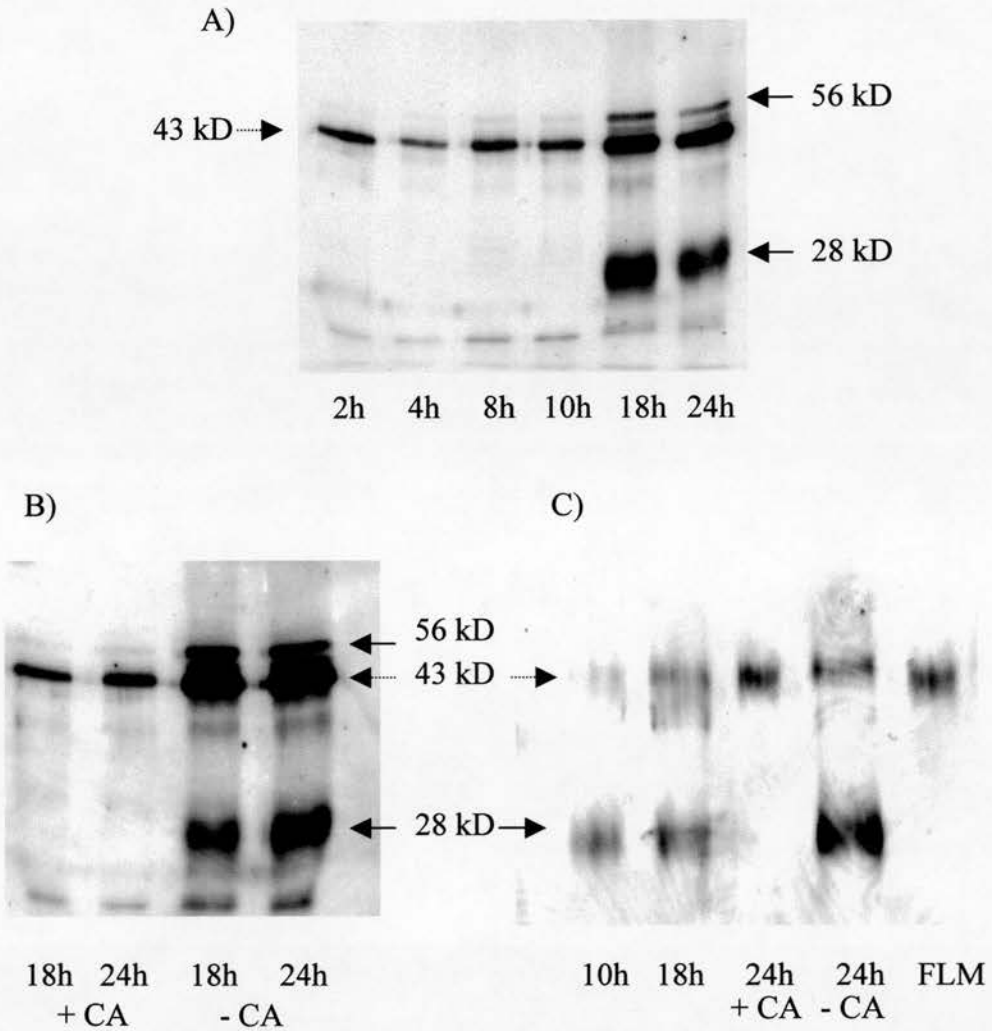

Fig. 3.11 Viral GIF expression in FLM cells after infection with orf virus NZ2.

A) Cell free supernatants collected from orf virus (NZ2) infected FLM cell cultures at various times after infection (2h-24h) and tested for the presence of GIF (both 28 kD and 56 kD GIF where present are arrowed) by Western blot analysis under non-reducing conditions using the rabbit anti-GIF.

B) A similar Western blot analysis of supernatants taken at 18h and 24h after infection from infected cells maintained in the presence and absence of cytosine arabinoside (CA: an inhibitor of viral replication and late viral protein expression).

C) Cell lysate material collected at 10h and 18h from infected FLM cells was compared under reducing conditions with cell lysate collected at 24h from infected cells maintained in the presence or absence of cytosine arabinoside and cell lysate from uninfected cells (FLM).

As previously shown the 43 kD protein was present (dashed arrow) in all samples tested including those from uninfected control cell cultures (FLM).

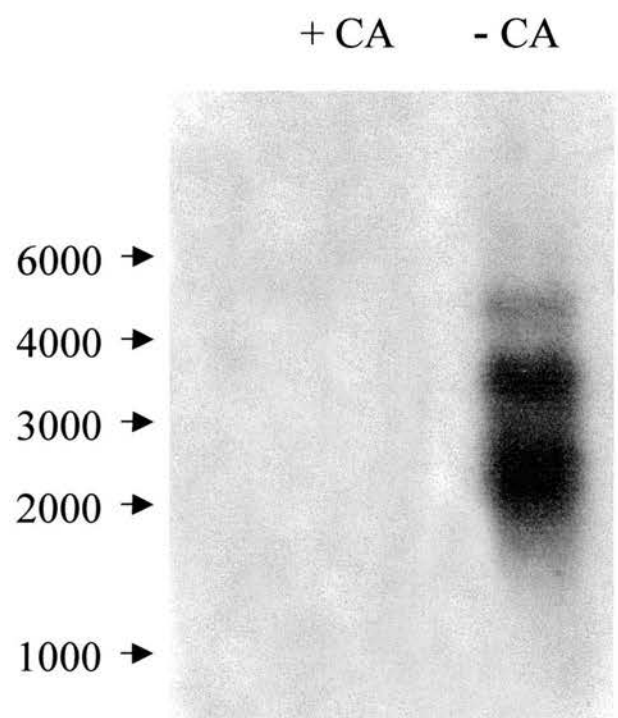

Fig. 3.12 Northern blot analysis of GIF mRNA expression (courtesy of Colin McInnes).
Viral RNA was isolated from FLM cell cultures 18 h after infection with NZ2 at a MOI of 20 $TCID_{50}$ in the presence or absence of cytosine arabinoside (CA).
Using a DNA probe derived from the GIF open reading frame, GIF mRNA was detected in infected FLM cultures maintained in the absence of CA.
The positions of RNA size markers (in bases) are indicated.

reading frame) detected GIF mRNA at 18 h after infection. GIF mRNA was not detected at 5 h after infection or at 18 h after cultures were treated with cytosine arabinoside (Fig. 3.12). This result along with the results from the Western blot analysis demonstrated that the GIF gene was expressed as an intermediate or late but not early viral gene. The detection of multiple mRNA bands instead of a single mRNA band (Fig. 3.12) supports this conclusion since the point at which intermediate and late gene transcription stops can vary.

3.2.5. Expression of GIF by other parapoxviruses

FLM cells infected with different orf virus strains, orf11, NZ2, scabbymouth and D1701, were all shown to express GIF when supernatants were analysed by GM-CSF clearance ELISA 18-20 h after infection (Fig. 3.13). GIF activity was not detected in supernatants taken (at > 90 % cytopathic effect) from FLM cells infected with the parapox viruses bovine papular stomatitis virus (BPSV) and pseudocowpox virus/milkers' nodule virus (MNV) and the control virus, Semliki forest virus (SFV).

Samples collected from FLM cell cultures that had been infected with different parapox viruses were found to contain high levels of serum protein that prevented protein separation by SDS-PAGE. Consequently Western blot analysis of these samples was not be carried out.

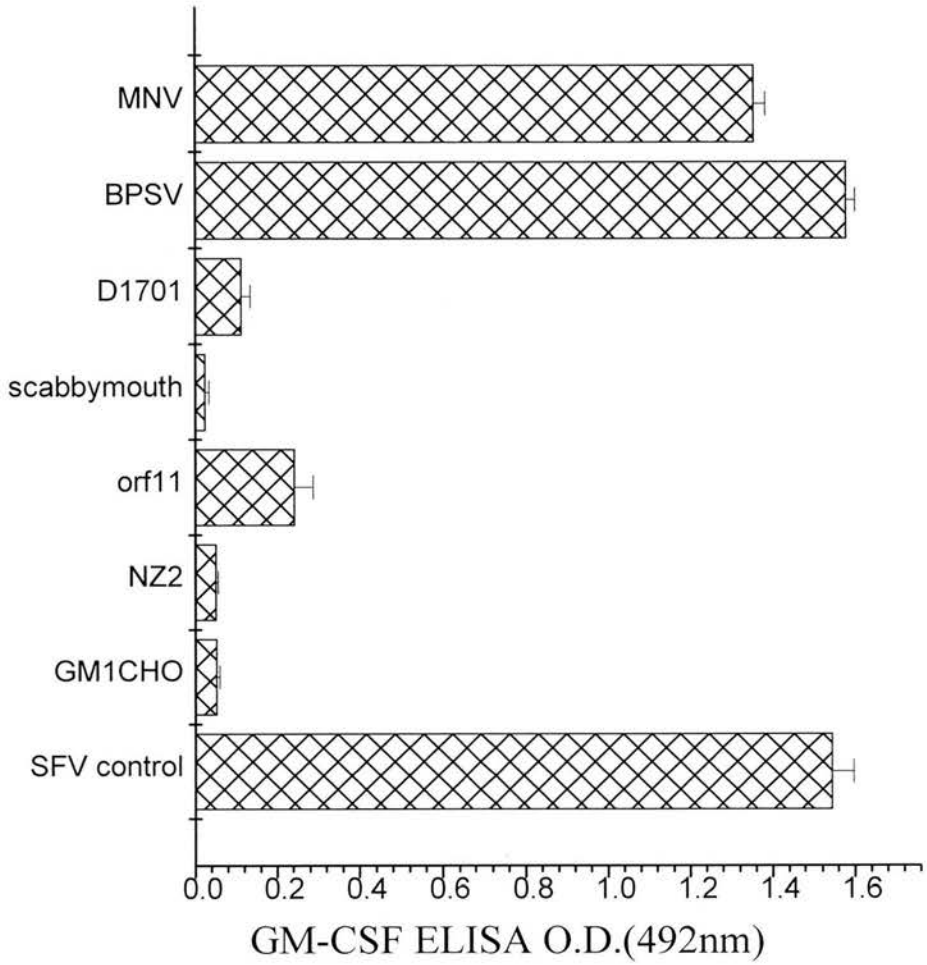

Fig. 3.13 GIF expression by parapoxviruses.
Different strains of orf virus, bovine papular stomatitis virus (BPSV) and milkers nodule virus/pseudocowpox virus (MNV) propagated in FLM cells were tested for expression of GIF by GM-CSF ELISA.
All orf virus strains tested expressed GIF as demonstrated by the low absorbance (x-axis, O.D. (492nm)).
Semliki forest virus (SFV), bovine papular stomatitis virus and milkers nodule virus-infected cultures did not express GIF.

3.3. Discussion

3.3.1. Mapping of the GIF gene

In this chapter the orf virus gene encoding the GIF protein mapped to a single ORF located 20.1 kb from the right terminus of the orf virus genome. From earlier studies, it was found that vaccinia virus did not express a protein that bound ovine GM-CSF and consequently use was made of the VVOV recombinant library to map the GIF gene to the orf virus genome. Without this library, the mapping of the GIF gene by the isolation of single ORFs would have been extremely difficult. Due to the high G+C content of the orf virus genome, it is difficult to identify individual stop codons and so determine single ORFs. This problem of ORF identification was highlighted in the orthopoxvirus, Molluscum contagiosum virus (MCV) which, like orf virus, has a high G+C content (63%). Senkevich *et al*, (1996) demonstrated that the genome of MCV contains approximately 163 ORFs instead of the 588 ORFs predicted by the analysis of apparent stop codons. This more realistic estimate was derived from statistical predictions of coding regions, signal peptides and putative promoters and correlates with the 187 and 198 ORFs for the orthopoxviruses, variola virus and vaccinia virus respectively (Goebel *et al*, 1990).

The vaccinia virus-controlled expression of plasmids containing subclones of the 10 kb VVOV85 orf virus DNA fragment allowed further mapping of the GIF gene to a 2.3 kb fragment (pVU13) at the right hand end of VVOV85. Improved expression of GIF activity was achieved when this fragment was recloned in the 5′-3′ orientation into the pEE14 mammalian expression vector and transfected into CHO cells.

3.3.2. GIF gene expression by parapoxviruses

Conservation of GIF expression was found in all orf virus strains tested. These included the tissue culture adapted strains; orf11, scabbymouth, D1701 and NZ2. Comparison of the GM1 sequences of orf 11 and MRI scab viruses with that of NZ2 revealed a high level of identity for the predicted protein product (>98%).

Binding to rovGM-CSF by samples from cultures infected with bovine papular stomatitis virus or pseudocowpox virus was not detected. Interestingly, although much of either genome has yet to be sequenced, Dr. Andy Mercer (University of Otago) has found sequences homologous to orf virus GIF in both the genomes of bovine papular stomatitis virus and pseudocowpox virus (personal communication). This failure to bind ovine cytokine may reflect the fact that these viruses infect cattle and through co-evolution with this host have selected viral receptors that are specific for cytokines of bovine origin. Therefore any future study into GIF expression by the bovine-specific parapoxviruses should be directed towards the analysis of GIF-bovine GM-CSF binding.

3.3.3. Identification of the GIF gene product

Purification of recombinant GIF by GM-CSF-Sepharose affinity chromatography resulted in the identification of 28 kD and 43 kD protein bands on SDS-PAGE under reducing conditions. Subsequent N-terminal sequence analysis identified the 28kD protein as the product of the GIF gene contained within the GM1 ORF. A BLAST search of protein sequence databases failed to find any match with the N-terminal amino acid sequence obtained for the co-eluting 43 kD protein. A less discriminatory search using the FASTA search tool provided by the Daresbury Laboratories

(Daresbury, U.K.) for any match of the 20 terminal amino acids of the 43 kD protein yielded no definitive match with any sequences held in the protein databases. There was however some indication of a common sequence (40-50% identity in a 15 amino acid overlap) with fungal/microbial chaperonins.

The GIF gene was predicted to encode a 265 amino acid (27.9 kD) protein (Colin McInnes). From the alignment with 20 amino acid terminal sequence of the recombinant GIF, the first 19 amino acids of the predicted sequence was thought to constitute a putative signal that is cleaved as part of a post-translational modification.

There were similarities between the predicted sequence of the GIF protein and the A41 protein precursor of variola virus and vaccinia virus strains Copenhagen and Lister (32% similarity over an 88 amino acid overlap). The alignments of A41 and GIF sequences based on identical amino acids and conserved amino acid substitutions were shown in the same central region of the peptide chain. The function of the A41 gene product is not known, the A41 protein sequence has been reported to have homology with the 35 kD/T1 family of chemokine soluble receptors (Lalani and McFadden, 1997; Lalani *et al*, 1998). These 35-40 kD secreted proteins (35 kD for orthopoxviruses and T1 for leporipoxviruses) bind CC- chemokines with high affinity. Whereas the 35kD/T1 proteins were shown to block CC-chemokines binding to target receptors *in vitro*, they did not block IL-8 (a CXC-chemokine) binding its receptor (Smith *et al*, 1997; Lalani *et al*, 1998; Alcami and Koszinowski, 2000). However no significant sequence homology was revealed when the sequences of GIF and Shope fibroma virus T1 protein (a representative of the 35 kD/T1 family, Graham *et al*, 1997) were compared.

3.3.4. Temporal expression of the GIF gene

From Western blot analysis and Northern blot analysis of samples collected from virus infected cells at different times and maintained in the presence or absence of cytosine arabinoside, it was shown that GIF was the product of an intermediate or late expressed orf virus gene. GIF was first detected by GM-CSF clearance ELISA in supernatant from FLM cell cultures approximately 18 hours after orf virus infection. Nonetheless, cytoplasmic GIF can be detected eight hours earlier and this correlates with the observation of Lear (1995) whereby constitutive GM-CSF production by keratinocytes is effectively shut down 10 hours after orf virus infection. This suggests that at least one role for GIF is to block GM-CSF in infected keratinocytes, the target cell of orf virus *in vivo*. The significance of this is not yet clear.

Alternatively, the proper folding and secretion of GIF may be dependent on additional factors that include host gene products (possibly the 43 kD protein). The roles of the 43 kD protein and the 56 kD protein (that was observed in the non-reduced electrophoresis of affinity-purified material and is possibly a dimeric form of the 28 kD GIF protein) in GIF-GM-CSF binding is investigated in Chapter 4.

CHAPTER 4

THE PHYSICO-CHEMICAL PROPERTIES OF THE GM-CSF-INHIBITORY FACTOR PROTEIN

4.1. Introduction

In chapter 3, it was shown that the orf virus GIF gene encodes a secreted protein of 28 kD and an additional 56 kD band in non-reduced gels. Like their cellular counterparts, many poxvirus cytokine receptors are present in solution as higher order oligomers (Lalani *et al*, 1997; Mossman *et al*, 1996; Loparev *et al*, 1998). The aims of this chapter were therefore to determine firstly whether GM-CSF was bound by GIF as a monomer and/or as an oligomer and secondly to investigate other physico-chemical properties of GIF including; glycosylation, isoelectric point and the stability of GIF across a range of pH values, salt concentrations and temperatures.

The initial approach was to further purify the GIF protein by gel filtration chromatography under physiological conditions (0.15M NaCl and pH 7.2). The isolated GIF was then tested for GM-CSF binding in the ELISA. The calibration of the gel filtration column with a range of markers of known molecular mass enabled the size of the GIF molecule to be determined.

In order to confirm that GIF bound GM-CSF directly, a ligand blot procedure was developed. This approach entailed the blotting of rovGM-CSF by ^{125}I-GIF. Analysis of chemically cross-linked cytokine-receptor complexes has revealed both the molecular mass of the complex and the stoicheometry of the reaction. Upton *et al* (1992) have characterised the binding of the M-T7 protein encoded by a myxoma virus gene to rabbit IFN-γ through SDS-PAGE analysis of the chemically cross-linked M-T7/IFN-γ complex. This approach was used to investigate the native conformation of the GIF molecule when bound to GM-CSF and whether GIF bound one or more GM-CSF molecules.

Forces such as hydrogen bonds, disulfide bridges, attractions between positive and negative charges, and hydrophobic and hydrophilic linkages cause a protein molecule to coil or fold into a secondary structure, examples of which are the alpha helix, the beta pleated sheet, turn and coil. The secondary structure of a protein can be predicted from the amino acid sequence by proteomic computer programs that are available on the world-wide web. These proteomics tools use a number of different mathematical algorithms to calculate not only the probability of the various secondary structures but also molecular mass, isoelectric point, regions of hydrophophilicity/hydrophobicity, regions of antigenicity and potential glycosylation sites. The tertiary and quaternary structures of some proteins have already been determined by X-ray crystallography and nuclear magnetic resonance analysis. These protein structures can be used as model templates for the mathematical prediction of the higher order stuctures of other proteins with amino acid sequence homology. Protein structure prediction tools provided the ExPASy proteomics server were used to investigate the structure of GIF.

Gel mobility-shift analysis by SDS-PAGE of GIF before and after treatment with endoglycosidases was used to investigate the level of glycosylation associated with the GIF molecule. This approach was used previously to identify glycosylated and non-glycosylated forms of secreted rovGM-CSF (Entrican *et al*, 1996)

Electrostatically-charged glycosidic residues such as neuraminic acid, N-acetyl glucosamine and N-acetyl galactosamine can contribute, along with charged amino acids, to the net charge of a protein molecule. Since the overall charge carried by a protein molecule can influence what methods may be applied to its isolation and characterisation (for example ion-exchange chromatography and isoelectric focusing)

it was considered important to determine the isoelectric point (pI) of the GIF protein. The pI is the pH at which a protein carries the same number of negative and positive charges. The pI of GIF was determined by the method outlined by Lampson and Tytell (1965), whereby the binding of GIF to an ion exchange resin, equilibrated with buffers of different pH, was tested. At the isoelectric point, GIF, with no net charge, would not bind to the resin. Unbound GIF was detected by the GM-CSF clearance ELISA.

Previously, Andrea Lear (1995), in addition to demonstrating that the clearance of GM-CSF by GIF was not due to proteolytic activity, had shown that the process of heating supernatants from infected cultures to 56°C affected the ability of GIF to clear GM-CSF detectable by ELISA. In this chapter, the physical and chemical nature of the GIF-rovGM-CSF binding reaction was further investigated. The effects of temperature, chemical reducing agents, high salt concentration and extremes of pH on GIF-GM-CSF binding was tested by GM-CSF clearance ELISA. The kinetics of GIF-GM-CSF reactivity over increasing time intervals was also investigated.

4.2. Results

4.2.1. The identification of GIF oligomers

Sephacryl-200HR gel filtration of recombinant GIF activity isolated by rovGM-CSF affinity chromatography (Section 2.3.1.) resulted in the identification of a protein complex of approximately 110-120 kD with GIF activity as measured by the GM-CSF clearance ELISA (Fig. 4.1A). Analysis by SDS-PAGE (Fig. 4.1B and C) revealed that this complex consisted of 28 kD peptides when run under reducing conditions. Under non-reducing conditions a 56 kD major protein band and a minor 28 kD band were observed.

GIF activity was not detected in the major absorbance peak (O.D. 280nm) from gel filtration which had an estimated molecular mass of 55-60 kD (Fig. 4.1A). SDS-PAGE analysis revealed that the major component of this peak was the 43kD peptide that co-eluted with GIF from the rovGM-CSF affinity column.

The reduction of the GIF protein complex by boiling in the presence of 5 mM dithiothreitol resulted in its dissociation to the 28 kD form as seen on SDS-PAGE analysis of GIF run under reducing conditions. The 28 kD GIF did not react with rovGM-CSF as measured by GM-CSF clearance ELISA even after extensive dialysis against PBS (Fig. 4. 2). GIF that had been boiled in the absence of dithiothreitol was found to clear rovGM-CSF.

The 110-120 kD GIF protein complex was radio-iodinated and the product evaluated by Sephacryl-200HR (Fig. 4.3). Since the protein load applied to the gel filtration column was no greater than 20 μg, separation was carried out in the

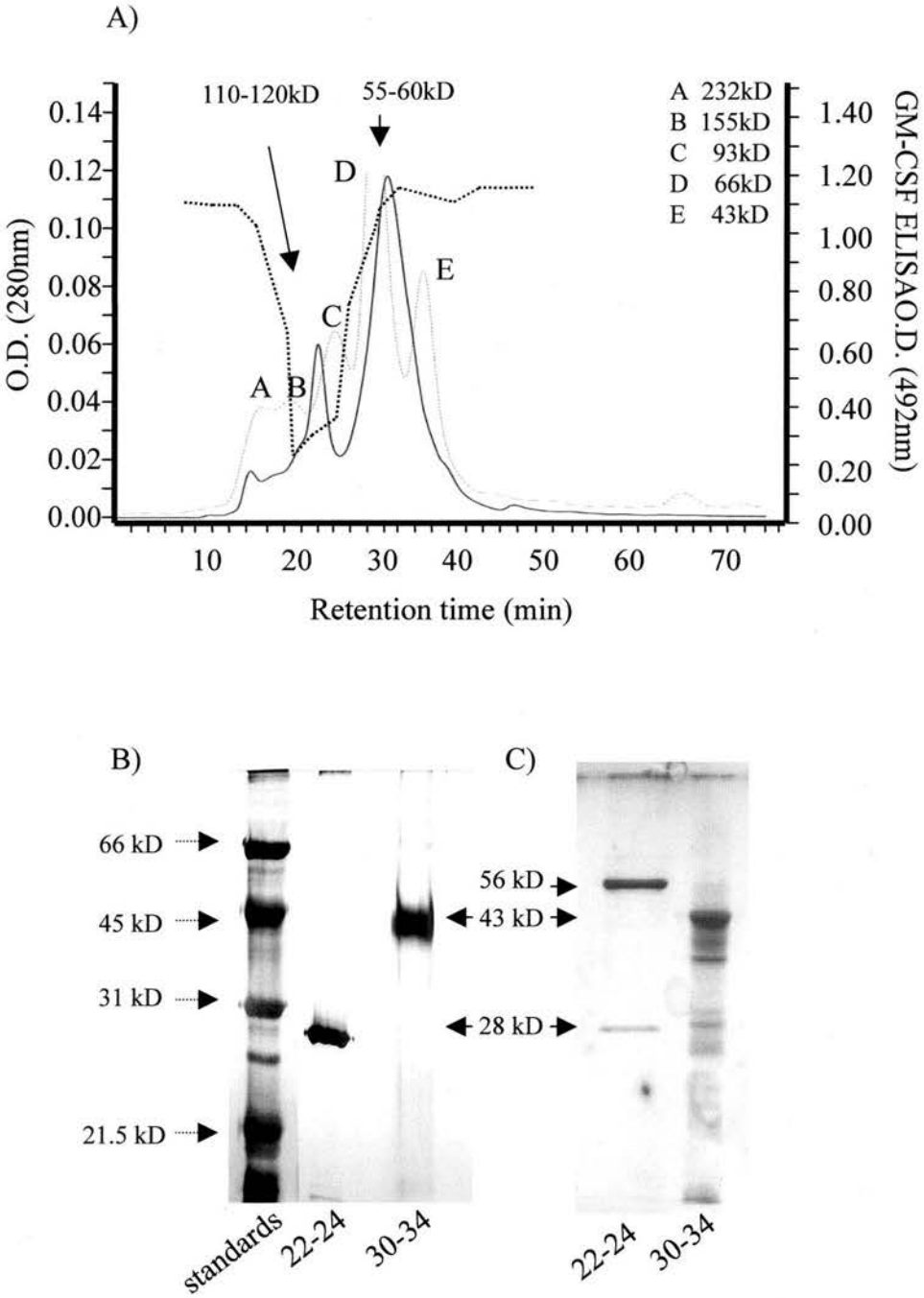

Fig.4.1 Purification of recombinant GIF.
A) The rovGM-CSF- affinity column eluate containing the 28 kD and 43 kD proteins was further separated by gel filtration on Sephacryl 200HR (solid line denoting retention time vs O.D. 280 nm). Fractions were tested for GIF activity in the GM-CSF ELISA (O.D. 492nm denoted by the dashed line and showing a decrease in O.D. associated with GIF activity). The molecular mass of each peak (110-120 kD and 55-60 kD) was estimated by comparison with a range of protein standards (denoted by the light dotted line joining peaks A-E) run previously under identical conditions.
Aliquots consisting of pooled peak fractions 22-24 and 30-34 were analysed by 12% SDS-PAGE under B) reducing conditions and C) non-reducing conditions. The molecular weights of the major protein bands isolated from the column fractions (arrowed, 28 kD, 43 kD and 56 kD) were calculated by comparison with a range of molecular mass protein standards (dashed arrows 21.5 kD - 66 kD).

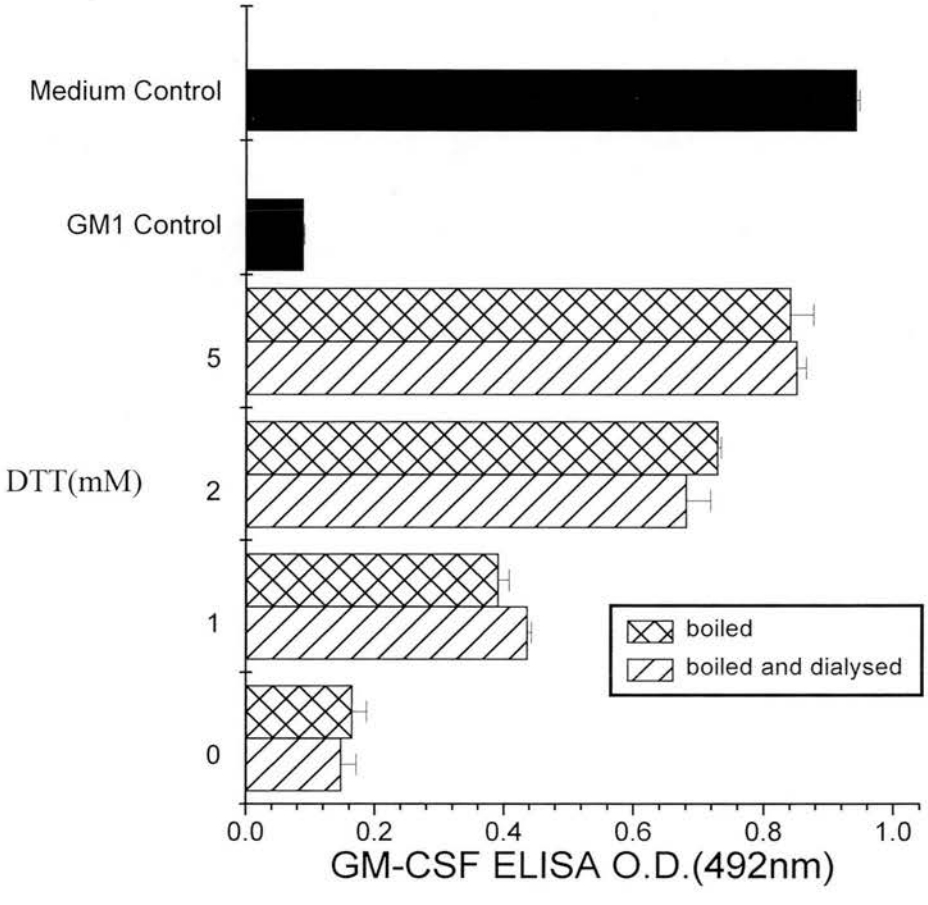

Fig. 4.2 The effect of dithiothreitol reduction on GIF activity.
To test the effect of reduction on GIF binding to GM-CSF, affinity purified GIF was boiled in the presence of increasing concentration of dithiothreitol (y axis, DTT (mM)). As shown by the increase in absorbance (cross hatched bars), reduction by DTT resulted in loss of GIF binding activity which was not recovered even after removal of the DTT by dialysis (diagonal hatched bars).
Values represent the mean of 4 samples and standard error of the mean.

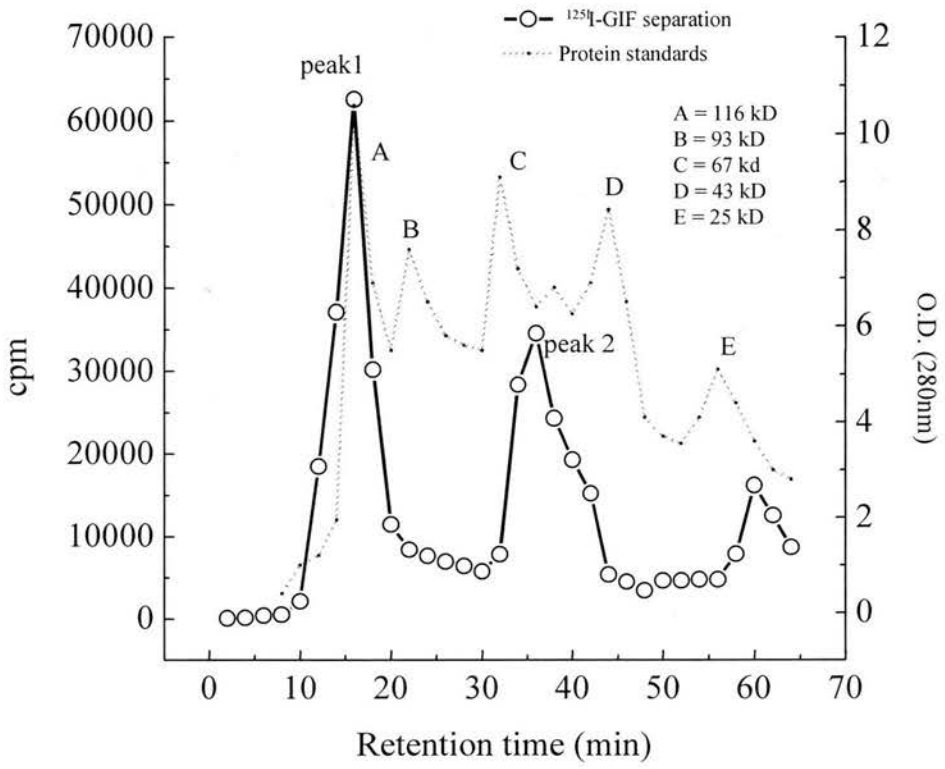

Fig. 4.3 Gel filtration of ^{125}I-GIF.
Purified GIF was radio-iodinated by the chloramine T method and after removal of free ^{125}Iodine was applied to Sephacryl 200HR. Aliquots were taken from each fraction collected and radioactivity (primary y-axis) measured by γ-counter (solid line). The approximate molecular mass of each peak of radio-labelled protein was estimated (peak 1 = 115 kD; peak 2 = 55/60 kD) by comparison with retention times of protein standards measured at O.D. at 280nm secondary y-axis and peaks A-E joined by dotted line and run previously under identical conditions.

presence of 0.5 M NaCl and 0.1% CHAPS to minimise adsorption to the column matrix. Two major peaks of radioactivity were measured with estimated molecular masses of 115 kD and 55/60 kD respectively. Both peaks were found to comprise the 28 kD ^{125}I- GIF subunit when analysed by SDS-PAGE under reducing conditions (Fig. 4.4). There was no peak of radioactivity corresponding to the molecular mass of the 28 kD subunit detected during the fractionation of ^{125}I-GIF by Sephacryl-200HR.

The reactivity of ^{125}I-GIF for rovGM-CSF was tested by GM-CSF clearance ELISA (Fig. 4.5) and Western blot analysis (Fig. 4.6). Comparison of equal concentrations of ^{125}I-GIF and unlabelled GIF for clearance of rovGM-CSF as measured in the GM-CSF clearance ELISA showed that radioiodination did not affect the ability of ^{125}I-GIF to bind rovGM-CSF. Nitrocellulose strips containing separated rovGM-CSF were incubated with ^{125}IGIF fractions collected during gel filtration. Those fractions that corresponded to both ^{125}I-GIF peaks were found to react with rovGM-CSF (Fig. 4.6). The doublet bands bound by ^{125}I-GIF represent different glycosylated forms of the rovGM-CSF protein (see below Section 4.2.2.).

In an attempt to determine the molecular structure of the GM-CSF-binding complex, the 115 kD ^{125}I-GIF was incubated with rovGM-CSF then crosslinked with EDC (Fig.4.7). The effectiveness of EDC in cross-linking the proteins in this study was found to be low. As with untreated ^{125}I-GIF (lane 2), cross-linked ^{125}I-GIF (lane 1), when analysed by SDS-PAGE under non-reducing conditions, comprised predominantly 56 kD and 28 kD peptides, although some of the 115 kD complex appears to be preserved (lane 2). A labelled complex can be seen in the presence of a molar excess of rovGM-CSF with apparent molecular mass in excess

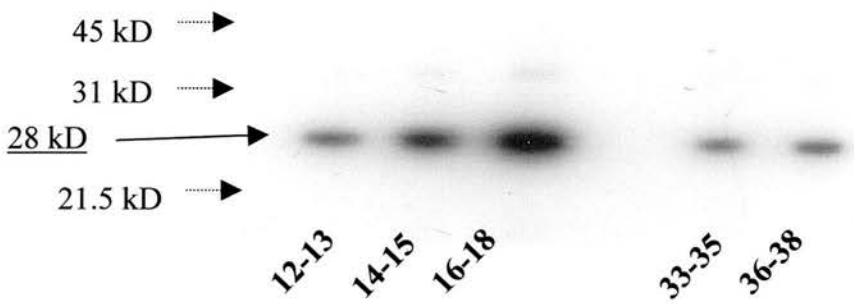

Fig. 4.4 SDS-PAGE analysis of S200 peak fractions of ^{125}I-GIF. Aliquots from pooled fractions (12-13, 14-15, 16-18 of peak 1 and 33-35, 36-38 of peak 2) of S200-separated ^{125}I-GIF were analysed by 12% SDS-PAGE run under reducing conditions.
Radio-labelled protein (28 kD, solid lined arrow) was identified by autoradiography of the fixed, stained and dried gel. The relative positions of protein standards run at the same time and identified by coomassie blue staining prior to autoradiography are shown (dashed line arrows).

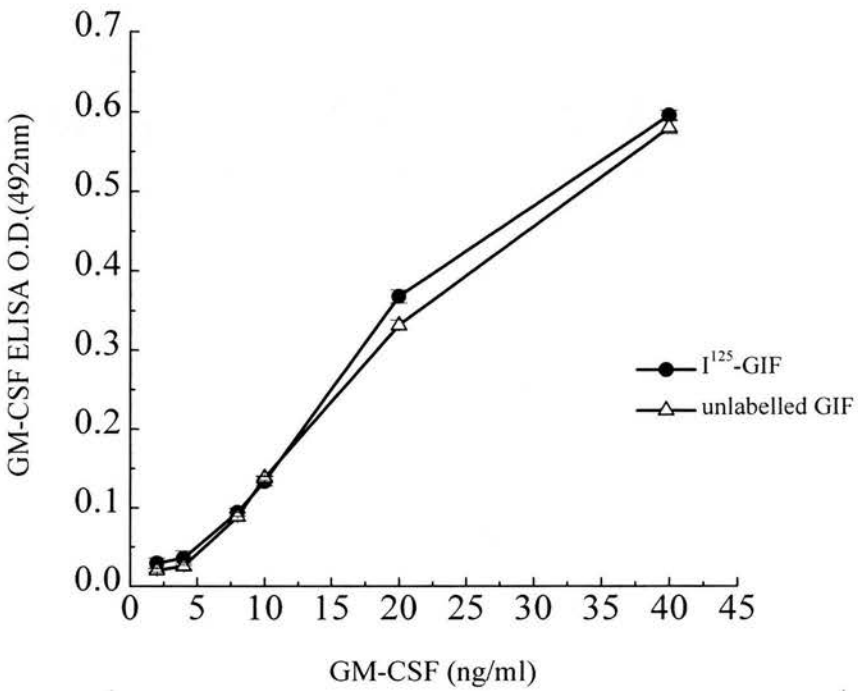

Fig. 4.5 Binding of ^{125}I-GIF to rovGM-CSF.
The binding of equal concentrations of ^{125}I-GIF (solid circles) and unlabelled GIF (solid triangles) to increasing amounts of rovGM-CSF (x-axis, ng/ml) was measured by GM-CSF ELISA (y-axis, O.D. 492nm).

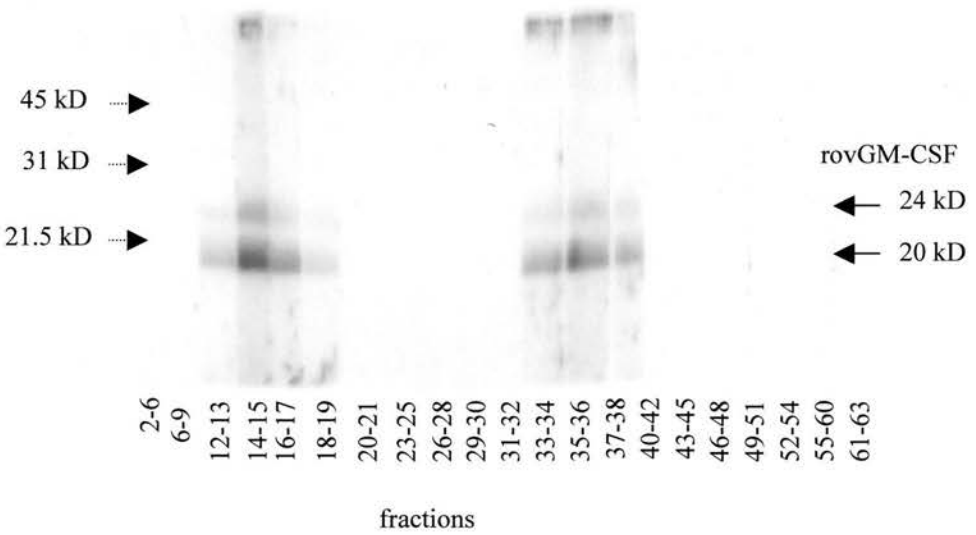

Fig 4.6 Ligand blot analysis of ^{125}I-GIF separated by gel filtration. The reactivity of ^{125}I-GIF separated by S200 gel filtration was tested against purified rovGM-CSF by ligand blot analysis. SDS-PAGE-separated rovGM-CSF (doublet bands of 20 kD and 24 kD) was transferred to nitrocellulose membrane which was cut into strips. Individual strips were incubated with column fractions (consecutive fractions pooled as numbered) that were collected over the duration of the run (63 min.) and tested for ^{125}I-GIF-rovGM-CSF reactivity by autoradiography. (The positions of molecular mass standards is marked by dashed arrows).

of 130 kD (lane 3). No complex (115 kD or 130+ kD) was observed when ^{125}I-GIF was crosslinked in the presence of an excess of rovIL-3 (lane 4). Due to low mobility of the cross-linked ^{125}I- GIF-GM-CSF complex, an accurate estimate of its molecular mass could not be made. Consequently the stoichiometry of the GIF-GM-CSF interaction could not be ascertained.

4.2.2 The predicted protein structure of GIF

The amino acid sequence of GIF was used as a template to predict the secondary structure of the protein. The Predator and ProSite proteomics tools supplied by the ExPASy proteomics server were used to predict the regions of the polypeptide chain that were likely to form alpha helix, beta-pleated sheet, turn or coil secondary structures. In addition, theoretical hydrophobic, hydrophilic and antigenic domains were also calculated by the ProSite tool. Potential O-linked and N-linked glycosylation sites were computed by the O-Glycbase tool and ProSite tool respectively. The various structural domains and glycosylation sites are shown aligned with the 246 amino acid sequence of GIF in Fig. 4.8. Much of the polypeptide chain of GIF is predicted to be hydrophilic and comprised of a number of extended alpha helical regions with smaller regions of beta-pleated sheet, turns and coils. The regions of polypeptide calculated as being potentially antigenic corresponded to the predicted turn secondary structures. Potential N-linked glycosylation sites were mapped to asparagine residues at position 30, 36, 63 and 114 on the GIF polypeptide chain. Possible O-linked glycosylation sites were given at threonine residues, 46, 81 and 243 and serine residues 232 and 240.

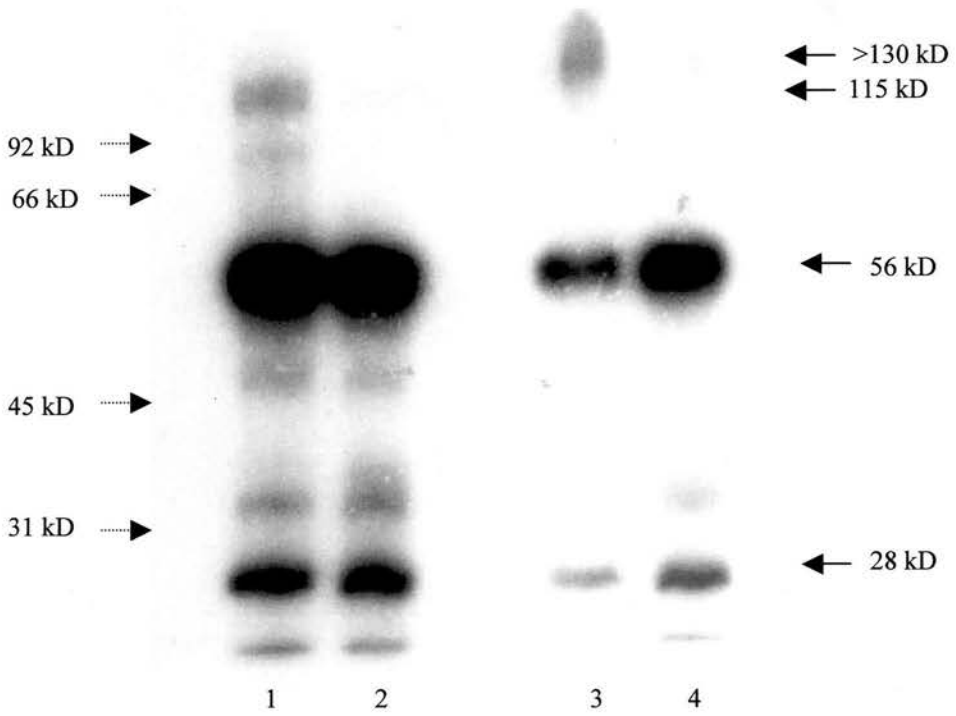

Fig. 4.7 The effect of EDC-crosslinking on ^{125}I-GIF-GM-CSF binding.
Samples of the 115 kD peak fraction of ^{125}I-GIF were analysed by SDS -PAGE (7.5% under non-reducing conditions) and autoradiography after treatment with EDC peptide crosslinker (lane 1) and before treatment (lane 2). EDC crosslinking was also carried out in the presence of a 50 fold molar excess of rovGM-CSF (lane 3) and a 50 fold molar excess of rovIL-3 as a non-specific control (lane 4). The molecular masses of GIF (solid line arrows) present as a monomer (28 kD), dimer (56 kD) and tetramer (115 kD) and complexed with rovGM-CSF (>130 kD) were estimated by comparison with protein standards run simultaneously (dashed line arrows).

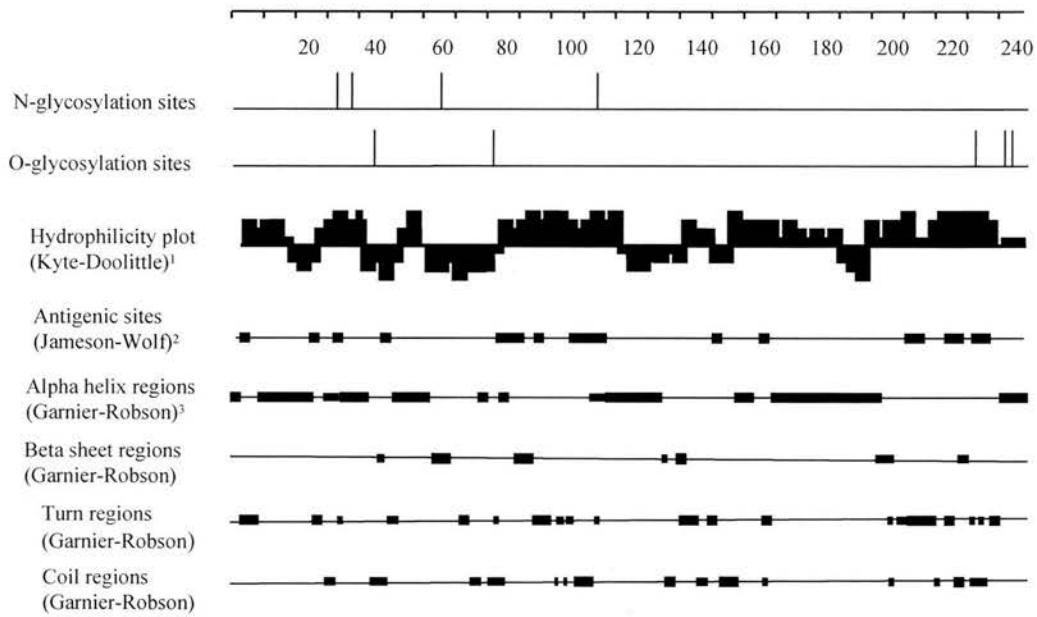

Fig. 4.8 Predicted secondary structure and glycosylation sites of GIF.
The secondary structure of GIF was predicted from the amino acid sequence using the Predator prediction tool.
Potential O-linked glycosylation sites were predicted by O-Glycbase tool that searched for serine and threonine residues in the sequence. Potential N-linked glycosylation sites were predicted by the ProSite tool based on the position of tri-peptide asparagine-unspecified amino acid -serine/threonine residues.
The various structural domains are shown aligned with the GIF amino acid sequence.
The secondary structure predictions were calculated according to the algorithms of [1]Kyte and Doolittle (1982), [2]Beattie *et al* (1992) and [3]Garnier *et al* (1978).

The theoretical isoelectric point and molecular mass was calculated as pH 6.5 and 27,848 Daltons, respectively, using the MultiIdent tool.

The Swiss-Model automated protein-modelling server was used unsuccessfully to predict tertiary and quaternary structures of GIF. This prediction tool calculates a model of the three-dimensional and oligomer structure for a protein based on a number of template structures derived by X-ray crystallography or nuclear magnetic resonance analysis. For successful modelling, it is necessary that the template proteins sequences closely match the sequence of the test protein. Template proteins that matched GIF were not found.

4.2.3. Endoglycosidase-F treatment of GIF

In spite of a number of potential glycosylation sites being present on the polypeptide chain, the measured (from SDS-PAGE) 28 kD molecular mass of GIF corresponded to the predicted molecular mass, suggesting that GIF was not significantly glycosylated. However, a mobility shift analysis (Fig. 4.9A) was performed on GIF before (lane 1) and after treatment (lane 2) with the N-linked specific endoglycosidase, PNGase-F. No change in molecular mass was observed on Western blot analysis with anti-GIF. To ensure the efficacy of endoglycosidase treatment, similar treatment was applied to rovGM-CSF (Fig. 4.9B). PNGase-F was shown to remove N-linked glycosidic moieties from the upper doublet of rovGM-CSF bands (lane 1) that are considered to represent N-glycosylated forms of the lower molecular mass rovGM-CSF bands that remain after treatment (lane 2).

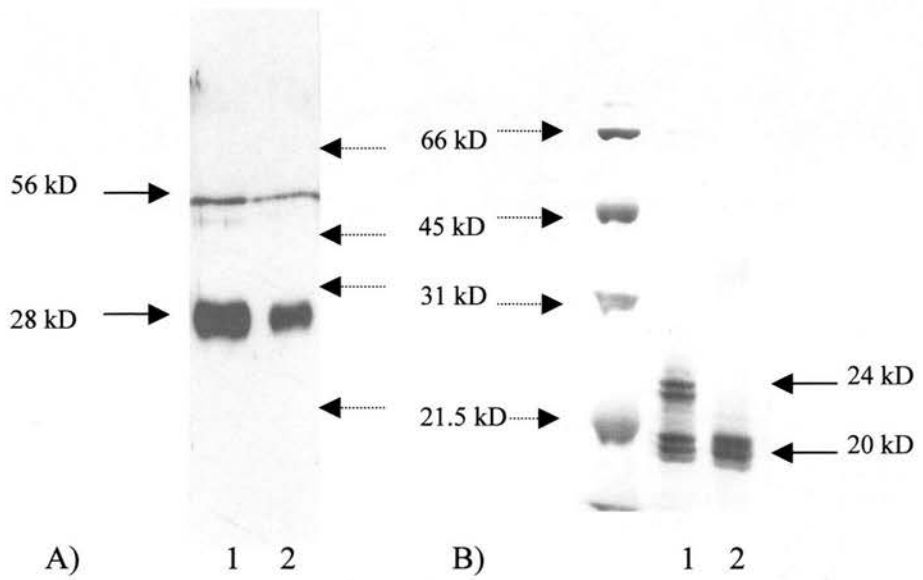

Fig. 4.9 The effect of N-linked de-glycosylation on GIF mobility.
A) Purified rGIF was treated with endoglycosidase F to remove N-linked glycosidic residues then analysed by Western blot analysis using rabbit anti-GIF. Before treatment (lane 1) is compared with post treatment (lane 2). No change in mobility of either 28 kD or 56 kD GIF (solid line arrows) is observed.
B) The effectiveness of the de-glycosylation procedure is demonstrated in a silver stained 12% SDS-PAGE gel, where glycosylated rovGM-CSF (the upper set of bands in lane 1, 24 kD) is converted to the non/lower glycosylated form (lane 2, 20 kD) by endoglycosidase F.
The relative positions of molecular mass standards on either gel is shown (dashed arrows).

4.2.4. The isoelectric point of GIF

GIF adsorption to the anion-exchange resin Q-Sepharose (that had been equilibrated in buffers at different pH values) was measured by GM-CSF clearance ELISA of the supernatants (Fig. 4.10). At pH less than 7, GIF did not bind to Q-Sepharose as shown by the high level of GIF activity in the supernatant. In contrast, at pH 7-9 the majority of GIF present bound to Q-Sepharose. For anion-exchange separations, it is considered that proteins bind at 0.5 pH unit above their isoelectric point (Himmelhoch, 1971). From these data, the isoelectric point of GIF was estimated between pH 6.5 and 7. This value correlates with a value of 6.5 that was computed by the MultiIdent proteomics tool from the amino acid sequence of the GIF protein.

4.2.5. The effect of temperature, salt concentration and extremes of pH

i). Temperature

GIF bound rovGM-CSF maximally at 37°C (Fig. 4.11). There was some reduction in this binding when the mixture was incubated at 20°C and 27°C. At lower temperatures such as 4°C and 10°C and at the higher temperature of 56°C, binding was significantly reduced ($p < 0.01$ when compared with GIF-rovGM-CSF binding at 37°C).

ii). Salt concentration

Increasing the salt concentration of the GIF-rovGM-CSF mixture buffer to 1 M NaCl, had little effect on GIF activity ($p > 0.1$ compared with GIF activity at physiological salt concentration [0.15 M NaCl]) as measured by GM-CSF clearance

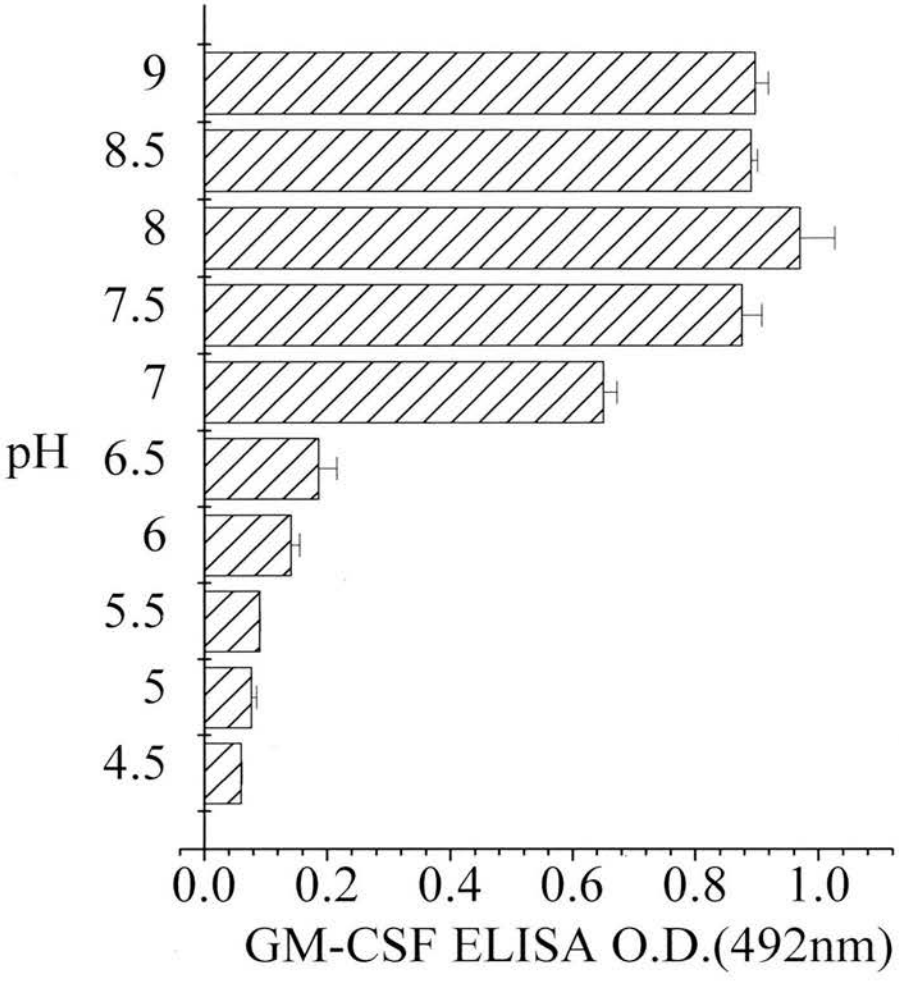

Fig. 4.10 Determination of the isoelectric point (pI) of GIF. Affinity purified GIF was applied to 0.5 ml volumes of Q-Sepharose, which had been equilibrated in buffer at different pH (y-axis pH 4.5 -9). After mixing the gel was allowed to settle and the supernatant was tested for GIF activity by ELISA. As shown by the higher absorbances (x-axis, O.D. 492nm) observed in supernatants taken from gel equilibrated in buffers at pH > 6.5, GIF has bound to the gel.
For anion exchangers, proteins bind at 0.5 pH unit above their pI. The pI of GIF is therefore between 6.5 and 7.
Values represent the mean of 4 samples and standard error of the mean. The values for the GIF positive control and medium negative control for this experiment were 0.104 +/- 0.003 and 0.91 +/- 0.01 respectively.

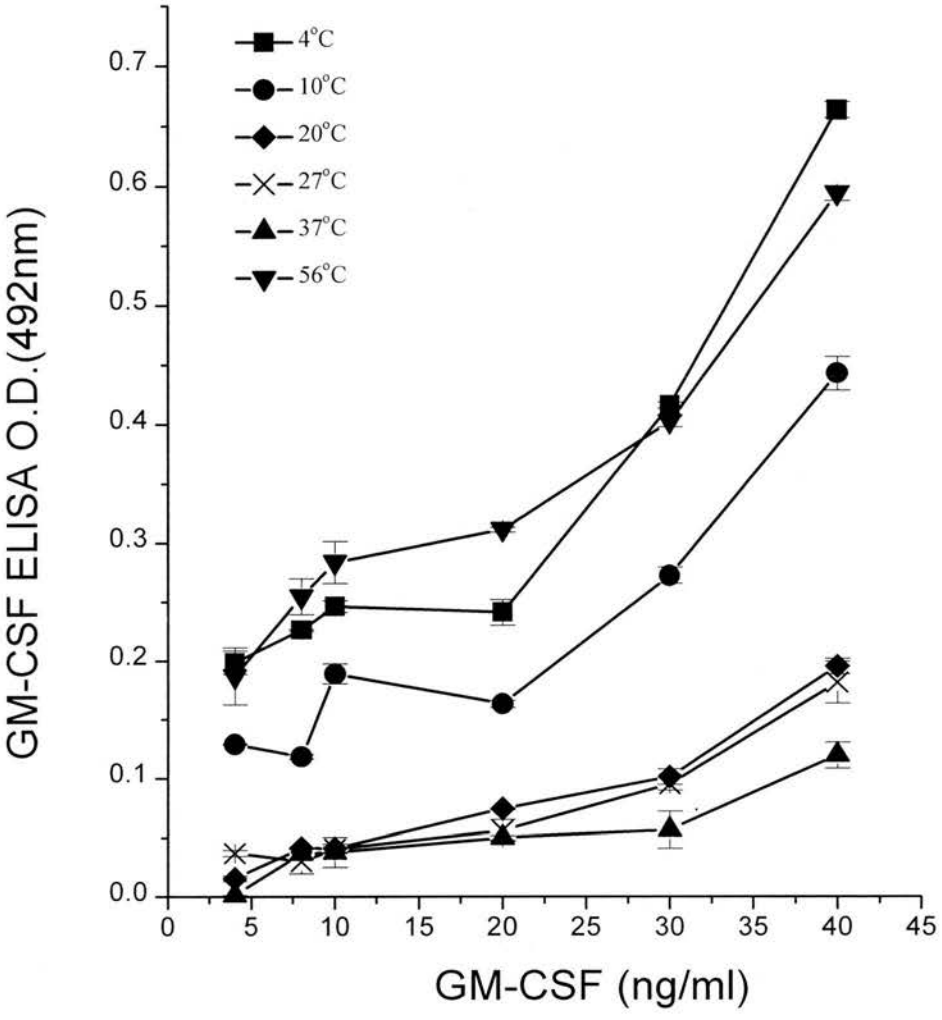

Fig. 4.11 The effect of temperature on GIF-rovGM-CSF binding.
The binding of GIF to increasing concentrations of rovGM-CSF (x-axis, GM-CSF ng/ml) at different temperatures (4°C-56°C) was measured by GM-CSF ELISA.
Maximum GIF-rovGM-CSF binding was observed at 37°C as shown by the lowest O. D. (492nm) values.

ELISA (Fig. 4.12). At this concentration, in the absence of GIF, some interference with GM-CSF detection by ELISA was observed.

iii). pH

GIF binding to rovGM-CSF was tested at pH 3.0, 4.0, 7.5, 10.0 and 11.0 (Fig. 4. 13). Lowering of the reaction mixture to pH 3.0 and pH 4.0 resulted in little or no rovGM-CSF binding to GIF. Incubation of the reaction mixture at pH 10.0 was shown to have less of an effect with 50-60% of the added GM-CSF binding GIF. However at pH 11.0, little rovGM-CSF bound GIF. Exposure of GIF to low pH prior to neutralisation and addition of rovGM-CSF resulted in the loss of approximately 45% of total rovGM-CSF binding after treatment at pH 3.0 and 30-35% of total binding at pH 4.0 when compared with control samples maintained at pH 7.5. A similar but less marked effect on GIF binding to rovGM-CSF was observed when GIF was exposed to pH 10.0 and pH 11.0. Acidic or basic pretreatment of rovGM-CSF had little effect on its detection by ELISA.

4.2.6. GIF-rovGM-CSF binding with time

GIF was incubated with increasing amounts of rovGM-CSF for 1 h and 20 h (Fig. 4.14). For a range of saturating concentrations of rovGM-CSF, no difference in GIF-rovGM-CSF binding was observed when the incubation time was increased to 20 h ($p > 0.1$).

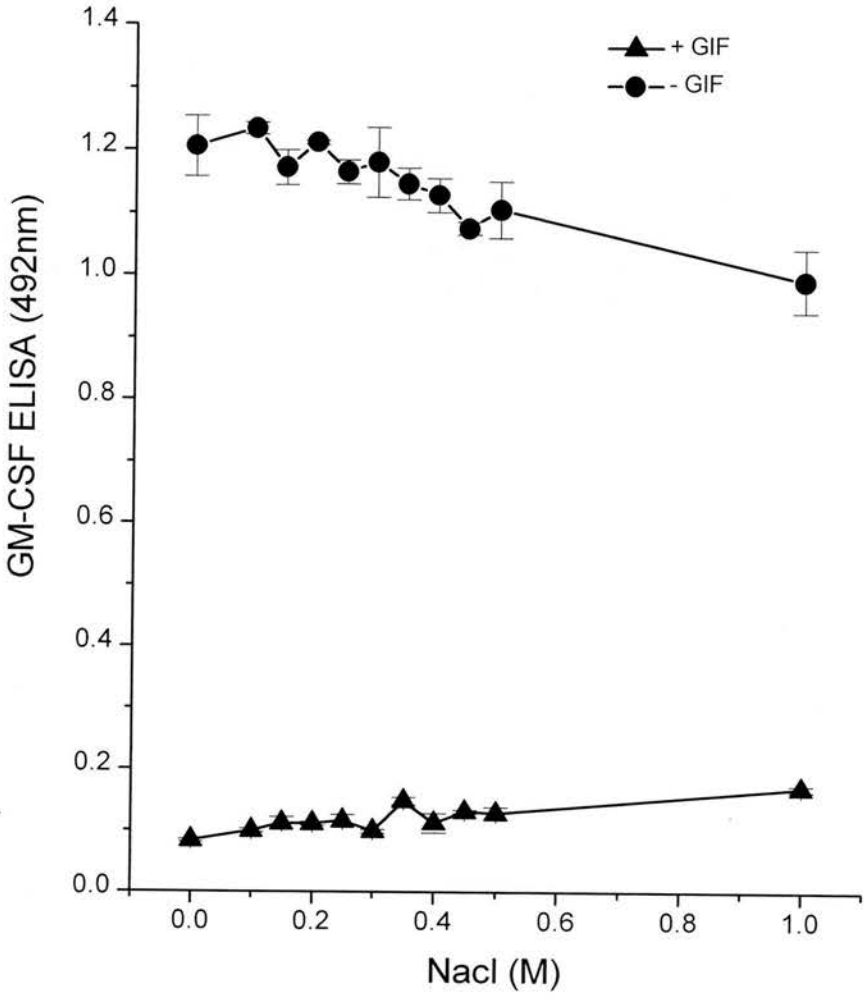

Fig. 4.12 The effect of increasing salt on GIF activity.
The binding of GIF to rovGM-CSF in the presence of increasing salt concentration (x axis, NaCl (M)) was assayed by ELISA (y axis, O.D. (492nm)). Salt concentrations up to 1M NaCl had little effect on GIF-rovGM-CSF binding but some interference with the detection of rovGM-CSF by ELISA was observed at high salt concentrations.

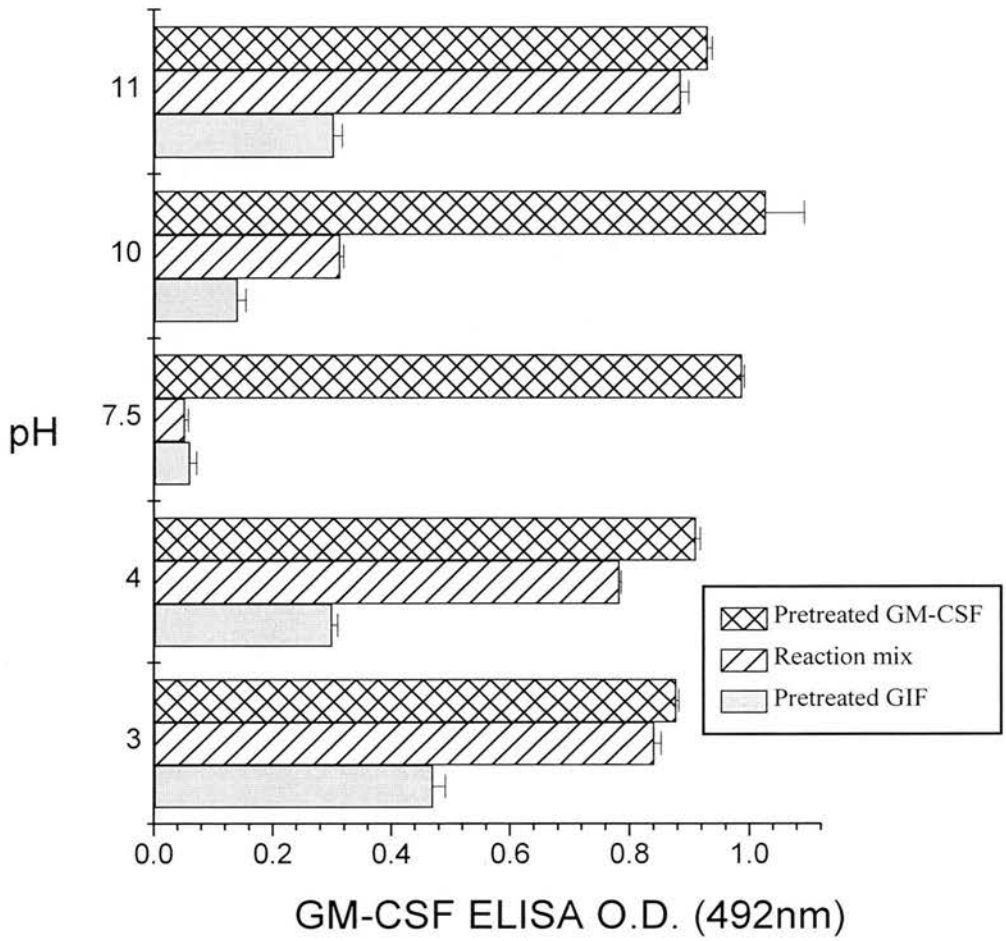

Fig. 4.13 The effect of pH on GIF binding.
The binding of GIF to rovGM-CSF was tested after the reaction mix had been exposed to different pH values for 1h before neutralisation to pH 7.5 (cross hatched bars) or after GIF had been exposed to the same treatment prior to neutralisation and addition of rovGM-CSF (solid bars).
The effect of pH on rovGM-CSF and its subsequent detection after neutralisation was also investigated (cross hatched bars).
Maximum GIF-rovGM-CSF binding was observed at pH 7.5 as shown by the lowest O.D. (492nm) values. Exposure of rovGM-CSF to high and low pH values had little significant effect on rovGM-CSF detection by ELISA ($p > 0.05$) when compared with that at pH 7.5.

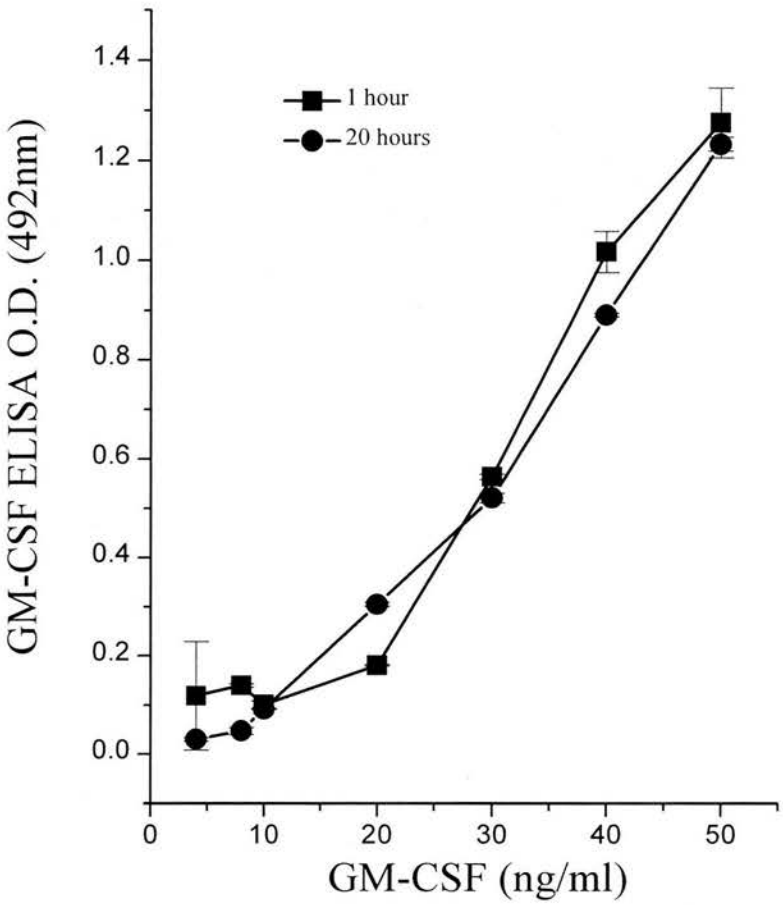

Fig. 4.14 GIF reactivity with GM-CSF as a function of time.
The clearance of increasing concentrations of rovGM-CSF (x-axis, ng/ml) by GIF was tested after incubations for 1 h and 20 h.
No significant increase or decrease ($p > 0.05$) in GIF-rovGM-CSF binding was observed after 20 h when compared with binding after 1 h.

4.3. Discussion

4.3.1. Characterisation of GIF multimer formation

In this chapter the monomer/multimer structure of the GIF molecule that bound ovine GM-CSF *in vitro* was investigated. Under physiological conditions (0.15 M NaCl and pH 7.2), GIF was present in solution predominantly as a homo-tetramer comprising 4 x 28 kD GIF subunits. This was evidenced by the isolation of a 115 kD GIF complex by Sephacryl-200HR gel filtration run in the presence of PBS and the dissociation of this complex into 28 kD subunits when exposed to reducing conditions. Formation of a higher order GIF molecule was required for ovGM-CSF binding since the 28 kD subunit did not bind ovGM-CSF. Both tetrameric and dimeric forms of GIF were shown to bind ovGM-CSF. In the presence of high salt and non-ionic detergent (as observed with gel filtration of ^{125}I-GIF), the tetrameric conformation was less stable and dissociation to the dimer form was favoured. This implied that tetrameric GIF comprised two dimers that were held together by non-covalent bonds. In contrast, dimeric GIF was disrupted by boiling in the presence of a reducing reagent and this suggests that intermolecular disulphide may be involved in dimer formation. Furthermore, the 28 kD subunit did not self-associate under physiological conditions *in vitro*, implying that oligomerisation may be part of post-translational modification of the GIF protein *in vivo*. The degree of GIF oligomerisation is clearly dependent on the ionic strength of the solution.

Ho and Shuman (1996) have shown that the dsRNA-binding protein encoded by the E3L gene of vaccinia virus is a dimer at high ionic strength (>0.5M NaCl) but as the ionic strength is reduced to 0.1M, self-associates to form higher order oligomers.

In contrast to this evidence that supports dimeric GIF-rovGM-CSF interaction, EDC-peptide cross-linking of both the ^{125}I-GIF and GIF-rovGM-CSF complexes suggested that rovGM-CSF was associated with tetrameric GIF whilst no mobility shift concomitant with dimeric ^{125}I-GIF binding rovGM-CSF was detected. Since the efficiency of crosslinking in this study was low (a similar observation of low cross-linking efficiency by EDC of M-T7/IFN-γ hetero-oligomers and IFN-γ homodimers was made by Upton *et al*, 1992), further analysis is needed to confirm this observation. One explanation for the presence of tetrameric GIF rather than dimeric GIF in the GIF-rovGM-CSF complex identified by cross-linking could be that the binding of rovGM-CSF to dimeric GIF promoted further oligomerisation even in the presence of high ionic strength. Stomski *et al*, (1996) and Guthridge *et al* (1998) postulate a model for cellular receptors for IL-3, GM-CSF and IL-5 whereby the cytokines bind their respective receptors and undergo oligomerisation which results in the activation of the receptors.

Similarly ligand–induced receptor conversion from a dimer to a tetramer has been reported for granulocyte colony-stimulating factor receptor (Hiraoka *et al*, 1994). Horan *et al* (1997) report that soluble granulocyte-colony stimulating factor receptor (G-CSFR) has a weak tendency to self-associate into a dimer in the absence of a ligand but this receptor-receptor binding is enhanced by ligand binding and the most stable complex occurs at 2:2 stoichiometry. Clearly the GIF-GM-CSF complex observed in the cross-linking experiment could fit this model of ligand-induced oligomerisation if GIF homodimers bound single GM-CSF molecules then oligomerised to form a more stable complex that comprised tetrameric GIF and two GM-CSF molecules.

The information obtained from protein structure prediction analysis was limited. The predicted secondary structure of GIF appeared typical of the structure of many soluble globular proteins. Future experiments that involve such techniques as X-ray crystallography are required to determine the structure of GIF and the GIF-GM-CSF complex.

4.3.2. Analysis of glycosidic residues linked to GIF

In contrast to a number of soluble virus cytokine receptors that are glycoproteins such as M-T7 (13% glycosylation, Lalani *et al*, 1997) and M-T1 (12% glycosylation, Lalani *et al*, 1999a) of myxoma virus, and cowpox virus CrmD (15% glycosylation, Loparev *et al*, 1998), GIF does not appear to be glycosylated. Indeed it seems likely that given that the observed and predicted molecular masses of GIF are essentially the same (28 kD), any contribution of carbohydrate (even O-linked) to GIF molecular structure must be minimal. Unlike the human GM-CSFR α subunit that is considered to modulate cellular responsiveness through differences in glycosylation (Budel *et al*, 1993; Ding *et al*, 1995), GIF is a protein in which N-glycosylation is not required for binding to GM-CSF *in vitro*. In addition, N-glycosylation of rovGM-CSF is not associated with GIF-rovGM-CSF since, from ligand blotting analysis, GIF was shown to bind both glycosylated and unglycosylated rovGM-CSF. In contrast to the GM-CSFR α subunit, glycosylation of GM-CSF is not required for its biological activity (Kaushansky *et al*, 1989).

4.3.3 Factors affecting GIF-rovGM-CSF binding

Considerable rovGM-CSF-binding capacity was lost when GIF was exposed to acidic pH. This was not recovered when the GIF solution was neutralised to pH 7.

Acid-induced unfolding of proteins can result in loss of tertiary structure but with retention of secondary structure. Narhi *et al* (1996) have shown that at acidic pH (below pH 4) TNF-α not only disassociates from trimers to the monomeric form but can convert from a native anti-parallel beta-sheet structure to an alpha-helix structure. Such a loss of native tertiary structure may account for the loss of GIF activity observed during affinity chromatography where GIF is eluted at low pH from the GM-CSF-Sepharose column.

Thermal disruption of the GIF complex by boiling appeared to be temporary with much of the GM-CSF-binding activity recovered after the solution cooled. This suggests that, in the absence of reducing agents or acidic conditions, the GIF molecule can refold into the native conformation.

Formation of the GIF-rovGM-CSF complex appeared characteristic of ligand–soluble receptor interactions, however a more detailed investigation into the binding affinity of GIF for its ligand(s) is described in the following chapter.

4.3.4. The role of the 43 kD protein in GIF-rovGM-CSF binding

The 43kD peptide that co-eluted with GIF from rovGM-CSF-Sepharose is not required for GIF activity *in vitro*. It appears to be a ubiquitous protein present in supernatant collected from a variety of cell types that include transfected and un-transfected CHO cells and orf virus infected and uninfected FLM cells. From Western blot analysis (carried out in the previous chapter) of samples collected from virus infected cells at different times, the level of 43kD expression appears to mirror that of GIF. Whether the 43kD peptide has any definitive role in the expression and secretion of GIF remains unclear.

CHAPTER 5

THE *IN VITRO* LIGAND-BINDING PROPERTIES OF GM-CSF-INHIBITORY FACTOR

5.1. Introduction

In the previous chapter, homo-tetrameric and homo-dimeric GIF complexes were shown to bind rovGM-CSF. In this chapter, the binding specificity of GIF was tested against a range of cytokines and GM-CSF of different species.

Ovine recombinant cytokines and chemokines have been produced that are biologically active (Entrican *et al*, 1989, 1996; McInnes *et al*, 1991, 1993, 1994; Seow *et al*, 1993, 1994). This allows GIF reactivity with ligands other than GM-CSF to be tested. The recombinant ovine cytokines and chemokines included in this study were; IL-1β, IL-2, IL-3, IL-4, IL-5, IL-8, IFN-γ, Stem cell factor (SCF), VEGF, TNF-α, monocyte chemotactic protein–1 (MCP-1), macrophage inflammatory protein 1α (MIP-1α) and RANTES. These were expressed from CHO cells that had been transfected with the pEE14 plasmid vector containing the respective cytokine cDNAs. (see Section 2.4.1 and McInnes *et al*, 1991). These cytokines were tested for their ability to compete with GM-CSF for binding with GIF as measured by the GM-CSF clearance ELISA.

Since the heparin-binding domains of a number of chemokines are thought to be involved in their binding by virus receptors, for example the M-T7 protein of myxoma virus (Lalani *et al*, 1997), heparin was also tested for GIF-binding.

Alpha$_2$-macroglobulin, a potent inhibitor of viral proteases (Menendez Aria *et al*, 1992; Kisselev *et al*, 1994; Ryan-Poirier and Kawaoka, 1993) was also included in the competition ELISA to monitor for any proteolytic activity.

A second approach was based on the ligand blotting method described by Schwabe *et al* (1988). In their report, the authors identified the human IFN-α

Schwabe *et al* (1988). In their report, the authors identified the human IFN-α receptor by probing nitrocellulose blots of SDS-PAGE-separated Burkitt lymphoma cell extracts with ^{125}I-IFN-α. In the present study, ligand blots of recombinant cytokines separated by SDS-PAGE were probed with ^{125}I-GIF.

Orf virus is also capable of infecting humans (Groves *et al*, 1991; Yirrell *et al*, 1994b; Haig and Mercer, 1998) and it was important to determine whether GIF could bind human GM-CSF. In order to test whether GIF reactivity was species-specific, a number of commercially available recombinant cytokines of human and murine origin were included in the analysis.

Finally, the binding affinity of ^{125}I-GM-CSF for GIF was measured in an assay based on that described to measure IL-1β-Il-1β-receptor interactions in man (Dower *et al*, 1985; Symons and Duff, 1990).

The specific aims of this study were;

1.) To investigate the ligand specificity of GIF for cytokines and chemokines of ovine origin.

2.) To determine whether this specificity is species restricted.

3.) To measure the binding affinity of the GIF-GM-CSF interaction.

5.2. Results

5.2.1. Ligand specificity of GIF

A number of ovine cytokines, ovine chemokines, heparin and α_2-macroglobulin were tested for their ability to compete with GIF binding to rovGM-CSF as measured by GM-CSF clearance ELISA (see Section 2.4.2.). Competitive ligand binding to GIF was measured by a rise in GM-CSF levels detected by the ELISA as GIF-GM-CSF binding was inhibited.

Only recombinant ovine IL-2 out of all potential ligands (tested at greater than ten-fold molar excess to rovGM-CSF) demonstrated binding to GIF in the competitive assay ($p < 0.001$ when compared with supernatant from CHO cell culture (CHOUTF) that was included as a negative control sample, Fig. 5.1). In a parallel control assay carried out in the absence of GIF, the measurement of rovGM-CSF by the ELISA was not affected by any other cytokine or chemokine.

5.2.2. Cross-species reactivity of GIF

The species range of GIF reactivity was investigated (see Section 2.4.2.). Recombinant murine, bovine and human GM-CSF and IL-2 samples were tested for inhibition of GIF-ovGM-CSF reactivity (Fig. 5.2). GIF did not react with recombinant IL-2 or GM-CSF from man or mouse but GIF did bind rbovGM-CSF ($p < 0.001$ when compared with the GIF positive control). Binding to rbovIL-2 was considerably lower ($p < 0.05$). The slight increase in O.D. (492nm) measured in samples of mouse and human GM-CSF that were incubated with GIF and rovGM-

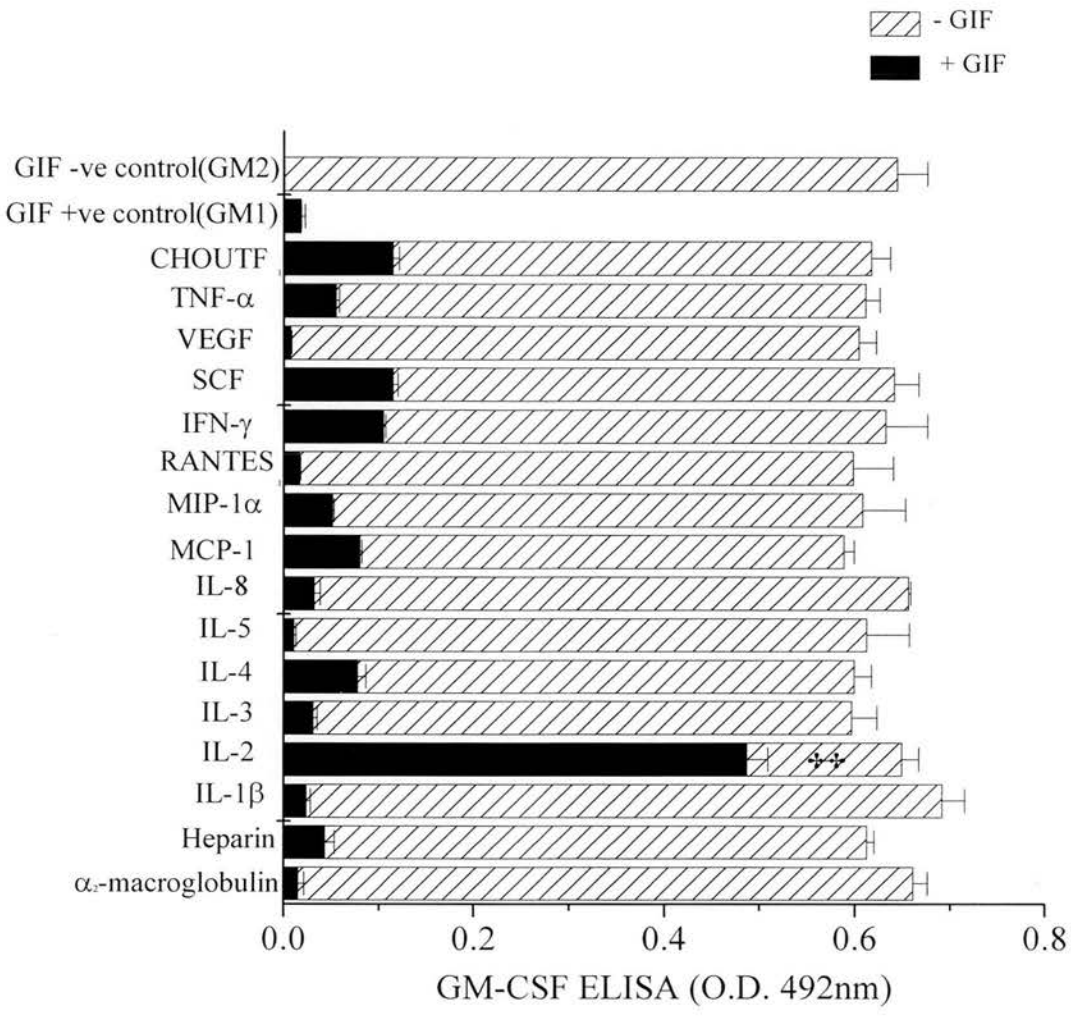

Fig. 5.1 GIF specificity by ligand competition assay.
The binding of ligands (labelled on the y-axis) to GIF (solid bar) was measured by a rise in absorbance (O.D. 402nm, x-axis) as rovGM-CSF clearance by GIF was inhibited. The cytokines and chemokines tested in this assay were recombinant proteins (100-200 ng/ml) and of ovine origin unless stated otherwise (i.e. prefixes bo = bovine and hu = human).
Alpha$_2$-macroglobulin, and heparin were used at between 1-2μg/ml. Recombinant ovine IL-2 was found to bind GIF (‡ $p < 0.001$ when compared with the GIF +ve control). Control samples included supernatants from GM1-CHO, GM2-CHO and untransfected CHO (CHOUTF) cell cultures.
Cytokines were tested, in the absence of GIF (hatched bar), for any interference with rovGM-CSF detection.

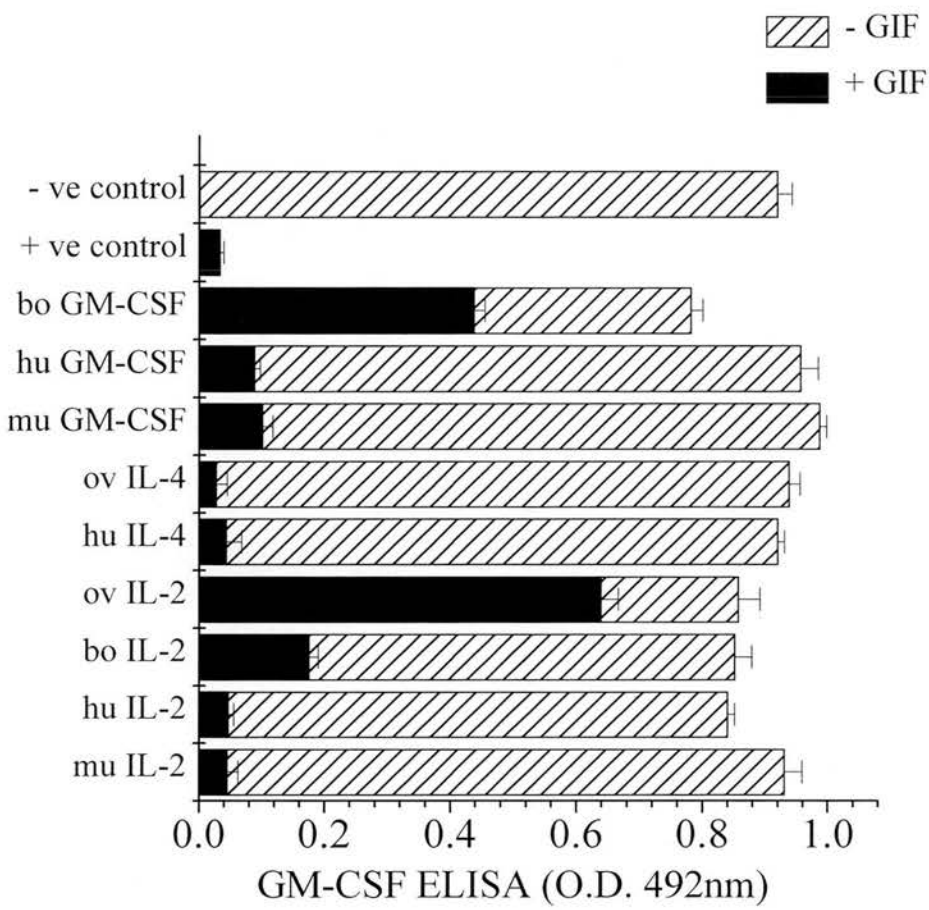

Fig. 5.2 Species specificity of GIF binding to various ligands. Recombinant cytokines from sheep (ov), cattle (bov), mouse (mu) and man (hu) were tested for inhibition of GIF-rovGM-CSF reactivity (solid bar) as measured by GM-CSF ELISA. Cytokines were tested, in the absence of GIF (hatched bar), for any interference with rovGM-CSFdetection.
(Assay was carried out as described in Fig. 5.1)

CSF was also seen in assays where GIF was absent and probably corresponds to low level non-specific binding of the cytokines to the anti-ovine GM-CSF mAbs of the ELISA. As already reported (Entrican *et al*, 1996), bovine GM-CSF was not detected by the GM-CSF ELISA used in this study.

5.2.3. Ligand blot analysis

The recombinant ovine cytokines that bound GIF by competitive ovGM-CSF clearance ELISA were identified and confirmed by ligand blot analysis (see Section 2.4.2.). This analysis was not performed on recombinant bovine GM-CSF and IL-2 due to lack of material.

Samples of human, murine and ovine cytokines were separated by 15% SDS-PAGE under both reducing and non-reducing conditions and electro-transferred to cellulose nitrate. ^{125}I-GIF was used to probe the separated and immobilised proteins (Fig. 5.3 A. and B.). ^{125}I-GIF bound only rovIL-2 and rovGM-CSF and was not reactive with other ovine cytokines/chemokines or cytokines from mouse or man tested in this study. No difference in ^{125}I-GIF binding to rovIL-2 and rovGM-CSF was observed when the cytokines were separated under reducing or non-reducing conditions. In the presence of a 100-fold excess of unlabelled GIF as a specificity control, ^{125}I-GIF binding to both rovIL-2 and rovGM-CSF was blocked (Fig. 5.3 C. and D.)

5.2.4. The effect of rovIL-2 on GIF-rovGM-CSF reactivity

In order to investigate whether GIF bound both rovIL-2 and rovGM-CSF through the same or proximal GIF binding site(s), increasing concentrations of rovIL-2 were tested for the effect on GIF-rovGM-CSF binding as measured by GM-CSF clearance

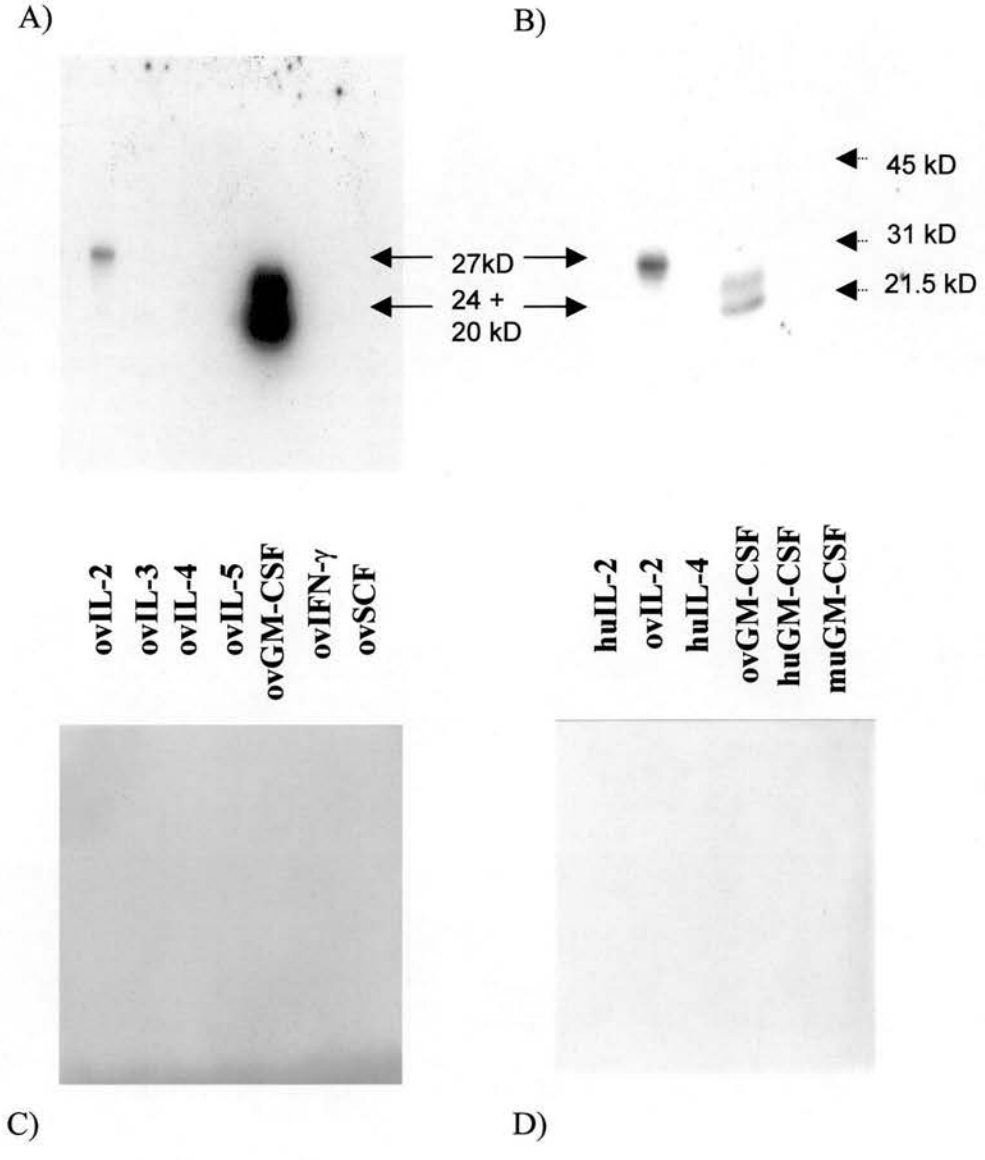

Fig. 5.3 ^{125}I GIF-cytokine ligand blot analysis.
^{125}I GIF was used to probe A) a range of ovine cytokines and B) human, murine and ovine cytokines which were separated by 15% SDS-PAGE and transferred to nitrocellulose membranes. ^{125}I GIF bound to rovGM-CSF (20kD + 24 kD) and rovIL-2 (27 kD). As a specificity control, 10 nM of unlabelled GIF was used to compete for ^{125}I GIF binding to the cytokines (C and D). The position of molecular weight markers (dashed arrows) are indicated.
This experiment was repeated four times with the same result (not shown).

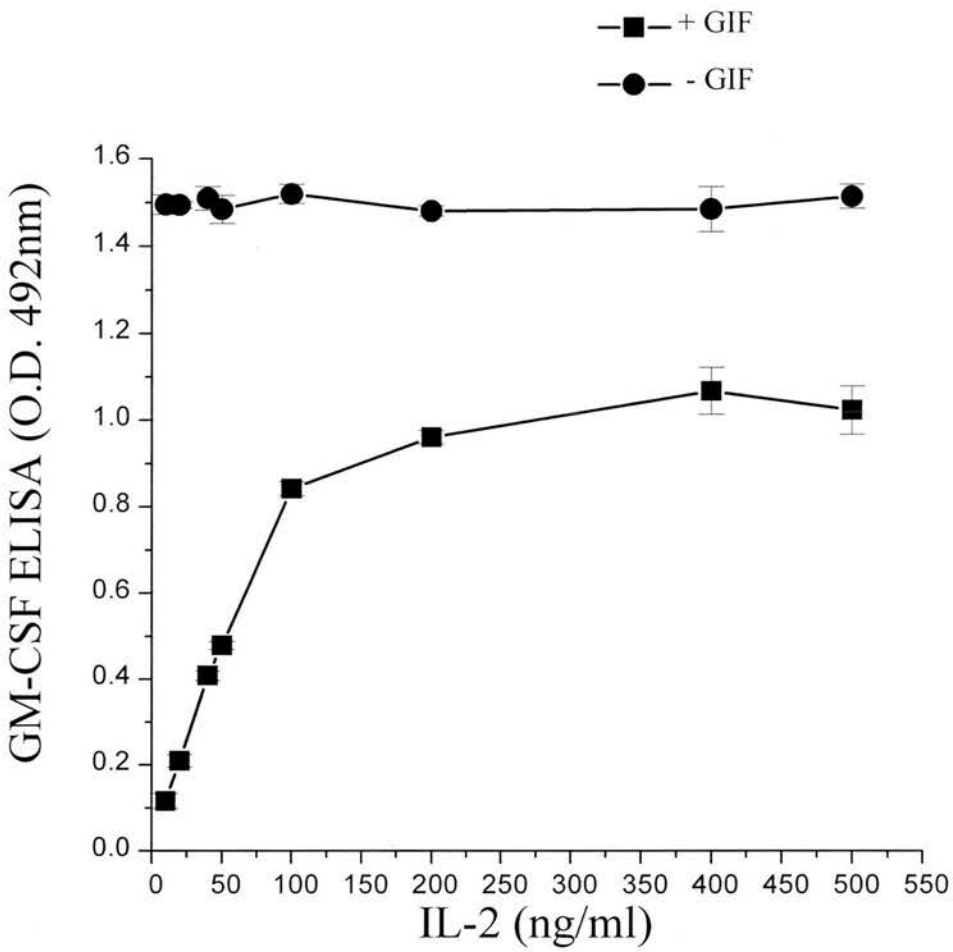

Fig. 5.4 The effect of IL-2 on GIF-GM-CSF reactivity.
Increasing amounts of purified rovIL-2 (10-500 ng/ml, x-axis) were tested for inhibition of GIF clearance of an 8ng/ml spike of rovGM-CSF in the GM-CSF ELISA (solid square). However, the inhibition of GIF-GM-CSF binding (as shown by the rise in O.D. (y-axis)) at saturating concentrations of rovIL-2 (200-500ng/ml) was shown to be incomplete ($p < 0.001$) when compared with either the GIF - ve control for this experiment (GM2-CHO supernatant O.D. (492nm) value of 1.42 +/- 0.02) or with rovIL-2 and rovGM-CSF (8ng/ml) in the absence of GIF (solid circle).
The value for the GIF positive control (GM1-CHO supernatant) in this experiment was 0.098 +/- 0.002 (not shown).

ELISA (Fig.5.4). Levels of purified rovIL-2 which were in 50-100 fold excess of the rovGM-CSF spike failed to completely inhibit rovGM-CSF binding to GIF.

5.2.5. The affinity of binding of GIF to GM-CSF and IL-2

The affinity-binding of GIF for rovGM-CSF and rovIL-2 was determined by a soluble binding assay using ^{125}I-rovGM-CSF and ^{125}I-rovIL-2 (Figs. 5.5 and 5.6). Specific binding of either cytokine to GIF was determined by subtracting the counts obtained by polyethylene glycol precipitation of each radio-labelled cytokine in the absence of GIF (see Section 2.4.3.). Scatchard analysis was applied to the mean values of the ^{125}I-ligand –GIF binding data that were collected from the soluble binding assays. GIF bound to rovGM-CSF with a K_d of 369 +/- 52 pM (Fig. 5.7) and to rovIL-2 with a K_d of 1040 +/- 79pM (Fig. 5.8). GIF bound to rovGM-CSF with a higher affinity than it bound to rovIL-2.

Processing the same data by the Scatchard plot analysis tool provided with the Equilibrate Ligand Binding Program (Version 1.2, G.J.C. Veenstra, Rockville, USA) gave the binding affinity of rovGM-CSF to GIF as K_d = 374 +/- 175 pM. For rovIL-2 binding to GIF, the K_d was 1044 +/- 282 pM.

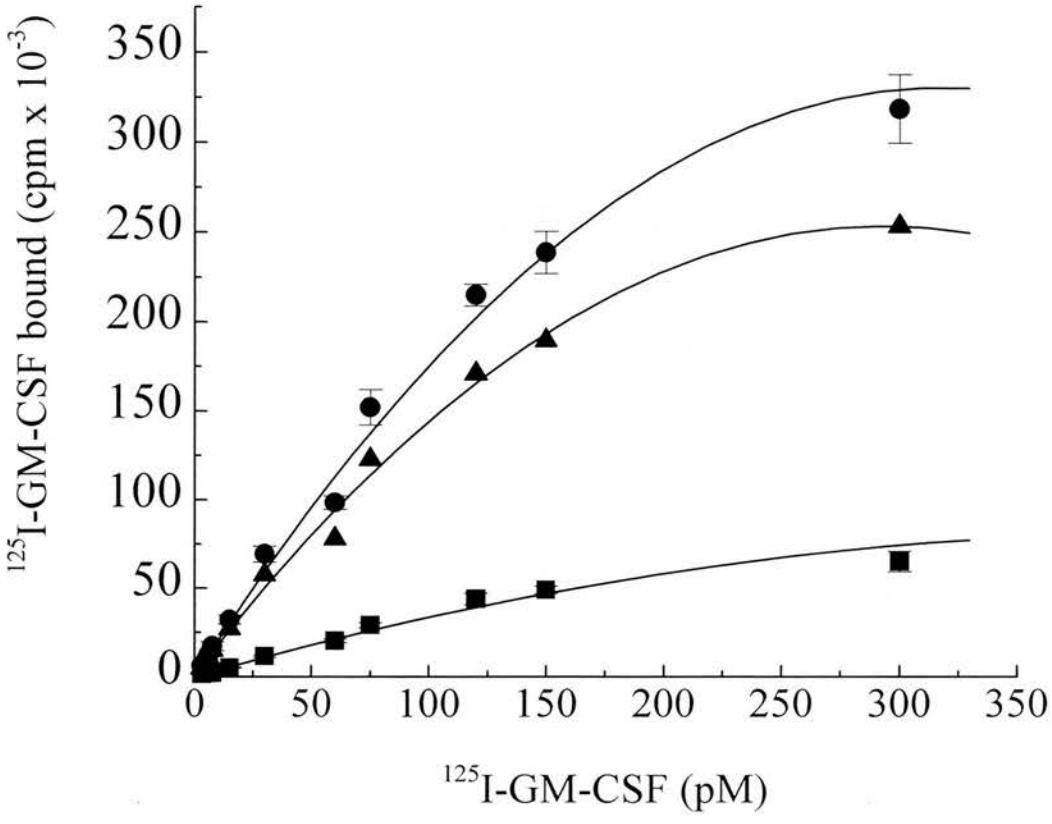

Fig. 5.5 Equilibrium binding of ^{125}I-rovGM-CSF to GIF in solution. Purified GIF (100 ng) was incubated with increasing concentrations of ^{125}I-rovGM-CSF (x-axis, pMoles). The PEG precipitated GIF-^{125}I-rovGM-CSF complex was collected onto fibre discs and bound ^{125}I-rovGM-CSF measured in a γ-counter.
To determine the specific binding of ^{125}I-rovGM-CSF to GIF (solid triangles and given as ^{125}I-rovGM-CSF bound cpm on the y axis), the binding of ^{125}I-rovGM-CSF to the discs in the absence of GIF (solid squares) was subtracted from the total binding (solid circles).
Data presented here represent the mean of quadruplicate samples.

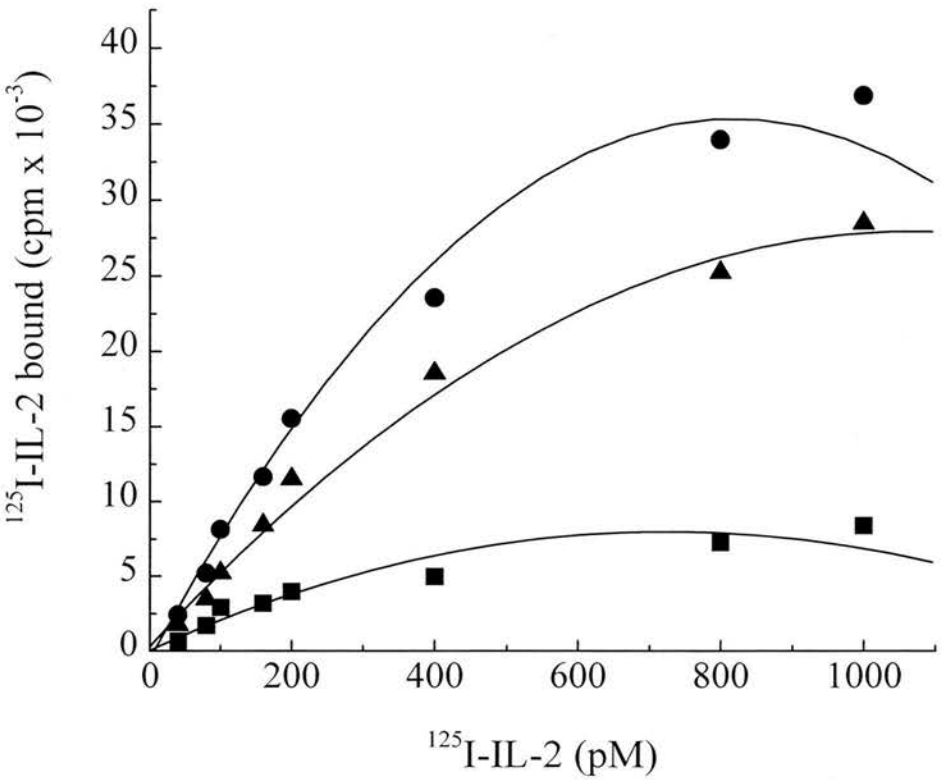

Fig. 5.6 Equilibrium binding of ^{125}I-rovIL-2 to GIF in solution.
Purified GIF (100 ng) was incubated with increasing concentrations of ^{125}I-rovIL-2 (x-axis, pMoles). The PEG precipitated GIF-^{125}I-rovIL-2 complex was collected onto fibre discs and bound ^{125}I-rovIL-2 measured in a γ-counter.
To determine the specific binding of ^{125}I-rovIL-2 to GIF (solid triangles), the binding of ^{125}I-rovIL-2 to the discs in the absence of GIF (solid squares) was subtracted from the total binding (solid circles).
Data presented here represent the mean of quadruplicate samples

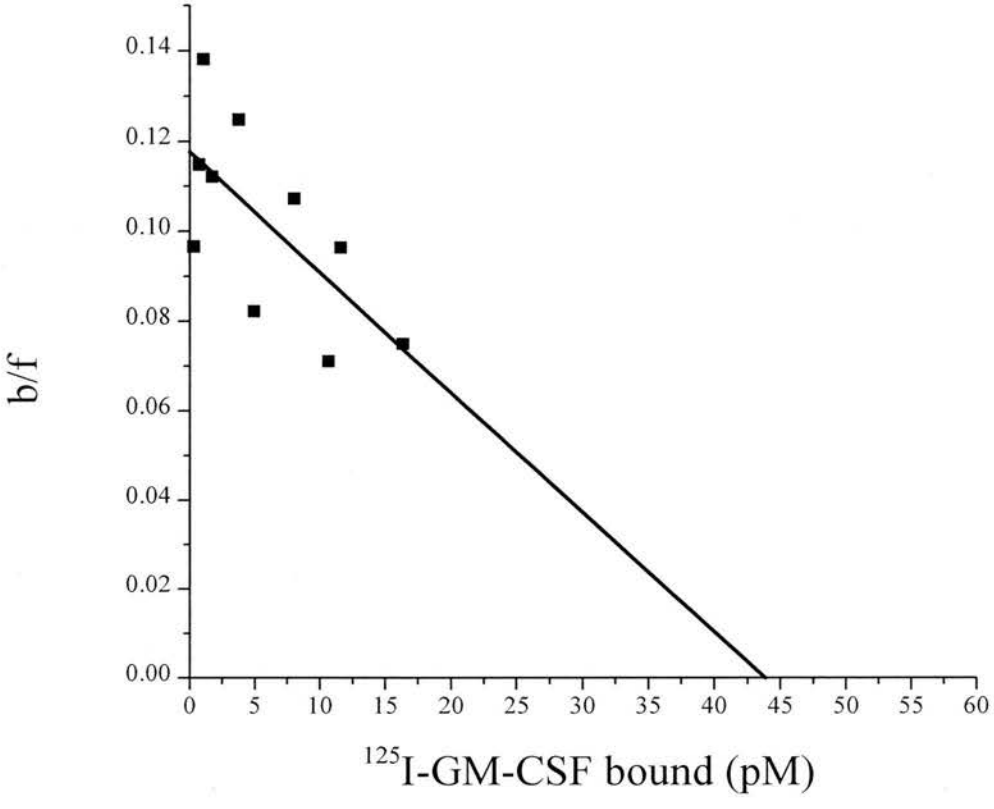

Fig. 5.7 GM-CSF-GIF binding: Scatchard plot analysis.
Scatchard analysis was applied to the mean of data collected from three ^{125}I-rovGM-CSF soluble binding assays and plotted as the concentration of ^{125}I-rovGM-CSF bound (x-axis, pM) versus the ratio of ^{125}I-rovGM-CSF bound/^{125}I-rovGM-CSF free (y-axis, b/f). A linear best line fit was applied to the data points in order to intercept both x-axis and y-axis (Origin, Microcal).
The affinity of rovGM-CSF-GIF binding (K_d) was determined from the modified Eadie-Scatchard equation (Segel, 1976):

$$[S]_b/[S]_f = - 1/K_d\ [S]_b + n[E]_t/K_d$$

where [S] = concentration of ligand, $[S]_b/[S]_f$ = b/f and $n[E]_t$ = the total concentration of ligand binding sites (the intercept at the x-axis). The slope of any line plotted through the points = -1/Kd and consequently the intercept on the y-axis = $n[E]_t/K_d$.
GIF bound rovGM-CSF with a K_d of 369 +/- 52 pM.

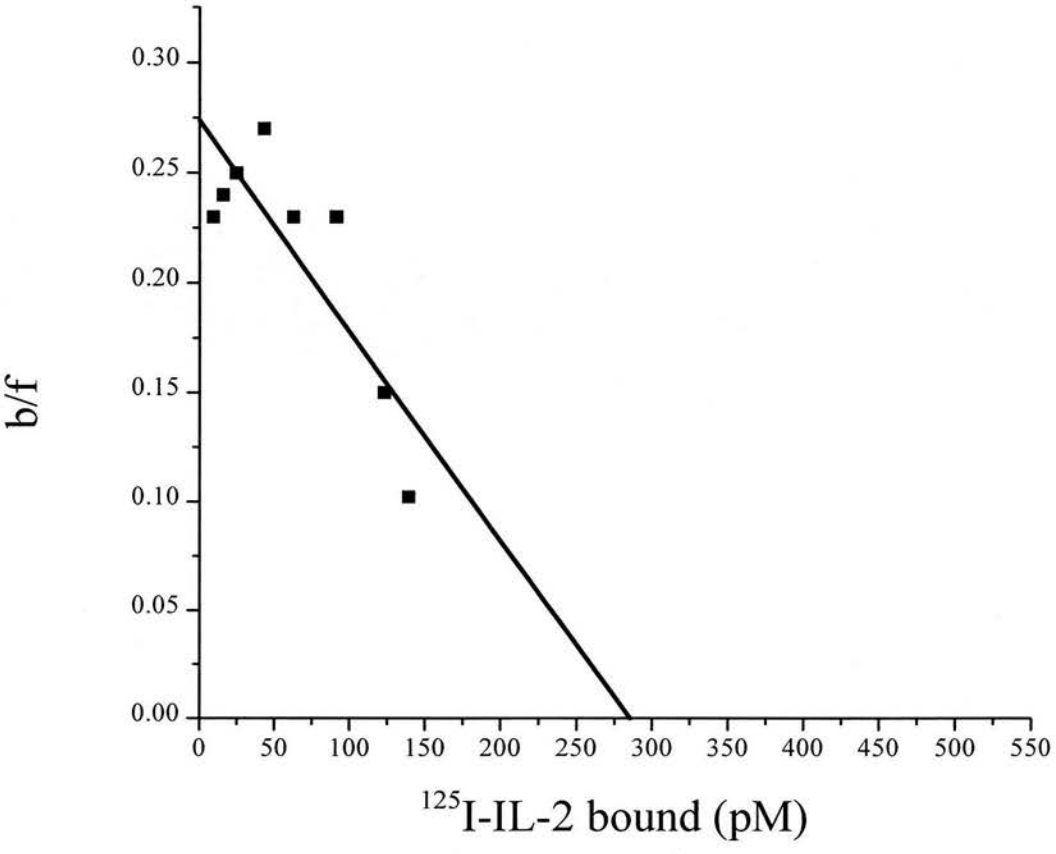

Fig. 5.8 IL-2-GIF binding: Scatchard plot analysis. Scatchard analysis was applied to the mean of data collected from ^{125}I-IL-2 soluble binding assays. GIF bound ovIL-2 with a K_d of 1040 +/- 79 pM

5.3. Discussion

5.3.1. Identification of the ligand specificity of GIF

A panel of recombinant ovine cytokines and chemokines from sheep were tested for binding to GIF by a competition ELISA assay. GIF was shown to bind rovGM-CSF with higher affinity than rovIL-2. Some poxvirus immunomodulatory proteins such as the MT-7 (binds IFN-γ and CXC, CC and C chemokines, Lalani *et al*, 1997) and MT-2 (binds TNFα and inhibits virus-induced apoptosis, Sedger and McFadden, 1996) of myxoma virus and the 38 kD glycoprotein of tanapox virus (binds IL-2, IL-5 and IFN- γ, Essani *et al*, 1994) have the ability to bind and inactivate multiple, sometimes apparently unrelated cytokines and this property represents an economical way of controlling host immunity. Whilst no homology could be established between GIF and any cytokine receptors identified to date, GIF appears to fit into this category with its ability to bind both rovGM-CSF and rovIL-2.

The question arose whether rovGM-CSF and rovIL-2 shared the same binding domain. The addition of a 100-fold excess of rovIL-2 to the reaction mixture was shown to compete up to approximately 75% of the GM-CSF binding to GIF. Kanakura *et al*, (1993) have reported that GM-CSF competed up to 75% with radio-labelled IL-2 for binding to the β form of IL-2R that is expressed on the human myeloid leukemia cell line, M07E, whereas no competition of GM-CSF binding was observed with IL-2 even at a 400-fold molar excess. This implied that whilst distinct binding domains for either cytokine were present within the IL-2 receptor, the binding of GM-CSF could sterically influence the binding of IL-2. Although this evidence may suggest that the respective binding domains of GIF for ovine GM-CSF

and ovine IL-2 are not shared, in the absence of an assay system for ovine IL-2, the reciprocal experiment whereby an excess of rovGM-CSF was tested for the effect on GIF binding rovIL-2 was not carried out. Consequently the exclusivity or otherwise of the GIF binding domains for ovGM-CSF and ovIL-2 remains uncertain. Alternatively, the failure of an excess of rovIL-2 to completely inhibit GIF binding rovGM-CSF may reflect the difference in binding affinities of GIF for ovGM-CSF and ovIL-2 or the effect of steric hindrance of one ligand by the other.

A structural comparison of human and ovine GM-CSF with human and ovine IL-2 (carried out by Colin McInnes) did not reveal any common features other than both human GM-CSF and human IL-2 are members of the short chain, four α-helical-bundle family of cytokines that also includes IL-4 (Von Feldt *et al*, 1994.). However ovine IL-4 did not bind GIF.

5.3.2. Investigation into species specificity of GIF-ligand binding

The binding of GIF appears to be restricted to ovine and bovine GM-CSF and IL-2. Although orf virus also infects humans, GIF did not bind human GM-CSF or human IL-2. This suggests that the gene encoding GIF had been acquired through the co-evolution of orf virus with sheep rather than with man. Whether the failure of GIF to bind human GM-CSF and human IL-2 could be associated with differences in the pathologies of ovine and human infections described by Yirrell and Vestey (1994) is unclear and warrants further investigation.

In spite of orf virus failing to infect cattle (Darbyshire and Huck, 1966), GIF did bind bovine GM-CSF. (GIF also bound bovine IL-2 but at a lower level.) Further investigation into GIF reactivity with bovine GM-CSF and IL-2 is clearly warranted.

Whilst the amino acid sequence of ovine GM-CSF is highly homologous to the published bovine sequence (80% identity, Leong *et al*, 1989) and human sequence (80% identity, Cantrell *et al*, 1985), some conservation of sequence between ovine and bovine GM-CSF is absent from the human sequence (Fig. 5.9). The sequences of ovine GM-CSF and murine GM-CSF are less homologous with 57 % identity, (Gough *et al*, 1985).

Ovine	APTRQPSPVT	RPWQHVDAIK	EALSLLNDST	TAAVMDETVE	40
Bovine	----P-NTA-	----------	-------H-S	-D---ND-*-	39
Human	--A-S---S-	Q--E--N--Q	--**RR**---L-R	---E-N----	40
Murine	----S-IT--	---K--E---	--N--D***-	MPVTLN-E--	37

Ovine	VVSEMFDSQE	PTCLQTRLEL	YKQGLRGSLT	SLTGSLTMMA	80
Bovine	----K-----	--------K-	--N--Q----	--M-------	79
Human	-I-----L--	----------	----------	K-K-P------	80
Murine	---NE-SFKK	L--V----KI	FE-----NF-	K-K-A-N-T-	77

Ovine	SHYKKHCPPT	QETSCETQII	TFKSFKENLK	DFLFIIPFDC	120
Bovine	T--E------	P----G--F-	S--N---D--	E---------	119
Human	----Q-----	P----A----	--E-------	---LV-----	120
Murine	-Y-QTY----	P--D----VT	-YAD-IDS--	T--TD---E-	117

Ovine	WEPVQK	126
Bovine	---A--	125
Human	-----E	126
Murine	KK----	123

Fig. 5.9 Alignment of the amino acid sequences of GM-CSF from sheep, cattle, man and mouse (adapted from McInnes and Haig, 1991).
The ovine sequence is given as the consensus with only those amino acids that are different being shown for the other sequences. The dashes indicate complete identity with the ovine sequence. Asterisks indicate amino acid deletions from the bovine and murine sequences.

Those regions of the human GM-CSF protein that are critical for species restricted biological activity via its cellular receptor have been identified (Kaushansky *et al*, 1989). The regions encompassing amino acids 21-31 and 78-94 are considered important (underlined, Fig. 5.9), with a single substitution of Arginine[23] to glutamine resulting in greatly reduced activity of the cytokine (Kaushansky *et al*, 1989). The sequence of human GM-CSF differs from both ovine and bovine GM-CSF sequences at amino acids 23 and 24 (bold type, Fig. 5.9) with neither change considered conservative (McInnes and Haig, 1991). Whether this region of the ovine GM-CSF protein contains the GIF binding domain would represent the basis for future study.

5.3.3. Analysis of binding affinities of GIF for rovGM-CSF and rovIL-2

In this study, the affinity of GIF-rovGM-CSF binding was calculated as Kd = 369 pM. As yet there is no record of any GM-CSF- receptor proteins having been characterised from ruminants. Consequently the activity of GIF as a soluble cytokine receptor cannot be directly compared with that of sheep GM-CSF receptors. A soluble ovine IL-2-receptor alpha chain has been identified (Verhagen *et al*, 1992) but with no structural similarity to the GIF protein. Nevertheless, human GM-CSF and IL-2 receptors have been well characterised (Dipersio *et al*, 1990, 1991; Raines *et al*, 1991; Brown *et al*, 1995 and Heaney *et al*, 1995) and for the purposes of this study will be taken as representative of mammalian GM-CSF and IL-2 receptors.

The α subunit of human GM-CSFR (huGM-CSFRα) exists in both transmembrane -anchored and soluble isoforms. The soluble isoform, a 55- to 60-kD glycosylated protein, lacks the transmembrane and cytoplasmic domains of the intact receptor. The soluble huGM-CSFRα binds to huGM-CSF in solution and has been shown to

inhibit huGM-CSF biological activity *in vitro* (Brown *et al*, 1995; Monfardini *et al*, 1998). Soluble huGM-CSFRα has been reported to bind huGM-CSF in solution with a dissociation constant range (Kd) of 500-3800 pM and when retained on the cell surface with a Kd of 331 pM (Chiba *et al*, 1990; Khwaja *et al*, 1993.). If similar soluble receptor-ligand interactions occur in sheep, then the antagonistic effect of GIF on ovGM-CSF binding to its cellular receptor would be seen as significant, particularly in the local environment of the responsive cell.

The receptor for IL-2 belongs to the same super-family of cytokine receptors as GM-CSF. Like the GM-CSFRα, the alpha subunit of IL-2R is expressed as a soluble or membrane-bound form. It has been proposed that soluble IL-2Rα (sIL-2Rα) could negatively modulate local immune responses (Verhagen *et al*, 1994). Jacques *et al*, (1987) have determined that the sIL-2Rα binds IL-2 with a dissociation constant (Kd = 30 nM) identical to a low affinity cell-surface IL-2R (p55/ Tac antigen). This is in contrast to the high affinity binding of IL-2 to the cell surface trimeric receptor complex (Kd = 25 pM). From Scatchard analysis, the affinity of GIF-rovIL-2 binding was calculated as Kd = 1.04 nM. As with the GIF-rovGM-CSF interaction, the binding of GIF-rovIL-2 is again of higher affinity than that recorded for the soluble IL-2Rα to IL-2 in man. Given that soluble forms of the cellular receptors for human GM-CSF and human IL-2 are produced in general to downregulate normal GM-CSF and IL-2 driven effector mechanisms, then clearly GIF has the potential to interfere with similar immune response mechanisms in the sheep to the advantage of orf virus. The effect of GIF on ovine GM-CSF and ovine IL-2 function is investigated in chapter 6.

CHAPTER 6

THE FUNCTION OF GM-CSF-INHIBITORY FACTOR

6.1. Introduction

In Chapter 5, GIF was shown to bind both ovine GM-CSF and IL-2. However the consequence of this binding on GM-CSF and IL-2 function was not determined. The role of GM-CSF and IL-2 in the anti-viral immune response to orf virus is unclear but since they are both targeted by GIF, this suggests they may be important in sheep cutaneous immunity to virus infection. The focus of this chapter was to investigate whether GIF inhibited GM-CSF and IL-2 activity by binding to the cytokines and preventing their interaction with their respective receptors.

Appropriate biological assays for ovine GM-CSF and ovine IL-2 were available for this study. The effect of GM-CSF on ovine bone marrow derived colony-forming cells has been assessed *in vitro*. (Haig *et al*, 1990; McInnes *et al*, 1993; Haig *et al*, 1994). GM-CSF stimulated increased numbers of neutrophils, macrophages and eosinophil colonies in soft agar haemopoietic clonogenic assays. In this study the approach was to investigate firstly, whether GIF inhibited the binding of ^{125}I-rovGM-CSF to its receptor on the surface of neutrophils as measured by a cell binding assay (based on Dower *et al*, 1985) and secondly, the effect of GIF on the stimulation of bone marrow haemopoietic cells by GM-CSF that is measured in a soft agar clonogenic assay described by Haig *et al* (1994).

Ovine IL-2 stimulates T cell blast proliferation (Bujdoso *et al*, 1990). The assay exploits the ability of IL-2 to stimulate the proliferation of sheep T cell blasts (generated by antigen or mitogen (Con A) stimulation of lymphocytes) as measured by a ^{3}H-thymidine uptake assay. In the present study, the approach was to determine firstly, the effect of GIF on ^{125}I-rovIL-2 binding to IL-2 receptors on an enriched

$CD4^+$ T cell subset isolated from ovine lymph node and measured by the ^{125}I-cytokine-cell binding assay, and secondly, the effect of GIF on IL-2 –induced proliferation of $CD4^+$ T cell blasts transformed with Con A and measured by cellular uptake of ^3H-thymidine.

The aims of this study were;

1.) To determine whether GIF can block the binding of GM-CSF and IL-2 to their respective cellular receptors.

2.) To show that in binding both GM-CSF and IL-2, GIF can also block the biological activities of the cytokines.

6.2. Results

6.2.1. The effect of GIF on cytokine-cell surface receptor interactions

In order to determine the effect of GIF on the binding of rovGM-CSF and rovIL-2 to their respective cell surface receptors, two separate cell-binding assays were developed (see Section 2.5.).

In the first analysis, the binding of increasing concentrations of ^{125}I-rovGM-CSF to GM-CSF receptors on neutrophils isolated from peripheral blood was measured. In the second, ^{125}I- rovIL-2 binding to a predominantly $CD4^+$ T cell population (90%), isolated from mesenteric lymph node, was measured.

^{125}I-rovGM-CSF was found to bind to neutrophils in a dose-dependent fashion (Fig. 6.1). This binding was inhibited across a range of ^{125}I-rovGM-CSF concentrations (100-1000 pM) by the addition of 10 nM purified GIF. The addition of 100 nM of unlabelled rovGM-CSF to the cell suspension served to demonstrate the specificity of ^{125}I-rovGM-CSF binding. Neutralisation of GIF inhibition of ^{125}I-rovGM-CSF binding to its receptor on neutrophils was achieved by pre-treatment of GIF with the rabbit anti-GIF (ra101).

A similar level of inhibition by GIF on ^{125}I-rovIL-2 binding to $CD4^+$ T cells was observed (Fig. 6.2). The specificity of both ^{125}I-rovIL-2 – T cell binding and ^{125}I-rovIL-2-GIF binding was demonstrated by inclusion of 100 nM unlabelled rovIL-2 and 2 μg/ml ra101 respectively.

In order to compare the binding affinities of both cytokines for their respective surface receptors with the affinities of GIF for rovGM-CSF and rovIL-2 that were determined by Scatchard plot analysis earlier, in Chapter 5, a similar analysis was

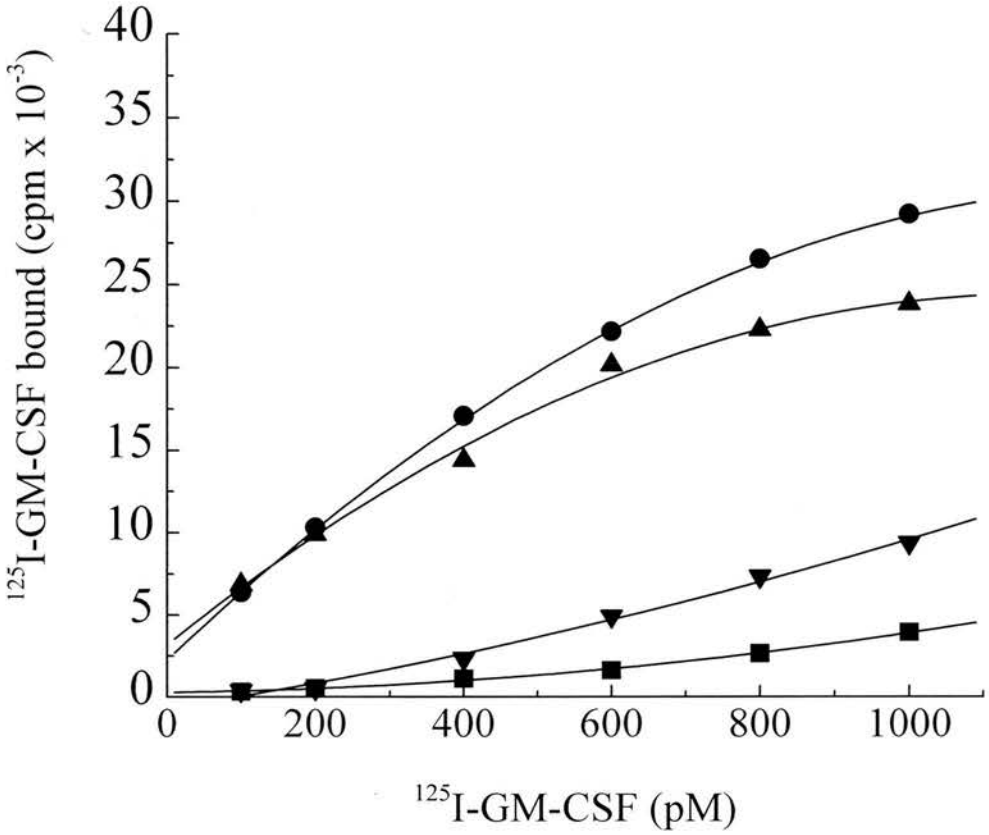

Fig. 6.1 Effect of GIF on ^{125}I-rovGM-CSF binding to neutrophils. ^{125}I-rovGM-CSF was found to bind to neutrophils in a dose-dependent fashion (solid circles). This binding (y-axis, cpm x $10^{3)}$ was inhibited across a range of ^{125}I-rovGM-CSF concentrations (x-axis, pM) by the addition of 10 nM GIF (inverted solid triangles). The addition of 100 nM of unlabelled rovGM-CSF (solid squares) to the cell suspension served to demonstrate the specificity of ^{125}I-rovGM-CSF binding. Specificity of GIF-^{125}I-rovGM-CSF binding was shown by the neutralisation of GIF-^{125}I-rovGM-CSF binding by pre-treatment with the rabbit anti-GIF ra101 (solid upright triangles). Data represent the mean of triplicate samples.
A further two independent experiments showed similar results.

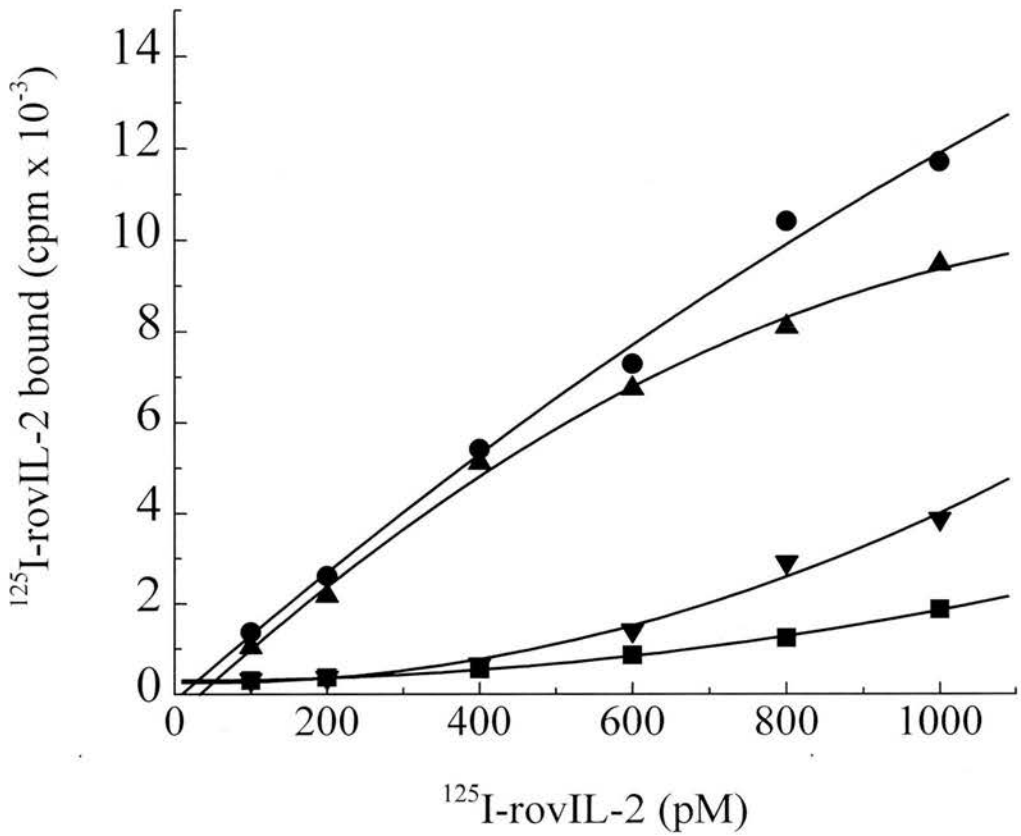

Fig. 6.2 Effect of GIF on ^{125}I-rovIL-2 binding to CD4$^+$ T cells. CD4$^+$ T cells were isolated from mesenteric lymph nodes. ^{125}I-rovIL-2 binding to CD4$^+$ T cells was measured (solid circles). GIF (10 nM) was found to inhibit ^{125}I-rovIL-2 binding across the range of ^{125}I-rovIL-2 concentrations tested (inverted triangles). Unlabelled rovIL-2 (100 nM) and anti-GIF were included as specificity controls for ^{125}I-rovIL-2 binding (squares) and GIF binding (upright triangles) respectively.

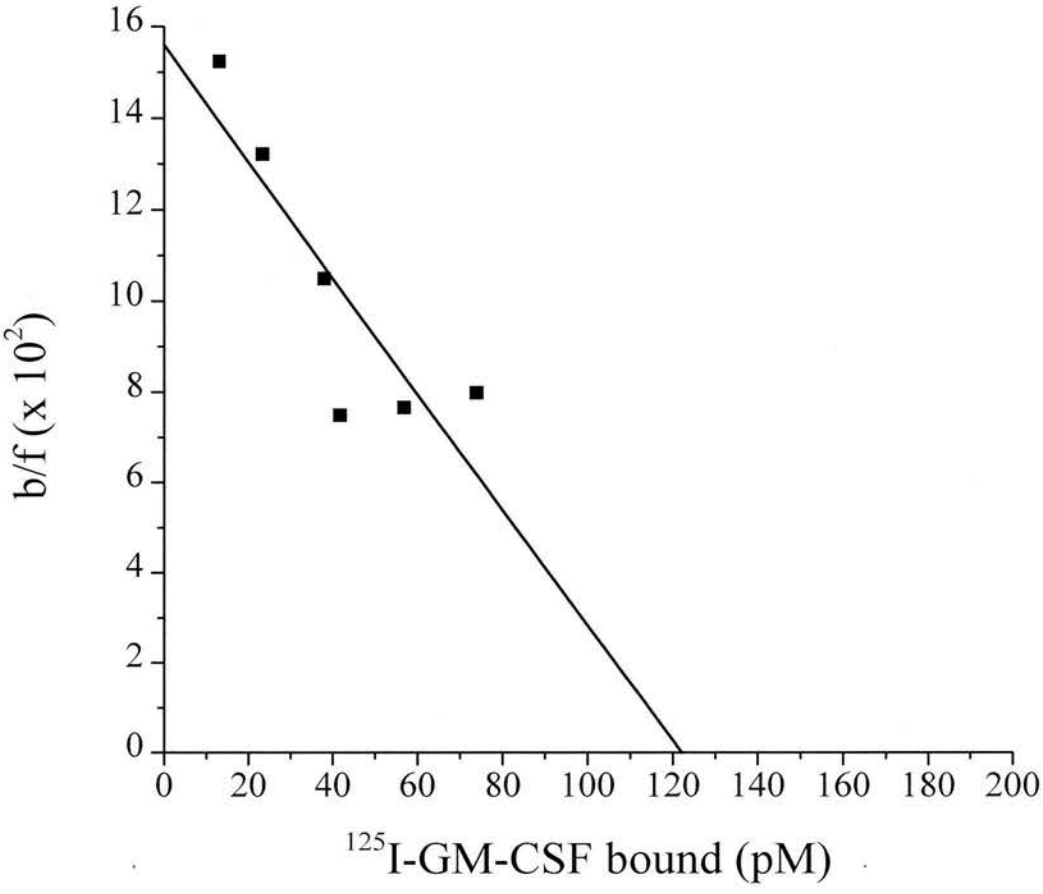

Fig. 6.3 Scatchard analysis of ^{125}I-rovGM-CSF binding to neutrophils.
Data from the mean of three assays of ^{125}I-rovGM-CSF binding to neutrophils (Fig. 6.1) were converted to the Scatchard coordinate system (as described for Fig.5.7).
Binding shown represents specific binding, with binding in the presence of excess unlabelled rovGM-CSF subtracted from total ^{125}I-rovGM-CSF binding.
The binding affinity of rovGM-CSF for GM-CSF cell surface receptor on neutrophils was computed as K_d = 784 pM
Scatchard plot analyses applied to the individual data sets showed a Kd range 718 to 850 pM.

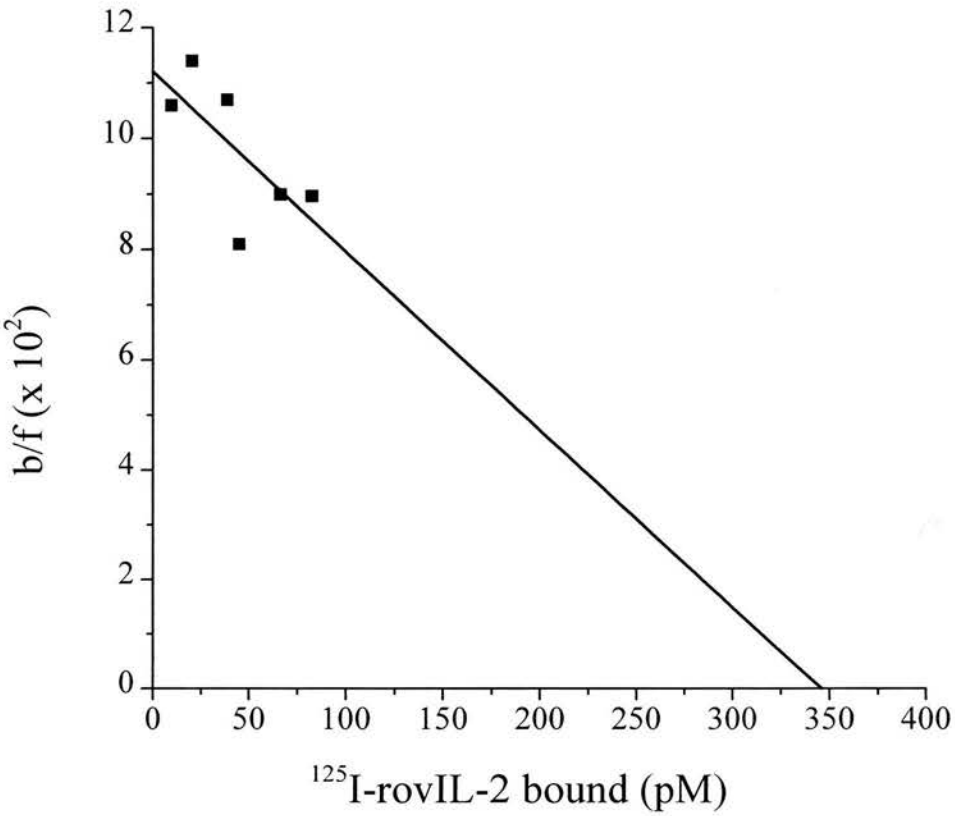

Fig. 6.4 Scatchard analysis of ^{125}I-rovIL-2 binding to CD4$^+$ T cells. The data from the mean of three assays measuring specific ^{125}I-rovIL-2 binding to CD4$^+$ T cell blasts were converted to the Scatchard coordinate system and the binding affinity of rovIL-2 for its cell surface receptor calculated as K_d = 3.084 nM. Scatchard plot analyses applied to the individual data sets showed a Kd range 1.88 to 4.24 nM.

performed on the data from both radio-labelled cytokine-cell binding assays (Figs 6.3 and 6.4). The binding affinity of rovGM-CSF for GM-CSFR on neutrophils was calculated as Kd = 784 +/- 66 pM. From the equilibrium binding data, as outlined by Porteu and Nathan (1990), the number of GM-CSF receptors present on sheep polymorphonuclear cells was estimated at 4000 +/- 960 per cell. For IL-2 binding to its receptor on $CD4^+$ T cells the binding affinity was estimated as Kd = 3040 +/- 1200 pM. The number of IL-2 R molecules bound per cell was calculated as 5250 +/- 807 per cell.

6.2.2. The effect of GIF on GM-CSF and IL-2 function

i). RovGM-CSF

The effect of GIF on rovGM-CSF activity was measured in a soft agar bone marrow haemopoietic clonogenic assay (Fig. 6.5). The results of a dose response experiment (typical of three repeat experiments) which measured the effect of increased rovGM-CSF concentrations on the development of cell-colonies from 10^5 bone marrow cells cultured for 14 days in soft agar are outlined in Fig. 6.5a. Maximum colony counts (73 +/- 2 colonies/10^5 cells) were obtained from cultures treated with 460 pg/ml rovGM-CSF. No further increase in colony formation was obtained with a 10-fold increase in rovGM-CSF concentration. The addition of GIF at 52 ng/ml and 520 ng/ml to the cultures inhibited the development of colonies from cultures responding to rovGM-CSF to different degrees but was most noticeable for both GIF concentrations when 460 pg/ml rovGM-CSF was used. The specificity of GIF activity was demonstrated by its neutralisation by anti-GIF.

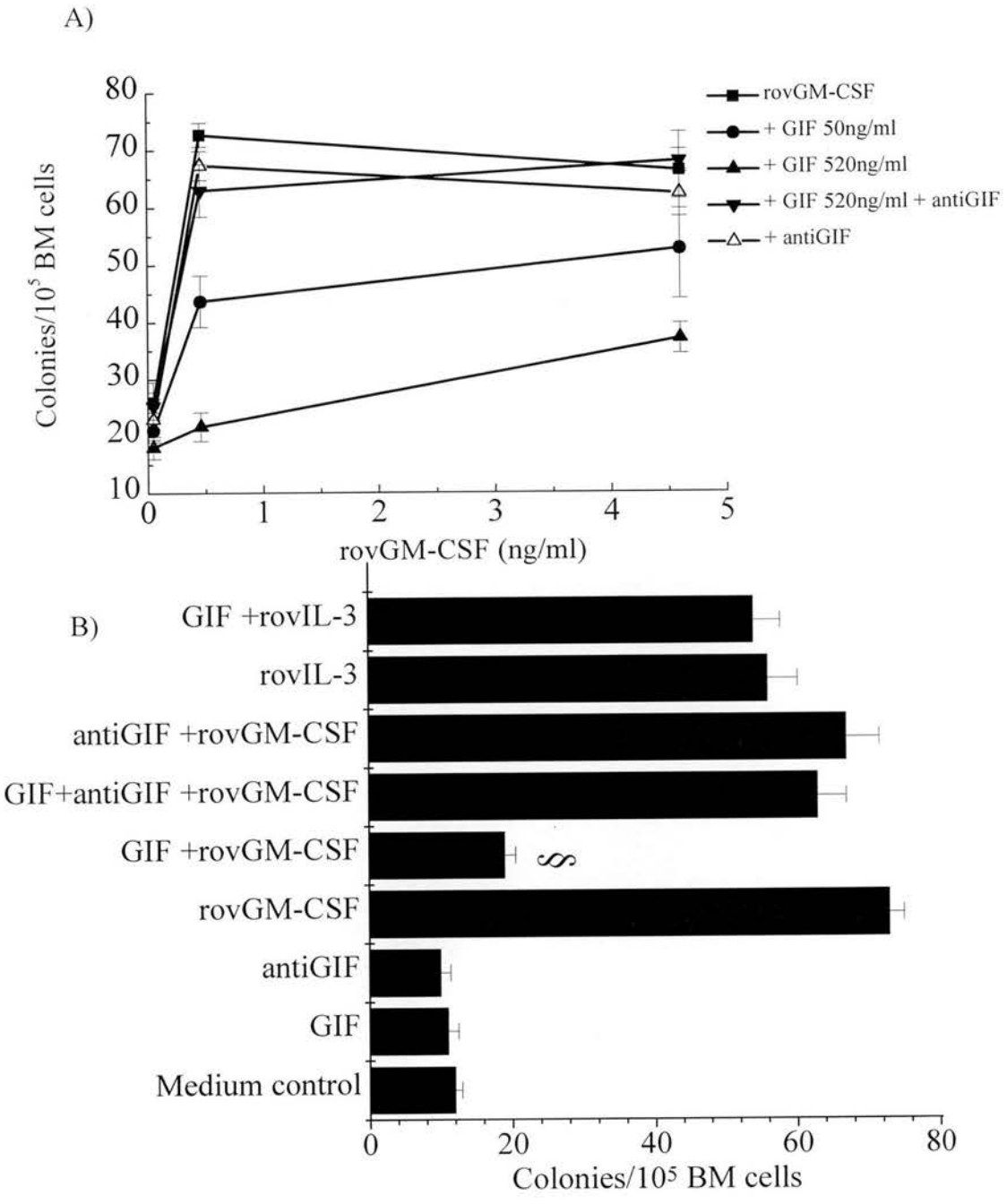

Fig.6.5 The effect of GIF on rovGM-CSF activity in the soft-agar bone marrow clonogenic assay.

A) Dose response experiment measuring the effect of increasing rovGM-CSF concentration alone (x-axis, solid squares) and in the presence of 50 ng/ml (solid circles) and 520 ng/ml (solid triangles) of GIF on the development of cell colonies (y-axis) from 10^5 bone marrow cells cultured for 14 days in soft agar. The inhibitory action of GIF was neutralised by pre-treatment of GIF with anti-GIF (solid inverted triangles), which had no effect on its own on colony development (open triangles).

B) Direct comparison of day 14 colony counts (x-axis) from cultures that were treated with rovGM-CSF (460 pg/ml), GIF (520 ng/ml) and rovIL-3 (50 ng/ml). GIF is shown inhibiting the stimulation of rovGM-CSF (§ $p < 0.005$ when compared with rovGM-CSF alone). Controls included cultures that were set up in the presence of medium, GIF or anti-GIF alone.

GIF specificity was further examined in the comparative analyses of colony counts from a number of repeat bone marrow cultures set up in either rovGM-CSF (460 pg/ml) or rovIL-3 (50 ng/ml) (Fig. 6.5B). Whilst GIF was shown to inhibit colony development stimulated by rovGM-CSF ($p < 0.005$ when compared with colony numbers from cultures set up in rovGM-CSF alone), it had no significant effect on rovIL-3-induced colony development ($p > 0.1$). Both GIF and anti-GIF were tested for any direct effect on colony formation. None was found.

ii). RovIL-2

The effect of increasing rovIL-2 concentrations (20-320 ng/ml) on $CD4^+$ T cell proliferation was measured by the incorporation of ^{3}H-thymidine into dividing cells (Fig. 6.6A). T cell proliferation in response to rovIL-2 was dose-dependent. GIF inhibition of ^{3}H-thymidine uptake by T cells was particularly significant at 40 and 160 ng/ml rovIL-2 concentrations ($p < 0.005$ when compared with cultures treated with rovIL-2 alone) but less so at 320 ng/ml ($p < 0.05$). The presence of anti-GIF neutralised the inhibitory effect of GIF.

Further analysis of $CD4^+$ T cell proliferation was carried out to compare cultures grown in the presence of rovIL-2 (40ng/ml) and GIF (520ng/ml) with control cultures maintained in the presence of either GIF, anti-GIF or medium alone (Fig. 6.6B). GIF inhibited rovIL-2 stimulation of T cells ($p < 0.001$ when compared with cultures treated with rovIL-2 alone). ^{3}H-thymidine uptake by control T cell cultures maintained in the presence of GIF or anti-GIF did not exceed the uptake by those cells grown in medium alone. Anti-GIF had no significant effect on ^{3}H-thymidine uptake by T cell cultures. The counts observed from cultures maintained in GIF alone were lower than other control cultures ($p < 0.01$) and may reflect

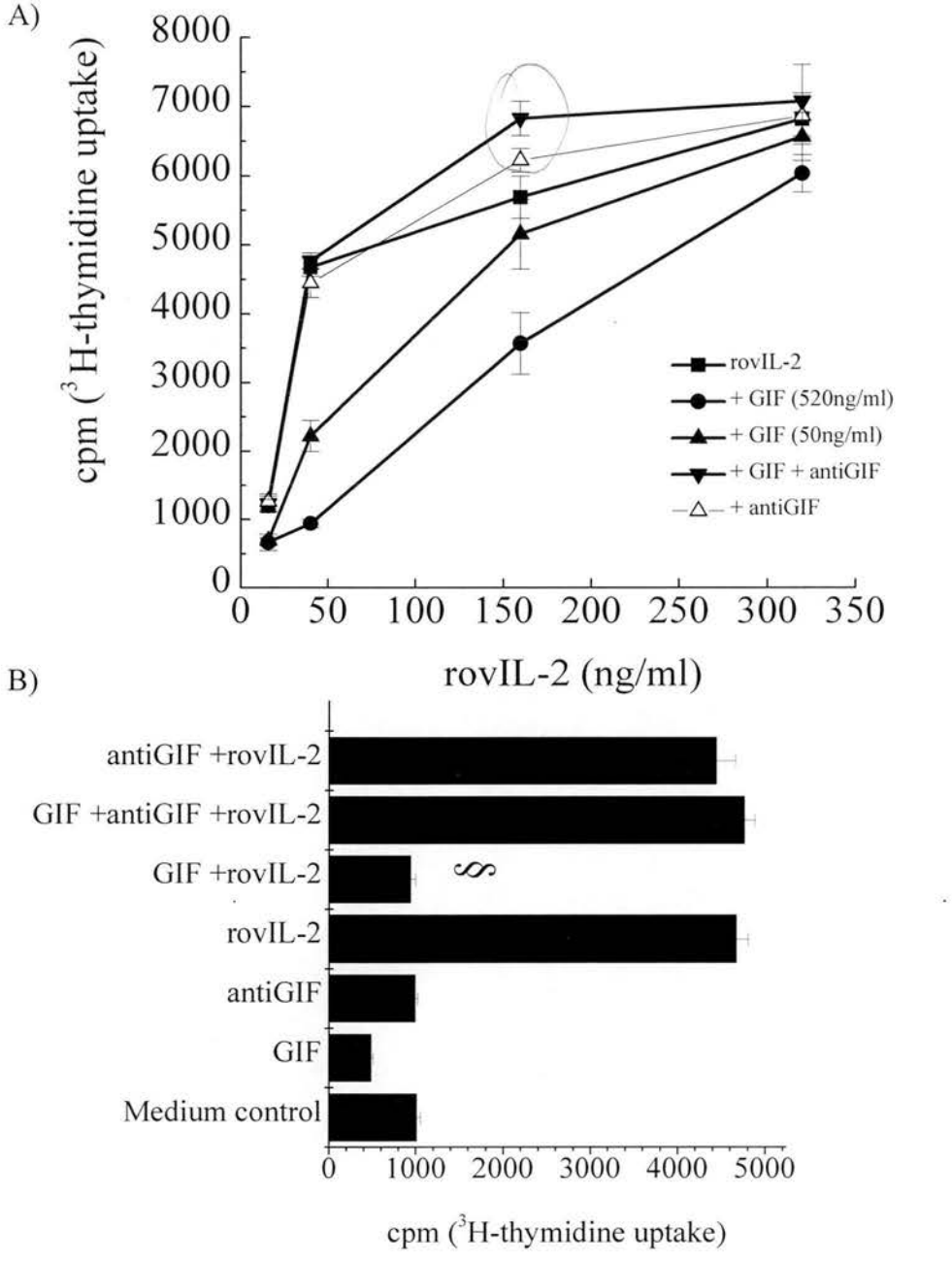

Fig. 6.6 GIF inhibition of rovIL-2 stimulation of $CD4^+$ T cells.
A) The effect of increasing rovIL-2 concentration (x-axis, nM) on $CD4^+$ T cell proliferation (y-axis, cpm ^{3}H-thymidine uptake) was measured 48 hours later (solid squares). Activation of $CD4^+$ T cells by rovIL-2 was compared in the presence of GIF +/- anti-GIF. GIF (520 ng/ml solid circles) was shown to inhibit rovIL-2 driven $CD4^+$ T cell proliferation across the range of rovIL-2 concentrations used. Values given represent the mean cpm of ^{3}H-thymidine incorporated into dividing cells in quadruplicate wells and standard error of the mean.
B) Comparison of $CD4^+$ T cell proliferation (x-axis) in the presence of rovIL-2 (40ng/ml) and GIF (100ng/ml). GIF is shown inhibiting the stimulation of rovIL-2 (§ $p < 0.001$ when compared with rovIL-2 alone). Cultures maintained in the presence of anti-GIF plus rovIL-2, GIF, anti-GIF and medium alone were included as specificity controls.

GIF reacting with traces of endogenous IL-2 present in the cultures (bovine IL-2 present in the FCS component of the medium and to which some T cell response was noted).

6.3. Discussion

6.3.1. GIF inhibition of cytokine binding to cell surface receptors

In this chapter GIF was shown to inhibit the binding of rovGM-CSF and rovIL-2 to their respective cellular receptors on neutrophils and $CD4^+$ T cells. The binding affinities (Kd) of rovGM-CSF for cell surface GM-CSF receptor (784 +/- 66 pM) and rov IL-2 for IL-2R (3064 +/- 1176 pM) were compared with the binding affinities calculated for GIF binding rovGM-CSF (369 +/- 52 pM) and rovIL-2 (1040 +/- 79 pM) in solution and described in Chapter 5. Given the apparent higher affinities of both cytokines for GIF, it is evident that if these values that were obtained *in vitro* reflect ligand-receptor binding *in vivo*, then GIF reactivity towards either cytokine in solution would be favoured over the interaction of the cytokine with its natural receptor.

Little is known concerning cytokine-receptor interactions in sheep but the range of Kd values that were obtained for rovGM-CSF- GM-CSF cell surface receptor and rovIL-2- IL-2 cell surface receptor interactions correspond to those values reported for GM-CSF and IL-2 binding to low affinity sites on human and murine neutrophils and T cells. For example, Khwaja *et al*, (1993) have identified low affinity receptors on human neutrophils that bound GM-CSF with a Kd = 1800 +/- 300 pM and at a density of 8600 +/- 1150 receptors per cell. This is in contrast to the high affinity GM-CSF transmembrane receptor that has been reported at lower density (2-5 $x10^2$) on cells of the granulocyte and monocyte lineages and that binds human GM-CSF with a Kd in the range 5-100 pM (Griffin *et al*, 1990, Brown *et al*, 1995, Murray *et al*, 1998). In spite of a two-site model of high and low affinity GM-CSF receptors

expressed by human monocytes (Elliot *et al*, 1989), the experimental data showed only one class of receptor for ovGM-CSF present on ovine neutrophils. This is consistent with the work of Onetto-Pothier *et al*, (1990) who identified a single class of GM-CSF receptors on human neutrophils (albeit of intermediate affinity, Kd = 100-160 pM).

Similarly, the rovIL-2-cellular receptor interaction appeared to follow the one site-low affinity model with little indication of higher order rovIL-2-receptor binding. As with GM-CSF-receptor interactions, little is known regarding IL-2-receptor dynamics in the sheep. From human studies, three distinct IL-2 receptor subunits with different binding affinities have been identified (Taniguchi and Minami, 1993, Caligiuri *et al*, 1990; Vanham *et al*, 1994). In the cell-binding assay, unlike the proliferation assay, the $CD4^+$ T cells had not been activated with ConA, and it is possible that those cells expressed only low affinity ovIL-2 receptors. This is in contrast to more activated/blast transformed $CD4^+$ T cells that may express receptors of high, low and intermediate binding affinities (Vanham *et al*, 1994). The IL-2 –receptor status of ovine $CD4^+$ T cell blasts warrants future investigation.

Whatever the nature of the cytokine receptors present on the effector cells targeted by orf virus *in vivo*, it is probable that GIF in solution can compete successfully with cell surface receptors exhibiting higher binding affinities like the soluble forms of both GM-CSF and IL-2 low affinity receptors (Brown *et al*, 1995 and Jacques *et al*, 1987 respectively).

6.3.2. GIF inhibition of cytokine biological function

i). GM-CSF function

GIF was shown to inhibit GM-CSF-driven myelopoiesis from bone marrow precursor cells in the soft agar clonogenic assay. Beside its haematopoietic action, GM-CSF also has a stimulatory effect on mature neutrophil, eosinophil and macrophage function particularly those related to recruitment and activation at the sites of inflammation (Rapoport *et al*, 1992; Gagnadoux *et al*, 1997; Bernasconi *et al*, 1995). The data from this study suggests that GIF expressed by infected cells could also block GM-CSF and IL-2 stimulation of responder cells recruited to the site of infection. GM-CSF alone and in concert with IL-1β and TNF-α has also been shown to mediate in the accessory cell function of epidermal Langerhans cell (immature DC) (Steinman, 1988; Heufler *et al*, 1988a and b). This accessory function of Langerhans cells involves the uptake and processing of antigens, followed by migration to lymph nodes where they interact with T cells (King and Katz, 1990). Thus, GIF blocking of GM-CSF function might also result in the failure of DC to activate the T cell mediated immune response.

ii). IL-2 function

In this study GIF was shown to inhibit IL-2-driven T cell proliferation. Apart from promoting T cell proliferation at sites of inflammation and within lymph nodes *in vitro* (Egan *et al*, 1996; Haig *et al*, 1996e), IL-2 has been shown to be responsible for human T cell and natural killer cell chemotaxis (Robbins *et al*, 1986; Cao *et al*, 1998). *In vivo*, IL-2 was shown to mediate the infiltration of neutrophils into sites of inflammation in mice (Tang *et al*, 1997). In each study, chemotaxis could be neutralised by anti-IL-2 antibodies.

6.3.3. Summary

By targeting both GM-CSF and IL-2, orf virus, through the action of GIF, has the potential to block their biological activities that may either directly or indirectly regulate cell mediated anti-viral immunity.

CHAPTER 7

TISSUE DISTRIBUTION OF GM-CSF-INHIBITORY FACTOR DURING ORF VIRUS REINFECTION

7.1. Introduction

In this study, the *in vivo* localisation of GIF in the skin of orf virus infected sheep and in lymph either entering (afferent lymph) or exiting a local draining lymph node was mapped. The immunohistological analysis of GIF in fixed and paraffin-embedded orf skin biopsy material is described. This investigation follows the same methodology employed by Jenkinson *et al* (1992) to define the changes in cutaneous T and B lymphocyte populations which follow experimental infection with orf virus. In the present study, sections were tested for the presence of orf virus antigen and GIF protein, using respectively, an anti-orf virus antigen mouse monoclonal antibody (Housawi *et al*, 1998) and mouse and rabbit polyclonal antibodies raised against purified recombinant GIF (described in Section 2.6.1.). In addition afferent and efferent lymph samples collected at various times from orf virus reinfected and control scarified sheep (as part of an earlier study) were analysed for the presence of GM-CSF and GIF by ELISA.

The aims of this study were;

1.) To determine whether GIF could be detected in orf virus-infected skin and lymph, and if so where in the skin and in which lymph compartment.

2.) To investigate whether the expression of GIF by orf virus-infected cells *in vivo* is associated with the fluctuations observed in lymph GM-CSF.

7.2. Results

7.2.1. Immunohistological analysis

Serial sections of sheep skin were taken from biopsies taken at various times before and during an orf virus reinfection and analysed for the presence of orf virus antigen (39kD envelope protein) and GIF (see Section 2.6.1.). Neither orf virus antigen nor GIF was detected in skin sections taken from experimental animals prior to orf virus reinfection (Fig. 7.1) nor control animals where PBS instead of live orf virus was applied to the scarification lines. Attempts to stain sections for GM-CSF with the anti-rovGM-CSF mAbs 3C2 and 8D8 proved unsuccessful.

In the experimental animals, staining for orf virus antigen was most intense on day 3 (Fig. 7.2A) and on day 5 (Fig. 7.3A) after reinfection but declined in intensity thereafter. Staining was observed in the region of epidermis close to the area of scarification and also in underlying hair follicles. In sections taken early in the course of reinfection, orf virus antigen was localised to the ballooning/vacuolated and degenerating epidermis seen in the outer stratum spinosum beneath the corneum and lining the hair follicle at the edge of the expanding lesion. A heavy infiltration of leucocytes (with intensely stained nuclei) was observed in the dermis beneath the lesion. By day 7 (Fig7.4A), staining for orf virus antigen was less intense and localised to the periphery of the original lesion where the epidermis had disintegrated into a large pustule heavily infiltrated with neutrophils. Sections taken on day 9, showed orf virus antigen present in a scab that had formed from the remnants of pustules above a highly proliferative layer of epidermal cells. By day 14, the scab

A)

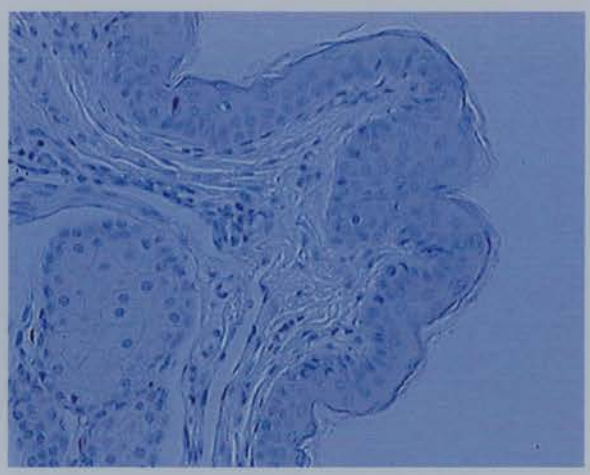

B)

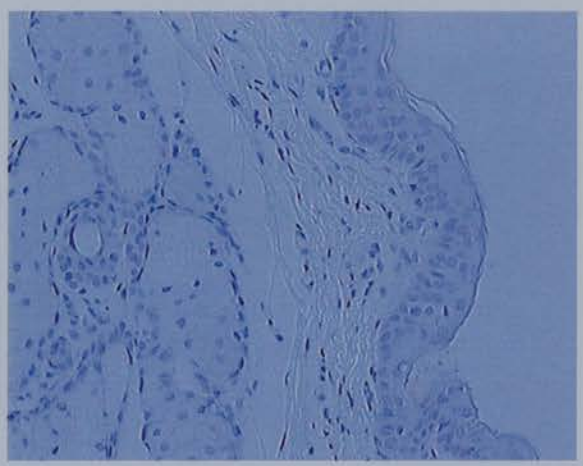

Fig. 7.1 Immunohistological staining of sheep skin for orf virus antigen and GIF prior to reinfection with orf virus. Serial sections from a skin biopsy specimen taken from the inner thigh prior to challenge with orf virus and tested for A) orf virus antigen using mAb 10E6 (reactive against the 39kD envelope protein, Housawi et al, 1998) and B) GIF using an IgG fraction of mouse anti-GIF serum, muLT1.
Staining for either orf virus antigen or GIF was not observed. (Immunoperoxidase; haematoxylin and eosin, x 250)

A)

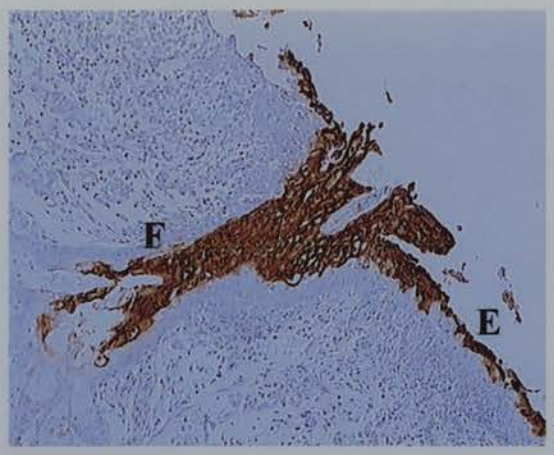

B)

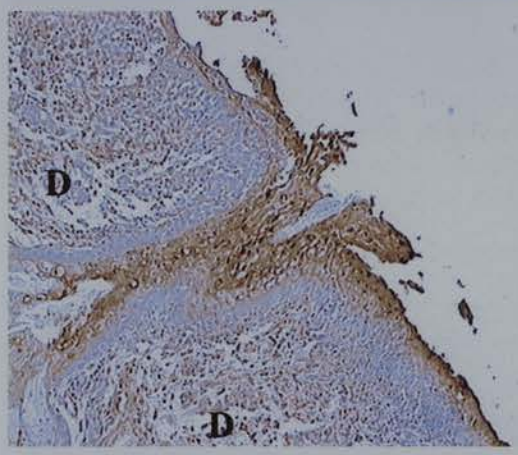

C)

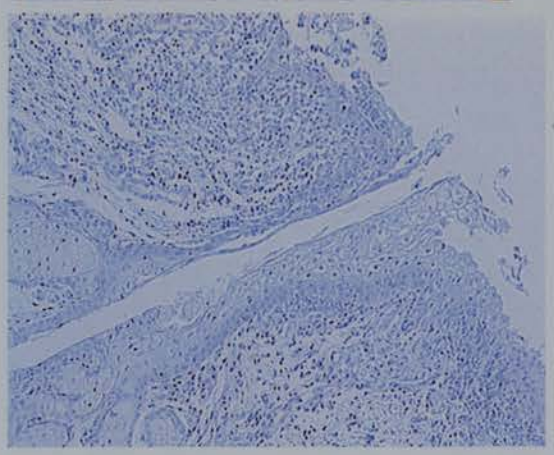

Fig. 7.2 Immunohistological staining of orf virus-infected skin at day 3 after reinfection.
A) A section from a skin biopsy specimen stained for orf virus antigen. Orf virus (intense dark brown staining) is shown present in the degenerating epidermis lining the hair follicle (F). The virus has spread laterally along the outer layers of the stratum spinosum (E) on both sides of the lesion.
B) A serial section to (A) stained for GIF and showing GIF present in the infected epidermis with less intense staining observed throughout the underlying dermis (D).
C) Section incubated with IgG fraction from pre-immune mouse serum as a negative control. (Immunoperoxidase; haematoxylin and eosin, x 112)

A)

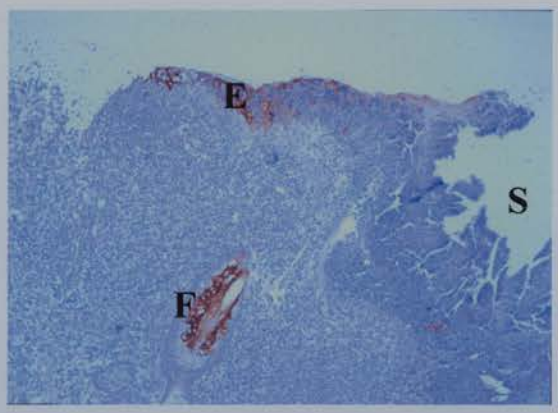

B)

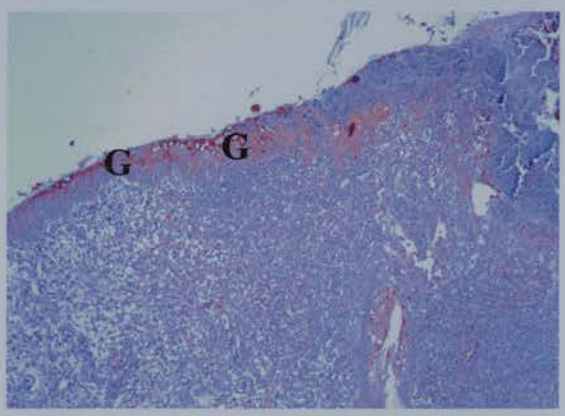

C)

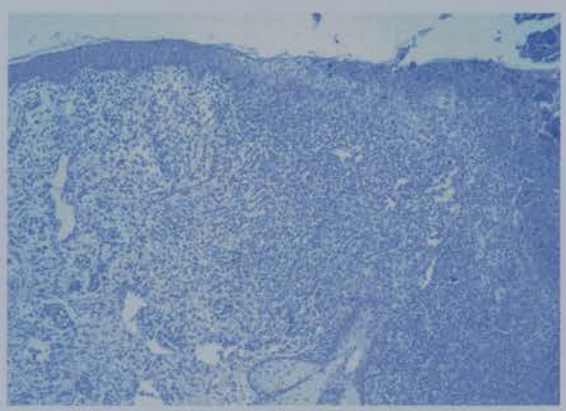

Fig. 7.3 Immunohistological staining of orf virus-infected skin at day 5 after reinfection.
A) A section from a skin biopsy specimen taken around the area of abraded skin (S) and stained for orf virus antigen. The localisation of orf virus (dark brown staining) is evident in the ballooning degenerating epidermis in the outer stratum spinosum (E), and lining the hair follicle (F). B) A serial section of (A) stained for GIF using muLT1. This section shows weak staining for GIF distributed throughout the tissue but with more intense staining (G) localised to the infected epidermis. C) A further serial section was incubated with an IgG fraction from pre-immune mouse serum as a negative control. (Immunoperoxidase; haematoxylin and eosin, x 112)

A)

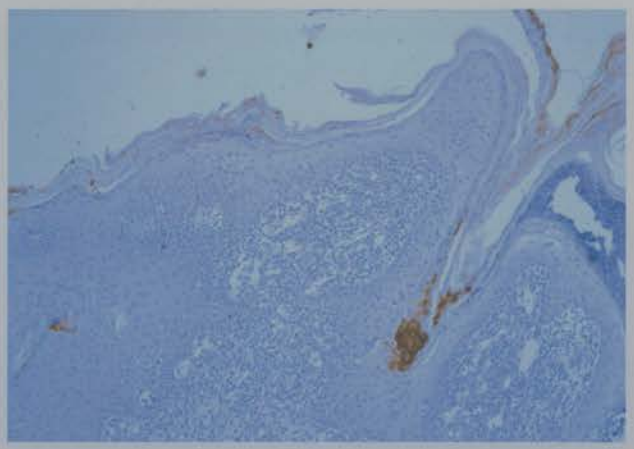

B)

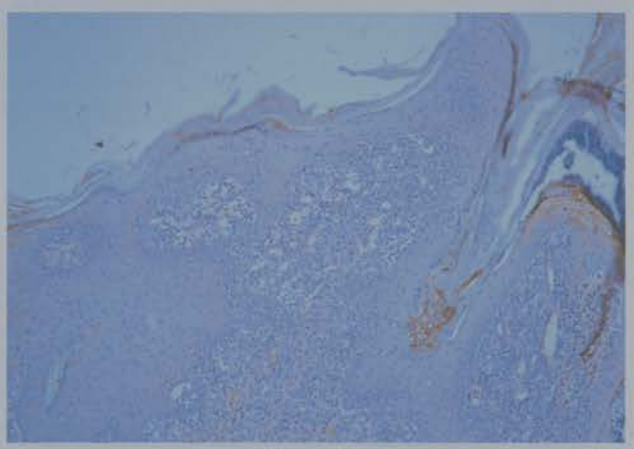

C)

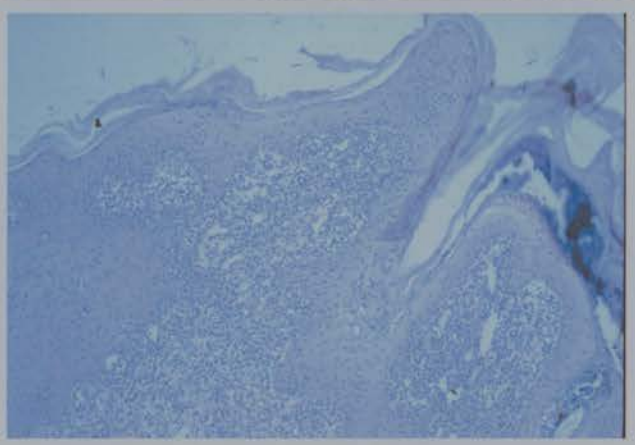

Fig. 7.4 Immunohistological staining of orf virus-infected skin at day 7 after reinfection.
A) A section taken and stained for orf virus antigen. Staining for orf virus antigen is still strong but not so extensive as in the section taken on day 5.
B) A serial section of (A) stained for GIF and showing reduced levels of GIF present in the epidermis of the lesion.
C) Section incubated with an IgG fraction from pre-immune mouse serum as a negative control. (Immunoperoxidase; haematoxylin and eosin, x 112)

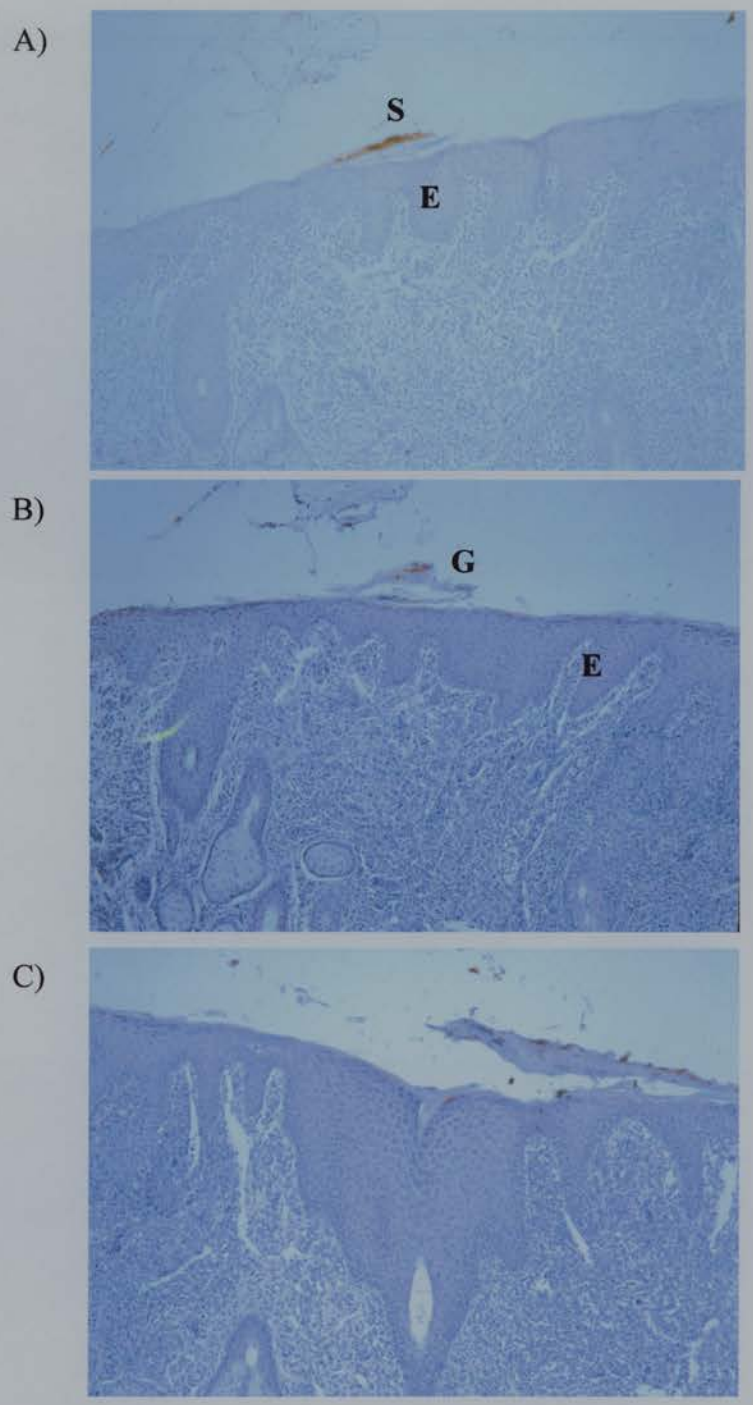

Fig 7.5 Immunohistological staining of orf virus-infected skin at day 9 after reinfection.
(A) Orf virus antigen was detected only within the newly formed scab (S). The remnant of pustules form a scab above a highly proliferative layer of epidermal cells (E).
(B) Trace amounts of GIF (G) were only detected in those areas of scab staining for orf virus antigen. Note the columns of epidermal cells (E) growing out of the stratum basale into the dermis and towards each other.
(C) Section treated with pre-immune mouse IgG fraction as control.
(Immunoperoxidase; haematoxylin and eosin, x 112)

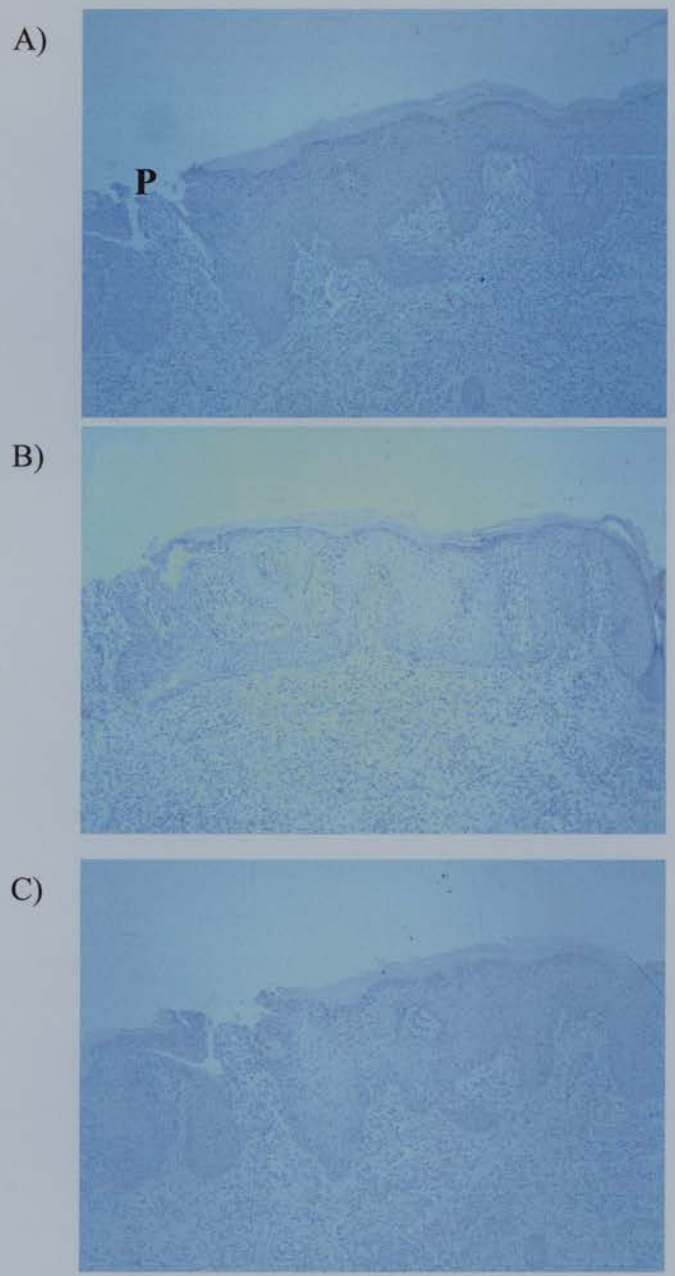

Fig. 7.6 Immunohistological staining of sheep skin at day 14 after orf virus reinfection.
Serial sections taken at day 14 after orf virus reinfection and stained for A) orf virus antigen and B) GIF. A further section C) was included as a negative control (IgG fraction of pre-immune mouse serum).
Orf virus antigen and GIF were not detected in sections taken at this time. The new epidermis is still hypertrophied but not yet fully cornified particularly around the site of the old lesion (P). Inflammatory cells can still be seen in the dermis underlying the site of the lesion.
(Immunoperoxidase; haematoxylin and eosin, x 112)

had sloughed off and with it the newly replicated orf virus. Orf virus antigen was not detected in these sections.

Staining for GIF was carried out initially with ra101, ra161 and muLT1. Non-specific staining was observed with ra101-treated control sections and consequently its use was discontinued. GIF was detected in sections taken on day 3 through to day 9 by both ra161 and muLT1. Sections presented are stained with muLT1. On day 3 after reinfection (Fig. 7.2B), heavy staining for GIF was observed in those areas of infected epidermis in the outer stratum spinosum and lining the hair follicles. There was also some staining present in the dermis immediately adjacent to the infected epidermis. By day 5 (Fig 7.3B), staining for GIF appeared less intense than on day 3 but with the most intense staining for GIF again coincident with that for orf virus antigen. GIF was also detected in the dermis underlying and adjacent to infected cells. GIF staining was much reduced by day 7 (Fig. 7.4B). It was most noticeable in the area of the resolving lesion coincident with orf virus antigen and also in and around the periphery of the newly formed pustules/scab. By day 9 (Figs 7.5B), with the resolution of the lesion in progress, only trace amounts of GIF were detected in those areas of scab containing orf virus (as antigen) and in the process of sloughing off. Neither GIF nor orf virus antigen was detected in sections taken on day 14 after infection.

7.2.2. Analysis of lymph for GIF activity

GIF activity was measured in afferent and efferent lymph plasma taken at various times after orf virus reinfection (see Section 2.6.2.). Supernatants from cultured afferent and efferent lymph cells were also tested for the presence of GIF.

GIF was detected in afferent lymph plasma samples (Fig. 7.7A) but not in efferent lymph plasma samples (Fig. 7.7B) from reinfected animals. GIF was not present in either afferent or efferent lymph plasma samples from control scarified animals or those that were injected intradermally with UV-inactivated virus (Fig. 7.7B). Moreover, GIF was not detected in supernatants from cultured afferent or efferent lymph cells. In afferent lymph, maximum GIF activity was measured in samples taken at days 5 and 6 from all three animals tested. Note that the lower O.D. [450nm] seen with sheep no. 1215 reflected a lower GM-CSF spike of 4ng/ml. As observed in the assays carried out on recombinant GIF, anti-GIF (ra101) was shown to neutralise the GM-CSF-binding capability of viral "natural" GIF.

The levels of GM-CSF in lymph plasma were measured by ELISA at various times after orf virus reinfection (Fig. 7.8). GM-CSF content of afferent lymph plasma was seen to vary between animals. Reduced levels in all 3 sheep were detected in samples taken between days 4 and 7 after reinfection. The biphasic GM-CSF response as described previously (Haig *et al*, 1996e, 1999) was clearly seen in samples collected from sheep no. 1215 ($p < 0.005$ value for reduction in GM-CSF levels when compared with pre-challenge levels). Such a GM-CSF response was not seen in efferent lymph collected from two orf virus infected sheep (sheep nos. 1118 and 1126). After an early rise, GM-CSF levels were observed to decline gradually as the infection was resolved.

Control sheep (358 and 567) challenged with UV-inactivated orf virus displayed considerable variation in afferent lymph GM-CSF content. Whereas the GM-CSF response in afferent lymph of sheep no. 358 showed some similarity to the biphasic response of those animals challenged with live virus, the GM-CSF response

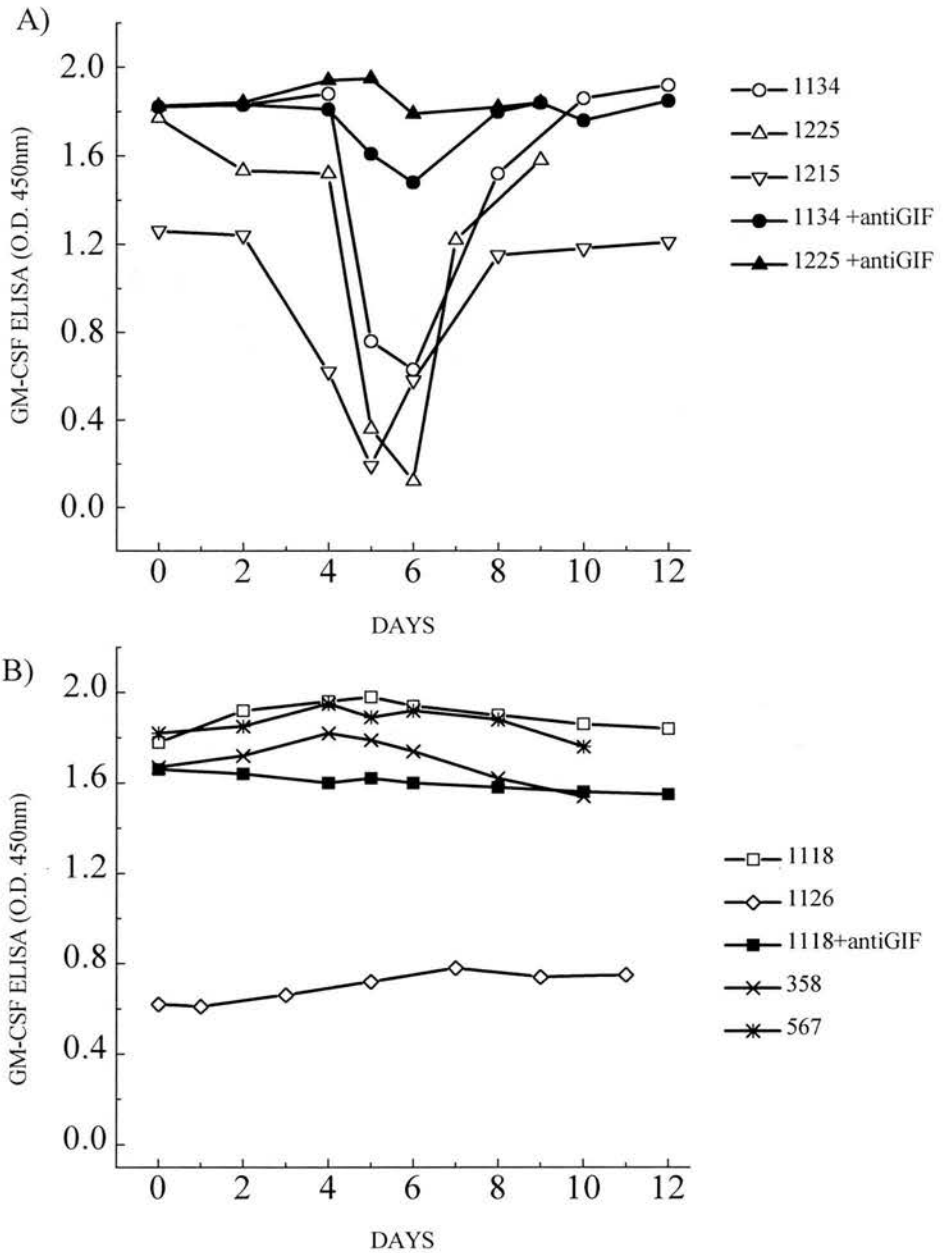

Fig. 7.7 GIF activity measured in lymph plasma from samples taken before and after orf virus re-infection.
Lymph plasma samples were spiked with rovGM-CSF at 8ng/ml (sheep nos. 1134, 1225, 1118, 358 and 567) or 4ng/ml (sample nos. 1215 and 1126) and tested for GIF activity by ELISA.
A) GIF activity (open symbols) measured in afferent lymph samples (sheep nos.1134,1215 and 1225). Addition of anti-GIF (solid symbols) was found to neutralise lymph plasma GIF activity.
B) Analysis of efferent lymph plasma (open symbols) from reinfected sheep (1134 and 1126) and afferent lymph plasma (crossed symbols) from control sheep (358 and 567; challenged with UV-inactivated orf virus) for GIF activity. Values represent the average of duplicate samples.

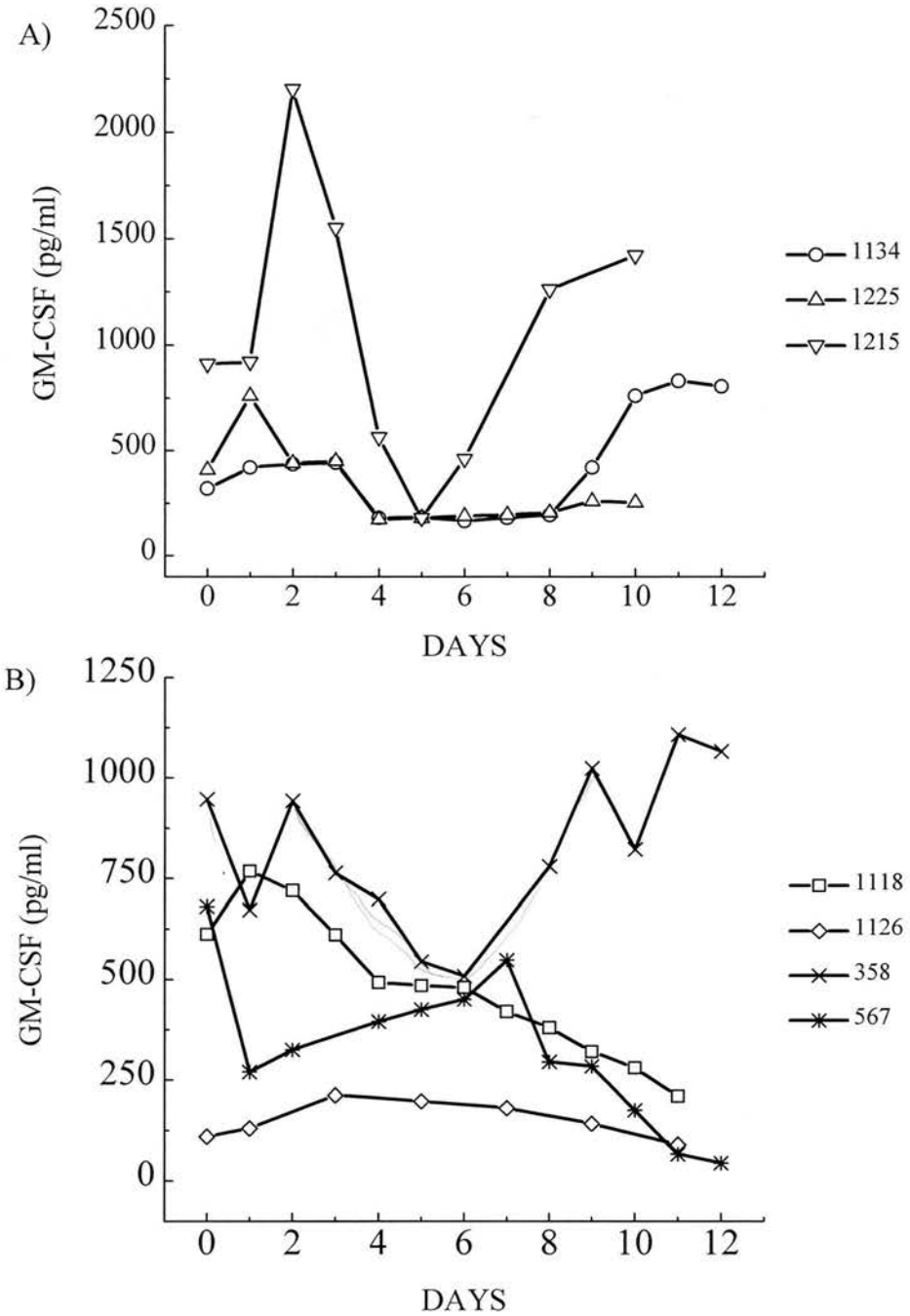

Fig. 7.8 Detection of GM-CSF in lymph plasma from samples taken before and after orf virus re-infection.
GM-CSF concentrations (y-axis, pg/ml) were measured by ELISA at various times after orf virus re-infection in A) afferent lymph plasma samples (sheep nos. 1134, 1225 and1215) and B) efferent lymph plasma samples (sheep nos. 1118 and 1126). Afferent lymph samples from control sheep (358 and 567) which were challenged with UV-inactivated orf virus were also assayed.

observed in lymph plasma from the other control animal (sheep no. 567) did not. Efferent lymph from control animals was not tested. In addition, due to the loss of material, GM-CSF was not measured in supernatant from cultured afferent and efferent lymph cells for this experiment.

7.3. Discussion

7.3.1. GIF in orf virus-infected skin

GIF was detected by specific antibody in sections taken from skin during an orf virus reinfection. Staining for GIF observed on day 3 through to day 7 coincided with the period of maximum virus replication as observed by the presence of virus antigen. Not only was GIF present in the area of regenerating epidermis that was the site of viral replication as shown by the staining for orf virus envelope antigen, but during this period GIF was also detected in the dermis adjacent to and underlying this site of infection. This indicates that it is secreted from infected cells. Counterstaining with hematoxylin revealed that the area of dermis, underlying infected cells, was infiltrated with leucocytes. Phenotypic analysis of orf virus-infected cells in sheep skin has shown that $CD4^+$ T cells in particular of the lymphocyte subsets, accumulate in large numbers adjacent to and underlying the site of the lesion (Haig *et al*, 1996d, 1997). Since these cells are the principal source of GM-CSF and IL-2 in afferent and efferent lymph after orf virus infection, it is likely that both cytokines are produced in sheep skin as part of the host immune response to orf virus reinfection. Indeed, mRNA encoding both GM-CSF and IL-2 has been detected in sheep skin biopsy specimens obtained during orf virus infection (Haig *et al*, 1996c). Thus, it is highly probable that the release of GIF during the period of viral replication (days 3-7 of an orf virus reinfection), would counteract at least part of the host cellular response due to the production of GM-CSF and IL-2 in the vicinity of the lesion site.

Whilst IL-2 has been implicated in the immune response to orf virus (Haig *et al*,

1996c and e, 1997; Lear, 1995; Lear *et al*, 1996) the role of GM-CSF is less clear. GM-CSF stimulates the recruitment and activation of neutrophils and macrophages either directly or indirectly. Both of these cell-types are present in orf lesions. Another possible point of GIF intervention would be GM-CSF regulation of antigen presentation by dendritic cells. Haig *et al* (1995a) have shown that GM-CSF and TNF-α are involved in the recruitment of Langerhans cells and other DC to the ovine dermis. Interestingly, a feature of orf virus infection is the dense network of DC that surrounds the lesion (Jenkinson *et al*, 1991). The inhibition of GM-CSF in the vicinity of orf virus infected epidermal keratinocytes could affect DC function, especially their role in antigen presentation to effector T cells and the induction of the cell -mediated immune response. Whatever the origin of the GM-CSF circulating through orf virus infected tissue, GIF has the capacity to inhibit GM-CSF function.

7.3.2. GIF in afferent lymph draining orf virus infected skin

After orf virus reinfection of sheep, GIF was detected in afferent lymph plasma samples that had low levels of GM-CSF and which corresponded to the period of maximum viral replication in the epidermis (Haig *et al*, 1996c). Orf virus has not been detected in lymph cells and GIF was not detected in supernatants taken from lymph cells in culture. This confirms that GIF is produced locally at the site of infection as a soluble mediator and appears in the afferent lymph plasma.

GIF was not detected in efferent lymph and this indicates that GIF either does not pass through the lymph node into efferent lymph or is diluted out by the large volume of efferent lymph that passes out of the node and is mainly derived from blood. As in infected skin, the inhibitory action of GIF on circulating IL-2 and GM-

CSF in afferent lymph or those cytokines in the lymph node remains undefined. Orf virus-specific $CD8^+$ cytotoxic T cells that are directly cytotoxic (effector rather than precursor CTL) for virus infected autologous epidermal cells are also enriched in afferent lymph (Haig *et al*, 1996b). Any mediation of CTL function by IL-2 would therefore constitute a target for GIF activity. Another possible target for GIF inhibition is a migrating population of dermal dendritic cells that transport antigen from the skin to the paracortical areas of the draining lymph node and are potent antigen-presenting cells for T cells in both primary and secondary immune responses (Bujdoso *et al*, 1989; McKeever *et al*, 1991). These afferent lymph dendritic or veiled cells (ALDC) have been shown to be stimulated to grow in culture in response to GM-CSF and TNF-α but not GM-CSF on its own (Haig *et al*, 1995a). It is suggested however that GM-CSF is required for the acquisition of accessory function by ALDC as measured by an increase in $CD4^+$ T cell autologous proliferation (Haig *et al*, 1995a).

7.3.3. GIF and the host immune response

By targeting GM-CSF function, GIF has the capability of regulating the migration, differentiation and the accessory function of dendritic cells in the skin and afferent lymph. In addition, GIF may also affect neutrophil and macrophage function. Similarly the clearance of IL-2 by GIF may also serve to down-regulate or delay the T-cell mediated response to orf virus infection.

CHAPTER 8

GENERAL DISCUSSION

In this study, the characterisation of the novel orf virus immunomodulatory protein, GM-CSF-inhibitory factor (GIF) has been described. GIF is the product of a gene located within the right terminal region of the viral genome, in an area associated with non-essential genes in poxvirus genomes. GIF has been expressed as a recombinant protein of 28 kD that associates with itself to form dimers and tetramers under physiological conditions. The dimer and tetramer forms of GIF are biologically functional, binding and inhibiting the activities of the ovine cytokines GM-CSF and IL-2. GIF is of *in vivo* relevance as it is produced by virus-infected cells in orf lesions and is detected in afferent lymph plasma draining the infection site. GIF is therefore a novel member of a growing family of immunomodulatory proteins produced by DNA viruses (Alcami and Koszinowski, 2000; McFadden *et al*, 1998). In orf virus it is one of several immuno-modulatory proteins that include a viral homologue of IL-10 (vIL-10, Fleming *et al*, 1997), and a interferon resistance protein (vIFNR, McInnes *et al*, 1998) and proteins active in inflammation such as vascular endothelial growth factor (vVEGF, Lyttle *et al*, 1994). It is probable that the GIF gene has been acquired during the co-evolution of orf virus and its host to function in a co-ordinated fashion with other immuno-modulatory genes and their products to interfere with host immunity and gain enough time for the virus to complete its life cycle in infected epidermal cells and produce infective progeny virions.

Studies carried out previously at Moredun Research Institute examined the immune response to orf virus in the skin and lymph of infected sheep. It was demonstrated that in both primary and secondary infections, there was an influx of immune and inflammatory cells into the dermis underlying the infected epidermis,

that were activated and produced cytokines and effector molecules typical of an anti-viral response (Jenkinson *et al*, 1990, 1991; Lear *et al*, 1996; Haig and Mercer, 1998). In spite of this vigorous immune and inflammatory response, orf virus is capable of reinfecting its host and replicating. Immunomodulatory proteins encoded by orf virus genes that target host defence mechanisms are probably a major factor in virus survival.

Binding of GM-CSF and IL-2 by GIF could interfere with immune and inflammatory responses at several levels. GM-CSF is produced by a wide variety of tissue types, including fibroblasts, endothelial cells, T cells, macrophages, mesothelial cells, epithelial cells and many types of tumor cells, in response to inflammatory mediators, such as IL-1, IL-6, TNF or endotoxin, (Griffin *et al*, 1990; Baldwin, 1992; Groves *et al*, 1996). GM-CSF stimulates the proliferation and maturation of myeloid progenitor cells in haemopoiesis (Clark, 1988), as well as functionally activating mature neutrophils, eosinophils, and monocytes (Ruef and Coleman, 1990; Burdach *et al*, 1991; Smith *et al*, 1995; Dale *et al*, 1998; Yagisawa *et al*, 1999). Haig *et al* (1995b) reported that the intradermal injection of recombinant ovine GM-CSF resulted in the accumulation over five days of MHC Class II^+ dendritic cells at the injection site, as well as increased numbers of neutrophils, eosinophils and lymphocytes. *In vitro*, Hu and Yasui (1997) found that GM-CSF suppressed anti-Fas antibody-induced apoptosis in mature human neutrophils and maintained their function of superoxide production and enzyme release in response to the invasion of micro-organisms.

GM-CSF is involved in the early stages of immune responses in the tissues particularly in regulating the differentiation and activation of antigen-presenting

dendritic cells, the most important cell type for the induction of primary T cell responses (Tarr, 1996; Stewart-Akers *et al*, 1993). In sheep, Haig *et al* (1995a) reported that together with TNF-α, GM-CSF supports the survival and growth in culture of afferent lymph DC which were found to retain MHC class II and ovine CD1 antigen expression and accessory function for antigen presentation to T cells. Vaccination of mice with irradiated tumour cells producing GM-CSF led to a ten-fold increase in DC infiltrating the vaccination site when compared with control sites vaccinated with β-galactosidase-producing cells (Kielian *et al*, 1999). Immunohistochemical analysis of the vaccination sites suggested that GM-CSF, through the local production of the chemokine MIP-1α, was responsible for the recruitment of DC (Kielian *et al*, 1999).

IL-2, a T-cell derived lymphokine that induces proliferation of antigen- or mitogen-stimulated T cells, was first described as "T-cell growth factor" by Morgan *et al*. in 1976. Inaba *et al* (1983) reported that in culture, DC induced T cells to produce and become responsive to IL-2. $CD4^+$ T helper cells and $CD8^+$ CTL both produce IL-2 (Farrar *et al*, 1982). $CD4^+$ T cells are thought to "help" CTL by producing IL-2 (Swain *et al*, 1991). In addition, IL-2 induces the production of IFN-γ (Kasahara *et al*, 1983). The stimulation of CTL and IFN-γ production, along with the activation of NK cells by IL-2 (Baume *et al*, 1992) are features of an anti-viral response.

In addition to the stimulation of T cell and NK cell activation and proliferation, IL-2 directly triggers the responsive T cells to release B cell helper factors (Inaba *et al*, 1983; Glassman, 1989; Farner *et al*, 1997). Purified natural or recombinant human IL-2 in the absence of exogenous antigen or mitogen has been shown to

induce the differentiation and activation of lymphokine-activated killer (LAK) cells from peripheral blood lymphocytes. LAK cells show an extensive target cell range and are capable of killing NK-resistant human tumour cells (Grimm *et al*, 1991). However the immunological consequences of IL-2 stimulation may be more complex than the mediation of T cell growth.

Both GM-CSF and IL-2 are members of the short chain, 4-α-helical-bundle family of cytokines that also includes IL-4 (Von Feldt *et al*, 1994). However GIF did not bind rovIL-4. A comparison of the ovGM-CSF and ovIL-2 sequences did not reveal any obvious feature other than some similarity (29% in a 38 amino acid overlap) towards the N-terminus of each of the proteins. Interestingly, this region of ovGM-CSF sequence encompasses the domain (amino acids 21-31 of the mature peptide) which is considered important in GM-CSF binding to its receptor in humans (Kaushansky *et al*, 1989). In addition, the conservation of amino acids Leucine^{23} and Serine^{24} in GM-CSF of sheep and cattle that is not present in human GM-CSF may reflect the failure of GIF to bind human GM-CSF. Construction of mutant human and ovine recombinant GM-CSF with appropriate substitutions at amino acids 23 and 24 would allow this to be tested experimentally.

The binding of GIF to both ovine GM-CSF and ovIL-2 and the blocking of GIF-rovGM-CSF interaction by rovIL-2, whilst reflecting the different binding affinities of GIF for each cytokine, suggests that the binding domain(s) for each cytokine is shared or overlapping and can be sterically inhibited. GM-CSF has been shown to compete with IL-2 for binding to IL-2 receptors on the myeloid leukemia cell line, MO7E, suggesting that human GM-CSF and human IL-2 may share a common receptor (Kanakura *et al*, 1993). Human keratinocytes have been shown to express a

cell surface IL-2 like molecule which binds the soluble IL-2 receptor α and may be involved in the activation of Langerhans cells and infiltrating T cells both of which carry surface IL-2 receptors (Dreno *et al*, 1989a and b). Interestingly, the authors describe the blocking of this IL-2 receptor-IL-2 binding by anti-IL-2 monoclonal antibodies that recognise epitopes that may be shared by both IL-2 and GM-CSF.

Although the receptor proteins for ovine GM-CSF have yet to be characterised, there is no evidence of any structural similarity between GIF and any known mammalian cytokine receptor. Apart from GIF, the only other natural inhibitor of GM-CSF identified to date is a secreted form of the human GM-CSF receptor α-chain (Brown *et al*, 1995; Raines *et al*, 1991). This is a post-translationally modified form of the low-affinity α subunit that is specific for GM-CSF but when crosslinked with a β subunit gives rise to a high affinity trans-membranous binding site for GM-CSF (Park *et al*, 1992). The soluble GM-CSFRα form has been shown to successfully compete with the high affinity oligomeric cell surface receptor for GM-CSF binding in spite of exhibiting a much lower affinity (Brown *et al*, 1997). Like GIF, the soluble GM-CSFRα forms oligomers in solution (Brown *et al*, 1997) but GIF bound ovGM-CSF with a ten-fold higher affinity than soluble GM-CSFRα bound huGM-CSF (Kd 369 pM and 3.9 nM respectively). In addition the soluble GM-CSFRα monomer exhibited the highest affinity of binding to human GM-CSF whereas the monomeric form of GIF did not bind either ovGM-CSF or ovIL-2.

The receptor for IL-2 belongs to the same super-family as the GM-CSF receptor. As yet the IL-2 receptor(s) of sheep have not been characterised (except the IL-2Rα chain, Bujdoso *et al*, 1992), but in man and mouse a high affinity IL-2R has been

identified that is expressed on the cell surface of lymphocytes as a trimeric protein complex consisting of an α, β and γ subunit (Nelson and Willerford 1998, Herrmann and Diamantstein 1987). Like the GM-CSFRα, the α subunit of IL-2R can be expressed in a soluble form. Following T cell activation with antigen or mitogens *in vitro*, there is an up-regulation of IL-2Rα chain expression, a high proportion of which is shed from the surface of the T cell in a soluble form (Verhagen *et al* 1994). It has been proposed that as with soluble GM-CSFRα, soluble IL-2Rα could negatively modulate local immune response. High levels of soluble IL-2Rα have been found in the serum and ascites of ovarian cancer patients (Elg *et al* 1997). Jacques *et al* (1987) have determined that the soluble IL-2Rα binds human IL-2 with a dissociation constant (kd = 30nM) identical to a low affinity cell-surface IL-2R (p55/ Tac antigen), this is in contrast to the high affinity binding of IL-2 to the cell surface trimeric complex (kd = 25pM). In this study GIF bound ovIL-2 with a 30-fold higher affinity than soluble human IL-2Rα bound huIL-2 and a 3-fold higher affinity than ovine IL-2 bound to T cells (Kd 1.04 nM, 30 nM and 3.084 nM respectively).

Clearly, if the binding affinities of the ovine receptors for GM-CSF and IL-2 reflect the binding affinities reported for human receptor-ligand binding then, from our studies, GIF has the potential to block either ovine GM-CSF or ovine IL-2 binding its cellular receptor.

GIF represents the first example of a microbial inhibitory protein for GM-CSF and for both GM-CSF and IL-2. A 38 kD protein encoded by tanapox virus, a pathogen of primates, binds human IL-2 but also human IL-5 and human IFN-γ

(Essani *et al*, 1994). Like GIF, the tanapox virus protein represents a group of poxvirus proteins that have the ability to bind and inactivate multiple cytokines and chemokines, some of which appear unrelated. Within the Poxvirus family, genome size appears to be controlled (Wittek, 1982). Consequently one gene product with the ability to bind and inhibit several important immune effector molecules confers a clear advantage to virus survival and efficiency. Another example of this genetic economy practised by the poxviruses, is the M-T7 protein encoded by the myxoma virus B8R gene that was not only shown to inhibit rabbit IFN-γ and human IL-8 but bound promiscuously through a conserved heparin-binding domain to all CXC, CC and C chemokines tested (Lalani *et al*, 1997).

GIF at present appears to have no direct homologue in any organism in the databases. Some sequence similarities have been identified between the genes encoding GIF and A41 of vaccinia virus, variola virus and Shope fibroma virus and the 35 KD/T1 family of CC chemokine binding proteins of rabbit pox (35 kD) and myxoma virus (T1). Like GIF, these genes may have evolved independently from their respective hosts (Graham *et al*, 1997; Lalani and McFadden 1997 and Lalani *et al*, 1998). It is conceivable that GIF has evolved from an ancestral poxvirus gene that has ultimately given rise to a number of cytokine receptors with different specificities. Alternatively the GIF gene could represent an acquired host gene that has undergone radical modification such that the host and viral protein no longer resemble one another except for short peptide sequences that are essential for ligand binding. However until the genes encoding ovGM-CSF receptors have been identified, the origin of the GIF gene remains speculative.

Common to these viral proteins which have been shown to bind a number of

different cytokines is their possession of 8 cysteine residues, some of which are in similar positions in their respective polypeptide chains (Graham *et al*, 1997). It is postulated that the cysteines, through intramolecular disulphide bridges, influence molecular conformation and ultimately ligand specificity of the proteins. From the present study, the involvement of disulphide bridges would appear to be crucial to the activity of GIF particularly in the formation of active homo-dimers that associate under physiological conditions to active homo-tetramers. The construction of single point GIF gene mutations whereby each of the eight cysteines is substituted in turn is proposed as part of a future study. The recombinant GIF proteins expressed from these mutated genes would be analysed for GIF activity in the GM-CSF clearance ELISA to determine which of the eight cysteines are crucial to the formation of an active GIF molecular complex. In addition to providing valuable structural information regarding the conformation of active GIF, this study would provide the basis whereby an orf virus mutant strain could be developed. This orf virus, carrying a defective GIF gene could then be used to infect sheep and by comparing the pathology of the infection with that resulting from a wild type orf virus infection, the contribution of GIF to orf virus infectivity/virulence could be more fully assessed.

The ability to form higher order oligomers is a feature of certain poxvirus receptors with multiple specificities (Lalani *et al*, 1997, 1999a; Loparev *et al*, 1998). These receptors are capable of binding multiple structurally-unrelated cytokines through different binding domains of the oligomeric complex. GIF appears to fall into this category, since even in the presence of molar excess of rovIL-2, GM-CSF binding is not completely inhibited. Whilst this might reflect the differences in binding affinities of GIF for GM-CSF and IL-2, it is possible that GIF possesses 2

separate binding domains for IL-2 and GM-CSF which are in close proximity to one another and consequently the binding of one ligand may partially block the binding of the other.

An investigation into the crystallographic structure of GIF and GIF-GM-CSF and GIF-IL-2 complexes would hopefully identify the natural structure of GIF and the complexes GIF forms with GM-CSF and IL-2. The molecular structures of a number of cytokines, cytokine receptors and the complexes they form have already been determined by X-ray crystallography. For example, the crystal structure of the ligand-binding domain of the common GM-CSF/IL-3/IL-5 receptor β chain has been determined and key amino acid residues identified (Rossjohn *et al*, 2000). In addition the crystal structures of ligand-receptor complexes that include; IFN-γ and IFN-γ receptor (Walter *et al*, 1995), IL-1 and IL-1 receptor (Schreuder *et al*, 1997), IL-10 and IL-10 receptor (Hoover *et al*, 1999) and G-CSF and G-CSF receptor (Aritomi *et al*, 1999) have been examined by X-ray crystallography and their molecular structure resolved. These studies have identified not only the binding domains of the ligands and their respective receptors but have revealed how the molecules are folded, their oligomeric structure and the stoichiometry of the ligand-receptor complexes.

GIF is essentially species-specific. Some reactivity towards bovine GM-CSF and IL-2 may reflect structural similarities between the ovine and bovine cytokines. Orf virus does not infect cattle and so the consequence of this binding is not known. GIF does not react with either human GM-CSF or IL-2 in spite of orf virus being capable of infecting humans. An obvious conclusion is that since GIF cannot bind human GM-CSF, those functions already outlined for GM-CSF in an anti-viral response may not be affected in man unless by some other viral agent acting independently.

Clearly the reservoir of orf virus in the environment is maintained through infection of sheep rather than man and the majority of viral immuno-modulatory proteins, such as viral VEGF and viral IL-10 which closely resemble their sheep homologues, could be considered to be the consequence of the co-evolution of virus and sheep. However it is possible that the virus has evolved additional virulence factors that counteract specific components of the human immune system. There may be differences in the pathology of the disease in man when compared with orf in sheep. A further investigation into differences/similarities in skin pathology of orf infections in sheep and man is therefore warranted.

GIF activity has not been reported in the other genera of the poxviruses. The expression of a GIF-like activity appears restricted to orf virus and possibly the other parapoxviruses bovine papular stomatitus virus and pseudocowpox virus, since GIF- like sequences in both genomes have recently been identified (Dr. A. Mercer, personal communication). Testing for exogenous ovGM-CSF clearance in supernatants from bovine fibroblasts infected with either BPSV or MNV failed to detect a GIF that bound ovGM-CSF. Although orf virus GIF was shown to bind bovGM-CSF and bovIL-2, it is possible that any GIF encoded by genes expressed by either BPSV- or MNV- infected cells binds only bovine cytokines. An ELISA that measures bovine GM-CSF is now available and a future study, similar to the investigation described here, would enable any BPSV and MNV gene products that bind bovGM-CSF to be identified.

GIF is detected at several local sites during orf virus reinfection: in the infected cell, in the vicinity of the infected cell and in the lymph draining the site of infection. This is likely to be a consequence of GIF being a soluble (secreted) mediator.

However, GIF must act primarily in and around the infected cell since this is where GIF is produced. By binding GM-CSF, GIF could down-regulate macrophage and neutrophil activation and the antigen-presenting function of DC. By binding IL-2, GIF could down-regulate $CD4^+$ T cell and $CD8^+$ CTL effector function, IFN-γ production and (through blocking helper T cell function) down-regulate the antibody response to orf virus.

Within the infected epidermal cell GIF may bind GM-CSF constitutively produced by keratinocytes (Lear, 1995), the host cell targeted by orf virus (Fig. 8.1). This is a selective action by orf virus since the expression of the chemokine IL-8 and the inflammatory cytokine TNF-α was not inhibited. Instead, expression of IL-8 has been reported to be increased in infected keratinocytes (Lear, 1995). The production of the orf virus immunomodulatory proteins, vIL-10 and vIFNR protein, along with GIF and vVEGF by infected keratinocytes may be part of a concerted strategy that is not only directed against certain key areas of the anti-viral immune response but also promotes conditions favourable to orf virus replication. IL-8 is thought to promote the proliferation of keratinocytes (Tuschil *et al*, 1992) and so expand the number of possible targets for further infection. At the same time the release of vVEGF will increase the vascularisation in and around the site of the lesion and may in so doing, provide the nutrients and growth factors required by the regenerating epidermis which orf virus targets (Savory *et al*, 2000). Although human IL-10 has been shown to inhibit antigen-specific T cell proliferation by down regulating MHC class II+ molecules on antigen-presenting cells (e.g. DC and macrophages, Allavena *et al*, 1998), this property has not been demonstrated for orf virus IL-10. The orf virus IFNR protein is thought to be involved in the inhibition of interferon-induced protein

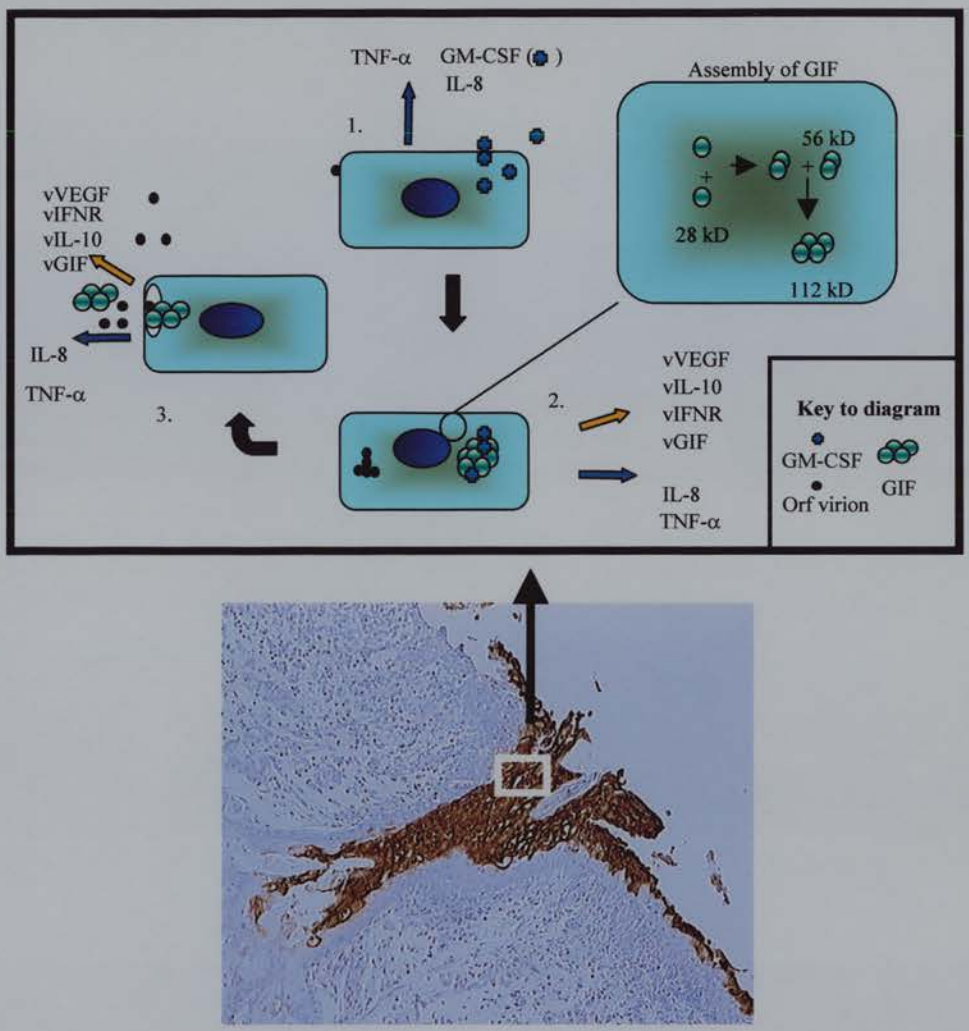

Fig. 8.1 GIF expression by orf virus infected keratinocytes (day 3 after infection).
Schematic representation of the proposed role of GIF in clearing GM-CSF constitutively produced by keratinocytes. (Insert showing skin section stained with anti-orf virus antigen-specific mAb 10E6).
1.) Orf virus targets the regenerating epidermis (keratinocytes) at the site of the orf lesion.
2.) Viral VEGF, IL-10, IFNR and GIF are expressed and secreted by the infected keratinocyte. GM-CSF, IL-8 and TNF-α are constitutively produced but whilst IL-8 and TNF- α are secreted, GM-CSF is bound by GIF. (Insert showing proposed assembly of active GIF within the infected keratinocyte).
3.) Virus-induced cell lysis results in the release of progeny virions and residual virus immunomodulatory proteins.
The vacuolated areas of the lesion as seen in the stained section are indicative of this cytopathic effect.

synthesis shutdown that is part of the anti-viral state within infected cells. This inteferon resistance property of vIFNR has been demonstrated by its ability to protect Semliki Forest virus from the anti-viral effects of both type 1 and type 2 interferons when the vIFNR gene was transfected into ovine fibroblasts prior to SFV infection (Haig *et al*, 1998).

Whilst the role of GM-CSF and IL-2 on keratinocyte function remains to be defined, GIF, by clearing GM-CSF produced by keratinocytes, would be capable of preventing the activation of local (to the epidermis) DC such as Langerhans cells. These cells are responsible for capturing and processing viral antigen prior to presentation to effector T cells. Futhermore, human keratinocytes have been shown to express a surface IL-2-like molecule that may also be implicated in Langerhans cell-directed T cell activation (Dreno *et al*, 1989a and b). Similarly, GIF has the potential to suppress this mechanism through binding ovIL-2.

Within several days of orf virus reinfection, GIF is present at detectable levels throughout the dermis underlying the site of infection. Whether this is as a result of active secretion of GIF by the infected keratinocytes or the release of accumulated GIF through virus-induced cell lysis is not yet clear but since recombinant GIF can be secreted by transfected CHO cells, both appear likely.

Except for GIF, the parapox immodulatory proteins identified so far are all products of early viral genes. GIF was expressed as an intermediate-late gene. This suggests that GIF activity is co-ordinated with those later stages of the viral life cycle within the infected cell, in particular the replication of DNA and the generation of new virus particles. The release of GIF prior to, and coincident with release of progeny virions could be seen as a mechanism by which orf virus encourages the

survival of the newly released virions which are vulnerable to phagocytosis and antibody clearance (Fig. 8.2). Through its reactivity with GM-CSF, GIF could neutralise the phagocytic response mounted by neutrophils and macrophages and inhibit the maturation of DC and ultimately the induction of cytotoxic T cells. Neutralisation of IL-2 function would have a similar effect on the activation on CTL and on NK cells. The accumulation of neutrophils and MHC class II^+ DC in the dermis surrounding the lesion site may be seen as a consequence of recruitment brought about by chemokines produced in response to orf virus infection. However the further signal(s) that these cells require to become functional in the anti-viral response, namely GM-CSF, is cleared by GIF circulating within the dermis and consequently their activation is delayed to the benefit of the virus.

In the skin, immuno-staining for GIF antigen increased in intensity from day 3 after orf virus reinfection, to reach a peak by day 5 and then declined over the next 2-3 days until by day 9 no GIF antigen could be detected. A similar pattern was seen when afferent lymph samples taken during the course of reinfection were tested for the presence of GIF. The presence of GIF, as measured by GM-CSF clearance ELISA, in afferent lymph plasma samples from days 5 and 7 after infection coincided with the period of maximum virus replication and the period of 2-3 days when afferent lymph cell output falls. This followed an initial rise in predominantly $CD4^+$ T cells (considered to be a transient anamnestic response to orf virus). Around day 7-8, CD4+ T cell output rose again but to considerably higher levels that reflect the predicted cell mediated anti-viral response (Fig. 8.3, Haig *et al*, 1999). This increase in $CD4^+$ T cell output in afferent lymph was shortly followed by an increase in the output of $CD8^+$ T cells, then B cells. In the skin it could be argued

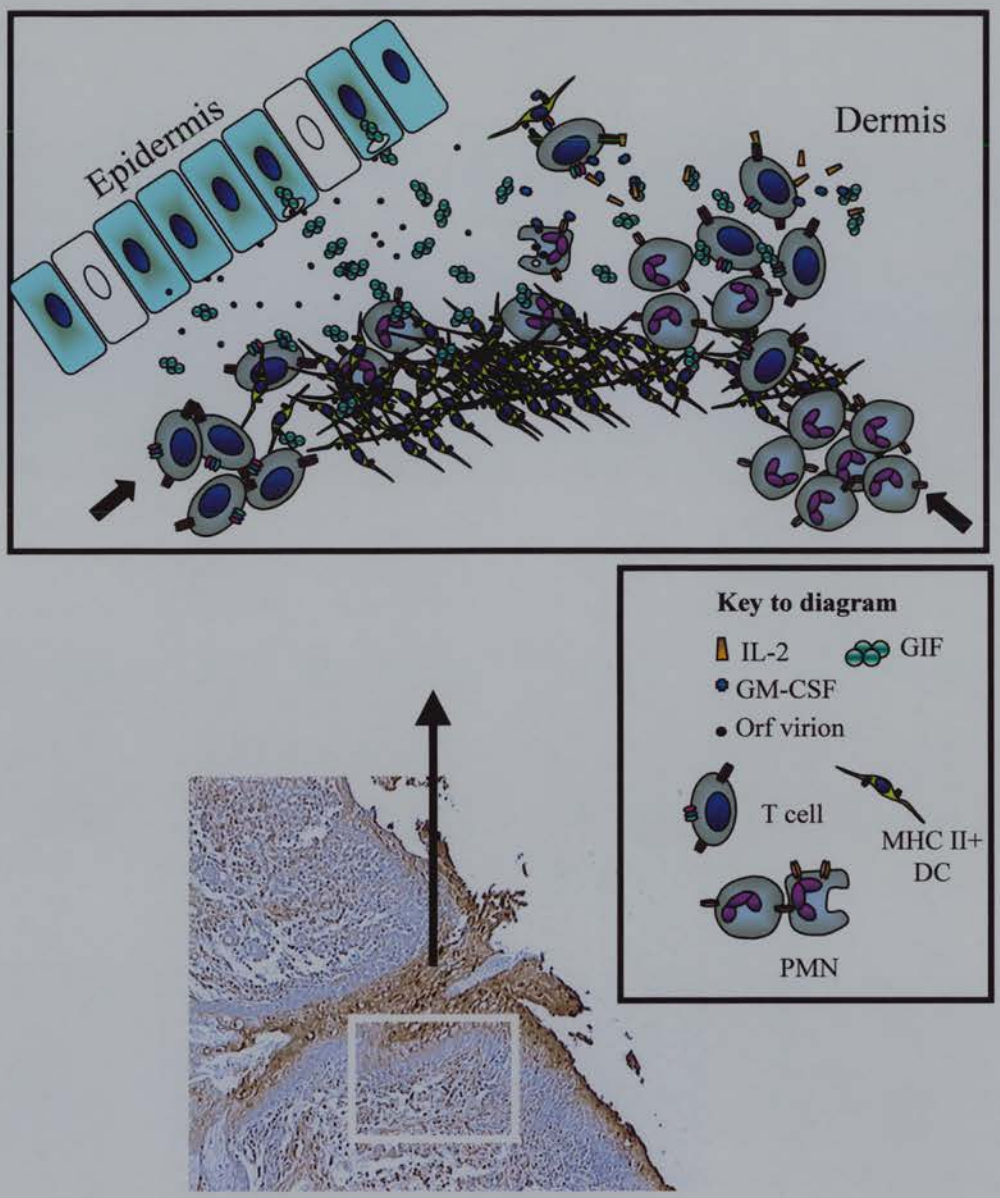

Fig. 8.2 Schematic representation of the proposed role of GIF in preventing GM-CSF and IL-2 mediated activation of effector cells recruited to the site of orf virus infection.

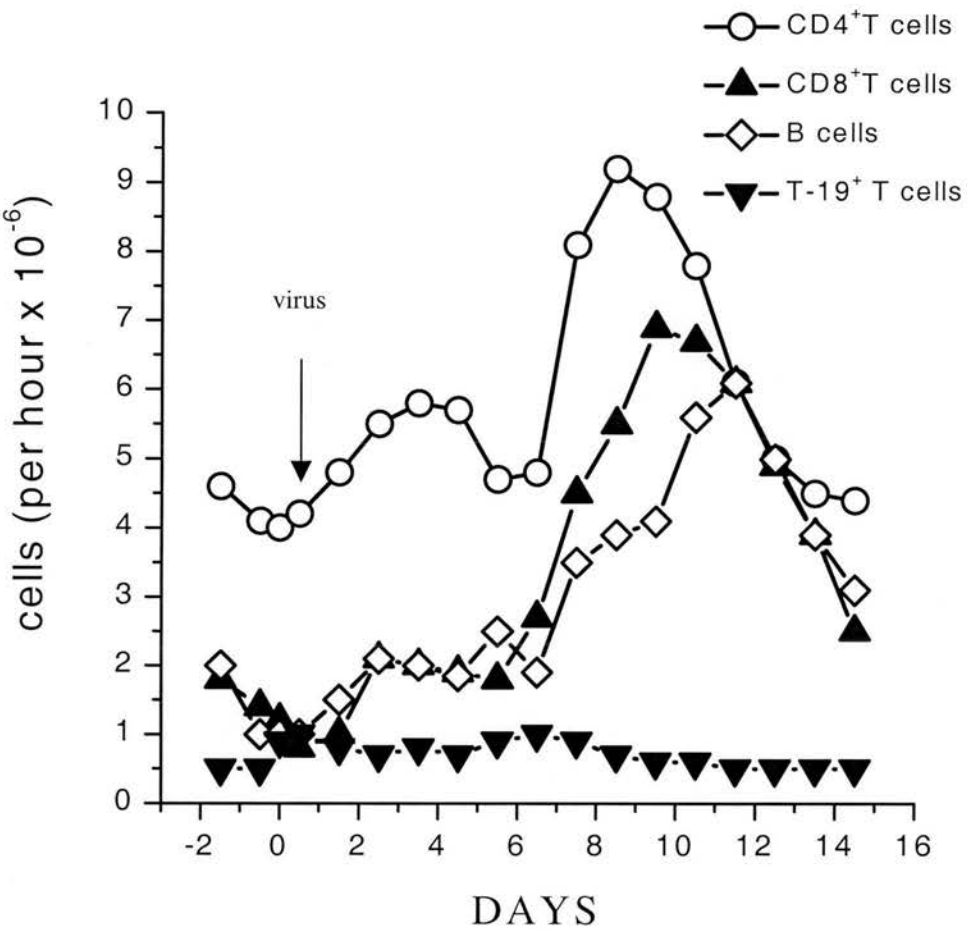

Fig. 8.3 Differential lymphocyte output analysis of afferent lymph draining the site of orf virus reinfection (Haig et al, 1996e).
Samples of afferent lymph collected daily (x-axis) prior to and after orf virus reinfection were analysed by flow cytometry (FACSCAN) for the output (cells per hour, y-axis) of $CD4^+$ -T cells (open circles), $CD8^+$ T cells (upright triangles), T-19^+ T cells (inverted triangles) and B cells (open diamonds) using specific mouse monoclonal antibodies. Data set presented is a representative example from a single animal.

that peak GIF levels preceded this later rise in afferent lymph cell output and that the role of GIF is to delay any local cell mediated response. Subsequently, as GIF percolates into the afferent lymph, it may contribute to the inhibition of further T and B cell mobilisation that is centred on the draining lymph node. Whether the influence of GIF extends to within the draining lymph node and those cell-cell interactions that include antigen presentation and lymphocyte clonal proliferation is not known. Unfortunately the draining lymph nodes were not available in this study but a future study may benefit from an immunohistological analysis of GIF within the draining lymph node. This analysis carried out in parallel with an assay (still to be developed) for ovIL-2 might clarify whether the targeting of IL-2 and GM-CSF by GIF is mutually exclusively or not. Furthermore, whether this specificity is influenced by local environment such as in and around the lesion site or within the afferent lymphatics and draining node. Of particular interest is whether IL-2 levels in afferent lymph draining the site of orf virus reinfection follow the same biphasic response whereby the fall of GM-CSF levels in the lymph, observed in samples taken at days 5-7, is coincident with the detection of GIF.

In conclusion, there is still much work to be done before the mode of action of GIF and its role in orf virus infection of sheep is fully elucidated. A future X-ray crystallographic study will hopefully determine the nature of the GIF and GIF-ligand molecular structures while the generation of a "knockout" orf virus, where the GIF gene is made dysfunctional, will enable the contribution of GIF activity to orf virus virulence to be tested.

The results presented in this thesis indicate that GIF represents a co-ordinated interference with host inflammatory and cell-mediated immune responses to orf virus

infection. These results also suggest that GM-CSF and IL-2 are important in host immunity to orf virus. GIF is a protein with unusual properties and part of a growing number of pathogen immunomodulators that will be useful not only in determining mechanisms of viral pathogenesis and the nature of host anti-viral immunity but also as templates for potentially therapeutic proteins and peptides.

BIBLIOGRAPHY

Abdulassam, M. (1957). Contagious pustular dermatitis: III Experimental infection. *Journal of Comparative Pathology* **67**: 305-319.

Abdulassam, M., Cosslet, V. E. (1957). Contagious pustular dermatitis; I Studies on morphology. *Journal of Comparative Pathology* **67**: 145-156.

Adachi, M., Torigoe, T., Takayama, S., Imai, K. (1998). BAG-1 and Bcl-2 in IL-2 signaling. *Leukemia and Lymphoma* **30**: 483-491.

Alcami, A., Khanna, A., Paul, N.L., Smith, G.L. (1999). Vaccinia virus strains Lister, USSR and Evans express soluble and cell- surface tumour necrosis factor receptors. *Journal of General Virology* **80**: 949-959.

Alcami, A., Koszinowski, U.H. (2000). Viral mechanisms of immune evasion. *Trends in Microbiology* **8**: 410-418.

Alcami, A., Smith, G.L. (1992). A soluble receptor for interleukin-1 beta encoded by vaccinia virus: a novel mechanism of virus modulation of the host response to infection. *Cell* **71**: 153-167.

Alcami, A., Smith, G.L. (1995). Vaccinia, cowpox, and camelpox viruses encode soluble gamma interferon receptors with novel broad species specificity. *Journal of Virology* **69**: 4633-4639.

Alcami, A., Smith, G.L. (1996). A mechanism for the inhibition of fever by a virus. *Proceedings of the National Academy of Science USA* **93**: 11029-11034.

Alcami, A., Symons, J.A., Collins, P.D., Williams, T.J., Smith, G.L. (1998). Blockade of chemokine activity by a soluble chemokine binding protein from vaccinia virus. *Journal of Immunology* **160**: 624-633.

Alcami, A., Symons, J.A., Smith, G.L. (2000). The vaccinia virus soluble alpha/beta interferon (IFN) receptor binds to the cell surface and protects cells from the Antiviral effects of IFN. *Journal of Virology* **74**: 11230-11239.

Allavena, P., Piemonti, L., Longoni, D., Bernasconi, S., Stoppacciaro, A., Ruco, L., Mantovani, A. (1998). IL-10 prevents the differentiation of monocytes to dendritic cells but promotes their maturation to macrophages. *European Journal of Immunology 28*: 359-369.

Altschul, S.F., Lipman, D.J. (1990). Protein database search for multiple alignments. *Proceedings of the National Academy of Science USA* **87**: 5509-5513.

Arakawa, T., Yphantis, D.A., Lary, J.W., Narhi, L.O., Lu, H.S., Prestrelski, S.J., Clogston, C.L., Zsebo, K.M., Mendiaz, E.A.,Wypych, J. (1991). Glycosylated and unglycosylated recombinant-derived human stem cell factors are dimeric and have extensive regular secondary structure. *Journal of Biological Chemistry* **266**: 18942-18948.

Archard, L.C. (1983). Synthesis of full-length, virus genomic DNA by nuclei of vaccinia-infected hela-cells. *Journal of General Virology* **64**: 2561-2575.

Aritomi, M., Kunishima, N., Okamoto, T., Kuroki, R., Ota, Y., Morikawa, K. (1999). Atomic structure of the GCSF-receptor complex showing a new cytokine- receptor recognition scheme. *Nature* **401**: 713-717.

Armstrong, J.A., Metz, D.H., Young, M.R. (1973). The mode of entry of vaccinia virus into L cells. *Journal of General Virology* **21**: 533-537.

Arnaud, J.P., Bernard, P., Souyri, N., Pecout, C., Dunoyer, J. (1986). Human ORF disease localized in the hand: a "false felon". A study of eight cases. *Annales de Chirurgie de Main* **5**: 129-132.

Arunachalam, B., Subba Rao, M.V., Ram, G.C. (1989). Bovine interleukin 2: biochemical and biological characterization. *Veterinary Immunology and Immunopathology* **23**: 377-383.

Aynaud, M. (1923) La stomatite pustuleuse contagieuse des ovins (chancre du mouton). *Annales de l'Institut Pasteur* **37**: 498-527.

Azwai, S.M., Carter, S.D., Woldehiwet, Z. (1995). Immune responses of the camel (*Camelus dromedarius*) to contagious ecthyma (Orf) virus infection. *Veterinary Microbiology* **47**: 119-131.

Balassu, T.C., Robinson, A.J. (1987). Orf virus replication in bovine testis cells: kinetics of viral DNA, polypeptide, and infectious virus production and analysis of virion polypeptides. *Archives of Virology* **97**: 267-281.

Baldwin, G.C. (1992). The biology of granulocyte-macrophage colony-stimulating factor: effects on hematopoietic and nonhematopoietic cells. *Developmental Biology* **151**: 352-367.

Ballingall, K.T., Wright, H., Redmond, J., Dutia, B.M., Hopkins, J., Lang, J., Deverson, E.V., Howard, J.C., Puri, N., Haig, D. (1992). Expression and characterization of ovine major histocompatibility complex class II (OLA-DR) genes. *Animal Genetics* **23**: 347-359.

Baroudy, B.M., Venkatesan, S., Moss, B. (1982a). Structure and replication of vaccinia virus telomeres. *Cold Spring Harbor Symposia on Quantitative Biology* **47**: 723-729.

Baroudy, B.M., Venkatesan, S., Moss, B. (1982b). Incompletely base-paired flip-flop terminal loops link the 2 DNA strands of the vaccina-virus genome into one uninterrupted polynucleotide chain. *Cell* **28**: 315-324.

Barry, M., Hnatiuk, S., Mossman, K., Lee, S.F., Boshkov, L., McFadden, G. (1997). The myxoma virus M-T4 gene encodes a novel RDEL-containing protein that is retained within the endoplasmic reticulum and is important for the productive infection of lymphocytes. *Virology* **239**: 360-377.

Barry, M., McFadden, G. (1997). Virus encoded cytokines and cytokine receptors. *Parasitology* **115**: S89-100.

Bassioukas, K., Orfanidou, A., Stergiopoulou, C.H., Hatzis, J. (1993). Orf. Clinical and epidemiological study. *Australian Journal of Dermatology* **34**: 119-123.

Baume, D.M., Robertson, M.J., Levine, H., Manley, T.J., Schow, P.W., Ritz, J. (1992). Differential responses to interleukin 2 define functionally distinct subsets of human natural killer cells. *European Journal of Immunology* **22**: 1-6.

Beattie, E., Denzler, K.L., Tartaglia, J., Perkus, M.E., Paoletti, E., Jacobs, B.L. (1995). Reversal of the interferon-sensitive phenotype of a vaccinia virus lacking e3l by expression of the reovirus s4 gene. *Journal of Virology* **69**: 499-505.

Beattie, J., Fawcett, H.A., Flint, D.J. (1992). The use of multiple-pin peptide synthesis in an analysis of the continuous epitopes recognised by various anti-(recombinant bovine growth hormone) sera. Comparison with predicted regions of immunogenicity and location within the three-dimensional structure of the molecule. *European Journal of Biochemistry* **210**: 59-66.

Beaud, G. (1995). Vaccinia virus DNA replication: a short review. *Biochimie* **77**: 774-779.

Becherel, P.A., Le Goff, L., Ktorza, S., Ouaaz, F., Mencia-Huerta, J.M., Dugas, B., Debre,

P., Mossalayi, M.D., Arock, M. (1995). Interleukin-10 inhibits IgE-mediated nitric oxide synthase induction and cytokine synthesis in normal human keratinocytes. *European Journal of Immunology* **25**: 2992-2995.

Beh, K.J., Haynes, S.E., Ward, K.A. (1986). Characterization of 2 mouse myeloma x sheep lymphocyte cell-lines secreting sheep antibody. *Molecular Immunology* **23**: 717-724.

Bernasconi, S., Matteucci, C., Sironi, M., Conni, M., Colotta, F., Mosca, M., Colombo, N., Bonazzi, C., Landoni, F., Corbetta, G. (1995). Effects of granulocyte-monocyte colony-stimulating factor (GM-CSF) on expression of adhesion molecules and production of cytokines in blood monocytes and ovarian cancer-associated macrophages. *International Journal of Cancer* **60**: 300-307.

Blasco, R., Moss, B. (1991). Extracellular vaccinia virus formation and cell-to-cell virus transmission are prevented by deletion of the gene encoding the 37:000-Dalton outer envelope protein. *Journal of Virology* **65**: 5910-5920.

Boshkov, L.K., Macen, J.L., McFadden, G. (1992). Virus-induced loss of class I MHC antigens from the surface of cells infected with myxoma virus and malignant rabbit fibroma virus. *Journal of Immunology* **148**: 881-887.

Boughton, I. B., Hardy, W. T. (1935). Immunisation of sheep and goats against sore mouth (contagious ecthyma). *Texas Agriculture Experimental Station Bulletin* No. 504.

Boulay, J.L., Paul, W.E. (1992). The interleukin-4 family of lymphokines. *Current Opinion in Immunology* **4**: 294-298.

Bowman, K.F., Barbery, R.T., Swango, L.J., Schnurrenberger, P.R. (1981). Cutaneous form of bovine papular stomatitis in man. *Journal of the American Medical Association* **246**: 2813-2818.

Brander, C., Walker, B.D. (2000). Modulation of host immune responses by clinically relevant human DNA and RNA viruses. *Current Opinion in Microbiology* **3**: 379-386.

Brazel, D., Nakanishi, S., Oster, W. (1991). Interleukin-1: characterization of the molecule, functional activity, and clinical implications. *Biotechnology Therapeutics* **2**: 241-267.

Brown, C.B., Beaudry, P., Laing, T.D., Shoemaker, S., Kaushansky, K. (1995). In vitro characterization of the human recombinant soluble granulocyte- macrophage colony-

stimulating factor receptor. *Blood* **85**: 1488-1495.

Brown, C.B., Pihl, C.E., Murray, E.W. (1997). Oligomerization of the soluble granulocyte-macrophage colony-stimulating factor receptor: identification of the functional ligand-binding species. Cytokine **9**: 219-225.

Buchan, J. (1996). Characteristics of orf in a farming community in mid-Wales. *British Medical Journal* **313**: 203-204.

Buddle, B.M., Pulford, H.D. (1984). Effect of passively-acquired antibodies and vaccination on the immune response to contagious ecthyma virus. *Veterinary Microbiology* **9**: 515-522.

Budel, L.M., Hoogerbrugge, H., Pouwels, K., van Buitenen, C., Delwel, R., Lowenberg, B., Touw, I.P. (1993). Granulocyte-macrophage colony-stimulating factor receptors alter their binding characteristics during myeloid maturation through up-regulation of the affinity converting beta subunit (KH97). *Journal of Biological Chemistry* **268**: 10154-10159.

Bugert, J.J., Lohmuller, C., Darai, G. (1999). Characterization of early gene transcripts of molluscum contagiosum virus. *Virology* **257**: 119-129.

Bujdoso, R., Hopkins, J., Dutia, B.M., Young, P., McConnell, I. (1989). Characterization of sheep afferent lymph dendritic cells and their role in antigen carriage. *Journal of Experimental Medicine* **170**: 1285-1301.

Bujdoso, R., Young, P., Hopkins, J., McConnell, I. (1990). IL-2-like activity in lymph fluid following in vivo antigen challenge. *Immunology* **69**: 45-51.

Bujdoso, R., Sargan, D., Williamson, M., McConnell, I. (1992). Cloning of a cDNA encoding the ovine interleukin-2 receptor 55-kDa protein, CD25. *Gene* **113**: 283-284.

Burdach, S. (1991). The granulocyte macrophage-colony stimulating factor (GM-CSF): basic science and clinical applications. *Klinische Paediatrie* **203**: 302-310.

Buttner, M., Czerny, C.P., Schumm, M. (1995). Behavior of Orf virus in permissive and non-permissive systems. *Tierarzthliche Praxis* **23**: 179-184.

Buttner, M., Czerny, C.P., Waldmann, R., Mayr, A. (1990). Recent information about the orf virus of small ruminants. *Tierarzthliche Praxis* **18**: 343-348.

Caligiuri, M.A., Zmuidzinas, A., Manley, T.J., Levine, H., Smith, K.A., Ritz, J. (1990). Functional consequences of interleukin-2 receptor expression on resting human-lymphocytes. Identification of a novel natural killer cell subset with high affinity receptors. *Journal of Experimental Medicine* **171**: 1509-1526.

Cantrell, M.A., Anderson, D., Cerretti, D.P., Price, V., McKereghan, K., Tushinski, R.J., Mochizuki, D.Y., Larsen, A., Grabstein, K., Gillis, S. (1985). Cloning, sequence, and expression of a human granulocyte/macrophage colony-stimulating factor. *Proceedings of the National Academy of Science USA* **82**: 6250-6254.

Cao, J.X., Gershon, P.D., Black, D.N. (1995). Sequence analysis of HindIII Q2 fragment of capripoxvirus reveals a putative gene encoding a G-protein-coupled chemokine receptor homologue. *Virology* **209**: 207-212.

Cao, X., Chen, G., He, L., Zhang, W., Yu, Y., Ye, T.X. (1998). Chemoattractive effect on the effector cells of the supernatants from melanoma cells transfected with the interleukin-2 (IL-2), IL-4 or IL-6 gene. *Journal of Cancer and Clinical Oncology* **124**: 88-92.

Carfi, A., Smith, C.A., Smolak, P.J., McGrew, J., Wiley, D.C. (1999). Structure of a soluble secreted chemokine inhibitor vCCI (p35) from cowpox virus. *Proceedings of the National Academy of Science USA* **96**: 12379-12383.

Carroll, K., Elroy-Stein, O., Moss, B., Jagus, R. (1993). Recombinant vaccinia virus K3L gene product prevents activation of double-stranded RNA-dependent, initiation factor 2 alpha-specific protein kinase. *Journal of Biological Chemistry* **268**: 12837-12842.

Chahidi, N., de Fontaine, S., Lacotte, B. (1993). Human orf. *British Journal of Plastic Surgery* **46**: 532-534.

Chand, P., Kitching, R.P., Black, D.N. (1994). Western blot analysis of virus-specific antibody responses for capripox and contagious pustular dermatitis viral infections in sheep. *Epidemiology and Infection* **113**: 377-385.

Chang, H.W., Watson, J.C., Jacobs, B.L. (1992). The e3l gene of vaccinia virus encodes an inhibitor of the interferon-induced, double-stranded RNA-dependent protein-kinase. *Proceedings of the National Academy of Sciences USA* **89**: 4825-4829.

Chiba, S., Tojo, A., Kitamura, T., Urabe, A., Miyazono, K., Takaku, F. (1990).

Characterization and molecular features of the cell surface receptor for human granulocyte-macrophage colony-stimulating factor. *Leukemia* **4**: 29-36.

Clark, S.C. (1988). Biological activities of human granulocyte-macrophage colony-stimulating factor. *International Journal of Cell Cloning* **6**: 365-377.

Cockett, M.I., Bebbington, C.R., Yarranton, G.T. (1990). High level expression of tissue inhibitor of metalloproteinases in Chinese hamster ovary cells using glutamine synthetase gene amplification. *Biotechnology* **8**: 662-667.

Corradi, A., Bajetto, A., Cozzolino, F., Rubartelli, A. (1993). Production and secretion of interleukin-1 receptor antagonist in monocytes and keratinocytes. *Cytotechnology* **11**: 50-52.

Cottone, R., Buttner, M., Bauer, B., Henkel, M., Hettich, E., Rziha, H.J. (1998). Analysis of genomic rearrangement and subsequent gene deletion of the attenuated Orf virus strain D1701. *Virus Research* **56**: 53-67.

Curling, E.M., Hayter, P.M., Baines, A.J., Bull, A.T., Gull, K., Strange, P.G., Jenkins, N. (1990). Recombinant human interferon-gamma. Differences in glycosylation and proteolytic processing lead to heterogeneity in batch culture. *Biochemical Journal* **272**: 333-337.

Czerny, C.P., Waldmann, R., Buttner, M. (1994). Recent developments in the diagnosis of parapoxviruses. *Tierarzthliche Praxis* **22**: 230-233.

Czerny, C.P., Waldmann, R., Scheubeck, T. (1997). Identification of three distinct antigenic sites in parapoxviruses. *Archives of Virology* **142**: 807-821.

Dale, DC, Liles, WC, Llewellyn, C, Price, T.H. (1998). Effects of granulocyte-macrophage colony-stimulating factor (GM-CSF) on neutrophil kinetics and function in normal human volunteers. *American Journal of Hematology* **57**: 7-15.

Darbyshire, J. H. (1961) A fatal ulcerative mucosal condition of sheep associated with the virus of contagious pustular dermatitis. *British Veterinary Journal* **117**: 97-105.

Darbyshire, J.H., Huck, R.A. (1966). Mucosal disease in Britain. *Bulletin de l' Office International Epizooties* **66**: 413-419.

Dashtseren, T., Solovyev, B.V., Varejka, F., Khokhoo, A. (1984). Camel contagious ecthyma (pustular dermatitis). *Acta Virologica* **28**: 122-127.

Davis-Poynter, N.J., Farrell, H.E. (1996). Masters of deception: a review of herpesvirus immune evasion strategies. *Immunology and Cell Biology* **74**: 513-522.

De Waal, M.R., Abrams, J., Bennett, B., Figdor, C.G., de Vries, J.E. (1991). Interleukin 10(IL-10) inhibits cytokine synthesis by human monocytes: an autoregulatory role of IL-10 produced by monocytes. *Journal of Experimental Medicine* **174**: 1209-1220.

Ding, D.X., Vera, J.C., Heaney, M.L., Golde, D.W. (1995). N-glycosylation of the human granulocyte-macrophage colony-stimulating factor receptor alpha subunit is essential for ligand binding and signal transduction. *Journal of Biological Chemistry* **270**: 24580-24584.

DiPersio, J.F., Golde, D.W., Gasson, J.D. (1990). GM-CSF: receptor structure and transmembrane signaling. *International Journal of Cell Cloning* **8**: 63-74.

DiPersio, J.F., Hedvat, C., Ford, C.F., Golde, D.W., Gasson, J.C. (1991). Characterization of the soluble human granulocyte-macrophage colony-stimulating factor receptor complex. *Journal of Biological Chemistry* **266**: 279-286.

Dobbelstein, M., Shenk, T. (1996). Protection against apoptosis by the vaccinia virus SPI-2 (B13R) gene product. *Journal of Virology* **70**: 6479-6485.

Dower, S.K., Kronheim, S.R., March, C.J., Conlon, P.J., Hopp, T.P., Gillis, S., Urdal, D.L. (1985). Detection and characterization of high affinity plasma membrane receptors for human interleukin 1. *Journal of Experimental Medicine* **162**: 501-515.

Dreno, B., Hallet, M.M., Moisan, J.P., Soulillou, J.P., Jacques, Y. (1989a). Interleukin 2-like material in human epidermis: a ligand for the human interleukin 2-receptor 55 kD alpha chain. *Journal of Investigative Dermatology* **93**: 78-82.

Dreno, B., Jacques, Y., Litoux, P., Soulillou, J.P. (1989b). The keratinocytes of the granular layer express a soluble IL-2R alpha-chain receptor. *Journal of Investigative Dermatology* **92**: 139.

Dubochet, J., Adrian, M., Richter, K., Garces, J., Wittek, R. (1994). Structure of intracellular mature vaccinia virus observed by cryoelectron microscopy. *Journal of Virology* **68**: 1935-1941.

Eck, M.J., Sprang, S.R. (1989). The structure of tumor necrosis factor-alpha at 2.6 A resolution. Implications for receptor binding. *Journal of Biological Chemistry* **264**: 17595-

17605.

Egan, P.J., Kimpton, W., Seow, H.F., Bowles, V.M., Brandon, M.R., Nash, A.D. (1996). Inflammation-induced changes in the phenotype and cytokine profile of cells migrating through skin and afferent lymph. *Immunology* **89**: 539-546.

Elg, S.A., Hill, R.B., Heldman, L., Ramakrishnan, S. (1997). The *in vitro* effect on T cell function of soluble IL-2R alpha from advanced ovarian cancer ascites. *Gynecologic Oncology* **66**: 133-137.

Elliott, M.J., Vadas, M.A., Eglinton, J.M., Park, L.S., To, L.B., Cleland, L.G., Clark, S.C., Lopez, A.F. (1989). Recombinant human interleukin-3 and granulocyte-macrophage colony-stimulating factor show common biological effects and binding characteristics on human monocytes. *Blood* **74**: 2349-2359.

Entrican, G., Deane, D., MacLean, M., Inglis, L., Thomson, J., McInnes, C., Haig, D.M. (1996). Development of a sandwich ELISA for ovine granulocyte/macrophage colony-stimulating factor. *Veterinary Immunology and Immunopathology* **50**: 105-115.

Entrican, G., Haig, D.M., Norval, M. (1989). Identification of ovine interferons: differential activities derived from fibroblast and lymphoid cells. *Veterinary Immunology and Immunopathology* **21**: 187-195.

Esposito, J.J., Knight, J.C. (1985). Orthopoxvirus DNA: a comparison of restriction profiles and maps. *Virology* **143**: 230-251.

Essani, K., Chalasani, S., Eversole, R., Beuving, L., Birmingham, L. (1994). Multiple anti-cytokine activities secreted from tanapox virus-infected cells. *Microbial Pathogenesis* **17**: 347-353.

Everett, H., Barry, M., Lee, S.F., Sun, X., Graham, K., Stone, J., Bleackley, R.C., McFadden, G. (2000). M11L: a novel mitochondria-localized protein of myxoma virus that blocks apoptosis of infected leukocytes. *Journal of Experimental Medicine* **191**: 1487-1498.

Farner, NL, Gan, J, deJong, JLO, Leary, TP, Fenske, TS, Buckley (1997). Alteration of the CD34(+) Tf-1 beta cell line profile in response to long-term exposure to IL-15. *Cytokine* **9**: 316-327.

Farrar, J.J., Benjamin, W.R., Hilfiker, M.L., Howard, M., Farrar, W.L., Fuller-Farrar, J.

(1982). The biochemistry, biology, and role of interleukin 2 in the induction of cytotoxic T cell and antibody-forming B cell responses. *Immunological Reviews* **63**: 129-166.

Fava, R.A., Olsen, N.J., Spencer-Green, G., Yeo, K.T., Yeo, T.K., Berse, B., Jackman, R.W., Senger, D.R., Dvorak, H.F., Brown, L.F. (1994). Vascular permeability factor/endothelial growth factor (VPF/VEGF): accumulation and expression in human synovial fluids and rheumatoid synovial tissue. *Journal of Experimental Medicine* **180**: 341-346.

Ferrara, N., DavisSmyth, T. (1997). The biology of vascular endothelial growth factor. *Endocrine Reviews* **18**: 4-25.

Fiorentino, D.F., Zlotnik, A., Vieira, P., Mosmann, T.R., Howard, M., Moore, K.W., O'Garra, A. (1991). IL-10 acts on the antigen-presenting cell to inhibit cytokine production by Th1 cells. *Journal of Immunology* **146**: 3444-3451.

Fleming, S.B., Blok, J., Fraser, K.M., Mercer, A.A., Robinson,A.J. (1993). Conservation of gene structure and arrangement between vaccinia virus and orf virus. *Virology* **195**: 175-184.

Fleming, S.B., Fraser, K.M., Mercer, A.A., Robinson, A.J. (1991). Vaccina virus-like early transcriptional control sequences flank an early gene in orf virus. *Gene* **97**: 207-212.

Fleming, S.B., Lyttle, D.J., Sullivan, J.T., Mercer, A.A., Robinson, A.J. (1995). Genomic analysis of a transposition-deletion variant of orf virus reveals a 3.3 kbp region of non-essential DNA. *Journal of General Virology* **76:** 2969-2978.

Fleming, S.B., McCaughan, C.A., Andrews, A.E., Nash, A.D., Mercer, A.A. (1997). A homolog of interleukin-10 is encoded by the poxvirus orf virus. *Journal of Virology* **71**: 4857-4861.

Fleming, S.B., Mercer, A.A., Fraser, K.M., Lyttle, D.J., Robinson, A.J. (1992). *In vivo* recognition of orf virus early transcriptional promoters in a vaccinia virus recombinant. *Virology* **187**: 464-471.

Florkiewicz, R.Z., Smith, A., Bergmann, J.E., Rose, J.K. (1983). Isolation of stable mouse cell lines that express cell surface and secreted forms of the vesicular stomatitis virus glycoprotein. *Journal of Cell Biology* **97**: 1381-1388.

Fraser, K.M., Hill, D.F., Mercer, A.A., Robinson, A.J. (1990). Sequence-analysis of the

inverted terminal repetition in the genome of the parapoxvirus, orf virus. *Virology* **176**: 379-389.

Freeman, G., Bron, A.J., Juel-Jensen, B. (1984). Ocular infection with orf virus. *American Journal of Ophthalmology* **97**: 601-604.

Gabrilovich, D., Ishida, T., Oyama, T., Ran, S., Kravtsov, V., Nadaf, S., Carbone, D.P. (1998). Vascular endothelial growth factor inhibits the development of dendritic cells and dramatically affects the differentiation of multiple hematopoietic lineages in vivo. *Blood* **92**: 4150-4166.

Gagnadoux, F, Diot, P, Boissinot, E, Lemarie, E (1997). Colony-stimulating factors and respiratory defences against infection. *Revue des Maladies Respiratoires* **14**: 93-99.

Garnier, J., Osguthorpe, D.J., Robson, B. (1978). Analysis of the accuracy and implications of simple methods for predicting the secondary structure of globular proteins. *Journal of Molecular Biologyy* **120**: 97-120.

Gill, M.J., Arlette, J., Buchan, K.A., Barber, K. (1990). Human orf. A diagnostic consideration? *Archives of Dermatology* **126**: 356-358.

Gilray, J.A., Nettleton, P.F., Pow, I., Lewis, C.J., Stephens, S.A., Madeley, J.D., Reid, H.W. (1998). Restriction endonuclease profiles of orf virus isolates from the British Isles. *Veterinary Record* **143**: 237-240.

Glassman, A.B. (1989). Interleuken-2 and lymphokine activated killer cells - promises and cautions. *Annals of Clinical and Laboratory Science* **19**: 51-55.

Glover, R. E. (1928). Contagious pustular dermatitis of sheep. *Journal of Comparative Pathology* 41: 318.

Goebel, S.J., Johnson, G.P., Perkus, M.E., Davis, S.W., Winslow, J.P., Paoletti, E. (1990). The complete DNA-sequence of vaccinia virus. *Virology* **179**: 247-266.

Golini, F., Kates, J.R. (1985). A soluble transcription system derived from purified vaccinia. *Journal of Virology* **53**: 205-213.

Gong, S., Lai, C.F., Esteban, M. (1990). Vaccinia virus induces cell-fusion at acid pH and this activity is mediated by the N-terminus of the 14-kDa virus envelope protein. *Virology*

178: 81-91.

Goodbourn, S., Didcock, L., Randall, R.E. (2000). Interferons: cell signalling, immune modulation, antiviral response and virus countermeasures. *Journal of General Virology* **81**: 2341-2364.

Gough, N.M., Metcalf, D., Gough, J., Grail, D., Dunn, A.R. (1985). Structure and expression of the mRNA for murine granulocyte-macrophage colony stimulating factor. *EMBO Journal* **4**: 645-653.

Gourreau, J.M., Mornet, M., Gressin, R., Fraisse, J.C., Gourvil, J., Lesouple, C. (1986). Orf: recontamination 8 months after the original infection. Review of the literature apropos of a case. *Annals of Dermatology and Venereology* **113**: 1065-1076.

Graham, G.J., MacKenzie, J., Lowe, S., Tsang, M.L., Weatherbee, J.A., Issacson, A., Medicherla, J., Fang, F., Wilkinson, P.C., Pragnell, I.B. (1994). Aggregation of the chemokine MIP-1 alpha is a dynamic and reversible phenomenon. Biochemical and biological analyses. *Journal of Biological Chemistry* **269**: 4974-4978.

Graham, K.A., Lalani, A.S., Macen, J.L., Ness, T.L., Barry, M., Liu, L.Y., Lucas, A., Clark-Lewis, I., Moyer, R.W., McFadden, G. (1997). The T1/35kDa family of poxvirus-secreted proteins bind chemokines and modulate leukocyte influx into virus-infected tissues. *Virology* **229**: 12-24.

Greig, A., Linklater, K.A., Clark, W.A. (1984). Persistent orf in a ram. *Veterinary Record* **115**: 149.

Griebel, P.J., Hein, W.R. (1996). Expanding the role of Peyer's patches in B-cell ontogeny. *Immunology Today* **17**: 30-39.

Griffin, J.D., Cannistra, S.A., Sullivan, R., Demetri, G.D., Ernst, T.J., Kanakura, Y. (1990). The biology of GM-CSF: regulation of production and interaction with its receptor. *International Journal of Cell Cloning* **8**: 35-44.

Grimm, E.A., Owen-Schaub, L. (1991). The IL-2 mediated amplification of cellular cytotoxicity. *Journal of Cellular Biochemistry* **45**: 335-339.

Groves, RW, Rauschmayr, T, Nakamura, K, Sarkar, S, Williams, IR, Kupper, TS (1996). Inflammatory and hyperproliferative skin disease in mice that express elevated levels of the

IL-1 receptor (type 1) on epidermal keratinocytes. *Journal of Clinical Investigation* **98**: 336-344.

Groves, R.W., Wilson-Jones, E., MacDonald, D.M. (1991). Human orf and milkers' nodule: a clinicopathologic study. *Journal of the American Academy of Dermatology* **25**: 706-711.

Gumbrell, R.C., McGregor, D.A. (1997). Outbreak of severe fatal orf in lambs. *Veterinary Record* **141**: 150-151.

Guthridge, M.A., Stomski, F.C., Thomas, D., Woodcock, J.M., Bagley, C.J., Berndt, M.C., Lopez, A.F. (1998). Mechanism of activation of the GM-CSF, IL-3: and IL-5 family of receptors. *Stem Cells* **16**: 301-313.

Haig, D.M. (1997). Isolation and Culture of Hematopoietic Cells. In: *Immunology Methods Manual*. (edited by I. Lefkovits) section 3.17, Academic Press Ltd. London.

Haig, D.M. (1998). Poxvirus interference with the host cytokine response. *Veterinary Immunology and Immunopathology* **63**: 149-156.

Haig, D.M., Brown, D., Mackellar, A. (1990). Ovine haemopoiesis: the development of bone marrow-derived colony-forming cells in vitro in the presence of factors derived from lymphoid cells and helper T-cells. *Veterinary Immunology and Immunopathology* **25**: 125-137.

Haig, D.M., Deane, D.L., Myatt, N., Thomson, J., Entrican, G., Rothel, J., Reid, H.W. (1996a). The activation status of ovine CD45R+ and CD45R- efferent lymph T cells after orf virus reinfection. *Journal of Comparative Pathology* **115**: 163-174.

Haig, D.M., Hutchinson, G., Thomson, J., Yirrell, D., Reid, H.W. (1996b). Cytolytic activity and associated serine protease expression by skin and afferent lymph CD8+ T cells during orf virus reinfection. *Journal of General Virology* **77**: 953-961.

Haig, D., McInnes, C., Deane, D., Lear, A., Myatt, N., Reid, H., Rothel, J., Seow, H.F., Wood, P., Lyttle, D., Mercer, A. (1996c). Cytokines and their inhibitors in orf virus infection. *Veterinary Immunology and Immunopathology* **54**: 261-267.

Haig, D.M., McInnes, C.J., Hutchison, G., Seow, H.F., Reid, H.W. (1996d). Cyclosporin A abrogates the acquired immunity to cutaneous reinfection with the parapoxvirus orf virus.

Immunology **89**: 524-531.

Haig, D.M., Deane, D.L., Percival, A., Myatt, N., Thomson, J., Inglis, L., Rothel, J., Seow, H-F., Wood, P., Miller, H.R.P., Reid, H.W. (1996e). The cytokine response following orf virus reinfection of sheep. *Veterinary Dermatology* **7**: 11-20.

Haig, D.M., Fleming, S. (1999). Immunomodulation by virulence proteins of the parapoxvirus orf virus. *Veterinary Immunology and Immunopathology* **72**: 81-86.

Haig, D.M., McInnes, C., Deane, D., Reid, H., Mercer, A. (1997). The immune and inflammatory response to orf virus. *Comparative Immunology Microbiology and Infectious Diseases* **20**: 197-204.

Haig, D.M., McInnes, C.J., Thomson, J., Wood, A., Bunyan, K., Mercer, A. (1998). The orf virus OV20.0L gene product is involved in interferon resistance and inhibits an interferon-inducible, double-stranded RNA-dependent kinase. *Immunology* **93**: 335-340.

Haig, D.M., Mercer, A.A. (1998). Ovine diseases. Orf. *Veterinary Research* **29**: 311-326.

Haig, D.M., Percival, A., Mitchell, J., Green, I., Sargan, D. (1995a). The survival and growth of ovine afferent lymph dendritic cells in culture depends on tumour necrosis factor-alpha and is enhanced by granulocyte-macrophage colony-stimulating factor but inhibited by interferon-gamma. *Veterinary Immunology and Immunopathology* **45**: 221-236.

Haig, D.M., Hutchinson, G., Green, I., Sargan, D., Reid, H.W. (1995b). The effect of intradermal injection of GM-CSF and TNF-α on the accumulation of dendritic cells in ovine skin. *Veterinary Dermatology* **6**: 221-234.

Haig, D.M., Thomson, J., Percival, A. (1994). The in-vitro detection and quantitation of ovine bone marrow precursors of multipotential colony-forming cells. *Journal of Comparative Pathology* **111**: 73-85.

Haig, D.M.,Hopkins, J.,Miller, H.R. (1999). Local immune responses in afferent and efferent lymph. *Immunology*, **96**: 155-163.

Hall, J. G., Morris, B. (1962). The ouput of cells in lymph from the popliteal node of sheep. *Quarterly Journal of Experimental Physiology* 4**8**: 360.

Hall, M. (1976). Letter: Orf in Britain. *British Medical Journal* **2**: 420.

Harkness, J.W., Scott, A.C., Hebert, C.N. (1977). Electron microscopy in the rapid diagnosis of ORF. *British Veterinary Journal* **133**: 81-87.

Harp, J.A., Runnels, P.L., Pesch, B., Dean, E.A., Moon, H.W. (1988). Lymphocyte traffic in sheep - site of entry into lymph-nodes and modulation by anti-sheep lymphocyte Fab fragments. *FASEB Journal* **2**: A1258.

Health and Safety Executive. (1993) In: *Occupational Zoonoses.* H.M.S.O. London.

Heaney, M.L., Vera, J.C., Raines, M.A., Golde, D.W. (1995). Membrane-associated and soluble granulocyte/macrophage-colony-stimulating factor receptor alpha subunits are independently regulated in HL-60 cells. *Proceedings of the National Academy of Science USA* **92**: 2365-2369.

Hedger, R.S., Barnett, I.T., Gray, D.F. (1980). Some virus diseases of domestic animals in the Sultanate of Oman. *Tropical Animal Health and Production* **12**: 107-114.

Hein, W. R. (1995). Sheep as experimental animals in immunological research. *Immunologist* **3**: [1], 12-18.

Hein, W.R., Dudler, L., Mackay, C.R. (1989). Surface expression of differentiation antigens on lymphocytes in the ileal and jejunal Peyer's patches of lambs. *Immunology* **68**: 365-370.

Hein, W.R., Mackay, C.R. (1991). Other surface antigens identified on sheep leukocytes. *Veterinary Immunology and Immunopathology* **27**: 115-118.

Herrmann, T., Diamantstein, T. (1987). The mouse high affinity IL 2 receptor complex. I. Evidence for a third molecule, the putative gamma-chain, associated with the alpha- and/or beta-chain of the receptor. *Immunobiology* **175**: 145-158.

Hessami, M., Keney, D.A., Pearson, L.D., Storz, J. (1979). Isolation of parapox viruses from man and animals: cultivation and cellular changes in bovine fetal spleen cells. *Comparative Immunology Microbiology and Infectious Diseases* **2:** 1-7.

Heufler, C., Koch, F., Schuler, G. (1988a). GM-CSF (Granulocyte-macrophage colony stimulating factor) promotes the maturation of epidermal Langerhans cells into potent immunostimulatory dendritic cells-invitro. *Journal of Investigative Dermatology* **90**: 244.

Heufler, C., Koch, F., Schuler, G. (1988b). Granulocyte macrophage colony-stimulating

factor and interleukin-1 mediate the maturation of murine epidermal Langerhans cells into potent immunostimulatory dendritic cells. *Journal of Experimental Medicine* **167**: 700-705.

Himmelhoch, S. R. Chromatography of proteins on ion-exchange adsorbents. *Methods in Enzymology* **22**: 273-286. 1971.

Hiramatsu, Y., Uno, F., Yoshida, M., Hatano, Y., and Nii, S. (1999). Poxvirus virions: their surface ultrastucture and interaction with the surface membrane of host cells. *Journal of Electron Microscopy (Tokyo)* **48**: [6], 937-946.

Hiraoka, A., Masaoka, T., Mizoguchi, H., Asano, S., Kodera, Y., Kitamura, K., Takaku, F., Komemushi, S. (1994). Recombinant human non-glycosylated granulocyte-macrophage colony- stimulating factor in allogeneic bone marrow transplantation: double- blind placebo-controlled phase III clinical trial. *Japanese Journal of Clinical Oncology* **24**: 205-211.

Ho, C.K., Shuman, S. (1996). Physical and functional characterization of the double-stranded RNA binding protein encoded by the vaccinia virus E3 gene. *Virology* **217**: 272-284.

Hollos, I., Lovas, B. (1968). The ultrastructure of vaccinia virus growing in the embryonated egg. *Acta Morphologica Academiae Scientiarum Hungaricae* **15**: 269-284.

Hoover, D.M., Schalk-Hihi, C., Chou, C.C., Menon, S., Wlodawer, A., Zdanov, A. (1999). Purification of receptor complexes of interleukin-10 stoichiometry and the importance of deglycosylation in their crystallization. *European Journal of Biochemistry. 262*: 134-141.

Hopkins, J., Dutia, B.M. (1990). Monoclonal antibodies to the sheep analogues of human CD45 (leucocyte common antigen), MHC class I and CD5. Differential expression after lymphocyte activation in vivo. *Veterinary Immunology and Immunopathology* **24**: 331-346.

Hopkins, J., Dutia, B.M., McConnell, I. (1986). Monoclonal antibodies to sheep lymphocytes. I. Identification of MHC class II molecules on lymphoid tissue and changes in the level of class II expression on lymph-borne cells following antigen stimulation *in vivo*. *Immunology* **59**: 433-438.

Horan, T.P., Martin, F., Simonet, L., Arakawa, T., Philo, J.S. (1997). Dimerization of granulocyte-colony stimulating factor receptor: the Ig plus CRH construct of granulocyte-colony stimulating factor receptor forms a 2:2 complex with a ligand. *Journal of*

Biochemistry (Tokyo) **121**: 370-375.

Housawi, F.M., Roberts, G.M., Gilray, J.A., Pow, I., Reid, H.W., Nettleton, P.F., Sumption, K.J., Hibma, M.H., Mercer, A.A. (1998). The reactivity of monoclonal antibodies against orf virus with other parapoxviruses and the identification of a 39 kDa immunodominant protein. *Archives of Virology* **143**: 2289-2303.

Hsiao, J.C., Chung, C.S., Chang, W. (1999). Vaccinia virus envelope D8L protein binds to cell surface. *Journal of Virology*, **73**: 8750-8761.

Hsu, D.H., Malefyt, R.D., Fiorentino, D.F., Dang, M.N., Vieira, P., Devries, J., Spits, H., Mosmann, T.R., Moore, K.W. (1990). Expression of interleukin-10 activity by Epstein-Barr-virus protein bcrf1. *Science* **250**: 830-832.

Hu, B., Yasui, K. (1997). Effects of colony-stimulating factors (CSFs) on neutrophil apoptosis: possible roles at inflammation site. *International Journal of Hematology* **66**: 179-188.

Hu, F.Q., Smith, C.A., Pickup, D.J. (1994). Cowpox virus contains two copies of an early gene encoding a soluble secreted form of the type II TNF receptor. *Virology* **204**: 343-356.

Hunig, T. (1985). The cell surface molecule recognized by the erythrocyte receptor of T lymphocytes. Identification and partial characterization using a monoclonal antibody. *Journal of Experimental Medicine* **162**: 890-901.

Hunkapiller, M.W., Hewick, R.M., Dreyer, W.J., Hood, L.E. (1983). High-sensitivity sequencing with a gas-phase sequenator. *Methods in Enzymology* **91**: 399-413.

Inaba, K., Granellipiperno, A., Steinman, R.M. (1983). Dendritic cells induce lymphocytes-T to release B-cell-stimulating factors by an interleukin 2-dependent mechanism. *Journal of Experimental Medicine* **158**: 2040-2057.

Ink, B.S., Gilbert, C.S., Evan, G.I. (1995). Delay of vaccinia virus-induced apoptosis in nonpermissive Chinese hamster ovary cells by the cowpox virus CHOhr and adenovirus E1B 19K genes. *Journal of Virology* **69**: 661-668.

Isaacs, S.N., Kotwal, G.J., Moss, B. (1992). Vaccinia virus complement-control protein prevents antibody-dependent complement-enhanced neutralization of infectivity and

contributes to virulence. *Proceedings of the National Academy of Science USA* **89**: 628-632.

Itoh, K., Inoue, T., Ito, K., Hirohata, S. (1994). The interplay of interleukin-10 (IL-10) And interleukin-2 (IL-2) In humoral immune-responses - IL-10 synergizes with IL-2 to enhance responses of human B-lymphocytes in a mechanism which is different from up-regulation of CD25 expression. *Cellular Immunology* **157**: 478-488.

Jacques, Y., Lemauff, B., Boeffard, F., Godard, A., Soulillou, J.P. (1987). A soluble interleukin-2 receptor produced by a normal alloreactive human T-cell clone binds interleukin-2 with low affinity. *Journal of Immunology* **139**: 2308-2316.

Janeczko, R.A., Rodriguez, J.F., Esteban, M. (1987). Studies on the mechanism of entry of vaccinia virus in animal-cells. *Archives of Virology*, **92**: 135-150.

Janeway, C.A., Jr., Jones, B., Hayday, A. (1988). Specificity and function of T cells bearing gamma delta receptors. *Immunology Today* **9**: 73-76.

Jenkinson, D. M., Hutchison G, Onwuka, S. K., Reid, H. W. (1991). Changes in the MHC class II^+ dendritic cell population of ovine skin in response to orf virus infection. *Veterinary Dermatology* **2**: 1-12.

Jenkinson, D. M., Hutchison G, Reid, H. W. (1990a). The polymorphonuclear and mast cell responses in ovine skin infected with orf virus. *Veterinary Dermatology* **1**: 71-86.

Jenkinson, D. M., McEwan, P. E., Moss, V. A., Elder, H. Y., Reid, H. W. (1990b). Location and spread of orf virus antigen in infected ovine skin. *Veterinary Dermatology* **1**: 189-197.

Jenkinson, D. M., McEwan, P. E., Onwuka, S. K., Moss, V. A., Elder, H. Y., Hutchison G., Reid, H. W. (1990c). The pathological changes and polymorphonuclear and mast cell responses in the skin of pathogen free lambs following primary and secondary challenge with orf virus. *Veterinary Dermatology* **1**: 139-149.

Jenkinson, D. M., Hutchison G., Reid, H. W. (1992). The B and T cell responses to orf virus infection of ovine skin. *Veterinary Dermatology* **3**: 57-69.

Johannessen, J.V., Krogh, H.K., Solberg, I., Dalen, A., van Wijngaarden, H., Johansen, B. (1975). Human orf. *Journal of Cutaneous Pathology* **2**: 265-283.

Kanakura, Y., Cannistra, S.A., Brown, C.B., Nakamura, M., Seelig, G.F., Prosise, W.W.,

Hawkins, J.C., Kaushansky, K., Griffin, J.D. (1991). Identification of functionally distinct domains of human granulocyte-macrophage colony-stimulating factor using monoclonal antibodies. *Blood* **77**: 1033-1043.

Kanakura, Y., Sugahara, H., Mitsui, H., Ikeda, H., Furitsu, T., Yagura, H., Kitayama, H., Kanayama, Y., Matsuzawa, Y. (1993). Functional expression of interleukin 2 receptor in a human factor-dependent megakaryoblastic leukemia cell line: evidence that granulocyte-macrophage colony-stimulating factor inhibits interleukin 2 binding to its receptor. *Cancer Research* **53**: 675-680.

Kasahara, T., Hooks, J.J., Dougherty, S.F., Oppenheim, J.J. (1983). Interleukin 2-mediated immune interferon (IFN-gamma) production by human T cells and T cell subsets. *Journal of Immunology* **130**: 1784-1789.

Kates, J.R., McAuslan, B.R. (1967). Relationship between protein synthesis and viral deoxyribonucleic acid synthesis. *Journal of Virology* **1**: 110-114.

Kaushansky, K., Shoemaker, S.G., Alfaro, S., Brown, C. (1989). Hematopoietic activity of granulocyte/macrophage colony-stimulating factor is dependent upon two distinct regions of the molecule: functional analysis based upon the activities of interspecies hybrid growth factors. *Proceedings of the National Academy of Science USA* **86**: 1213-1217.

Kawagishi-Kobayashi, M., Cao, C., Lu, J., Ozato, K., Dever, T.E. (2000). Pseudosubstrate inhibition of protein kinase PKR by swine pox virus C8L gene product. *Virology* **276**: 424-434.

Khwaja, A., Carver, J., Jones, H.M., Paterson, D., Linch, D.C. (1993). Expression and dynamic modulation of the human granulocyte-colony- stimulating factor-receptor in immature and differentiated myeloid cells. *British Journal of Haematology* **85**: 254-259.

Kielian, T., Nagai, E., Ikubo, A., Rasmussen, C.A., Suzuki, T. (1999). Granulocyte/macrophage-colony-stimulating factor released by adenovirally transduced CT26 cells leads to the local expression of macrophage inflammatory protein 1alpha and accumulation of dendritic cells at vaccination sites in vivo. *Cancer Immunology and Immunotherapy* **48**: 123-131.

King, P.D., Katz, D.R. (1990). Mechanisms of dendritic cell function. *Immunology Today* **11**: 206-211.

Kisselev, A.F., von der Helm, K. (1994). Human immunodeficiency virus type 1 proteinase is rapidly and efficiently inactivated in human plasma by alpha 2-macroglobulin. *Biological Chemistry Hoppe-Seyler* **375**: 711-714.

Klement, V., Nicolson, M.O. (1977). Methods for Assays of RNA Tumour Viruses. In: *Methods in Virology* (edited by K.Maramorosch, H.Koprowski) pp 59-108, Academic Press Ltd., London.

Kluge, J.P., Cheville, N.F., Peery, T.M. (1972). Ultrastructural studies of contagious ecthyma in sheep. *American Journal of Veterinary Research* **33**: 1191-1200.

Kotwal, G.J. (2000). Poxviral mimicry of complement and chemokine system components: what's the end game? *Immunology Today* **21**: 242-248.

Kummeneje, K., Krogsrud, J. (1979). Contagious ecthyma (orf) in reindeer (Rangifer tarandus). *Veterinary Record* **105**: 60-61.

Kyhse-Andersen, J. (1984). Electroblotting of multiple gels: a simple apparatus without buffer tank for rapid transfer of proteins from polyacrylamide to nitrocellulose. *Journal of Biochemical and Biophysical Methods* **10**: 203-209.

Kyte, J., Doolittle, R.F. (1982). A simple method for displaying the hydropathic character of a protein. *Journal of Molecular Biology* **157**: 105-132.

Laemmli, U.K., Beguin, F., Gujer-Kellenberger, G. (1970). A factor preventing the major head protein of bacteriophage T4 from random aggregation. *Journal of Molecular Biology* **47**: 69-85.

Lalani, A.S., Graham, K., Mossman, K., Rajarathnam, K., Clark-Lewis, I., Kelvin, D., McFadden, G. (1997). The purified myxoma virus gamma interferon receptor homolog M-T7 interacts with the heparin-binding domains of chemokines. *Journal of Virology* **71**: 4356-4363.

Lalani, A.S., Masters, J., Graham, K., Liu, L., Lucas, A., McFadden, G. (1999a). Role of the myxoma virus soluble CC-chemokine inhibitor glycoprotein, M- T1: during myxoma virus pathogenesis. *Virology* **256**: 233-245.

Lalani, A.S., Masters, J., Zeng, W., Barrett, J., Pannu, R., Everett, H., Arendt, C.W.,

McFadden, G. (1999b). Use of chemokine receptors by poxviruses. *Science* **286**: 1968-1971.

Lalani, A.S., McFadden, G. (1997). Secreted poxvirus chemokine binding proteins. *Journal of Leukocyte Biology* **62**: 570-576.

Lalani, A.S., Ness,T.L., Singh, R., Harrison, J.K., Seet, B.T., Kelvin, D.J., McFadden, G., Moyer, R.W. (1998). Functional comparisons among members of the poxvirus T1/35kDa family of soluble CC-chemokine inhibitor glycoproteins. *Virology* **250**: 173-184.

Lampson,G.P., Tytell,A.A. (1965). A simple method for estimating isoelectric points. *Analytical Biochemistry* **11**: 374-377.

Lance,W.R., Hibler,C.P., DeMartini,J. (1983). Experimental contagious ecthyma in mule deer, white-tailed deer, pronghorn and wapiti. *Journal of Wildlife Disease* **19**: 165-169.

Lang, H. A. (1962). Human orf. *British Medical Journal* ii, 1566.

Lear, A. (1995). The characterisation of the ovine skin response to orf virus infection. *PhD Thesis*, University of Edinburgh .

Lear, A., Hutchison, G., Reid, H.W., Norval, M., Haig, D.M. (1996). Phenotypic characterisation of the dendritic cells accumulating in ovine dermis following primary and secondary orf virus infections. *European Journal of Dermatology* **6**: 135-140.

Leavell, U.W., McNamara, M.J., Muelling, R., Talbert, W.M., Rucker, R.C., Dalton, A.J. (1968). Orf. Report of 19 human cases with clinical and pathological observations. *Journal of the American Medical Association* **203**: 657-664.

Leong, S.R., Flaggs, G.M., Lawman, M.J., Gray, P.W. (1989). Cloning and expression of the cDNA for bovine granulocyte-macrophage colony-stimulating factor. *Veterinary Immunology and Immunopathology* **21**: 261-278.

Liu, Z.G., Haelens, A., Wuyts, A., Struyf, S., Pang, X.W., Proost, P., Chen, W.F., Van Damme, J. (1996). Isolation of a lymphocyte chemotactic factor produced by the murine thymic epithelial cell line MTEC1: identification as a 30 kDa glycosylated form of MCP-1. *European Cytokine Network* **7**: 381-388.

Livingston, G. W., Hardy, W. T. (1960). Longevity of contagious ecthyma virus. *Journal of the American Veterinary Medical Association* **137**: 651.

Lloyd, J.B., Gill, H.S., Haig, D.M., Husband, A.J. (2000). In vivo T-cell subset depletion suggests that CD4(+) T-cells and a humoral immune response are important for the elimination of orf virus from the skin of sheep. *Veterinary Immunology and Immunopathology* **74**: 249-262.

Lo, C., Mathisen, G. (1996). Human orf in Los Angeles County. *Western Journal of Medicine* **164**: 77-78.

Lober, C.W., Mendelsohn, H.E., Datnow, B., Fenske, N.A. (1983). Clinical and histologic features of orf. *Cutis* **32**: 142-147.

Loparev,V.N., Parsons, J.M., Knight, J.C., Panus, J.F., Ray, C.A., Buller, R.M., Pickup, D.J., Esposito, .J. (1998). A third distinct tumor necrosis factor receptor of orthopoxviruses. . *Proceedings of the National Academy of Science USA* **95**: 3786-3791.

Loubet, A., Leboutet, M.J., Pestre, M., Bonnetblanc, J.M., Loubet, R. (1980). Human orf disease. Ultrastructural study of six cases. *Archives of Anatomy Cytology and Pathology* **28**: 303-306.

Luttichau, H.R., Stine, J., Boesen, T.P., Johnsen, A.H., Chantry, D., Gerstoft, J., Schwartz, T.W. (2000). A highly selective CC chemokine receptor (CCR)8 antagonist encoded by the poxvirus molluscum contagiosum. *Journal of Experimental Medicine* **191**: 171-180.

Lyttle, D.J., Fraser, K.M., Fleming, S.B., Mercer, A.A., Robinson, A.J. (1994). Homologs of vascular endothelial growth factor are encoded by the poxvirus orf virus. *Journal of Virology* **68**: 84-92.

Mackay, C.R., Hein, W.R. (1989). A large proportion of bovine T cells express the gamma delta T cell receptor and show a distinct tissue distribution and surface phenotype. *International Immunology* **1**: 540-545.

Mackay, C.R., Hein, W.R., Brown, M.H., Matzinger, P. (1988). Unusual expression of CD2 in sheep: implications for T cell interactions. *European Journal of Immunology* **18**: 1681-1688.

Mackay, C.R., Beya, M.F., Matzinger, P. (1989). Gamma/delta T cells express a unique surface molecule appearing late during thymic development. *European Journal of*

Immunology **19**: 1477-1483.

Mackay, C.R., Maddox, J.F., Brandon, M.R. (1986). Three distinct subpopulations of sheep T lymphocytes. *European Journal of Immunology* **16**: 19-25.

Mackett, M., Archard, L.C. (1979). Conservation and variation in Orthopoxvirus genome structure. *Journal of General Virology* **45**: 683-701.

Martinez-Pomares, L., Thompson, J.P., Moyer, R.W. (1995). Mapping and investigation of the role in pathogenesis of the major unique secreted 35-kDa protein of rabbitpox virus. *Virology* **206**: 591-600.

Mathiesen, S.D., Jorgensen, T., Traavik, T., Blix, A.S. (1985). On contagious ecthyma and its treatment in muskoxen (Ovibos moschatus). *Acta Veterinaria Scandinavica* **26**: 120-126.

Matsudaira, P. (1987). Sequence from picomole quantities of proteins electroblotted onto polyvinylidene difluoride membranes. *Journal of Biological Chemistry* **262**: 10035-10038.

Mayr, A., Bachmann, P. A., Bibrack, B., Wittman, E. (1974). Zellkulturen, Bebrutete Huhnereier, Versuchtiere. In: *Virologische Arbeitsmethoden.* Gustav Fischer, Stuttgart.

McConahey, P.J., Dixon, F.J. (1980). Radioiodination of proteins by the use of the chloramine-T method. *Methods in Enzymology*. **70**: 210-213.

McElroy, M. (1997). Studies on the pathological and immunological responses of sheep to infection with orf virus. *PhD thesis*, University College Dublin.

McFadden, G., Graham, K., Ellison, K., Barry, M., Macen, J., Schreiber, M., Mossman, K., Nash, P., Lalani, A., Everett, H. (1995). Interruption of cytokine networks by poxviruses: lessons from myxoma virus. *Journal of Leukocyte Biology* **57**: 731-738.

McFadden, G., Lalani, A., Everett, H., Nash, P., Xu, X. (1998). Virus-encoded receptors for cytokines and chemokines. *Seminars in Cell and Developmental Biology* **9**: 359-368.

McFadden, G., Schreiber, M., Sedger, L. (1997). Myxoma T2 protein as a model for poxvirus TNF receptor homologs. *Journal of Neuroimmunology* **72**: 119-126.

McInnes, C., Haig, D., Logan, M. (1993). The cloning and expression of the gene for ovine interleukin-3 (multi-CSF) and a comparison of the in vitro hematopoietic activity of ovine

IL-3 with ovine GM-CSF and human M-CSF. *Experimental Hematology* **21**: 1528-1534.

McInnes, C.J., Deane, D., Thomson, J., Broad, A., Haig, D.M. (1999). The cloning and expression of the cDNA for ovine stem cell factor (kit-ligand) and characterization of its in vitro haematopoietic activity. *Cytokine* **11**: 249-256.

McInnes, C.J., Haig, D.M. (1991). Cloning and expression of a cDNA encoding ovine granulocyte-macrophage colony-stimulating factor. *Gene* **105**: 275-279.

McInnes, C.J., Logan, M., Haig, D., Wright, F. (1994). Cloning of a cDNA encoding ovine interleukin-3. *Gene* **139**: 289-290.

McInnes, C.J., Wood, A.R., Mercer, A.A. (1998). Orf virus encodes a homolog of the vaccinia virus interferon-resistance gene E3L. *Virus Genes* **17**: 107-115.

McInnes, C.J., Wood, A.R., Nettleton, P.F., Gilray, J.A. Genomic comparison of an avirulent strain of orf virus with that of a virulent wild type isolate, reveals that the orf virus G2L gene is non-essential for replication. *Virus Genes* (in press).

McKeever, D. J. (1986). Studies on the immunology and epidemiology of orf. *PhD Thesis,* University of Edinburgh.

McKeever, D.J., Reid, H.W. (1986a). Survival of orf virus under British winter conditions. *Veterinary Record* **118**: 613-614.

McKeever, D. J., Reid, H. W. (1986b). The ovine immune response to orf virus infection. *Proceedings of the Sheep Veterinary Society* **11**: 12-16.

McKeever, D. (1984). Persistent orf. *Veterinary Record* **115**: 334-335.

McKeever, D.J., Jenkinson, D.M., Hutchison, G., Reid, H.W. (1988). Studies of the pathogenesis of orf virus infection in sheep. *Journal of Comparative Pathology* **99**: 317-328.

McKeever, D.J., MacHugh, N.D., Goddeeris, B.M., Awino, E., Morrison, W.I. (1991). Bovine afferent lymph veiled cells differ from blood monocytes in phenotype and accessory function. *Journal of Immunology* **147**: 3703-3709.

McKeever, D.J., Reid, H.W. (1987). The response of the supramammary lymph node of the sheep to secondary infection with orf virus. *Veterinary Microbiology* **14**: 3-13.

McKeever, D.J., Reid, H.W., Inglis, N.F., Herring, A.J. (1987). A qualitative and quantitative assessment of the humoral antibody response of the sheep to orf virus infection. *Veterinary Microbiology* **15**: 229-241.

Melder, R.J., Koenig, G.C., Witwer, B.P., Safabakhsh, N., Munn, L.L., Jain, R.K. (1996). During angiogenesis, vascular endothelial growth factor and basic fibroblast growth factor regulate natural killer cell adhesion to tumor endothelium. *Nature Medicine* **2**: 992-997.

Menendez-Arias, L., Risco, C., Oroszlan, S. (1992). Isolation and characterization of alpha 2-macroglobulin-protease complexes from purified mouse mammary tumor virus and culture supernatants from virus-infected cell lines. *Journal of Biological Chemistry* **267**: 11392-11398.

Mercer, A., Fleming, S., Robinson, A., Nettleton, P., Reid, H. (1997a). Molecular genetic analyses of parapoxviruses pathogenic for humans. *Archives of Virology* Suppl **13**: 25-34.

Mercer, A.A., Yirrell, D.L., Whelan, E.M., Nettleton, P.F., Pow, I., Gilray, J.A., Reid, H.W., Robinson, A.J. (1997b). A novel strategy for determining protective antigens of the parapoxvirus, orf virus. *Virology* **229**: 193-200.

Mercer, A.A., Fraser, K., Barns, G., Robinson, A.J. (1987). The structure and cloning of orf virus DNA. *Virology* **157**: 1-12.

Mercer, A.A., Yirrell, D.L., Reid, H.W., Robinson, A.J. (1994). Lack of cross-protection between vaccinia virus and orf virus in hysterectomy-procured, barrier-maintained lambs. *Veterinary Microbiology* **41**: 373-382.

Mercer, A.A. Personal communication.

Meyer, M., Clauss, M., Lepple-Wienhues, A., Waltenberger, J., Augustin, H.G., Ziche, M., Lanz, C., Buttner, M., Rziha, H.J., Dehio, C. (1999). A novel vascular endothelial growth factor encoded by Orf virus, VEGF- E, mediates angiogenesis via signalling through VEGFR-2 (KDR) but not VEGFR-1 (Flt-1) receptor tyrosine kinases. *EMBO Journal* **18**: 363-374.

Mitchner, M. B. (1969). The envelope of vaccinia and orf viruses: an electron-cytochemical investigation. *Journal of General Virology* **5**: 211-220.

Moens, U., Wold, I., Mathiesen, S.D., Jorgensen, T., Sorensen, D., Traavik, T. (1990). Parapoxvirus papillomatosis in the muskoxen (Ovibos moschatus): genetical differences between the virus causing new outbreak in a vaccinated herd, the vaccine virus and a local orf virus. *Acta Veterinaria Scandinavica* **31**: 17-25.

Monfardini, C., Ramamoorthy, M., Rosenbaum, H., Fang, Q., Godillot, P.A., Canziani, G., Chaiken, I.M., Williams, W.V. (1998). Construction and binding kinetics of a soluble granulocyte-macrophage colony-stimulating factor receptor alpha-chain-Fc fusion protein. *Journal of Biological Chemistry* **273**: 7657-7667.

Moore, K. W., Vieira, P, Fiorentino, D. F., Trounstine, M. L., Khan, T. A., and Mosmann, T. R. (1990). Homology of cytokine synthesis inhibitory factor (IL-10) to the Epstein-Barr virus gene BCRF1. *Science* 248: 1230-1234.

Moore, D.M., MacKenzie, W.F., Doepel, F., Hansen, T.N. (1983). Contagious ecthyma in lambs and laboratory personnel. *Laboratory Animal Science* **33**: 473-475.

Moore, K.W., O'Garra, A., de Waal, M.R., Vieira, P., Mosmann, T.R. (1993). Interleukin-10. *Annual Review of Immunology* **11**: 165-190.

Moore, N.F., Patzer, E.J., Wagner, R.R., Yeagle, P.L., Hutton, W.C., Martin, R.B. (1977). The structure of vesicular stomatitis virus membrane. A phosphorus nuclear magnetic resonance approach. *Biochimica et Biophysica Acta* **464**: 234-244.

Moore, R.M. (1973). Human Orf in the United States, 1972. *Journal of Infectious Diseases* **127**: 731-732.

Morgan, C. (1976). Vaccinia virus reexamined: development and release. *Virology* **73**: 43-58.

Morgan, D.A., Ruscetti, F.W., Gallo, R. (1976). Selective in vitro growth of T lymphocytes from normal human bone marrows. *Science* **193**: 1007-1008.

Mosmann, T. R. (1994). Properties and functions of interleukin-10. *Advances in Immunology* 56: 1-25.

Mosmann, T.R., Moore, K.W. (1991). The role of IL-10 in cross-regulation of TH1 and TH2 responses. *Immunology Today* **12**: A49-A53.

Moss, B. (1996). Poxviridae; The viruses and their replication. In: *Fields Virology* 3rd edition. (edited by B. N. Fields) pp. 2637- 2672, Raven Publications, Philadelphia.

Moss, B. (1991). Vaccinia virus - a tool for research and vaccine development. *Science* **252**: 1662-1667.

Mossman, K., Lee, S.F., Barry, M., Boshkov, L., McFadden, G. (1996). Disruption of M-T5: a novel myxoma virus gene member of poxvirus host range superfamily, results in dramatic attenuation of myxomatosis in infected European rabbits. *Journal of Virology* **70**: 4394-4410.

Mossman, K., Upton, C., Buller, R.M., McFadden, G. (1995). Species specificity of ectromelia virus and vaccinia virus interferon- gamma binding proteins. *Virology* **208**: 762-769.

Mourtada, I., Le Tournuer, M., Chevrant-Breton, J., Le Gall, F. (2000). Human orf and erythema multiforme. *Annals of Dermatology and Venereology* **127**: 397-399.

Moyer, R.W., Graves, R.L. (1981). The mechanism of cytoplasmic orthopoxvirus DNA replication. *Cell* **27**: 391-401.

Mullbacher, A., Wallich, R., Moyer, R.W., Simon, M.M. (1999). Poxvirus-encoded serpins do not prevent cytolytic T cell-mediated recovery from primary infections. *Journal of Immunology* **162**: 7315-7321.

Munro, R., Gilmour, J., Nettleton, P., Buxton, D., Cornwell, C., Thompson, H., Mccandlish, I., Ross, H. (1988). Veterinarians and seals. *Veterinary Record* **123**: 451.

Munyon, W., Paoletti, E., Grace, J.T.J. (1967). RNA polymerase activity in purified infectious vaccinia virus. *Proceedings of the National Academy of Science USA* **58**: 2280-2287.

Murray, E.W., Pihl, C., Robbins, S.M., Prevost, J., Mokashi, A., Bloomfield, S.M., Brown, C.B. (1998). The soluble granulocyte-macrophage colony-stimulating factor receptor's carboxyl-terminal domain mediates retention of the soluble receptor on the cell surface through interaction with the granulocyte-macrophage colony-stimulating factor receptor beta-subunit. *Biochemistry* **37**: 14113-14120.

Nagington, J., Horne, N. W. (1962). Morphological studies of orf and vaccinia viruses. *Virology* **16**: 248-260.

Nagington, J., Newton, A. A., Horne, N. W. (1964). The structure of orf virus. *Virology* **23**: 461-472.

Nagington, J., Lauder, I.M., Smith, J.S. (1967). Bovine papular stomatitis, pseudocowpox and milker's nodules. *Veterinary Record* **81**: 306-313.

Nagington, J., Tee, G.H., Smith, J.S. (1965). Milker's nodule virus infections in Dorset and their similarity to orf. *Nature* **208**: 505-507.

Narhi, L.O., Philo, J.S., Li, T., Zhang, M., Samal, B., Arakawa, T. (1996). Induction of alpha-helix in the beta-sheet protein tumor necrosis factor-alpha: acid-induced denaturation. *Biochemistry* **35**: 11454-11460.

Nash, A.D., Andrews, A.E., Martin, H.M., Colditz, I.G., Wood, P.R., Seow, H.F. (1997). Neutrophil chemotaxis bioassay for the detection of IL-8. In: *Immunology Methods Manual.* (edited by I. Lefkovits) Section 3.13, Academic Press Ltd. London.

Nash, P., Lucas, A., McFadden, G. (1997). SERP-1: a poxvirus-encoded serpin, is expressed as a secreted glycoprotein that inhibits the inflammatory response to myxoma virus infection. *Advances in Experimental Medicine and Biology* **425**: 195-205.

Nelson, B.H., Willerford, D.M. (1998). Biology of the interleukin-2 receptor. *Advances in Immunology* **70**: 1-81.

Nettleton, P.F., Gilray, J.A., Yirrell, D.L., Scott, G.R., Reid, H.W. (1996a). Natural transmission of orf virus from clinically normal ewes to orf- naive sheep. *Veterinary Record* **139**: 364-366.

Nettleton, P.F., Brebner, J., Pow, I., Gilray, J.A., Bell, G.D., Reid, H.W. (1996b). Tissue culture-propagated orf virus vaccine protects lambs from orf virus challenge. *Veterinary Record* **138**: 184-186.

Okada, H.M., Okada, K., Numakunai, S., Ohshima, K. (1984). Electron microscopy on mucosal and cutaneous lesions in contagious papular dermatitis of Japanese Serow (*Capricornis crispus*). *Nippon Juigaku Zasshi* **46**: 297-302.

Okada, K., Fujimoto, Y. (1975). The fine structure of cytoplasmic inclusions and virus particles of bovine papular stomatitis. *Japanese Journal of Veterinary Research* **23**: 33-40.

Okamoto, M., Nakai, M., Nakayama, C., Yanagi, H., Matsui, H., Noguchi, H., Namiki, M., Sakai, J., Kadota, K., Fukui, M. (1991). Purification and characterization of three forms of differently glycosylated recombinant human granulocyte-macrophage colony- stimulating factor. *Archives of Biochemistry and Biophysics* **286**: 562-568.

Onetto-Pothier, N., Aumont, N., Haman, A., Park, L., Clark, S.C., De Lean, A., Hoang, T. (1990). IL-3 inhibits the binding of GM-CSF to AML blasts, but the two cytokines act synergistically in supporting blast proliferation. *Leukemia* **4**: 329-336.

Onwuka, S.K., Jenkinson, D.M., Inglis, L., Pow, I., Gray, E.W., Reid, H.W. (1995). Ultrastructural studies of orf virus-infection and replication in fetal lamb fibrocytes. *Veterinary Dermatology* **6**: 85-92.

Oswald, I.P., Lantier, F., Bourgy, G. (1990). Classical and alternative pathway haemolytic activities of ovine complement: variations with age and sex. *Veterinary Immunology and Immunopathology* **24**: 259-266.

Paiba, G.A., Thomas, D.R., Morgan, K.L., Bennett, M., Salmon, R.L., Chalmers, R., Kench, S.M., Coleman, T.J., Meadows, D., Morgan-Capner, P., Softley, P., Sillis, M., Green, L.E. (1999). Orf (contagious pustular dermatitis) in farmworkers: prevalence and risk factors in three areas of England. *Veterinary Record* **145**: 7-11.

Palatsi, R., Oksanen, A., Sormunen, R., Kallioinen, M., Karvonen, J. (1993). The first Orf virus epidemic diagnosed in man and reindeer in 1992-1993 in Finland. *Duodecim* **109**: 1945-1950.

Palumbo, G.J., Buller, R.M., Glasgow, W.C. (1994). Multigenic evasion of inflammation by poxviruses. *Journal of Virology* **68**: 1737-1749.

Park, L.S., Martin, U., Sorensen, R., Luhr, S., Morrissey, P.J., Cosman, D., Larsen, A. (1992). Cloning of the low-affinity murine granulocyte-macrophage colony- stimulating factor receptor and reconstitution of a high-affinity receptor complex. *Proceedings of the National Academy of Science USA* **89**: 4295-4299.

Pask, V. M., Mackerras, I. M., Sutherland, A. K., Simmons G. C. (1951). Transmission of

contagious ecthyma from sheep to man. *Medical Journal of Australia* **2**: 628-632.

Payne, L.G., Norrby, E. (1978). Adsorption and penetration of enveloped and naked vaccinia virus particles. *Journal of Virology* **27**: 19-27.

Pearse, A. G. E. (1980). The chemistry and practice of fixation. In: *Histochemistry, theoretical and applied.* 4th Edition. London, Churchill.

Perrin, G.O., Subramaniam, P.S., Johnson, H.M. (1999). Interleukin-10 (IL-10) directly inhibits the proliferation of CD4(+) cells at the level of the cell cycle by suppressing the MAP kinase cascade. *FASEB Journal* **13**: A654.

Pickup, D.J., Bastia, D., Stone, H.O., Joklik, W.K. (1982). Sequence of terminal regions of cowpox virus-DNA - arrangement of repeated and unique sequence elements. *Proceedings of the National Academy of Sciences USA* **79**: 7112-7116.

Plikaytis, B.D., Carlone, G.M., Edmonds, P., Mayer, L.W. (1986). Robust estimation of standard curves for protein molecular weight and linear-duplex DNA base-pair number after gel electrophoresis. *Analytical Biochemistry* **152**: 346-364.

Porteu, F., Nathan, C. (1990). Shedding of tumor-necrosis-factor receptors by activated human neutrophils. *Journal of Experimental Medicine* **172**: 599-607.

Pospischil, A., Bachmann, P.A. (1980). Nuclear changes in cells infected with parapoxviruses stomatitis papulosa and orf: an in vivo and in vitro ultrastructural study. *Journal of General Virology* **47**: 113-121.

Prideaux, C.T., Kumar, S., Boyle, D.B. (1990). Comparative analysis of vaccinia virus promoter activity in fowlpox and vaccinia virus recombinants. *Virus Research* **16**: 43-57.

Purdy, M. J. (1955). Orf. *New Zealand Medical Journal* 54: 572-575.

Pye, D. (1990). Vaccination of sheep with cell culture grown orf virus. *Australian Veterinary Journal* **67**: 182-186.

Raines, M.A., Liu, L., Quan, S.G., Joe, V., DiPersio, J.F., Golde, D.W. (1991). Identification and molecular cloning of a soluble human granulocyte-macrophage colony-stimulating factor receptor. *Proceedings of the National Academy of Science USA* **88**: 8203-8207.

Rapoport, A.P., Abboud, C.N., DiPersio, J.F. (1992). Granulocyte-macrophage colony-stimulating factor (GM-CSF) and granulocyte colony-stimulating factor (G-CSF) - receptor biology, signal transduction, and neutrophil activation. *Blood Reviews* **6**: 43-57.

Ray, C.A., Black, R.A., Kronheim, S.R., Greenstreet, T.A., Sleath, P.R., Salvesen, G.S., Pickup, D.J. (1992). Viral inhibition of inflammation: cowpox virus encodes an inhibitor of the interleukin-1 beta converting enzyme. *Cell* **69**: 597-604.

Reid, H. W. (1991). Orf. In: *Diseases of Sheep*. (edited by W.B.Martin) pp. 265-269 Blackwell Scientific Publications, Oxford.

Reid, H. W. (1999). Orf virus infection of sheep. *Moredun Foundation News* 3: 4.

Reisner, A.H. (1985). Similarity between the vaccinia virus 19k early protein and epidermal growth factor. *Nature* **313**: 801-803.

Reynaud, C.A., Garcia, C., Hein, W.R., Weill, J.C. (1995). Hypermutation generating the sheep immunoglobulin repertoire is an antigen-independent process. *Cell* **80**: 115-125.

Riske, F.J., Cullen, B.R., Chizzonite, R. (1991). Characterization of human interferon-gamma and human interleukin-2 from recombinant mammalian cell lines and peripheral blood lymphocytes. *Lymphokine Cytokine Research* **10**: 213-218.

Robbins,R.A., Klassen,L., Rasmussen,J., Clayton,M.E.M., Russ,W.D. (1986). Interleukin-2-induced chemotaxis of human T-lymphocytes. *Journal of Laboratory and Clinical Medicine* **108**: 340-345.

Robinson, A. J., Balassu, T. C. (1981). Contagious pustular dermatitis (orf). *The Veterinary Bulletin* **51**: [No.10], 771.

Robinson, A.J., Mercer, A.A. (1988). Orf virus and vaccinia virus do not cross-protect sheep. *Archives of Virology* **101**: 255-259.

Robinson, A.J., Mercer, A.A. (1995). Parapoxvirus of red deer: evidence for its inclusion as a new member in the genus parapoxvirus. *Virology* **208**: 812-815.

Robinson, R.A. (1983). Sheep and goat zoonoses. *Veterinary Clinics of North America [Large Animal Practice]* **5**: 711-717.

Rodriguez, J.F., Esteban, M. (1987). Mapping and nucleotide-sequence of the vaccinia virus gene that encodes a 14-kilodalton fusion protein. *Journal of Virology*, **61**: 3550-3554.

Romagnani, S. (1992). Induction of TH1 and TH2 responses: a key role for the 'natural' immune response? *Immunology Today* **13**: 379-381.

Romagnani, S. (1997). The Th1/Th2 paradigm. *Immunology Today* **18**: 263-266.

Romero-Mercado, C.H., McPherson, E.A., Laing, A.H., Lawson, J.B., Scott, G.R. (1973). Virus particles and antigens in natural orf. *Archiv fur Gesamte der Virusforsch* **40**: 159-160.

Rosel, J., Moss, B. (1985). Transcriptional and translational mapping and nucleotide-sequence analysis of a vaccinia virus gene encoding the precursor of the major core polypeptide 4b. *Journal of Virology* **56**: 830-838.

Rosenbusch, R.F., Reed, D.E. (1982). Comparisons between 2 isolates of stomatitis papulosa virus. *Veterinary Microbiology* **7**: 109-116.

Rosengard, A.M., Alonso, L.C., Korb, L.C., Baldwin, W.M., III, Sanfilippo, F., Turka, L.A., Ahearn, J.M. (1999). Functional characterization of soluble and membrane-bound forms of vaccinia virus complement control protein (VCP). *Molecular Immunology* **36**: 685-697.

Rosliakov, A.A. (1972). Comparative ultrastructure of viruses of camel pox, pox-like disease of camels ("auzdyk") and contagious ecthyma of sheep. *Voprosy Virusologii* **17**: 26-30.

Rossjohn, J., McKinstry, W.J., Woodcock, J.M., McClure, B.J., Hercus, T.R., Parker, M.W., Lopez, A.F., Bagley, C.J. (2000). Structure of the activation domain of the GM-CSF/IL-3/IL-5 receptor common beta-chain bound to an antagonist. *Blood* **95**: 2491-2498.

Ruef, C., Coleman, D.L. (1990). Granulocyte-macrophage colony-stimulating factor - pleiotropic cytokine with potential clinical usefulness. *Reviews of Infectious Diseases* **12**: 41-62.

Ryan-Poirier, K.A., Kawaoka, Y. (1993). Alpha 2-macroglobulin is the major neutralizing inhibitor of influenza A virus in pig serum. *Virology* **193**: 974-976.

Sainsbury, T., Ward, L. (1996). Parapoxvirus infection in red squirrels. *Veterinary Record* **138**: 400.

Sato, H., Nakayama, T., Tanaka, Y., Yamashita, M., Shibata, Y., Kondo, E., Saito, Y., Taniguchi, M. (1999). Induction of differentiation of pre-NKT cells to mature Valpha14 NKT cells by granulocyte/macrophage colony-stimulating factor. *Proceedings of the National Academy of Science USA* **96**: 7439-7444.

Savory, L.J., Stacker, S.A., Fleming, S.B., Niven, B.E., Mercer, A.A. (2000). Viral vascular endothelial growth factor plays a critical role in orf virus infection. Journal of Virology **74**: 10699-10706.

Sawhney, A.N., Toschkov, A. (1972). Cytopathogenicity of contagious pustular dermatitis virus in primary cell culture with special reference to the formation of intracytoplasmic inclusions. *Indian Journal of Experimental Biology* **10**: 234-235.

Schagger, H., Aquila, H., Von Jagow, G. (1988). Coomassie blue-sodium dodecyl sulfate-polyacrylamide gel electrophoresis for direct visualization of polypeptides during electrophoresis. *Analytical.Biochemistry* **173**: 201-205.

Schall, T.J. (1991). Biology of the RANTES/SIS cytokine family. *Cytokine* **3**: 165-183.

Schmidt, D., Hardy, W. T. (1932). Soremouth (contagious ecthyma) in sheep and goats. *Extension Agricultural Experiment Station Bulletin.* 457.

Schreiber, M., Sedger, L., McFadden, G. (1997). Distinct domains of M-T2: the myxoma virus tumor necrosis factor (TNF) receptor homolog, mediate extracellular TNF binding and intracellular apoptosis inhibition. *Journal of Virology* **71**: 2171-2181.

Schreiber, S.L., Crabtree, G.R. (1992). The mechanism of action of cyclosporin A and FK506. *Immunology Today* **13**: 136-142.

Schreuder, H., Tardif, C., Trump-Kallmeyer, S., Soffientini, A., Sarubbi, E., Akeson, A., Bowlin, T., Yanofsky, S., Barrett, R.W. (1997). A new cytokine-receptor binding mode revealed by the crystal structure of the IL-1 receptor with an antagonist. *Nature* **386**: 194-200.

Schwabe, M., Princler, G.L., Faltynek, C.R. (1988). Characterization of the human type I interferon receptor by ligand blotting. *European Journal of Immunology* **18**: 2009-2014.

Sedger, L., McFadden, G. (1996). M-T2: a poxvirus TNF receptor homologue with dual

activities. *Immunology and Cell Biology* **74**: 538-545.

Segel, L.A. (1976). Incorporation of receptor kinetics into a model for bacterial chemotaxis. *Journal of Theoretical Biology* **57**: 23-42.

Seifert, H.W., Saito, Y. (1977). Contagious ecthyma with virus demonstration in a negative staining method. *Hautarzt* **28**: 188-191.

Selbie, F. R. (1944). Experiments on the transmission to the rabbit of infectious labial dermatitis of sheep. *Veterinary Research Report*: Department of Agriculture, New South Wales. **6**: 109.

Senkevich, T.G., Koonin, E.V., Bugert, J.J., Darai, G., Moss, B. (1997). The genome of molluscum contagiosum virus: analysis and comparison with other poxviruses. *Virology* **233**: 19-42.

Seow, H.F., David, M.J., McWaters, P., Hurst, L., Wood, P.R. (1996). Cloning and sequencing of an ovine interleukin-5 cDNA. *DNA Sequence* **6**: 331-335.

Seow, H.F., Mucha, M.J., Hurst, L., Rothel, J.S., Wood, P.R. (1997). Expression of ovine interleukin-2 cDNA in *Escherichia coli*. *Veterinary Immunology and Immunopathology* **56**: 107-117.

Seow, H.F., Rothel, J.S., Radford, A.J., Wood, P.R. (1990). The molecular cloning of ovine interleukin 2 gene by the polymerase chain reaction. *Nucleic Acids Research* **18**: 7175-7175.

Seow, H.F., Rothel, J.S., Wood, P.R. (1993). Cloning and sequencing an ovine interleukin-4-encoding cDNA. *Gene* **124**: 291-293.

Seow, H.F., Yoshimura, T., Wood, P.R., Colditz, I.G. (1994). Cloning, sequencing, expression and inflammatory activity in skin of ovine interleukin-8. *Immunology and Cell Biology* **72**: 398-405.

Smith, C.A., Davis, T., Wignall, J.M., Din, W.S., Farrah, T., Upton, C., McFadden, G., Goodwin, R.G. (1991). T2 open reading frame from the Shope fibroma virus encodes a soluble form of the TNF receptor. *Biochemical and Biophysical Research Communications* **176**: 335-342.

Smith, C.A., Hu, F.Q., Smith, T.D., Richards, C.L., Smolak, P., Goodwin, R.G., Pickup, D.J. (1996). Cowpox virus genome encodes a second soluble homologue of cellular TNF receptors, distinct from CrmB, that binds TNF but not LT alpha. *Virology* **223**: 132-147.

Smith, G.L. (1993). Vaccinia virus glycoproteins and immune evasion. The sixteenth Fleming Lecture. *Journal of General Virology* **74**: (Pt 9), 1725-1740.

Smith, G.L. (1999). Vaccinia virus immune evasion. *Immunology Letters* **65**: 55-62.

Smith, G.L., Chan, Y.S. (1991). Two vaccinia virus proteins structurally related to the interleukin-1 receptor and the immunoglobulin superfamily. *Journal of General Virology* **72**: 511-518.

Smith, G.L., Symons, J.A., Khanna, A., Vanderplasschen, A., Alcami, A. (1997). Vaccinia virus immune evasion. *Immunological Reviews* **159**: 137-154.

Smith, G.L., Vanderplasschen, A. (1998). Extracellular enveloped vaccinia virus. Entry, egress, and evasion. *Advances in Experimental Medicine and Biology* **440**: 395-414.

Smith, V.P., Bryant, N.A., Alcami, A. (2000). Ectromelia, vaccinia and cowpox viruses encode secreted interleukin-18- binding proteins. *Journal of General Virology* **81**: 1223-1230.

Smith, W.B., Guida, L., Sun, Q., Korpelainen, E.I., Gillis, D., Hawrylowicz, C.M., Vadas, M.A., Lopez, A.F. (1995). Neutrophils activated by granulocyte-macrophage colony-stimulating factor express receptors for interleukin-3 which mediate class II expression. *Blood* **86**: 3938-3944.

Steinman, R.M. (1988). Cytokines amplify the function of accessory cells. *Immunology Letters* **17**: 197-202.

Stewart-Akers, A.M., Cairns, J.S., Tweardy, D.J., McCarthy, S.A. (1993). Effect of granulocyte-macrophage colony-stimulating factor on lymphokine-activated killer cell induction. *Blood* **81**: 2671-2678.

Stomski, F.C., Sun, Q., Bagley, C.J., Woodcock, J., Goodall, G., Andrews, R.K., Berndt, M.C., Lopez, A.F. (1996). Human interleukin-3 (IL-3) induces disulfide-linked IL-3 receptor alpha- and beta-chain heterodimerization, which is required for receptor activation but not

high-affinity binding. *Molecular Cell Biology* **16**: 3035-3046.

Sullivan, J.T., Fleming, S.B., Robinson, A.J., Mercer, A.A. (1995). Sequence and transcriptional analysis of a near-terminal region of the orf virus genome. *Virus Genes* **11**: 21-29.

Sullivan, J.T., Mercer, A.A., Fleming, S.B., Robinson, A.J. (1994). Identification and characterization of an orf virus homologue of the vaccinia virus gene encoding the major envelope antigen p37K. *Virology* **202**: 968-973.

Swain, S.L., Bradley, L.M., Croft, M., Tonkonogy, S., Atkins, G., Weinberg, A.D., Duncan, D.D., Hedrick, S.M., Dutton, R.W., Huston, G. (1991). Helper T-cell subsets: phenotype, function and the role of lymphokines in regulating their development. *Immunological Reviews* **123**: 115-144.

Symons, J.A., Duff, G.W. (1990). A soluble form of the interleukin-1 receptor produced by a human B cell line. *FEBS Letters* **272**: 133-136.

Symons, J.A., Eastgate, J.A., Duff, G.W. (1990). A soluble binding protein specific for interleukin 1 beta is produced by activated mononuclear cells. *Cytokine* **2**: 190-198.

Takatsu, K., Tominaga, A. (1991). Interleukin 5 and its receptor. *Progress in Growth Factor Research* **3**: 87-102.

Takatsu, K., Tominaga, A., Harada, N., Mita, S., Matsumoto, M., Takahashi, T., Kikuchi, Y., Yamaguchi, N. (1988). T cell-replacing factor (TRF)/interleukin 5 (IL-5): molecular and functional properties. *Immunological Reviews* **102**: 107-135.

Tan, S.T., Blake, G.B., Chambers, S. (1991). Recurrent orf in an immunocompromised host. *British Journal of Plastic Surgery* **44**: 465-467.

Tang, Q., Chen, W., Hendricks, R.L. (1997). Proinflammatory functions of IL-2 in herpes simplex virus corneal infection. *Journal of Immunology* **158**: 1275-1283.

Taniguchi, T., Minami, Y. (1993). The IL-2/IL-2 receptor system - a current overview. *Cell* **73**: 5-8.

Tarr, P.E. (1996). Granulocyte-macrophage colony-stimulating factor and the immune system. *Medical Oncology* **13**: 133-140.

Tartaglia, J., Winslow, J., Goebel, S., Johnson, G.P., Taylor, J., Paoletti, E. (1990). Nucleotide-sequence analysis of a 10.5 kbp HindIII fragment of fowlpox virus - relatedness to the central portion of the vaccinia virus HindIII D-region. *Journal of General Virology* **71**: 1517-1524.

Telford, E.A.R., Watson, M.S., Aird, H.C., Perry, J., Davison, A.J. (1995). The DNA-sequence of equine herpesvirus-2. *Journal of Molecular Biology* **249**: 520-528.

Tuschil, A., Lam, C., Haslberger, A., Lindley, I. (1992). Interleukin-8 stimulates calcium transients and promotes epidermal cell proliferation. *Journal of Investigative Dermatology* **99**: 294-298.

Upton, C., Macen, J.L., Schreiber, M., McFadden, G. (1991). Myxoma virus expresses a secreted protein with homology to the tumor necrosis factor receptor gene family that contributes to viral virulence. *Virology* **184**: 370-382.

Upton, C., Mossman, K., McFadden, G. (1992). Encoding of a homolog of the IFN-gamma receptor by myxoma virus. *Science* **258**: 1369-1372.

Vanderplasschen, A., Mathew, E., Hollinshead, M., Sim, R.B., Smith, G.L. (1998). Extracellular enveloped vaccinia virus is resistant to complement because of incorporation of host complement control proteins into its envelope. *Proceedings of the National Academy of Science USA* **95**: 7544-7549.

Vanham, G., Kestens, L., Vingerhoets, J., Penne, G., Colebunders, R., Vandenbruaene, M., Goeman, J., Ceuppens, J.L., Sugamura, K., Gigase, P. (1994). The interleukin-2 receptor subunit expression and function on peripheral-blood lymphocytes from HIV-infected and control persons. *Clinical Immunology and Immunopathology* **71**: 60-68.

Vazquez, M.I., Esteban, M. (1999). Identification of functional domains in the 14-kilodalton envelope protein (A27L) of vaccinia virus. *Journal of Virology* **73**: 9098-9109.

Verhagen, A.M., Andrews, A.E., Brandon, M.R., Nash, A.D. (1992). Molecular cloning, expression and characterization of the ovine IL-2R alpha chain. *Immunology* **76**: 1-9.

Verhagen, A.M., Kimpton, W.G., Nash, A.D. (1994). Development of a sandwich immunoassay for the detection of soluble ovine IL-2R alpha chain. *Veterinary Immunology and Immunopathology* **42**: 287-300.

Von Feldt, J.M., Monfardini, C., Kieber-Emmons, T., Voet, D., Weiner, D.B., Williams, W.V. (1994). Granulocyte-macrophage colony-stimulating factor mimicry and receptor interactions. *Immunologic Research* **13**: 96-109.

Wada, H., Noguchi, Y., Marino, M.W., Dunn, A.R., Old, L.J. (1997). T cell functions in granulocyte/macrophage colony-stimulating factor deficient mice. *Proceedings of the National Academy of Science USA* **94**: 12557-12561.

Waltenberger, J., Lange, J., Weich, H.A., Breier, G., Rockl, W., Clauss, M. (1996). Vascular endothelial growth factor and placenta growth factor stimulate monocyte activation and chemotaxis via the VEGF-receptor 1. *Circulation* **94**: 3475.

Walter, M.R., Windsor, W.T., Nagabhushan, T.L., Lundell, D.J., Lunn, C.A., Zauodny, P.J., Narula, S.K. (1995). Crystal structure of a complex between interferon-gamma and its soluble high-affinity receptor *Nature* **376**: 230-235.

Wang, B., Kondo, S., Shivji, G.M., Fujisawa, H., Mak, T.W., Sauder, D.N. (1996). Tumour necrosis factor receptor II (p75) signalling is required for the migration of Langerhans' cells. *Immunology* **88**: 284-288.

Wang, P., Wu, P., Anthes, J.C., Siegel, M.I., Egan, R.W., Billah, M.M. (1994). Interleukin-10 inhibits interleukin-8 production in human. *Blood* **83**: 2678-2683.

Ward, B.M., Moss, B. (2000). Golgi network targeting and plasma membrane internalization signals in vaccinia virus B5R envelope protein. *Journal of Virology* **74**: 3771-3780.

Wheeler, C. E., Cawley, E. P. (1956). The microscopic appearance of ecthyma contagiosum (orf) in sheep, rabbits and man. *Journal of Pathology* 3**2**: 535-545.

Wise, L.M., Veikkola, T., Mercer, A.A., Savory, L.J., Fleming, S.B., Caesar, C., Vitali, A., Makinen, T., Alitalo, K., Stacker, S.A. (1999). Vascular endothelial growth factor (VEGF)-like protein from orf. *Proceedings of the National Academy of Science USA* **96**: 3071-3076.

Wittek, R., Kuenzle, C.C., Wyler, R. (1979). High C + G content in parapoxvirus DNA. *Journal of General Virology* **43**: 231-234.

Wittek, R. (1982). Organization and expression of the poxvirus genome. *Experientia* **38**: 285-297.

Xing, Z., Gauldie, J., Tremblay, G.M., Hewlett, B.R., Addison, C. (1997). Intradermal transgenic expression of granulocyte-macrophage colony- stimulating factor induces neutrophilia, epidermal hyperplasia, Langerhans' cell/macrophage accumulation, and dermal fibrosis. *Laboratory Investigation* **77**: 615-622.

Yagisawa, M., Saeki, K., Okuma, E., Kitamura, T., Kitagawa, S., Hirai, H., Yazaki, Y., Takaku,F., Yuo, A. (1999). Signal transduction pathways in normal human monocytes stimulated by cytokines and mediators: comparative study with normal human neutrophils or transformed cells and the putative roles in functionality and cell biology. *Experimental Hematology* **27**: 1063-1076.

Yeh, H.P., Soltani, K. (1974). Ultrastructural studies in human orf. *Archives of Dermatology* **109**: 390-392.

Yirrell, D. L., Vestey, J. P. (1994). Human orf infections. *Journal of the European Academy of Dermatology and Venerealogy* **4**: 451-459.

Yirrell, D.L., Norval, M., Reid, H.W. (1994a). Local epidermal viral infections: comparative aspects of vaccinia virus, herpes simplex virus and human papillomavirus in man and orf virus in sheep. FEMS *Immunology and Medical Microbiology* **8**: 1-12.

Yirrell, D.L., Vestey, J.P., Norval, M. (1994b). Immune responses of patients to orf virus infection. *British Journal of Dermatology* **130**: 438-443.

Yirrell, D.L., Reid, H.W., Norval, M., Entrican, G., Miller, H.R. (1991). Response of efferent lymph and popliteal lymph node to epidermal infection of sheep with orf virus. *Veterinary Immunology and Immunopathology* **28**: 219-235.

Yirrell, D.L., Reid, H.W., Norval, M., Howie, S.E. (1989). Immune response of lambs to experimental infection with Orf virus. *Veterinary Immunology and Immunopathology* **22**: 321-332.

Yoshimura, T., Leonard, E.J. (1990). Secretion by human fibroblasts of monocyte chemoattractant protein-1: the product of gene JE. *Journal of Immunology* **144**: 2377-2383.

Zenke, G., Lokker, N.A., Strittmatter, U., Fagg, B., Geisse, S., Huber-Wegmann, G., Kocher, H.P. (1991). Purification and characterization of natural human interleukin-3. *Lymphokine*

and Cytokine Research **10**: 329-335.

Zhou, Q., Snipas, S., Orth, K., Muzio, M., Dixit, V.M., Salvesen, G.S. (1997). Target protease specificity of the viral serpin CrmA. Analysis of five caspases. *Journal of Biological Chemistry* **272**: 7797-7800.

APPENDIX

PUBLICATIONS ARISING FROM THIS THESIS

JOURNAL OF VIROLOGY, Feb. 2000, p. 1313–1320
0022-538X/00/$04.00+0

Vol. 74, No. 3

Orf Virus Encodes a Novel Secreted Protein Inhibitor of Granulocyte-Macrophage Colony-Stimulating Factor and Interleukin-2

DAVID DEANE,[1] COLIN J. McINNES,[1]* ANN PERCIVAL,[1] ANN WOOD,[1] JACKIE THOMSON,[1] ANDREA LEAR,† JANICE GILRAY,[1] STEPHEN FLEMING,[2] ANDREW MERCER,[2] AND DAVID HAIG[1]

Moredun Research Institute, International Research Centre, Penicuik, Scotland,[1] and HRC Virus Research Unit, University of Otago, Dunedin, New Zealand[2]

Received 2 August 1999/Accepted 4 November 1999

The parapoxvirus orf virus encodes a novel soluble protein inhibitor of ovine granulocyte-macrophage colony-stimulating factor (GM-CSF) and interleukin-2 (IL-2). The GM-CSF- and IL-2-inhibitory factor (GIF) gene was expressed as an intermediate-late viral gene in orf virus-infected cells. GIF formed homodimers and tetramers in solution, and it bound ovine GM-CSF with a K_d of 369 pM and ovine IL-2 with a K_d of 1.04 nM. GIF did not bind human GM-CSF or IL-2 in spite of the fact that orf virus is a human pathogen. GIF was detected in afferent lymph plasma draining the skin site of orf virus reinfection and was associated with reduced levels of lymph GM-CSF. GIF expression by orf virus indicates that GM-CSF and IL-2 are important in host antiviral immunity.

Poxviruses stimulate a vigorous immune response in their hosts. In spite of this, these viruses can replicate and induce lesions. A possible explanation for this is that poxviruses, along with other large DNA viruses, express immunomodulatory virulence proteins that inhibit or mimic key effector molecules of the host immune and inflammatory response to infection (35, 56, 57). A common general mechanism is the production of viral proteins inhibiting early events in the host response to infection, including inflammatory cytokine, interferon, chemokine, and complement function and apoptosis. Many of the immunomodulatory genes are orthologues of host cellular genes that have been acquired and modified by the viruses. For example, the orthopoxviruses vaccinia virus and cowpox virus encode soluble receptor proteins that bind to and inactivate the host cytokines interleukin-1β (IL-1β), tumor necrosis factor alpha (TNF-α), and interferons (IFNs) as well as complement components (1, 2, 8, 31, 50, 58, 62). Viral proteins that do not bind directly to IFNs but instead interfere with downstream signalling molecules following ligand-receptor coupling also inhibit the antiviral activity of interferons (10, 27, 44). By studying these viral immunomodulator proteins, insight into the mechanisms of not only virus virulence but also host protective immunity to virus infection is gained.

We have been studying the mechanisms of immune system evasion by the prototype parapoxvirus orf virus (contagious ecthyma virus). Orf virus is a ~140-kb double-stranded DNA (dsDNA) parapoxvirus that has a worldwide distribution and infects sheep, goats, and man (reviewed in references 26 and 49). Infections are acute, giving rise to pustular lesions that turn to scabs. Virus is contained locally and shed with the scab. The virus infects via broken or scarified skin and replicates in regenerating epidermal keratinocytes. The immune response to orf virus is characterized by a local accumulation of $CD4^+$ and $CD8^+$ T cells, B cells, neutrophils, and a dense network of dermal dendritic cells (32, 33, 38). Immune system evasion by orf virus is implicated because the virus can repeatedly infect previously exposed lambs in spite of an apparently normal host antivirus immune and inflammatory response (21–24, 64, 65). Host immunity has some effect, since the size of the lesions and the time to resolution in reinfections are diminished compared to those of the initial infection.

Most of the orf virus genome of 140 kbp has been sequenced. However, only 31 gene sequences (or partial gene sequences) spanning the genome are presently in the databases. Several putative immunomodulating genes have been discovered: a viral orthologue of mammalian vascular endothelial growth factor (VEGF) (40), a viral orthologue of IL-10 (16), and an orf virus orthologue of the vaccinia virus E3L gene, which codes for an interferon resistance protein (27, 44). In a study of cytokine production in orf virus-infected keratinocytes, IL-8, TNF-α, and granulocyte-macrophage colony-stimulating factor (GM-CSF) mRNAs and IL-8 and TNF-α protein, but not GM-CSF protein, were detected (37). In this article, we describe the isolation and characterization of a novel protein, GM-CSF-inhibitory factor (GIF), derived from a gene within the right terminal quarter of the orf virus genome, that binds to and inhibits the ovine cytokines GM-CSF and IL-2.

MATERIALS AND METHODS

Viruses. The orf virus strains NZ-2 (47), orf 11 (generated at the Moredun Research Institute [unpublished]), and scabbymouth (52) were tissue culture adapted from field isolates and were maintained by passage in primary bovine testis or fetal lamb muscle (FLM) cells. Semliki Forest virus was used as an unrelated virus control; it was maintained by passage in ST-6 ovine fibroblasts (12). MRI scab virus (45) was obtained by infection of sheep and harvesting of virus from the resultant scabs; it has not been adapted to grow in cell culture. Ovine primary keratinocytes were obtained, cultured, and characterized as described previously (37). Vaccinia virus-orf virus recombinants (VVOVs) containing approximately 95% of the orf virus genome in overlapping DNA fragments have been described previously (48) and were propagated in CV-1 cells in Dulbecco's modified Eagle's medium (DMEM) supplemented with 10% fetal bovine serum (FBS).

Lymph samples were from previous experiments (21, 23). In these experiments, scabbymouth virus was used to infect Suffolk cross sheep in the hind flank (i.e., the prefemoral lymph node drainage region) by scarification with a needle

* Corresponding author. Mailing address: Moredun Research Institute, International Research Centre, Pentlands Science Park, Bush Loan, Penicuik EH26 0PZ, Scotland, United Kingdom. Phone: 44 (0)131 445 5111. Fax: 44 (0)131 445 6111. E-mail: mcinc@mri.sari.ac.uk.

† Present address: Astra Clinical Research Unit, Edinburgh, Scotland.

and topical application of orf virus (10^6 50% tissue culture infective doses [$TCID_{50}$]). For controls, the virus was inactivated by UV irradiation (21) and the equivalent of ~10^6 $TCID_{50}$ of virus was injected intradermally into the hind flank. Cannulated pseudo-afferent lymph (herein referred to as afferent lymph) and efferent lymph samples were obtained from reinfected sheep as described previously (21, 23).

DNA and RNA techniques. dsDNA templates were sequenced by using a LI-COR 4200 automated DNA sequencing system and manufacturer-recommended procedures. Single-stranded DNA (ssDNA) templates were sequenced by using a T7 DNA Sequencing Kit (Amersham Pharmacia Biotechnology [APB], St. Albans, United Kingdom). Viral RNA was prepared from FLM cells, infected for 5 or 18 h with NZ2 orf virus at a multiplicity of infection (MOI) of 20 $TCID_{50}$, by an acid phenol-guanidine hydrochloride method (6). Cells were grown in the presence and absence of cytosine arabinoside (CA) (40 μg/ml), which inhibits viral DNA replication but not the expression of early viral genes (27). Preparation of dsDNA and ssRNA probes and Northern analysis were performed as described previously (44).

Expression and purification of recombinant GIF. A 908-bp DNA fragment containing the entire open reading frame (ORF) of the GIF gene was amplified by PCR with oligonucleotides 5′-GGAAAGCTTGCGCCGGCTCTAGGAAA GAT-3′ and 5′-GGGGAATTCAAGGATAAGGTCCACGGCGT-3′. The PCR product was ligated into the pEE14 expression vector (Celltech, Slough, United Kingdom) (7, 13) in tandem with a glutamine synthetase selectable marker gene and verified by sequencing prior to transfection into CHO cells by the use of Superfect transfection reagent (Qiagen, Crawley, United Kingdom) in accordance with the manufacturer's recommended procedures. The stable transfected CHO cells were maintained in glutamine-free Glasgow's modified Eagle's medium (Gibco BRL, Paisley, United Kingdom) supplemented with 7.5% heat-inactivated dialyzed FBS (PAA Laboratories, Kingston upon Thames, United Kingdom) and methionine sulfoxamine (an inhibitor of glutamine synthetase) (Sigma, Poole, United Kingdom) to select cells with high levels of production of GIF. GIF was purified from CHO cell-free supernatants (CFSs) (serum-free medium) by affinity chromatography with purified recombinant ovine GM-CSF (rovGM-CSF) bound to CNBr-Sepharose (APB) followed by gel filtration on a Sephacryl S-200 column (APB). The rabbit anti-GIF immunoglobulin G (IgG) was prepared by injecting affinity-purified GIF (10 μg) and 20 μg of Quil-A saponin adjuvant intramuscularly followed by two booster injections. An IgG fraction was prepared by protein A-Sepharose affinity chromatography. Western blot analysis of proteins was performed with phosphate-buffered saline (PBS) plus 4% nonfat milk (blocking buffer) and PBS (0.5 M NaCl) plus 0.5% Tween 80 (antibody dilution and blot wash buffer) by the enhanced chemiluminescence technique (ECL; APB). Proteins were electrotransferred (Schleicher & Schuell) to BA 83 nitrocellulose membranes (Anderman, Kingston upon Thames, United Kingdom).

N-terminal amino acid sequencing of the soluble recombinant protein was achieved by liquid-phase Edman degradation chemistry on a model 492 Procise Protein Sequencer (Perkin-Elmer Applied Biosystems, Warrington, Cheshire, United Kingdom). The purified protein was applied to a Polybrene-treated glass fiber filter prior to sequencing. The N-terminal 20 amino acids of two separate samples were analyzed.

Cytokines and GIF-binding assays. The recombinant ovine cytokines IL-1β, IL-2, IL-3, IL-4, IL-5, IL-8, GM-CSF, MCP-1, macrophage inflammatory protein 1α, RANTES, TNF-α, and IFN-γ were prepared by transfection of the cytokine cDNAs (from Ian Colditz, T. Yoshimura, Heng-Fong Seow, Paul Wood, J.-P. Scheerlink, and Paul Chaplin, CSIRO, Melbourne, Australia, and Gary Entrican, Moredun Research Institute) into CHO cells and purification of the recombinant proteins by fast protein liquid chromatography, anion-exchange chromatography, and/or gel filtration chromatography. Purified human (hu) and murine (mu) GM-CSF, huIL-2, and huIL-4 recombinant proteins produced in *Escherichia coli* were purchased from R&D Systems (Abington, United Kingdom). Heparin was purchased from Sigma.

For GIF-cytokine ligand blots, purified GIF was radioiodinated (^{125}I labelled) by the chloramine T method (42) and further purified on Sephadex G-25 and Sephacryl 200 HR (APB) columns in PBS with 0.15% (vol/vol) 3-[(3-cholamidopropyl)-dimethylammonio]-1-propanesulfonate (CHAPS) buffer, pH 7.2. Two hundred to 350 ng of each cytokine was separated by sodium dodecyl sulfate (SDS)–15% polyacrylamide gel electrophoresis (PAGE) under reducing and nonreducing conditions and then transferred to nitrocellulose membranes. The membranes were blocked in blocking buffer, washed in PBS plus 0.05% Tween 20 (wash buffer), and then incubated with ^{125}I-GIF (20 pM) for 2 h at room temperature. After the membranes were washed three times in wash buffer, cytokine-GIF binding was detected by autoradiography, using Hyperfilm MP X-ray film (APB). A 100 nM concentration of unlabeled ("cold") GIF was used for competitive inhibition of binding of ^{125}I-GIF to the cytokines.

GIF activity was assayed by inhibition of ovine (ov) GM-CSF detection in an ovGM-CSF capture enzyme-linked immunosorbent assay (ELISA) using two monoclonal murine antibodies: 8D8 as the capture antibody and horseradish peroxidase-conjugated 3C2 as the detection antibody (13). 1,2 Diaminobenzene and tetramethylbenzidine peroxidase substrates were used (determined by optical densities at 450 and 492 nm [OD_{450} and OD_{492}], respectively). Samples containing GIF and control samples were incubated (spiked) with either 4 or 8 ng of ovGM-CSF/ml (in 20-μl volumes) for 1 h at 37°C. These samples were then assayed by ovGM-CSF ELISA. Binding of GIF to ovGM-CSF results in the loss of antibody binding to ovGM-CSF and a reduction in ELISA optical density (OD). The specificity of the ovGM-CSF inhibition ELISA was demonstrated by preincubation of samples for 1 h at room temperature with the rabbit anti-GIF IgG prior to spiking of the mixture with ovGM-CSF and proceeding as described above. The antibody-GIF complex inhibits the binding of GIF to exogenously added ovGM-CSF, which is detected in the ELISA. This is not a quantitative assay for GIF. Cytokines were assayed for GIF binding by competition with ovGM-CSF in the ovGM-CSF ELISA. Cytokines (10 to 20 ng/ml) were added to GIF prior to the addition of 4 ng of ovGM-CSF/ml and subsequent ELISA.

Scatchard analysis of GIF reactivity. Purified cytokines were radioiodinated by the chloramine T method. A soluble-ligand-binding assay was performed for each cytokine as described by Symons et al. (61) with some modifications. Briefly, 50-μl volumes of a range of ^{125}I-GM-CSF and ^{125}I-IL-2 concentrations (2 to 20 nmol) were incubated with 100 μl of GIF (100 ng) containing 5% FBS for 2 h at room temperature. Bound proteins were precipitated by the addition of 300 μl of 20% polyethylene glycol (PEG 6000; Sigma) in PBS and incubation on ice for 30 min. The material precipitated from each sample was collected by filtering through GF/C filter discs (Whatman, Maidstone, United Kingdom) under a vacuum and washing with four 10-ml volumes of ice-cold 10% PEG 6000 in PBS. Radiolabelled complex was detected and quantified in a gamma scintillation counter (Cobra II Auto-Gamma Counter; Packard, Pangbourne, United Kingdom). The levels of nonspecific binding of ^{125}I-cytokines to the filters were obtained in the absence of GIF, and the data were adjusted accordingly. Scatchard analysis was performed on best-fit plots (bound counts per minute/free counts per minute [y axis] versus bound counts per minute [x axis]) generated by using Origin software (Microcal, Northampton, Mass.).

GIF bioassays. The soft-agar hematopoietic cell clonogenic assay has been described in detail elsewhere (25, 43). Briefly, sternal bone marrow cells (5×10^4/ml of culture) in Iscove's modification of DMEM (Gibco BRL) containing 20% FCS and 3% (vol/vol) Bacto Agar (Difco) were set up in 35-mm-diameter petri dishes. Dilutions of rovGM-CSF and rovIL-3 with and without dilutions of GIF were added, and the cultures were incubated in a highly humidified atmosphere of 5% CO_2 in air. Cell colonies (>40 cells) were analyzed on day 14 of culture.

GIF inhibition of ovIL-2 activity was measured in a T-cell proliferation assay. Briefly, mesenteric lymph node cells were enriched (>85%) for $CD4^+$ T cells by magnetic activated cell sorting (Miltenyi Biotec, Bergisch Gladbach, Germany) depletion of $CD8^+$, γδ T-cell receptor-positive, and B lymphocytes, using 7C2, 86D, and VPM8 (anti-light chain) antibodies, respectively (22). Lymphoblasts that developed after stimulation with 5 μg of concanavalin A (Sigma)/ml for 3 days were expanded in ovIL-2 or huIL-2 for 3 days. After the lymphoblasts were thoroughly washed with medium containing 2% FBS to remove IL-2, 100 μl of T-cell blasts at a density of 5×10^5/ml were added to each well of a 96-well plate (Costar). Additional 100-μl volumes containing a range of ovIL-2 dilutions (final concentration range, 10 pg/ml to 100 ng/ml) in Iscove's modification of DMEM with and without GIF were added to quadruplicate wells. After 24 h, the cells were pulsed with [^{3}H]thymidine (18.5 MBq/well) for a further 24 h before being harvested onto glass fiber sheets in a Micromate 196 cell harvester (Packard). Incorporated [^{3}H]thymidine in each sample was measured with a Matrix 96 direct beta counter (Packard).

Statistical analysis. Where appropriate, Student's t test was applied to data normalized by $\log_{10}$ transformation.

Nucleotide sequence accession number. The nucleotide sequence of the GIF cDNA has been deposited in the GenBank database under accession no. AF 192803.

RESULTS

Identification and isolation of the GIF gene. In preliminary studies, orf virus infection of ovine skin keratinocytes prior to a cytopathic effect occurring at around 20 to 24 h after infection stimulated ovGM-CSF mRNA expression. However, ovGM-CSF was at a low or undetectable level in cell lysates or CFSs as measured by ovGM-CSF ELISA. In contrast, the ovIL-8 and ovTNF-α cytokine concentrations increased in the same cultures. The ovGM-CSF inhibition was not due to proteolytic activity, since the addition of proteinase inhibitors to the CFSs did not result in ovGM-CSF detection (37).

To determine whether the ovGM-CSF inhibition was due to the product of a viral gene(s), FLM cells were infected with 18 VVOVs containing among them >95% of the NZ2 orf virus genome in overlapping fragments. CFSs were analyzed for ovGM-CSF inhibition by adding 4 ng of ovGM-CSF/ml and then testing for ovGM-CSF clearance by ELISA. VVOV 85, containing a ~10-kb DNA fragment from within the right terminal quarter of the orf virus genome, expressed ovGM-CSF-inhibitory activity. Subclones of this fragment in the

```
TCGGGTAAAAACGTACACCGTCGCCTTGTCGCGGCGGTGTACGCTTTTTTCACGCCCTTT   60

                                          M  A  C  L  R  V  F
TTGCAAAATTTAAATTGTACCCGCGCCGGCTCTAGGAAAGATGGCGTGCCTCAGAGTGTT  120

 L  A  V  L  A  L  C  G  S  V  H  S  A  Q  W  I  G  E  R  D
CCTGGCGGTGCTCGCGCTGTGCGGGAGCGTGCACTCGGCGCAATGGATCGGCGAGCGCGA  180

 F  C  T  A  H  A  Q  D  V  F  A  R  L  Q  V  W  M  R  I  D
CTTCTGCACGGCCCACGCGCAGGACGTCTTCGCGCGGCTGCAGGTGTGGATGCGCATTGA  240

 R  N  V  T  A  A  D  N  S  S  A  C  A  L  A  I  E  T  P  P
CCGGAACGTGACCGCCGCGGACAACAGCTCGGCCTGCGCGCTGGCGATAGAGACGCCGCC  300

 S  N  F  D  A  D  V  Y  V  A  A  A  G  I  N  V  S  V  S  A
GAGCAACTTCGACGCGGACGTCTACGTCGCCGCGGCCGGCATAAACGTCAGCGTGTCCGC  360

 I  N  C  G  F  F  N  M  R  Q  V  E  T  T  Y  N  T  A  R  R
GATCAACTGCGGCTTCTTCAACATGCGCCAGGTAGAGACGACGTACAACACGGCACGCCG  420

 Q  M  Y  V  Y  M  D  S  W  D  P  W  V  I  D  D  P  Q  P  L
GCAGATGTACGTGTACATGGACTCCTGGGACCCTTGGGTGATCGACGACCCCCAGCCGCT  480

 F  S  Q  E  Y  E  N  E  T  L  P  Y  L  L  E  V  L  E  L  A
CTTCAGCCAGGAGTACGAAAACGAAACGCTTCCGTACCTGCTGGAGGTTCTGGAGCTAGC  540

 R  L  Y  I  R  V  G  C  T  V  P  G  E  Q  P  F  E  V  I  P
GAGGCTGTACATTCGCGTGGGCTGCACGGTGCCCGGAGAGCAGCCCTTCGAGGTGATCCC  600

 G  I  D  Y  P  H  T  G  M  E  F  L  Q  H  V  L  R  P  N  R
GGGGATCGACTACCCGCACACCGGCATGGAGTTTCTCCAGCACGTTCTACGGCCGAACCG  660

 R  F  A  P  A  K  L  H  M  D  L  E  V  D  H  R  C  V  S  A
CCGGTTCGCTCCGGCGAAGCTGCACATGGACCTCGAGGTGGACCACCGGTGCGTGAGCGC  720

 V  H  V  K  A  F  L  Q  D  A  C  S  A  R  K  A  R  T  P  L
CGTCCACGTGAAGGCGTTCCTGCAGGACGCCTGTAGCGCCCGCAAGGCGCGGACGCCACT  780

 Y  F  A  G  H  G  C  N  H  P  D  R  R  P  K  N  P  V  P  R
CTACTTCGCGGGGCATGGCTGCAACCATCCAGATCGCCGGCCAAAAAACCCAGTACCGCG  840

 P  Q  H  V  S  S  P  I  S  R  K  C  S  M  Q  T  A  R
CCCTCAGCACGTATCGTCGCCGATCTCCAGGAAGTGCAGCATGCAGACGGCGCGCTAAGG  900

GCGCTCACCGCGCTGACGGCGGCCGTGGTGTGCGCGATCGCCATCGCGCTCGAGCGCGGG  960

GCGGAGGCCGACGCCGTGGACCTTATCCTTATAAAATT  998
```

FIG. 1. DNA sequence of, and predicted amino acid sequence encoded by, the NZ2 orf virus GIF cDNA. The entire GIF ORF together with 100 bases of flanking sequence on either side of the ORF is shown. The initiator methionine is 20.1 kb from the right terminus of the orf virus genome. The gene is transcribed toward this terminus. The mature secreted protein starts with Ala^{20}. The region containing potential transcription promoter and/or initiator sequences is underlined.

pEE14 mammalian expression vector were assayed as described above. A single ORF, located 20.1 kb from the right terminus of the viral genome that encoded GIF was identified. The sequence of the ORF plus 100 bases of flanking sequence on either side, as well as the predicted amino acid sequence of GIF, is shown in Fig. 1. The GIF gene is predicted to encode a 265-amino-acid (27.9-kDa) protein, the first 19 amino acids of which constitute a putative signal peptide. A comparison of the predicted GIF protein sequence with that of the vaccinia virus A41L gene product by the use of the Swiss-Prot (release 37.0) and TREMBL (release 10.0) databases revealed 32% amino acid similarity (over the entire protein) (17, 18, 55). Although the vaccinia virus A41L protein has sequence similarity to the T1 secreted chemokine-binding proteins of leporipoxviruses, its function is not known. Furthermore, a comparison of the GIF amino acid sequence with that of the Shope fibroma virus T1 protein did not reveal any similarity. The GIF gene sequences from orf 11 and MRI scab viruses were also obtained. These were predicted to encode proteins that were 98% identical to the NZ2 sequence. The GIFs of orf 11 and MRI scab viruses, expressed in CV-1 cells transfected with the GIF cDNAs, inhibited ovGM-CSF as detected by ELISA. Furthermore, NZ2, orf 11, and scabbymouth virus GIF activities were demonstrated in CFSs of virus-infected ovine keratinocyte cultures (Table 1).

TABLE 1. GIF activity in ovine keratinocytes infected with tissue culture-adapted orf virus strains[a]

Sample	OD_{492} (SEM)
NZ2 virus	0.032 (0.008)
Orf 11 virus	0.05 (0.002)
Scabbymouth virus	0.012 (0.004)
SFV control	0.62 (0.02)
Mock infection	0.86 (0.004)
ovGM-CSF, 4 ng/ml[b]	0.71 (0.03)

[a] Ovine primary keratinocytes were infected with each of the viruses at an MOI of 2 $TCID_{50}$/cell or were mock infected (control). Twenty-four hours later, CFSs were harvested. GIF activity was detected by adding 4 ng of ovGM-CSF/ml to the CFS samples and analyzing them by ovGM-CSF ELISA. Results are expressed as ELISA OD_{492} units. Semliki forest virus (SFV) was used as a control.

[b] ovGM-CSF in culture medium (not keratinocyte CFS).

The NZ2 GIF cDNA was expressed as a secreted protein in CHO cells. Recombinant GIF was purified by ovGM-CSF affinity chromatography and Sephacryl S-200 gel filtration (Fig. 2A). Sequence analysis of the 20 N-terminal amino acids of the secreted recombinant GIF revealed that the mature protein started with Ala^{20} (Fig. 1).

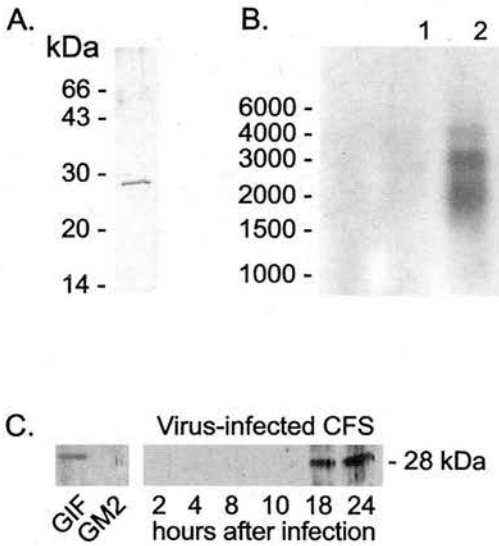

FIG. 2. Expression of recombinant and nonrecombinant GIF in virus-infected FLM cells. (A) Silver stain of recombinant GIF produced in CHO cells and purified by GM-CSF affinity chromatography followed by Sephacryl S-200 gel filtration. The positions of molecular mass markers are shown on the left. (B) Northern analysis of GIF mRNA expression in FLM cells at 18 h after infection with NZ2 virus at an MOI of 20 $TCID_{50}$ in the presence (lane 2) or absence (lane 1) of CA. Positions of RNA size markers (in bases) are indicated. (C) GIF expression in FLM CFSs at various times after infection with NZ2 (MOI = 2 $TCID_{50}$) in the absence of CA. Shown is a Western blot, prepared with rabbit anti-GIF, of samples subjected to SDS–15% PAGE. Recombinant GIF and GM2 (the product of an uncharacterized ORF adjacent to the GIF gene) were included as a positive and negative control, respectively. Both the recombinant and native GIFs are 28-kDa proteins.

GIF is an intermediate-late viral gene. In orf virus-infected cells in culture, progeny virions are detected at approximately 12 h after infection. Maximum titers are obtained between 24 and 72 h, concomitant with the virus-induced cytopathic effect (37). Using a DNA probe derived from sequence entirely within the GIF ORF, GIF mRNA was detected at 18 h after infection of FLM cells with orf virus in the absence of CA, an inhibitor of late viral gene expression and viral DNA replication (Fig. 2B). GIF mRNA was not detected at 5 h after infection of FLM cells in either the presence or the absence of CA. This demonstrated that the GIF gene was expressed as an intermediate or late, but not early, viral gene. The detection of multiple bands rather than a single mRNA also supports this conclusion, since the point at which intermediate and late poxvirus gene transcription stops can be heterogeneous (9, 41, 63). An equivalent ssRNA probe gave the same result as the DNA probe. Confirmation that the GIF gene was expressed as an intermediate or late viral gene was obtained by Western blot analysis of GIF protein production in FLM cells after virus infection, using the rabbit anti-GIF IgG. GIF was detected at 18 and 24 h after infection in CFSs (Fig. 2C).

GIF forms functional dimers and tetramers. During GIF purification it was observed that two peaks of GIF activity were separated by Sephacryl S-200 gel filtration. To determine whether GIF forms dimers and/or oligomers, purified recombinant ^{125}I-GIF was separated by S-200 gel filtration. Two ^{125}I-GIF peaks eluted from the column, at approximately 56- and 112-kDa-equivalent volumes (Fig. 3A). Both of these ^{125}I-GIF peaks contained ovGM-CSF-binding activity, as determined by ligand blot analysis (Fig. 3B). The 56- and 112-kDa GIF moieties correspond in mass to homodimers and tetramers, respectively, of 28-kDa GIF. There was no S-200 ^{125}I-GIF (or protein) peak at the elution point predicted for a GIF monomer mass of 28 kDa. Furthermore, each of the 56- and 112-kDa GIF moieties dissociated to the 28-kDa monomer form in the presence of SDS in PAGE performed under nonreducing conditions (Fig. 3C).

GIF binds ovGM-CSF and ovIL-2. Currently available ovine cytokines expressed in CHO cells, a selection of human and murine cytokines, and heparin were screened for the ability to bind GIF by the competitive ovGM-CSF inhibition ELISA. Only ovIL-2 inhibited the binding of GIF to ovGM-CSF (data not shown). Binding of GIF to ovGM-CSF and ovIL-2 was confirmed by a direct cytokine-GIF ligand blot assay (Fig. 4). Unlabelled (cold) GIF inhibited the binding of ^{125}I-GIF to ovGM-CSF and ovIL-2 (data not shown). The affinity binding of GIF to ovGM-CSF and ovIL-2 was determined by Scatchard analysis. GIF bound to ovGM-CSF with a K_d of 369 pM (range, 317 to 421 pM) and to ovIL-2 with a K_d of 1.04 nM (range, 0.961 to 1.124 nM). GIF therefore binds to ovGM-CSF with a higher affinity than it binds to ovIL-2. GIF did not bind to human or murine GM-CSF (Fig. 4a) or to human IL-2 (Fig. 4b). In the presence of SDS, GIF dimers and tetramers dissociated to the monomer form, which did not bind ^{125}I-ovGM-CSF or ^{125}I-ovIL-2 in SDS-PAGE ligand blot assays (data not shown).

GIF inhibits GM-CSF and IL-2 biological activities. Figure 5 shows that GIF inhibited the hematopoietic activity of ovGM-CSF, but not that of the control, IL-3, in the soft-agar bone marrow cell colony assay and that GIF inhibited the activity of ovIL-2 in the T-cell proliferation assay. Neutralization of GIF by rabbit anti-GIF prevented the inhibition of each of the cytokines in the assays.

GIF is produced in vivo during orf virus reinfection. To determine whether orf virus produces GIF in vivo, samples of cannulated afferent and efferent lymph draining the skin site

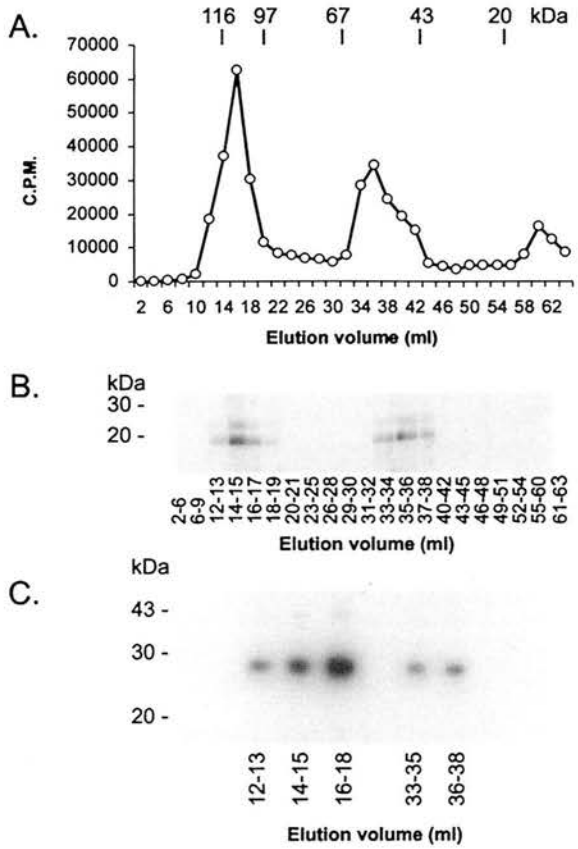

FIG. 3. GIF forms dimers and tetramers under physiological conditions. (A) Separation of ^{125}I-GIF on a Sephacryl S-200 column in 0.15% (vol/vol) CHAPS buffer at pH 7.4. Each fraction contained 1 ml of eluate. Two peaks of GIF eluted, with apparent molecular masses of ~112 and ~56 kDa. The arrows indicate the elution positions of protein standards (β-galactosidase, phosphorylase B, bovine serum albumin, ovalbumin, and chymotrypsinogen A) used to construct the molecular mass-versus-elution volume standard curve. (B) ovGM-CSF–GIF ligand blot showing the pooled and concentrated (10-fold) Sephacryl S-200 fractions of ^{125}I-GIF that bound to ovGM-CSF (19–21-kDa dimer), subjected to SDS–15% PAGE under nonreducing conditions and electrotransferred onto nitrocellulose strips. (C) Pooled and concentrated ^{125}I-GIF fractions from the S-200 column, subjected to SDS–15% PAGE under nonreducing conditions and revealed by autoradiography. Fractions 12 to 18 contained the 112-kDa GIF peak from the S-200 column, and fractions 33 to 38 were from the 56-kDa peak. All fractions showed a 28-kDa protein band. To the left of panels B and C are shown the positions of molecular mass markers.

(prefemoral lymph node drainage area) of orf virus reinfection from previous studies (21, 23) were analyzed for GIF activity by GM-CSF inhibition ELISA. Afferent lymph plasma from virus-infected sheep contained GIF (Fig. 6b). The presence of GIF was associated with reduced levels of GM-CSF in the lymph plasma (Fig. 6a). GIF was detected only in afferent lymph plasma samples from infected animals, not in those from control animals injected intradermally with UV-inactivated virus (data not shown). GIF was not detected in efferent lymph plasma or in CFSs from cultured afferent or efferent lymph cells. IL-2 was not tested for clearance by GIF because an IL-2-specific antibody was not available.

DISCUSSION

Poxviruses as a group encode a large number of immunomodulatory proteins that interfere with host immune and inflammatory responses to infection and, consequently, aid virus

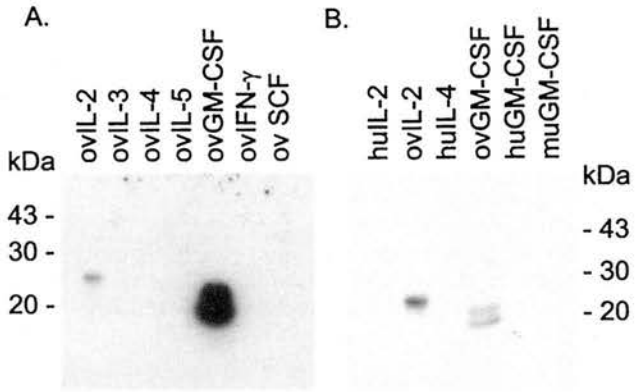

FIG. 4. GIF binding of ovGM-CSF and ovIL-2: ^{125}I-GIF–cytokine ligand blot analysis. ^{125}I-GIF was used to probe a range of ovine cytokines (A) and ovine, human, and murine cytokines (B) which were separated by SDS–15% PAGE and transferred to nitrocellulose membranes. ^{125}I-GIF bound to ovGM-CSF and ovIL-2. As a specificity control, 100 nM of unlabelled GIF was used to compete for ^{125}I-GIF binding to the cytokines. This inhibited ^{125}I-GIF binding to ovGM-CSF and ovIL-2. The positions of molecular mass markers are indicated.

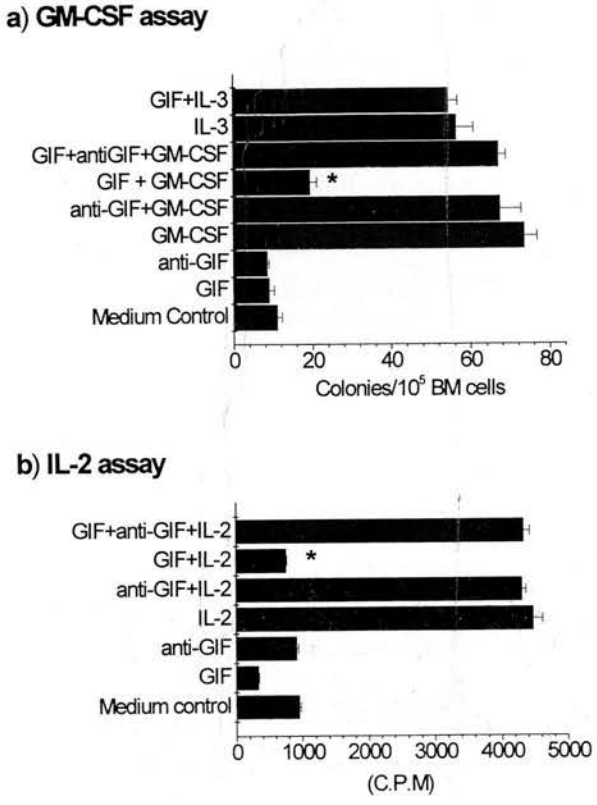

FIG. 5. GIF inhibits ovGM-CSF and ovIL-2 activities. (a) GIF inhibition of ovGM-CSF activity in the soft-agar bone marrow cell clonogenic assay. Colonies in triplicate cultures were counted on day 14 of culture, and the numbers were adjusted to represent the mean number of colonies, ± the standard error of the mean, that developed from 10^5 bone marrow cells plated on day zero. ovGM-CSF was used at 460 pg/ml; ovIL-3 and GIF were used at 520 and 50 ng/ml, respectively, based on dose-response experiments. (b) GIF inhibition of ovIL-2 activity in the 48-h T-cell proliferation assay. C.P.M., mean counts per minute of [^{3}H]thymidine incorporated into dividing cells in quadruplicate wells ± standard error of the mean. ovIL-2 and GIF were used at 40 and 100 ng/ml, respectively, based on dose-response experiments. *, $P < 0.002$ versus ovGM-CSF-stimulated colonies, (a) or IL-2-stimulated T-cell proliferation counts per minute (b).

replication. A proportion of these proteins bind to and inhibit cytokines that regulate the host response to infection. In this study, we isolated and characterized GIF, a novel cytokine-inhibitory protein encoded by several strains of the parapoxvirus orf virus.

GIF bound to and inhibited the biological function of ovGM-CSF and ovIL-2. GM-CSF is produced by a variety of cell types, including T cells. It stimulates neutrophil, monocyte, and eosinophil myelopoiesis and the recruitment and/or activation of these cell types in the tissues (46). GM-CSF is also involved in early events in immune responses, regulating the differentiation and function of antigen-presenting dendritic cells. IL-2 is a T-cell-derived lymphokine that stimulates T-cell and NK cell activation and proliferation and activated-B-cell proliferation (15). This is the first description, to our knowledge, of a microbial inhibitory protein for GM-CSF or for both GM-CSF and IL-2. huIL-2 was bound by a 38-kDa protein, encoded by tanapox virus, a poxvirus pathogen of primates, which was secreted from infected cells and bound huIL-5 and huIFN-γ (14). The ability to bind and inactivate multiple, sometimes apparently unrelated cytokines is a property of some poxvirus proteins and represents an economical way of controlling host immunity. Another example of such a protein is the M-T7 gene product of myxoma virus, which inhibited rabbit IFN-γ and CXC, CC, and C family chemokines (36). The chemokine binding was via a conserved chemokine heparin-binding domain. The binding of GIF to both GM-CSF and IL-2 indicates the existence of a binding domain(s) shared by both cytokines. A comparison of the ovGM-CSF and ovIL-2 sequences did not reveal any obvious common feature other than the fact that both GM-CSF and IL-2 are members of the short-chain, four-α-helical-bundle family of cytokines that also includes IL-4. However, ovIL-4 did not bind to GIF. Interestingly, GM-CSF has been shown to compete with IL-2 for binding to IL-2 receptors on the myeloid leukemia cell line MO7E (34), indicating that there may be a common receptor-binding domain in huGM-CSF and huIL-2.

Many of the viral cytokine-binding proteins are orthologues of host cytokine receptor molecules. GIF has no counterpart in the amino acid sequence databases. This may be because the ovGM-CSF receptor proteins have not been characterized. The human and murine cellular GM-CSF receptors consist of a low-affinity-binding α subunit that is specific for GM-CSF and a β subunit that is common to GM-CSF, IL-3, and IL-5 receptors (51). Cross-linking of the α and β subunits gives rise to a high-affinity binding site for GM-CSF. The IL-2 receptor (IL2R) consists of α, β, and γ chains. The α subunit (p55) has a low affinity for IL-2 but forms a high-affinity IL-2-binding site when cross-linked with the β and γ subunits (60). The ovIL-2R α chain has been cloned and sequenced (5), but there are no regions of homology between this sequence and GIF. There is a natural secreted form of the IL-2R α subunit and evidence of secreted forms of the IL-2R β and γ subunits (11, 30). All of these subunits have a low affinity for IL-2.

The only other natural inhibitor of GM-CSF described to date is a posttranslationally modified secreted form of the GM-CSF receptor alpha chain (GMRα) (3, 29, 53). The secreted form of GMRα was produced by myeloid but not lymphoid cell lines, and it bound ligand with a K_d of 3.8 nM (3, 29). Both GIF and GMRα form oligomers in solution in the absence of ligand (this study and reference 4). However, GIF bound ovGM-CSF with a 10-fold-higher affinity than GMRα bound huGM-CSF (K_d, 369 and 3.8 nM, respectively). In addition, GIF dimers and tetramers bound ovGM-CSF, whereas the monomer of the multimeric forms of GMRα exhibited the

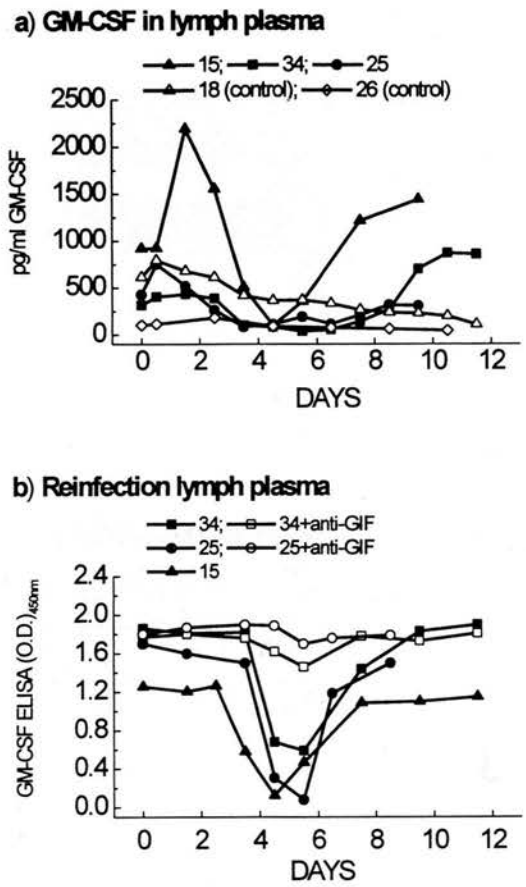

FIG. 6. GIF and ovGM-CSF in virus reinfection and control afferent lymph plasma. (a) GM-CSF concentrations in afferent lymph plasma samples from reinfected and control sheep. Control sheep (no. 18 and 26) received UV-inactivated virus intradermally. (b) Detection of GIF, by ovGM-CSF inhibition ELISA, in afferent lymph plasma samples obtained at various times after orf virus reinfection of sheep 15, 25, and 34 on day zero. Lymph plasma samples were spiked with 8 ng of GM-CSF/ml (4 ng/ml for sheep 15 samples, hence the lower OD) and analyzed for GM-CSF by ELISA. Rabbit anti-GIF was used as a specificity control to neutralize GIF in the assay.

highest-affinity binding of huGM-CSF (4). We did not observe binding of ^{125}I-ovGM-CSF or ^{125}I-ovIL-2 to the 28-kDa GIF monomer in SDS-PAGE ligand blot assays.

However, the lack of homology to host cytokine receptors by viral cytokine-binding proteins is not without precedent. The 35-kDa virulence proteins of variola and cowpox viruses inhibit β-chemokines but have no sequence homology to known proteins (54). The B18R gene product of vaccinia virus binds IFN-α/β but is in a protein superfamily different from that of known host IFN-α/β receptor proteins (62). It is possible that in the coevolution of virus and host, radical modification of the acquired host gene occurred such that the host and virus proteins no longer resemble each other except for short stretches of sequence that are important for ligand binding. Viral genome sizes for different families of viruses tend to be critically controlled. The ability to acquire host genes and modify them to produce minimally sized immunomodulatory proteins that inhibit one, or preferably several, important immune effector molecules has a clear advantage with regard to survival of the virus.

After orf virus reinfection of sheep, GIF was detected in afferent lymph plasma samples that had low levels of ovGM-CSF. Coupled with the fact that GIF was detected only in the afferent lymph plasma and not in cultured afferent lymph CFS, this demonstrated that GIF is produced from virus-infected epidermal cells and has in vivo relevance. The inability to detect GIF in efferent lymph plasma indicates that GIF either does not pass through the lymph node into efferent lymph or is diluted out by the large volume of efferent lymph plasma carrying lymphocytes derived from the blood via high endothelial venules (for a review of lymph, refer to reference 28). The time at which GIF was detected in afferent lymph corresponded to the period of maximum viral replication in the epidermis of the cannulated sheep, which occurred between 5 and 7 days after reinfection (21).

We can only speculate the function of GIF in orf virus infection. ovGM-CSF and ovIL-2 mRNAs have been detected in skin biopsy specimens obtained during orf virus reinfection (24). ovGM-CSF and ovIL-2 have been detected in afferent and efferent lymph after orf virus reinfection (21, 22). The principal source of these cytokines in both lymph compartments is the $CD4^+$ T cell. $CD4^+$ T cells, in particular of the lymphocyte subsets, accumulate in large numbers adjacent to and underlying orf virus-infected cells in sheep skin. IL-2 and IFN-γ have been implicated in protective immunity to orf virus reinfection (21, 24, 37, 39). The role of GM-CSF is less clear. GM-CSF is involved in the activation of neutrophils and macrophages, both of which are present in orf lesions. Macrophage colony-stimulating factor (M-CSF; CSF-1), granulocyte colony-stimulating factor, and IL-3 are also hematopoietic growth factors that support the development and activation of neutrophils and macrophages. Recently, an M-CSF-inhibitory protein encoded by the Epstein-Barr virus *BARF1* gene was identified (59). The *BARF1* product has sequence homology to the M-CSF receptor protein (c-fms). The function of macrophages in orf or Epstein-Barr virus infection is not clear. However, GM-CSF also regulates antigen presentation by dendritic cells, and this would be a useful point of intervention for viral immunomodulator proteins. We have previously shown that ovGM-CSF and ovTNF-α are involved in the recruitment of dendritic cells to the ovine dermis (19) and in supporting the survival and proliferation of afferent lymph veiled dendritic cells in culture (20). The inhibition of GM-CSF in the vicinity of orf virus-infected epidermal keratinocytes could affect dendritic cell function. Ovine keratinocytes in culture produce ovGM-CSF both constitutively and after stimulation with phorbol ester and calcium ionophore (37). A role for GIF in aiding virus replication in infected keratinocytes must also be considered.

ovGM-CSF and ovIL-2 were bound by GIF, whereas huGM-CSF, muGM-CSF, and huIL-2 were not. In the broader context, the orf virus IL-10 and VEGF protein sequences are most homologous to those of ovIL-10 and ovVEGF, respectively (16, 40). Taken together, these data demonstrate that orf virus has adapted to sheep, rather than man, as its principal host. Orf virus lesions in man are grossly similar to those in sheep, but they have not been studied in the same detail. The consequences (if any) of orf virus immunomodulatory proteins that are active in sheep but not active in man are of interest but are not known.

Except for GIF, the parapoxvirus immunomodulatory proteins discovered so far are all the products of early viral genes. GIF was expressed as an intermediate-late viral gene. orf virus expression of vIL-10 (16), the orf virus interferon resistance protein (27, 44), and GIF represents a coordinated interference with host inflammatory and type 1 immune responses to virus infection. This suggests that GM-CSF, along with IFN-γ,

IFN-α/β, and IL-2, are important in host immunity to orf virus (24).

GIF, a protein with unusual properties, is part of a growing number of pathogen immunomodulators that will be useful not only in determining mechanisms of viral pathogenesis and the nature of host antipathogen immunity but also as templates for potentially therapeutic proteins or peptides.

ACKNOWLEDGMENTS

David Deane and Colin McInnes contributed equally to this work.

We thank the following individuals for intellectual and/or material help with this project: Mary Norval and Hugh Miller, Edinburgh University; Peter Nettleton, Hugh Reid, and Gary Entrican, Moredun Research Institute; and Ian Colditz and Paul Chaplin, CSIRO, Melbourne, Australia.

The Scottish Executive for Rural Affairs Department (SERAD) funded this work.

REFERENCES

1. **Alcamí, A., and G. L. Smith.** 1992. A soluble receptor for interleukin-1β encoded by vaccinia virus: a novel mechanism of virus modulation of the host response to infection. Cell **71:**153–167.
2. **Alcamí, A., and G. L. Smith.** 1995. Vaccinia, cowpox, and camelpox viruses encode soluble gamma interferon receptors with novel broad species specificity. J. Virol. **69:**4633–4639.
3. **Brown, C. B., P. Beaudry, T. D. Laing, S. Shoemaker, and K. Kaushansky.** 1995. *In vitro* characterisation of the human recombinant soluble granulocyte-macrophage colony-stimulating factor receptor. Blood **85:**1488–1495.
4. **Brown, C. B., C. E. Pihl, and E. W. Murray.** 1997. Oligomerization of the soluble granulocyte-macrophage colony-stimulating factor receptor: identification of the functional ligand-binding species. Cytokine **9:**219–225.
5. **Bujdoso, R., D. Sargan, M. Williamson, and I. McConnell.** 1992. Cloning of a cDNA encoding the ovine interleukin-2 receptor 55-kDa protein, CD25. Gene **113:**283–284.
6. **Chomczynski, P., and N. Sacchi.** 1987. Single step method of RNA isolation by acid guanidinium thiocyanate-phenol-chloroform extraction. Anal. Biochem. **162:**156–159.
7. **Cockett, M. I., C. R. Bebbington, and G. T. Yarrington.** 1990. High level expression of tissue inhibitor metalloproteinases in Chinese hamster ovary cells using glutamine synthetase gene amplification. Bio/Technology **8:**662–667.
8. **Colamonici, O. R., P. Domanski, S. M. Sweitzer, A. Larner, and R. M. L. Buller.** 1995. Vaccinia virus B18R gene encodes a type 1 interferon-binding protein that blocks interferon-α transmembrane signalling. J. Biol. Chem. **270:**15974–15978.
9. **Cooper, J. A., and B. Moss.** 1979. *In vitro* translation of immediate early, early and late classes of RNA from vaccinia virus-infected cells. Virology **96:**368–380.
10. **Davies, M. V., H.-W. Chang, B. L. Jacobs, and R. J. Kaufman.** 1993. The E3L and K3L vaccinia virus gene products stimulate translation through inhibition of the double-stranded RNA-dependent protein kinase by different mechanisms. J. Virol. **67:**1688–1692.
11. **Dummer, R., G. Posseckert, K. Sugamura, H. Grundmann, and G. Burg.** 1996. Circulating interleukin-2 receptors are a group of multimeric proteins with immunoreactivity for interleukin-2 receptor alpha, beta and gamma chains. J. Interferon Cytokine Res. **16:**315–320.
12. **Entrican, G., D. M. Haig, and M. Norval.** 1989. Identification of ovine interferons: differential activities derived from fibroblast and lymphoid cells. Vet. Immunol. Immunopathol. **21:**187–195.
13. **Entrican, G., D. Deane, M. MacLean, L. Inglis, J. Thomson, C. McInnes, and D. M. Haig.** 1996. Development of a sandwich ELISA for ovine granulocyte macrophage-colony stimulating factor. Vet. Immunol. Immunopathol. **50:**287–298.
14. **Essani, K., S. Chalasani, R. Eversole, L. Beuving, and L. Birmingham.** 1994. Multiple anti-cytokine activities secreted from tanapox virus-infected cells. Microb. Pathog. **17:**347–353.
15. **Farner, N. L., J. A. Hank, and P. M. Sondel.** 1997. Interleukin-2: molecular and clinical aspects, p. 29–41. *In* D. G. Remick and J. S. Friedland (ed.), Cytokines in health and disease, 2nd ed. Marcel Dekker, Ann Arbor, Mich.
16. **Fleming, S. B., C. A. McCaughan, A. E. Andrews, A. D. Nash, and A. A. Mercer.** 1997. A homolog of interleukin-10 is encoded by the poxvirus orf virus. J. Virol. **71:**4857–4861.
17. **Goebel, S. J., G. P. Johnson, M. E. Perkus, S. W. Davis, J. P. Winslow, and E. Paoletti.** 1990. The complete DNA sequence of vaccinia virus. Virology **179:**247–266.
18. **Goebel, S. J., G. P. Johnson, M. E. Perkus, S. W. Davis, J. P. Winslow, and E. Paoletti.** 1990. The complete DNA sequence of vaccinia virus. Virology **179:**517–563.
19. **Haig, D. M., G. Hutchison, I. Green, D. Sargan, and H. W. Reid.** 1995. The effect of intradermal injection of GM-CSF and TNF-α on the accumulation of dendritic cells in ovine skin. Vet. Dermatol. **6:**211–220.
20. **Haig, D. M., A. Percival, J. Mitchell, I. Green, and D. Sargan.** 1995. The survival and growth of ovine afferent lymph dendritic cells in culture depends on tumour necrosis factor-α and is enhanced by granulocyte-macrophage colony-stimulating factor but inhibited by interferon-γ. Vet. Immunol. Immunopathol. **45:**221–236.
21. **Haig, D. M., D. L. Deane, A. Percival, N. Myatt, J. Thomson, L. Inglis, J. Rothel, H.-F. Seow, P. Wood, H. R. P. Miller, and H. W. Reid.** 1996. The cytokine response of afferent lymph following orf virus reinfection of sheep. Vet. Dermatol. **7:**11–20.
22. **Haig, D. M., G. Hutchison, J. Thomson, D. Yirrell, and H. W. Reid.** 1996. Cytolytic activity and associated serine protease expression by skin and afferent lymph $CD8^+$ T cells during orf virus reinfection. J. Gen. Virol. **77:**953–961.
23. **Haig, D. M., D. L. Deane, N. Myatt, J. Thomson, G. Entrican, J. Rothel, and H. W. Reid.** 1996. The activation status of ovine $CD45R^+$ and $CD45R^-$ efferent lymph T cells after orf virus reinfection. J. Comp. Pathol. **115:**163–174.
24. **Haig, D. M., C. J. McInnes, G. Hutchison, H.-F. Seow, and H. W. Reid.** 1996. Cyclosporin-A abrogates the acquired immunity to cutaneous reinfection with the parapoxvirus orf virus. Immunology **89:**524–531.
25. **Haig, D. M.** 1997. Techniques for the culture of ovine haemopoietic cells, p. 2098–2106. *In* I. Lefkovits (ed.), Immunological methods manual, vol. 4. Academic Press, London, United Kingdom.
26. **Haig, D. M., and A. Mercer.** 1998. Ovine diseases. Orf. Vet. Res. **29:**311–326.
27. **Haig, D. M., C. J. McInnes, J. Thomson, A. Wood, K. Bunyan, and A. A. Mercer.** 1998. The orf virus OV20.0L gene product is involved in interferon resistance and inhibits an interferon-inducible, double-stranded RNA-dependent kinase. Immunology **93:**335–340.
28. **Haig, D. M., J. Hopkins, and H. R. P. Miller.** 1999. Local immune responses in afferent and efferent lymph. Immunology **96:**155–163.
29. **Heaney, M. L., J. C. Vera, M. A. Raines, and D. W. Golde.** 1995. Membrane-associated and soluble granulocyte-macrophage colony-stimulating factor receptor alpha subunits are independently regulated in HL60 cells. Proc. Natl. Acad. Sci. USA **92:**2365–2369.
30. **Honda, M., K. Kitamura, T. Takeshita, K. Sugamura, and T. Tokunaga.** 1990. Identification of a soluble IL-2 receptor beta chain from human lymphoid cell line cells. J. Immunol. **145:**4131–4135.
31. **Hu, F.-Q., C. A. Smith, and D. J. Pickup.** 1994. Cowpox virus contains two copies of an early gene encoding a soluble secreted form of the type II TNF receptor. Virology **204:**343–356.
32. **Jenkinson, D. M., G. Hutchison, S. K. Onwuka, and H. W. Reid.** 1991. Changes in the MHC class II dendritic cell population of ovine skin in response to orf virus infection. Vet. Dermatol. **2:**1–9.
33. **Jenkinson, D. M., G. Hutchison, and H. W. Reid.** 1992. The B and T cell responses to orf virus infection of ovine skin. Vet. Dermatol. **3:**57–64.
34. **Kanakura, Y., H. Sugahara, H. Mitsui, H. Ikeda, T. Furitsu, H. Yagura, H. Kitayama, Y. Kanayama, and Y. Matsuzawa.** 1993. Functional expression of interleukin-2 receptor in a human factor-dependent megakaryoblastic leukaemia cell line: evidence that granulocyte-macrophage colony-stimulating factor inhibits interleukin-2 binding to its receptor. Cancer Res. **53:**675–680.
35. **Lalani, A. S., and G. McFadden.** 1997. Secreted poxvirus chemokine binding proteins. J. Leukoc. Biol. **62:**570–576.
36. **Lalani, A. S., K. Graham, K. Mossman, K. Rajarathnam, I. Clark-Lewis, D. Kelvin, and G. McFadden.** 1997. The purified myxoma virus gamma interferon receptor homolog M-T7 interacts with the heparin-binding domains of chemokines. J. Virol. **71:**4356–4363.
37. **Lear, A.** 1995. The characterisation of the ovine skin response to orf virus infection. Ph.D thesis. University of Edinburgh, Edinburgh, Scotland.
38. **Lear, A., G. Hutchison, H. W. Reid, M. Norval, and D. M. Haig.** 1996. Phenotypic characterization of the dendritic cells accumulating in the ovine dermis following primary and secondary orf virus infections. Eur. J. Dermatol. **6:**135–140.
39. **Lloyd, J., H. S. Gill, D. M. Haig, and A. J. Husband.** *In vivo* T cell subset depletion reveals that $CD4^+$ T cells and a humoral immune response are important for the elimination of orf virus from the skin of sheep. Vet. Immunol. Immunopathol., in press.
40. **Lyttle, D. J., K. M. Fraser, S. B. Fleming, A. A. Mercer, and A. J. Robinson.** 1994. Homologs of vascular endothelial growth factor are encoded by the poxvirus orf virus. J. Virol. **68:**84–92.
41. **Mahr, A., and B. E. Roberts.** 1984. Arrangement of late RNAs transcribed from a 7.1-kilobase *Eco*RI vaccinia virus DNA fragment. J. Virol. **49:**510–520.
42. **McConahey, P. J., and F. J. Dixon.** 1980. Radio-iodination of proteins by use of the chloramine-T method. Methods Enzymol. **70:**210–213.
43. **McInnes, C., D. Haig, and M. Logan.** 1993. The cloning and expression of the gene for ovine interleukin-3 (multi-CSF) and a comparison of the *in vitro* hematopoietic activity of ovine IL-3 with ovine GM-CSF and human M-CSF. Exp. Hematol. **21:**1528–1534.
44. **McInnes, C. J., A. Wood, and A. A. Mercer.** 1998. Orf virus encodes a gene

with homology to the vaccinia virus interferon-resistance E3L gene. Virus Genes **17:**107–115.
45. **McKeever, D. J., and H. W. Reid.** 1986. Survival of orf virus under British winter conditions. Vet. Rec. **118:**613–614.
46. **McNiece, I.** 1997. Interleukin-3 and the colony-stimulating factors, p. 41–53. *In* D. G. Remick and J. S. Friedland (ed.), Cytokines in health and disease, 2nd ed. Marcel Dekker, Ann Arbor, Mich.
47. **Mercer, A. A., K. Fraser, G. Barns, and A. J. Robinson.** 1987. The structure and cloning of orf virus DNA. Virology **157:**1–12.
48. **Mercer, A. A., D. L. Yirrell, E. M. Whelan, P. F. Nettleton, I. Pow, J. A. Gilray, H. W. Reid, and A. J. Robinson.** 1997. A novel strategy for determining protective antigens of the parapoxvirus orf virus. Virology **229:**193–200.
49. **Mercer, A. A., and D. M. Haig.** 1999. Parapoxviruses p. 1140–1146. *In* A. Granoff and R. Webster (ed.), The encyclopaedia of virology, vol. 2. Academic Press, London, United Kingdom.
50. **Mossman, K., C. Upton, and G. McFadden.** 1995. The myxoma virus soluble interferon-γ receptor homolog, M-T7, inhibits interferon-γ in a species-specific manner. J. Biol. Chem. **270:**3031–3038.
51. **Park, L. S., U. Martin, R. Sorensen, S. Luhr, P. J. Morrissey, D. Cosman, and A. Larsen.** 1992. Cloning of the low-affinity murine granulocyte-macrophage colony-stimulating factor receptor and reconstitution of a high-affinity receptor complex. Proc. Natl. Acad. Sci. USA **89:**4295–4299.
52. **Pye, D.** 1990. Vaccination of sheep with cell culture grown orf virus. Aust. Vet. J. **67:**182–186.
53. **Raines, M. A., L. Liu, S. G. Quan, V. Joe, J. F. DiPersio, and D. W. Golde.** 1991. Identification and molecular cloning of a soluble human granulocyte-macrophage colony-stimulating factor receptor. Proc. Natl. Acad. Sci. USA **88:**8203–8207.
54. **Smith, C. A., T. D. Smith, P. J. Smolak, D. Friend, H. Hagen, M. Gerhart, L. Park, D. J. Pickup, D. Torrance, K. Mohler, K. Schooley, and R. G. Goodwin.** 1997. Poxvirus genomes encode a secreted, soluble protein that preferentially inhibits beta chemokine activity yet lacks sequence homology to known chemokine receptors. Virology **236:**316–327.
55. **Smith, G. L., Y. S. Chan, and S. T. Howard.** 1991. Nucleotide sequence of 42kbp of vaccinia virus strain WR from near the right inverted terminal repeat. J. Gen. Virol. **72:**1349–1376.
56. **Smith, G. L.** 1996. Virus proteins that bind cytokines, chemokines or interferons. Curr. Opin. Immunol. **8:**467–471.
57. **Spriggs, M. K.** 1996. One step ahead of the game: viral immunomodulatory molecules. Annu. Rev. Immunol. **14:**101–130.
58. **Spriggs, M. K., D. E. Hruby, C. R. Maliszewski, D. J. Pickup, J. E. Sims, R. M. L. Buller, and J. Vansiyke.** 1992. Vaccinia and cowpox viruses encode a novel secreted interleukin-1-binding protein. Cell **71:**145–152.
59. **Strockbine, L. D., J. I. Cohen, T. Farrah, S. D. Lyman, F. Wagener, R. F. DuBose, R. J. Armitage, and M. K. Spriggs.** 1998. The Epstein-Barr virus BARF1 gene encodes a novel, soluble colony-stimulating factor-1 receptor. J. Virol. **72:**4015–4021.
60. **Sugamura, K., H. Asao, M. Kondo, N. Tanaka, N. Ishii, M. Nakamura, and T. Takeshita.** 1995. The common gamma-chain for multiple cytokine receptors. Adv. Immunol. **59:**225–277.
61. **Symons, J. A., J. A. Eastgate, and G. A. Duff.** 1990. A soluble binding protein specific for interleukin 1 beta is produced by activated mononuclear cells. Cytokine **2:**190–198.
62. **Symons, J. A., A. Alcami, and G. L. Smith.** 1995. Vaccinia virus encodes a soluble type 1 interferon receptor of novel structure and broad species specificity. Cell **81:**551–560.
63. **Vos, J. C., M. Sasker, and H. G. Stunnenberg.** 1991. Vaccinia virus capping enzyme is a transcription initiation factor. EMBO J. **10:**2553–2558.
64. **Yirrell, D. L., H. W. Reid, M. Norval, and H. R. P. Miller.** 1991. Qualitative and quantitative changes in ovine afferent lymph draining the site of epidermal orf virus infection. Vet. Dermatol. **2:**133–138.
65. **Yirrell, D. L., H. W. Reid, M. Norval, G. Entrican, and H. R. P. Miller.** 1991. Response of efferent lymph and popliteal lymph node to epidermal infection of sheep with orf virus. Vet. Immunol. Immunopathol. **28:**219–235.